ISBN 978-82-471-2584-7 (printed ver.)
ISBN 978-82-471-2585-4 (electronic ver.)
ISSN 1503-8181

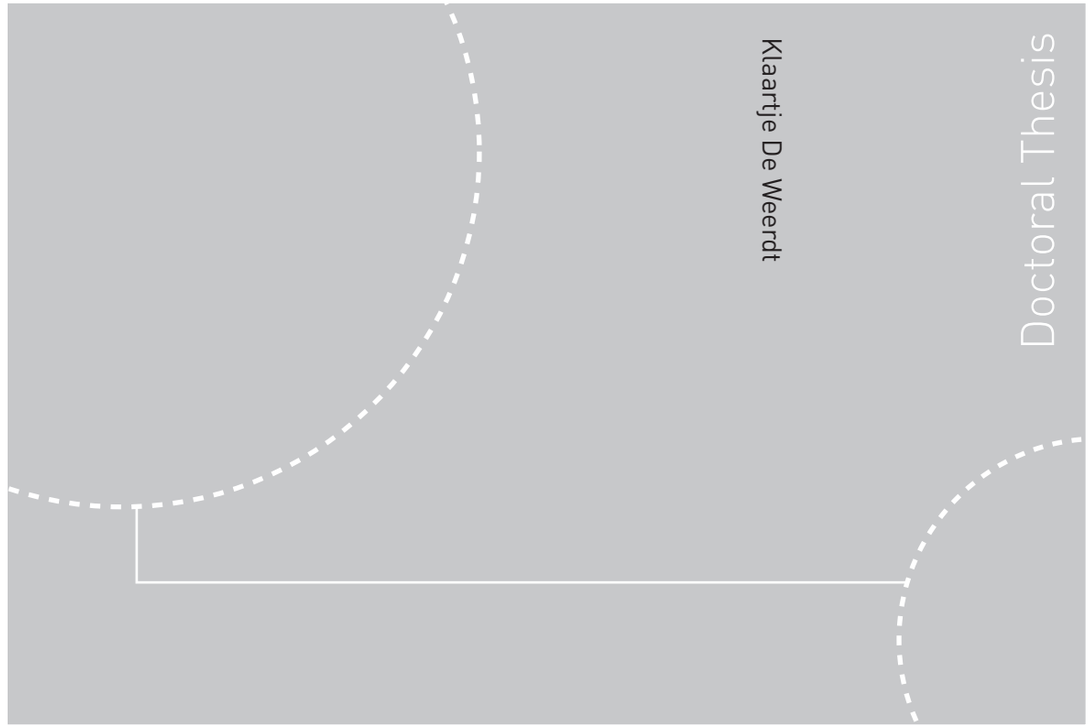

Doctoral theses at NTNU, DBCCL32

Klaartje De Weerdt

Blended Cement with Reduced CO_2 Emission - Utilizing the Fly Ash-Limestone Synergy

NTNU
Norwegian University of
Science and Technology
Thesis for the degree of
doctor philosophiae
Faculty of Engineering Science and Technology
Department of Structural Engineering

NTNU
Norwegian University of
Science and Technology

Doctoral theses at NTNU, 2011:32

NTNU

NTNU
Norwegian University of
Science and Technology

Klaartje De Weerdt

Blended Cement with Reduced CO_2 Emission - Utilizing the Fly Ash-Limestone Synergy

Thesis for the degree of doctor philosophiae

Trondheim, February 2011

Norwegian University of
Science and Technology
Faculty of Engineering Science and Technology
Department of Structural Engineering

NTNU
Norwegian University of
Science and Technology

NTNU
Norwegian University of Science and Technology

Thesis for the degree of doctor philosophiae

Faculty of Engineering Science and Technology
Department of Structural Engineering

ISBN 978-82-471-2584-7 (printed ver.)
ISBN 978-82-471-2585-4 (electronic ver.)
ISSN 1503-8181

Doctoral Theses at NTNU, 2011:32

Printed by Tapir Uttrykk

Acknowledgements

The research project presented in this thesis was carried out at SINTEF Building and Infrastructure in cooperation with the Department of Structural Engineering at the Norwegian University of Technology (NTNU) in Trondheim.

This project is part of the Concrete Innovation Centre (COIN), a centre for research based innovation, funded by the Norwegian Research Council and industrial partners (www.coinweb.no). I acknowledge COIN for the financial support, and for facilitating the interaction between experts, students and industry.

It would not have been possible to complete this thesis without the help and support of many.

First and foremost, I would like to express my gratitude to my co-supervisor Professor Harald Justnes for giving me the opportunity to come to Norway, for coming up with the fascinating idea which lead to this thesis, and for watching over me during four years while travelling the world. I would like to thank my supervisor Professor Knut O. Kjellsen for his enthusiasm and solid support, and Professor Erik J. Sellevold, for spending many hours of his spare time correcting my drafts, encouraging me and always being ready for a good discussion.

Special thanks go to Dr. Barbara Lothenbach for inviting me to EMPA, Dübendorf in Switzerland, giving me the opportunity to work in their excellent laboratories during 6 months, and for introducing me into the world of GEMS as well as charming Switzerland. I would like to thank Dr. Mohsen Ben Haha and Dr. Gwenn Lesaout for their assistance with respectively scanning electron microscopy techniques and XRD-Rietveld analysis. The discussions with Florian Deshner, Dr. Frank Winnefeld and Dr. Josef Kaufmann were inspiring, and their help with the experiments was much appreciated. I should not forget the invaluable support in the laboratory from Angela Steffen, Luigi Brunetti, Boris Ingold and Walter Trindler. Further, I want to thank the whole crew for making my stay at EMPA unforgettable.

I want to thank Dr. Maciej Zajac from the Heidelberg Technology Centre for his interest in the project, his advice, and the invitation to the research centre in Leimen.

The “concrete”-colleagues at “grønn bygget” have contributed immensely to my personal and professional time in Trondheim. The colleagues have been a source of optimism, passion for research, warmth and joy; thanks Hedda, Marit, Bjørn Erik, Hans, Randi, Gudrun, Erik T., Helge, Per Arne, Lars, Harald, Anja, Ola, Tone, Mari, Tore, Sindre, Jan, Gunrid, Kristin, Knut, Stig, Chris, Roger, Eirik and Tor Arne. I want to express my gratitude to Knut Lervik, Stig Roar Rudolfsen, Øystein Mortensvik and Ove Loraas for their assistance with the mortar tests, and Tone Østnor and Kristin Mjøen for helping me with the analyses in the chemistry lab. Special thanks go to Hedda Vikan and Tone Østnor for being so supportive and inspiring, and for the laughter and good times we shared.

I am very grateful to my family and friends for supporting me and reminding me that the world does not only turn around concrete or cement.

My final thanks go to Robert for his love, support and patience.

Klaartje, February 2011

Abstract

During cement production large amounts of CO_2 are emitted, about 1 tonne CO_2 per tonne clinker, if no measures are taken. About 40% originates from fuel combustion, grinding and other operations, and 60% from the de-carbonation of limestone to form the clinker phases. One way to reduce these emissions on the short term is by replacing part of the clinker with other materials such as slag, limestone powder, fly ash, silica fume and natural pozzolans. The type of replacement materials used depends on their availability (e.g. amount available, price and transportation) and is therefore dependent on the geographical location of the cement plant. The aim of this study is to contribute to the development of a novel all-round Portland composite cement for the Norwegian market. When this study was started, the cements produced at the Norwegian cement plants were: CEM I Portland cements containing up to 5% limestone powder and CEM II/A-V Portland fly ash cements containing up to 18% fly ash but no limestone powder. In this study, the effect of increasing the replacement levels of the ordinary Portland cement (OPC) (up to 35% replacement), and combining siliceous fly ash (FA) and limestone powder (L) to replace OPC are investigated.

Using a combination of fly ash and limestone to replace OPC seems to be better than using only one of them. Limestone powder accelerates the early hydration more than fly ash, but fly ash contributes to strength development at later ages due to its pozzolanic reaction. Additionally a chemical interaction between fly ash and limestone has been observed, first in simplified cementitious system and later also in Portland composite cement. Limestone powder interacts with the AFm and AFt phases formed during the hydration of OPC. At first, ettringite forms during the hydration of OPC. When all gypsum is consumed, ettringite will react with the remaining aluminates and form monosulphate. In the presence of limestone, hemi- and monocarboaluminate are formed instead of monosulphate. The ettringite does, therefore, not decompose. This leads to higher volume of the hydrates, which on its turn might reduce the porosity and enhance the compressive strength. The effect of limestone powder on OPC is limited due to its low aluminate content. However, when part of the OPC is replaced by fly ash, the fly ash will introduce additional aluminates to the system as it reacts. This will lower the SO_3/Al_2O_3 and increase the AFm/AFt ratio and thereby amplify the impact of limestone powder. These changes in the AFm and AFt phases have been experimentally observed by TGA, XRD and EDX, and predicted using thermodynamic modelling.

Only a few percent of limestone powder are required to prevent ettringite from decomposing to monosulphate. The changes in hydration products resulting from these small limestone powder contents coincides with an increase in compressive strength. Replacement of 5% fly ash with 5% limestone powder in a 65%OPC+35%FA cement resulted in a compressive strength increase ranging between 8 and 13% after 28 days of curing. At higher limestone contents the compressive strength decreases again as the additional limestone mainly serves as an inert filler. Replacing 5% of OPC with limestone powder resulted, on the other hand, in a strength reduction or a slight increase up to 4% after 28 days of curing. The beneficial effect of limestone is maximal at 28 days, and reduces slightly upon further curing. It is furthermore valid at 5, 20 and 40°C. However, at 40°C the fly ash reaction is accelerated and over time the fly ash content is more important than the synergetic effect.

The observed increase in compressive strength has to be partly due to the chemical interaction described above as an inert filler (crystalline quartz) with a similar psd does not have the same beneficial impact on strength as limestone. Additionally, the presence of limestone powder does not seem to affect the reactivity of OPC and fly ash significantly.

The observed effect between fly ash and limestone enables higher replacement levels than when only one of them is used. The applicability of the study is demonstrated by the fact that cement with the

optimal composition found in this study (65%OPC+30%FA+5%L) has recently been used in the construction of the Meteorological Centre in Oslo and the Science Centre in the county of Østfold.

List of papers

This thesis includes the following papers:

I. **Microstructure of binder from the pozzolanic reaction between lime and siliceous fly ash, and the effect of limestone addition.**
De Weerdt K. & Justnes H.
Proceedings of the First International Conference on Microstructure Related Durability of Cementitious Composites, Ed. W. Sun, K. Van Breugel, C. Miao, G. Ye and H. Chen, 2008, Nanjing, RILEM PRO 61, Vol. 1 pp.107-116 (ISBN 978-2-35158-065-3, e-ISBN 978-2-35158-084-4).

II. **Fly ash-limestone ternary cements: effect of component fineness.**
De Weerdt K., Sellevold E.J., Kjellsen K.O. & Justnes H.
Advances in Cement Research. Accepted.

III. **Fly ash -limestone ternary composite cements: synergetic effect at 28 days.**
De Weerdt K., Justnes H., Kjellsen K.O. & Sellevold E.J.
Nordic Concrete Research, 2010, Vol.42 (2) pp. 51-70

IV. **Synergy between fly ash and limestone powder in ternary cements**
De Weerdt K., Kjellsen K.O., Sellevold E.J. & Justnes H.
Cement and Concrete Composites,2011, Vol. 33 (1) pp.30-38,
doi:10.1016/j.cemconcomp.2010.09.006

V. **Quantification of the degree of reaction of fly ash**
Ben Haha M., De Weerdt K. & Lothenbach B.
Cement and Concrete Research, 2010, Vol. 40 (11) pp.1620-9,
doi:10.1016/j.cemconres.2010.07.004

VI. **Hydration mechanisms of ternary Portland cements containing limestone powder and fly ash**
De Weerdt K., Ben Haha M., Le Saout G., Kjellsen K.O., Justnes H. & Lothenbach B.
Cement and Concrete Research, 2010, in press,
doi:10.1016/j.cemconres.2010.11.014

VII. **The effect of limestone powder additions on strength and microstructure of fly ash blended cements**
De Weerdt K., Justnes H., Ben Haha M. & Lothenbach B.
13th International Congress on the Chemistry of Cement, 2011, Madrid, in review.

VIII. **The effect of temperature on the hydration of Portland composite cements containing limestone powder and fly ash**
De Weerdt K., Ben Haha M., Le Saout G., Kjellsen K.O., Justnes H. & Lothenbach B.
Materials and Structures, 2010, in review.

Klaartje De Weerdt's contribution to the publications:

Paper I-IV and paper VI-VIII Major part of writing.
Paper V Major part of writing except writing concerning image analysis

Content

Acknowledgements I
Abstract II
List of papers IV
Content V
Glossary of notations and terms VI
Chapter 1 – Introduction 1
Chapter 2 – Objective and limitations 3
Chapter 3 – Summary of used methods 4
Chapter 4 – Background 6
Chapter 5 – Main findings 9
Chapter 6 – Concluding remarks 14
Chapter 7 – Future research 16
References 18

Glossary of notations and terms

The cement chemist's short hand:

C = CaO	S = SiO_2	A = Al_2O_3	F = Fe_2O_3
H = H_2O	$\underline{S}$ = SO_3	$\underline{C}$ = CO_2	

The notation of the anhydrous phases and hydrates are subsequently:

C_3S	$3CaO{\cdot}SiO_2$	tricalcium silicate
C_2S	$2CaO{\cdot}SiO_2$	dicalcium silicate
C_3A	$3CaO{\cdot}Al_2O_3$	tricalcium aluminate
C_4AF	$4CaO{\cdot}Al_2O_3{\cdot}Fe_2O_3$	Ferrite or brownmillerite
$C\underline{S}H_2$	$CaSO_4$	gypsum
$C\underline{C}$	$CaCO_3$	calcium carbonate
CH	$Ca(OH)_2$	calcium hydroxide or Portlandite
$C_6A\underline{S}_3H_{32}$	$3CaO{\cdot}Al_2O_3{\cdot}3CaSO_4{\cdot}32H_2O$	ettringite
$C_4A\underline{S}H_{12}$	$3CaO{\cdot}Al_2O_3{\cdot}CaSO_4{\cdot}12H_2O$	calcium monosulphoaluminate hydrate
$C_4A\underline{C}H_{11}$	$3CaO{\cdot}Al_2O_3{\cdot}CaCO_3{\cdot}11H_2O$	calcium monocarboaluminate hydrate
$C_4A\underline{C}_{0.5}H_{11.5}$	$3CaO{\cdot}Al_2O_3{\cdot}0.5Ca(OH)_2{\cdot}0.5CaCO_3{\cdot}11.5H_2O$	calcium hemicarboaluminate hydrate

Terms:

C-S-H: Amorphous calcium silicate hydrate with a varying composition is able to take up A, $\underline{S}$, Na^+, K^+ etc. It is the main hydration product of ordinary Portland cement and can also be formed by the reaction of pozzolans with CH.

C-A-S-H: C-S-H with a relatively high aluminate content.

C-A-H: calcium aluminate hydrates e.g. C_2AH_8, C_3AH_6 etc.

Alite: Impure C_3S as found in Portland cement containing other oxides in solid-state substitution

Belite: Impure C_2S as found in Portland cement containing other oxides in solid-state substitution.

AFt-phases: The phase formed in the hydration of Portland cement which is derived from pure ettringite with partial substitution of A by F, and SO_4^{2-} by other ions.

AFm-phases: The phase formed in the hydration of Portland cement which is derived from the pure mono-sulphoaluminate with the partial substitution of A by F, and SO_4^{2-} by other ions.

Additional abbreviations:

OPC	ordinary Portland cement	FA	fly ash
L	limestone powder	Q	quartz
PSD	particle size distribution	SEM	scanning electron microscopy
BSE	backscattered electron	IA	image analysis
EDX or EDS	energy dispersive X-ray spectroscopy	TGA	thermogravimetric analysis
DTA	differential thermal analysis	XRD	X-ray diffraction
XRF	X-ray fluorescence	IC	ion chromatography

Chapter 1 – Introduction

Concrete is the most widely used material on earth apart from water, with nearly three tonnes used annually per capita [1]. It is strong, durable, water- and fire-resistant, castable and relatively inexpensive. This in addition to its versatile nature, as it can be transported and poured into required shape, makes it to a valuable building material.

During the production of concrete about 0.08 to 0.32 tonnes CO_2 is emitted per tonne of concrete, depending on cement type, strength and durability class [2, 3]. Due to the rising environmental awareness related to greenhouse gasses (e.g. CO_2) and the growing demand of construction materials, governments have put out incentives to reduce these emissions. Compared to other construction materials, rather low levels of CO_2 are emitted during the production of concrete i.e. about 1 - 1.4 tonne of CO_2 is emitted per tonne steel produced, and about 0.64 tonne CO_2 per ton timber [2, 3]. However, concrete, steel and timber cannot be compared on either a weight or volume basis. The materials have different properties and are used in different applications. A steel column supporting a certain load will be much more slender, than a concrete or a wooden column. Comparing the CO_2 efficiency of different materials should therefore be related to a specific application [3]. Additionally, one should take into account the CO_2 emissions associated with the use and maintenance of the structure, and its estimated lifetime. Intelligent architectural design combined with an optimized material choice, is one possible way to reduce the carbon footprint of buildings and infrastructure.

Portland cement, the reactive component in concrete, reacts with water and forms the binder between aggregates and sand. The major part of the CO_2 embodied in concrete originates from the cement. The cement industry is responsible for about 5-8% of the global man-made CO_2 emissions [4]. This can be attributed to enormous amount of cement produced each year, about $1.7 \cdot 10^9$ tonne [2], and the high level of CO_2 emitted during the production process. On average 0.8-0.9 tonne CO_2 is emitted for the production of 1 tonne of cement [1, 4, 5]. The raw meal used to produce cement clinker consist for about 75-79% of calcium carbonate, which is added in the form of limestone powder and/or marl [6]. During the clinkerization process the calcium carbonate decomposes to calcium oxide (see Equation (1)), thereby liberating CO_2. This source of CO_2 represents about 50-60% of the total amount of CO_2 emitted during cement production [4, 7].

$$CaCO_3\,(s) \rightarrow CaO\,(s) + CO_2\,(g) \qquad (1)$$

The remaining 40-50% of the CO_2 emissions, originate mainly form the heating of the cement kiln up to the clinkerization temperature of approximately 1450°C, and a minor part comes from grinding and transportation [7].

There are different possibilities to reduce CO_2 emissions in cement production [2, 4]. In order to reduce the fuel or electricity-related CO_2, one can optimize the heat transfer and the grinding process, and burn waste materials to heat the cement kiln (e.g. car tires, municipal waste and bone meal). The CO_2 originating from the de-carbonation (calcination) can be reduced by either producing an alternative type of cement clinker containing less CaO, or reducing the clinker content in the cement by replacing it with supplementary cementitious materials (SCMs).

This thesis focuses on the last named option: replacing part of the ordinary Portland cement by SCMs. Commonly used SCMs are: blast furnace slag, fly ash, silica fume, limestone powder, calcined clay,

natural pozzolans. These products, except for limestone powder, calcined clay and natural pozzolans are by-products form other industries. A major advantage of the use of these SCMs in concrete, besides the clinker replacement, is the reduction in the amount of waste materials dumped in landfills.

The use of SCMs is strongly dependent on their availability. Silica fume, one of the most efficient SCMs, has become increasingly scarce due to rising demand. The availability of granulated blast furnace slag and fly ash is strongly dependent on the supply and accessibility of respectively the steel industry and coal-fired power plants. Therefore the geographic position and accessibility of the cement plant plays a crucial role in the use of SCMs and hence the cement types produced. But besides availability, tradition also seems to play an important role. In Central Europe for example the use of limestone filler is very common [8], whereas in Scandinavia it appears to be rather rare, only in recent years Swedish and Danish cement manufacturers have introduced a cement with 15% limestone on the market. This difference cannot be explained by an availability difference as cement plants generally are positioned in the vicinity of limestone depositions.

Table 1: Classification of the cement types according to EN 197-1

% clinker replacement			0 10 20 30 40 50 60 70 80 90 100
Portland cement	CEM I		
Portland composite cement	CEM II	A	6-20
		B	21-35
Blastfurnace cement	CEM III	A	36-65
		B	66-80
		C	81-95
Pozzolanic cement	CEM IV	A	11-35
		B	36-55
Composite cement	CEM V	A	36-60
		B	61-80

In order to be able to sell a certain cement type on the European market, it has to conform with the European standards EN 197-1. It should however be noted that there is a higher degree of freedom for replacing part of the cement with SCMs in concrete when done at the concrete mixing plants.

Table 1 shows the different cement classes allowed within EN 197-1. CEM I represents ordinary Portland cement (OPC). This cement type can contain additional constituents up to 5%. All the cement types presented in Table 1 except CEM I are blended cements. CEM II cement types can contain SCMs up to 35%. This is the most commonly used cement type in Europe. They are subdivided into two classes, namely A and B. Most used is the A class with lowest cement replacement level (up to 20%). The other cement types, CEM III, CEM IV and CEM V, are less common. They are mostly tailor-made for specific construction projects. Nowadays in Europe, the CEM II cement is more common than plain ordinary Portland cement (CEM I). In 2004, CEMBUREAU reported that plain OPC, CEM I, only had a market share of 32% compared to 55% for CEM II, for all the strength classes. Furthermore, for the strength class 32.5, the market share of CEM I was about 9%, and 70% for CEM II [9]. This demonstrates the interest for CEM II cements on the European market.

Chapter 2 – Objective and limitations

Currently in Norway, two blended cements (CEM II) are produced, containing up to 20% fly ash (Standardsement FA and Anleggssement FA). The objective of this study is to contribute to the development an all-round Portland composite cement (CEM II/B-M) with clinker replacement levels higher than 30%. The study focuses on the use of a combination of limestone powder and class F fly ash. Limestone is available in different grades of purity in Norway, but fly ash has to be imported from coal-fired power plants in Germany, Denmark or the Netherlands. A possible synergetic interaction between fly ash and limestone powder was postulated at the start of the project.

In order to formulate this ternary Portland composite cement, exploiting the potential of the components both chemically and physically, the following research steps were undertaken:

- Examining the interaction between fly ash and limestone powder in cementitious systems
- Optimizing the fineness of the components of the ternary Portland composite cement
- Optimizing the replacement levels of the different components
- Evaluating the hydration mechanisms of the ternary Portland composite cement
- Evaluating the effect of curing time and temperature on the hydration of the ternary Portland composite cement

The cement is primarily meant to be used in concrete for buildings and not for infrastructure, thus relatively high water-to-cement ratios e.g. 0.5-0.6 will be applied. Therefore it was opted not to optimize the particle packing and rheological properties and all tests have been performed with a water-to-cement ratio of 0.5.

Documentation of the optimal gypsum content, mechanical properties (except for mortar strength) and durability is beyond the scope of the thesis.

Chapter 3 – Summary of used methods

Particle characterization: helium pycnometry – Blaine specific surface – laser granolumetry

The specific weight and the particle size distribution of the materials were determined using respectively an AccuPyc helium pycnometer from Micrometrics and a Mastersizer laser diffractometer from Malvern. The Blaine specific surface was measured using the air permeability method described in EN 196-6.

Compressive and flexural strength

The compressive and flexural strength were determined according to EN 196-1. Mortar prisms (40×40×160 mm) with cement – sand – water proportions of (1/3/0.5) were prepared. The samples were cured in $Ca(OH)_2$ saturated solution until testing.

Isothermal calorimetry

The isothermal rate of heat of hydration was measured on 6 g of paste with water-to-binder ratio of 0.5. The paste was prepared in a glass vial using a slow stirring IKA-WERKE RW16 mixer. Subsequently, the vial was sealed and loaded into a TAM Air isothermal calorimeter in which the rate of heat of hydration was measured at 20˚C during the first 24 hours after water addition.

Chemical shrinkage (CS)

Cement pastes were prepared with a water-to-binder ratio of 0.4. About 5 g of paste was weighed into an empty glass vial. The vial was filled with de-aerated water and sealed with a rubber stopper with an inserted graduated capillary tube. Care was taken to avoid air bubbles in vial and tube. A drop of paraffin was placed in the top of the capillary tube to minimize water evaporation. The samples were stored in a water bath at 20°C. Periodically the height of the water column in the capillary was noted together with the time expired since water addition to the cement. Three replicas were made. This method is described in ASTM C 1608-07.

Pore solution analysis – ion chromatography (IC)

The pore solution of a cylindrical cement paste sample of 500 ml cured under sealed conditions at 20°C, was extracted using the steel die method [10]. Immediately after extraction, the solution was filtrated using a 0.45 µm nylon filter. The pore solution was analysed with a pH electrode, calibrated with known KOH concentrations. The concentration of Na, K, S, Ca, Si and Al in the pore solution was determined using a Dionex Ion Chromatography system (ICS) 3000 using standards from Fluka.

Thermogravimetric analysis (TGA)

Cement paste samples were prepared with water-to-binder ratio of 0.5 and stored at 20°C in 20 ml sealed plastic vessels. The samples, used for thermogravimetric analysis and X-ray diffraction, were crushed (< 63 µm). The hydration was stopped by solvent exchange using either ethanol or a combination of isopropanol and ether. The samples were either dried in the TGA at 40°C while flushing with N_2, or stored for about 1 hour in a dessicator over silica gel prior to analysis.

The amount of bound water (H) and calcium hydroxide (CH) are determined with thermogravimetric analysis using a Mettler Toledo TGA/SDTA851 by measuring the weight loss of a 50 mg sample in the

respective temperature intervals 40-550˚C and 450-550˚C. The exact boundaries for the temperature interval of CH are read from the derivative curve (DTG). The values are expressed as %wt. of the sample mass at 550˚C.

Generally the amount of bound water is determined by the weight loss between 105 and 1000°C. It was decided to use the weight loss between 40 and 550°C, as at 105˚C the decomposition of ettringite and C-S-H has already started, and in the temperature interval 550-900°C the weight loss is mainly due to the decomposition of carbonates originating from the limestone powder.

X-ray diffraction (XRD)

The crystalline anhydrous and hydrous phases were identified using X-ray diffraction (XRD). Two different diffractometers were used in the course of the study, Bruker AXS D8 focus and Phillips PANalytical X'Pert Pro MPD, equipped with respectively a LynxEye and an X'celerator detector. Both have a θ-2θ configuration and a CuKα source (λ=1.54 Å). The powder samples of about 3 g were scanned between 5° and 70° 2θ. The powder samples used for XRD are the same as those used for TGA.

A selection of phases was quantified by Rietveld analysis using an external CaF_2 standard according to the method described in [11, 12].

Scanning electron microscopy (SEM) – energy dispersive X-ray spectroscopy (EDS)

The degree of hydration of OPC and fly ash, and the coarse porosity was determined using image analysis applied on backscattered electron (BSE) images taken by a Philips ESEM FEG XL 30 of a epoxy resin impregnated, polished and carbon coated piece of hydrated cement paste. The hydration of the hydrated cement paste was stopped by immersing it in isopropanol or ethanol and subsequent drying at 40°C. Over sixty images were taken per sample at a magnification of 1600. The minimum pore radius measured is reported to be 0.17 µm by the operator. The analyses were carried out using an accelerating voltage of 15kV to ensure a good compromise between spatial resolution and adequate excitation of the FeKα peak.

The variations in the chemical composition of the crypto crystalline C-S-H phase due to changes in curing temperature and the ongoing reaction of fly ash, e.g. Ca/Si ratio and Al incorporation, were investigated using Energy dispersive X-ray spectroscopy (EDX).

Thermodynamic modeling (GEMS)

The hydration of the tested cements was modelled using the Gibbs free energy minimization program, GEMS [13]. The thermodynamic data from the PSI-GEMS database [14, 15] was supplemented with cement specific data [16-18]. GEMS computes the equilibrium phase assemblage in a multi-component system based on the bulk composition of the materials.

Chapter 4 – Background

Ordinary Portland cement

Ordinary Portland cement is produced by burning finely ground raw meal consisting of mainly limestone, and to a lesser degree marl, clay or even shale, at about 1450°C in a rotary kiln. The material obtained after burning is called clinker. The clinker is cooled rapidly and blended with gypsum and subsequently ground to a fine powder.

The main oxides present in ordinary Portland clinker are: CaO (60-70%), SiO_2 (18-22%), Al_2O_3 (4-6%) and Fe_2O_3 (2-4%) [19]. They represent about 95% of the clinker, the remaining 5% includes MgO, K_2O, Na_2O, TiO_2, Mn_2O_3, SO_3. The main oxides constitute the main mineralogical phases of the clinker namely [19]:

• Alite	$3CaO{\cdot}SiO_2$	C_3S	55-65%
• Belite	$2CaO{\cdot}SiO_2$	C_2S	15-25%
• Aluminate	$3CaO{\cdot}Al_2O_3$	C_3A	8-14%
• Ferrite or brown millerite	$4CaO{\cdot}Al_2O_3{\cdot}Fe_2O_3$	C_4AF	8-12%

Alite and belite react with water to form C-S-H gel and CH according to Equations (2) and (3) respectively.

$C_3S + zH \rightarrow C_xSH_y + (3-x)\ CH$ (2)
$C_2S + zH \rightarrow C_xSH_y + (2-x)\ CH$ (3)
With z = y+3-x for alite and z = y+2-x for belite, and Z typically falls in the range 3-4.

Alite is the main clinker mineral and is much more reactive than belite during the first days of hydration. It is therefore the most important of the constituent phases for the strength development during the first 28 days. Belite reacts slowly, but can contribute to the strength development after 28 days. A great part of it can remain unreacted even after one year of hydration.

The aluminate phase reacts with water and gypsum to form ettringite (Equation 4). Within the first day the gypsum is consumed and the ettringite starts to react with the remaining aluminate to form calcium monosulphaluminate (also referred to as monosulphate) as described by Equation (5).

$C_3A + 3C\underline{S}H_2 + 26H \rightarrow C_6A\underline{S}_3H_{32}$ (4)
$C_6A\underline{S}_3H_{32} + 2\ C_3A + 4H \rightarrow 3C_4A\underline{S}H_{12}$ (5)

The hydration of the ferrite phase is analogous to the hydration of aluminate phases. The Al in ettringite and monosulphate can be partly replaced by Fe. The phases derived from pure monosulphate and pure ettringite with partial substitution of Al by Fe, and SO_4^{2-} by other ions and are referred to respectively as the AFm and AFt phases.

The clinker contains alkalis, easy soluble or incorporated in the clinker phases. This together with the formation of CH results in a high pH pore solution in the hydrated paste.

Portland-fly ash cement

Fly ash is a by-product from coal-fired power plants. Pulverized coal is injected in the furnace and incinerated to heat up water and produce steam for the turbine driven generators. Fly ash is the residuum of the coal particles, which are collected from the exhaust by electrostatic or mechanical precipitation [6]. Due to the high temperatures reached in the furnace, 1000-1600°C depending on

whether a dry or a slag-tap furnace is used [6], most of the mineral components contained in the coal melt and form small fused droplets which upon rapid air cooling transform into spherical glassy particles. They consist predominantly of SiO_2, Al_2O_3, Fe_2O_3 and alkalis. However, their chemical composition can vary considerably and depends on the composition of the inorganic fraction of the coal. Fly ash used in cement production generally has a glass content that varies between 50-90%, the remaining part consists of crystalline phases such as mullite, quartz and hematite, and often some left over unburned carbon particles.

Fly ash is classified according to composition regarding international cement and concrete standards. In the European standard, EN-197-1, fly ash is divided into siliceous and calcareous fly ash based on the reactive calcium oxide content. The former contains less than 10% reactive calcium oxide and the latter more. Additionally it should contain more than 25% reactive silicon oxide in order to be used in blended cements to conforming to EN-197-1. The American ASTM C618 uses two classes: class F and class C fly ash. This classification gives requirements for the total reactive SiO_2, Al_2O_3 and Fe_2O_3 content of the fly ash, requiring a total content higher than 70% for the former and higher than 50% for the latter. Indirectly, this classification refers to the reactive calcium oxide content.

Siliceous ash and Class F fly ash are often referred to as pozzolanic materials. Whereas, calcareous and Class C fly ash are considered partially hydraulic. Pozzolanic materials principally consist of reactive SiO_2 and Al_2O_3 which in an alkaline solution react with CaO and form reaction products. When a pozzolan is combined with ordinary Portland cement (OPC), calcium hydroxide is provided by the hydration of the OPC and the highly alkaline pore solution activates the pozzolanic reaction. The reaction products formed by the pozzolan are similar to the ones formed by OPC (see Equation 6). Class C or calcareous fly ashes provide part of the CaO themselves and are therefore referred to as partially hydraulic. The pozzolanic reaction can qualitatively be described as (AS = aluminosilicate);

$$\text{AS (fly ash)} + \text{CH (OPC)} + \text{H} \rightarrow \text{C-(A-)S-H} + \text{C-A-H} \qquad (6)$$

Fly ash has been used in concrete for many years, resulting in numerous publications. Malhotra and Mehta [20] provide a concise overview of the impact of fly ash on the properties of concrete: Replacing part of the cement with fly ash generally results in slower setting and hardening rates at early ages, especially at lower curing temperatures. However, over time, the mechanical properties can be superior compared to concrete prepared with plain OPC. Due to the spherical shape of the majority of the particles, fly ash can improve the flowability of the concrete due to its “ball-bearing-effect”. Therefore fly ash has been referred to as a water reducer as less water is needed to obtain the same flow when part of the OPC is replaced by fly ash. From a durability point of view fly ash has proved to be able to lower the permeability (higher resistance to chloride intrusion) and reduce alkali-silica-reaction (ASR) and sulphate attack, when used in correct proportions and cured properly.

Portland-limestone cement

The effect of limestone powder on the hydration of OPC has been a point of discussion for many years. The “aktivitt”-case in post-war Norway is a good example of this [21]. Engineer Arne Daniels patented the addition of metamorphic limestone powder under the brand name “aktivitt” to concrete, claiming that it would increase the strength and improve the resistant of concrete to marine environment [22-26]. It led to heated discussions in Scandinavia. An expert committee was appointed to evaluate the claim. Several series of tests were performed and the committee concluded that the effect of the “aktivitt” was no different compared to other limestone and rocks, and was merely due to its physical effect also referred to as filler effect.

Nowadays, it is generally accepted that 5% replacement of OPC with limestone powder does not impair the properties of the concrete to large extent. The majority of the current regulations allow the replacement of 5% of the cement with limestone for all standard cement types e.g. Brazil (NBR-5732), Canada (CAN3-A5-M83), Europe (EN-196) and USA (ASTM C150). Adding 5% of limestone powder is both economical and environmental advantageous as 5% less clinker has to be burned. As limestone is the main ingredient for the raw meal of the Portland clinker (about 80%), it is always available at cement plants.

When replacing more than 5% of the OPC, limestone powder has to fulfil the following requirements to conform with the European regulations EN-197: more than 75% of its mass has to consist of $CaCO_3$, the clay content determined by methyl adsorption has to be limited to 1.2g/100g and the total organic carbon content should not exceed 0.20% or 0.50% by mass.

The hydration of OPC is accelerated by the presence of limestone powder [27-32]. The finer the limestone, the greater is the effect [27, 32]. This has been attributed to its filler effect: the surface of the limestone particles serves as a nucleation and precipitation surface of the hydration products and the effective water to OPC ratio increases when the water to binder ratio is kept constant. It should be mentioned that the effect of limestone powder on the hydration of OPC is stronger with decreasing water-to-binder ratio [33].

Limestone powder interacts with the hydration of the calcium aluminates [34]. The AFm and AFt phases formed in a hydrating cement paste alter in the presence of limestone powder: calcium hemi- or mono-carboaluminate hydrate forms instead of calcium monosulphoaluminate hydrate [35-38] (see Equation 7 and 8). Therefore the ettringite will not decompose to monosulphate and remains stable.

$$C_3A + C\underline{C} + 11H \rightarrow C_4A\underline{C}H_{11} \quad (7)$$

$$C_3A + 0.5\ C\underline{C} + 0.5\ CH + 11H \rightarrow C_4A\underline{C}_{0.5}H_{11.5} \quad (8)$$

Replacing 5 to 10% of the OPC with limestone powder does generally not impair the compressive strength to a great extent [21]. This can be attributed to the filler effect and the chemical interaction between the calcium carbonate from the limestone powder and the aluminate hydrates.

Fly ash & limestone Portland composite cements

The chemical effect of limestone powder on OPC is limited due to the low aluminate content in the clinker, about 5-10% [39]. However, when part of the OPC is replaced by fly ash, additional aluminates are added to the system as the fly ash reacts. Fly ash can have a considerably higher aluminate content than OPC, typically around 30% [39]. These aluminates may react with the limestone powder and can therefore amplify the effect of the limestone powder.

Portland composite cements containing limestone and fly ash [32, 40-42] or other alumina containing SCM's such as slag [43-45] and natural pozzolans [46] have been studied. The combination of limestone powder and fly ash, slag or natural pozzolan appeared to be complementary: the limestone powder improves the early strength, while the slag, fly ash or natural pozzolan improves the later strength by its pozzolanic or hydraulic reaction. The interaction between limestone powder and alumina containing SCM's has however not been investigated, except for Hoshino et al. [45], who attributed the observed interaction between slag and limestone powder to changes in the AFm and AFt phases, using XRD-Rietveld analysis.

The main objective of this study is to obtain a better understanding of the interaction between limestone powder and fly ash when replacing part of the cement.

Chapter 5 – Main findings

The main findings of this study will be reported by discussing the major conclusions of each of the papers. They are presented in an order which follows the progression of the study.

Interaction between fly ash and limestone in a simplified system (Paper I)

In the first paper, the interaction between fly ash (FA) and limestone powder was studied in cement free-pastes. Pastes composed of lime/FA and lime/FA/limestone, respectively, were compared. Clinker was excluded to simplify the system. Instead an excess of calcium hydroxide ($Ca(OH)_2$) and alkaline mixing water (i.e. pH 13.2 and K/Na = 2:1) was used to simulate the conditions in a hydrating cement paste.

The mixes were cured at 5, 20, 38 and 80°C, and the reactions were stopped after 1, 3, 7, 28 and 88 days of curing.

The addition of limestone resulted in a slight increase in the amount of chemically bound water relative to the amount of FA. FA also appeared to bind more water than what was provided by calcium hydroxide. The XRD patterns of the pastes confirmed an interaction between the limestone and the FA, which resulted in the formation of calcium carboaluminate hydrates when limestone was included. At higher temperatures (80°C) the calcium carboaluminate phase appeared to be unstable and other hydration phases (e.g. hydrogarnet type phases) were observed.

Effect of component fineness (Paper II)

Composite cements in which the ordinary Portland cement (OPC) is party replaced by limestone powder and/or siliceous fly ash (FA) at levels up to 35% have been studied using three different finenesses for each material. The aim was to evaluate the influence of fineness and replacement level on the development of the compressive strength, the amount of bound water and calcium hydroxide and the heat of hydration of the composite cements.

The OPC fineness is the major parameter regarding the early hydration. At 28 days the fineness of the fly ash also plays an important role due to its contribution to the pozzolanic reaction. Indeed, intensive grinding of the fly ash appears to accelerate the reaction of the fly ash as observed from the calcium hydroxide consumption. Varying the fineness of the limestone powder within the tested range (362 – 812 m^2/kg) had no effect on the hydration of the OPC and the composite cement.

Limestone powder slightly accelerates the hydration of the OPC during the first day, whereas fly ash retards. When both are combined, limestone powder is able to compensate for the retardation caused by the fly ash. Additionally, replacing part of the OPC with fly ash and limestone powder increases the heat emitted by OPC during the first 24 hours of hydration. This can be attributed to the filler effect of the fly ash and the limestone. It was found that for a water-to-binder ratio of 0.50, this filler effect is not related to the increase of the effective water-to-OPC ratio.

Up to 10 % of the fine OPC can be replaced by fine limestone powder without impairing the compressive strength. Replacing 5% of OPC with limestone powder gives rise to a strength increase of about 2% after

28 days. Using 5% fine limestone powder instead of 5% fine FA in a cement containing 35% FA resulted, on the other hand, in a considerable strength increase of 13% at 28 days, indicating a synergetic effect between limestone powder and fly ash.

The finenesses of the materials used for further research are based on the results obtained in paper II, keeping in mind production conditions at the cement plant. The OPC was ground to 450 m^2/kg which was the medium fineness tested. The fineness has to be high enough to obtain sufficient reactivity at early ages. On the other hand, the fineness is limited due to the cost associated with grinding. The limestone was ground to a fineness of 800 m^2/kg. In production limestone powder would be interground with the OPC. Limestone powder is a softer material than clinker and would therefore be concentrated in the finer fraction. In the current production process, fly ash is added in the air separator at the end of the mill in which the larger particles are returned to the inlet of the mill whereas the others pass. Therefore, only the larger particles of the fly ash are ground in this setup. During the first 15 to 20 minutes, the density of the fly ash increases after which it does not change considerably. This indicates that during this period the coarser and porous particles are crushed. Hence, it was opted to grind the fly ash only for 15 minutes to simulate the effect of adding fly ash at the end of the mill, even though fly ash turns more reactive upon progressive grinding.

Synergy between fly ash and limestone after 28 days (Paper III)

In the previous paper, a positive effect on the compressive strength was observed when replacing part of the fly ash with limestone powder in fly ash blended cement. The materials used in that study were, however, ground very fine, too fine from an industrial point of view. A new experimental matrix was set up using coarser OPC and fly ash. The results on mortar and paste after 28 days of curing at 20°C are presented in Paper III.

A similar synergetic effect between fly ash and limestone powder was observed as in Paper II, however, using coarser OPC and FA. Replacing 5% of fly ash with 5% of limestone powder in a 65% OPC + 35% FA cement resulted in a strength increase of about 10% (4 MPa). Additionally, in the same mix, 20% of fly ash can be replaced by 20% limestone powder without impairing the strength. The 65%OPC + 30% FA + 5% limestone blend had a slightly higher strength than the 70%OPC + 30% FA blend, showing that due to the synergetic effect between fly ash and limestone powder, 5% additional OPC can be replaced.

Limestone powder has a greater beneficial effect on the fly ash blended cement than on the OPC. The replacement of 5% OPC with only limestone powder resulted in a strength increase of about 4% (2 MPa). The greater effect when fly ash is included might be partly attributed to the chemical interaction between fly ash and limestone powder, as observed in Paper I. The additional aluminates provided by the fly ash, amplifying the effect of the limestone powder on the aluminate hydrates formed.

The replacement of 5% of fly ash or OPC with limestone powder did result in an enhanced compressive strength, and also in an increase in the amount of bound water and remarkably in a decrease in the calcium hydroxide content. The combination of an increase in bound water and a decrease in calcium hydroxide indicates a change in the nature of the hydration products formed.

Thermogravimetric tests pointed toward a change in hydration products when limestone powder was included in the system. This was confirmed by X-ray diffraction showing the formation of calcium carboaluminate hydrates in the presence of limestone powder. The effect appears to be more pronounced for the fly ash blended cements.

This change in the nature of the hydration products is suggested as an explanation for the observed increase in compressive strength.

Synergy between fly ash and limestone (Paper IV)

In Paper IV, the same experimental matrix as in Paper III was used, with the main goal of evaluating the synergistic effect over longer times. The experiments were performed with a new batch of OPC and FA, in the laboratories of EMPA, Dübendorf, instead of the SINTEF laboratories in Trondheim. The aim of Paper IV was to evaluate whether the interaction would last over time or not. The paste and mortar samples were cured for 1, 28, 90 and 180 days at 20°C.

In this study, replacing part of the OPC with limestone powder resulted in a strength decrease at all tested ages, whereas experiments in Paper II and III had shown that up to 10% of the OPC could be replaced by only limestone powder without impairing the compressive strength at 28 days. There is no satisfactory explanation for this except for possible aging and carbonation of the clinker.

The beneficial effect of limestone powder on fly ash blended cement was also reduced compared to the results from Paper III, as only about 5 to 10% of the fly ash could be replaced by limestone powder without impairing the strength, whereas in Paper III up to 25% could be replaced. Nevertheless, 5-10% of the fly ash can be replaced by limestone powder at all tested ages without impairing the compressive strength. The beneficial effect of the limestone, however, decreases with curing time, as expected since the slow fly ash reaction dominates over longer times.

From the results of Paper IV, it can be concluded that the synergistic effect between fly ash and limestone powder observed in Paper III remains over time (1-180 days), but becomes weaker at later ages.

Quantification of the degree of reaction of fly ash (Paper V)

In order to study the hydration of Portland composite cement containing fly ash, the degree of reaction of the fly ash should be quantified. In Paper V, different methods are compared.

The first method is based on selective dissolution. The idea is to dissolve the unreacted OPC and hydration products, leaving the unreacted fly ash undissolved. The residues after the selective dissolution were compared by mass and examined by SEM. Some of the tested methods tended to dissolve part of the unreacted fly ash, whereas others were not able to dissolve the hydration products or part of the unreacted OPC.

The second method tested monitored the dissolution of Al and Si from the fly ash which was highly diluted in a strong alkaline solution. Over time, products started to precipitate, indicating that this method does not function over longer time.

The third and final method was based on image analysis of BSE images taken from hydrated pastes. By combining different mathematical filters, the amount of unreacted fly ash was segmented from the images.

The third method resulted in the most consistent set of results and was therefore used in the subsequent articles.

Hydration mechanisms (Paper VI)

The synergetic effect between fly ash and limestone powder is most significant for small limestone replacement levels as observed from results obtained in Paper IV. To investigate this effect more

thoroughly four cement types were selected for further examination: 100% OPC, 95%OPC+5%L, 65%OPC+35%FA and 65%OPC+30%FA+5%L with FA = fly ash and L = limestone powder.

Limestone powder was replaced by crystalline quartz (considered inert) to eliminate the chemical effect. The presence of 5% limestone increases, relative to blends containing the same amount of quartz, the compressive strength and the amount of bound water. Additionally, the effect was more pronounced in the presence of fly ash.

Quantification of the unreacted clinker and fly ash indicated that the presence of limestone powder did not alter significantly the reactivity of either of them.

The effect of limestone powder on the hydration of OPC and OPC-FA appears to be due to its interaction with the hydration products formed. At 1 day, the hydrates formed are similar for all tested combinations: C-S-H, portlandite, ettringite. But after 1 day, when the reaction of the clinkers continues while the gypsum has been depleted, the kind and amount of AFm and AFt phases start to differ between the limestone containing and limestone–free OPC and OPC-FA blends. In the absence of limestone powder, ettringite decomposes to monosulphate. However, in the presence of calcium carbonate, the main constituent of limestone powder, the decomposition of ettringite to monosulphate is prevented as monosulphate is rendered unstable and instead calcium mono- and hemicarboaluminate hydrates are formed as observed experimentally and predicted by the thermodynamic modelling. The changes in AFm and AFt phases are reflected in the sulphur concentrations of the pore solution. The effect appears to be greater for the fly ash blended cement due to a lower SO_3/Al_2O_3 ratio. This on its turn is caused by replacing part of the OPC with fly ash, which as it reacts introduces additional aluminates to the system. As predicted by the thermodynamic modelling, the XRD patterns show a larger amount of AFm and AFt phases when fly ash is present. However, aluminates liberated by fly ash do not only go into AFm and AFt phases as part of it also is incorporated in the C-S-H gel as observed by EDX measurements.

The stabilisation of ettringite and the formation of carboaluminate hydrates, when limestone is present, lead to an increase in the volume of hydration products, as indicated by the increased chemical shrinkage. This on its turn leads to a decrease in porosity and thus to an increase in compressive strength. While a clear increase in strength was observed, the experimental determination of the porosity of the cement paste did not show a clear difference between the blends with and without limestone powder. This might be associated with the relatively large error of measurement or to the dehydration of ettringite during the sample preparation.

Alternative model (Paper VII)

The experimental results obtained in Paper IV and Paper VI are combined with a different kind of model. The model predicts the effect of gradual replacement of OPC or fly ash with limestone powder on the hydrate assemblage, and enables to calculate the impact of the variation of certain parameters.

The model shows that the presence of limestone powder results in the formation of hemi-and monocarboaluminate hydrate instead of monosulphate and hydrogarnet, thereby stabilizing the ettringite as also shown by the experiments in Paper III, IV and VI and the model in Paper VI. As limestone powder replaces the OPC or fly ash, monosulphate transforms to ettringite, resulting in an increase of the volume of the hydrates as monosulphate has a higher density than ettringite, 2.01 vs. 1.77 [39]. At the same time hemicarboaluminate is formed. Upon continued limestone powder addition, the hemicarboaluminate will transform to the more carbonate rich monocarboaluminate resulting in a decrease of the total volume of hydrates as the former has a slightly lower density than the latter, 1.98

vs. 2.17 g/cm^3 [39]. These two mechanisms result in a maximum solid volume predicted for limestone powder additions of 2-3% for the tested cements. Upon further replacement of OPC or fly ash with limestone powder, the total solid volume starts to decline again, as the additional limestone does no longer react and therefore acts as filler replacing the more reactive components, OPC and fly ash.

The model predicts a larger increase in total solid volume as more of the fly ash has reacted, and at the same time, the optimal limestone replacement increases. Varying the percentage of the calcium carbonate of the limestone powder reacted, showed that the optimal limestone replacement increases when less calcium carbonate has reacted.

The effect of curing temperature (Paper VIII)

Cement paste and mortar prepared with the four cement types studied in Paper VI together with one extra, 70%OPC+30%FA, were cured at 5˚C, 20˚C and 40˚C (with FA = fly ash and L = limestone powder).

After the first day of hydration, increasing of curing temperature accelerates significantly the OPC hydration and thus increases the compressive and flexural strength and the amount of bound water and Portlandite. After about 7 days of hydration, the compressive strength of OPC and OPC-L cements exhibit a crossover. The higher curing temperature, initially yielding higher strength, turns out to be detrimental from 7 days and onwards. After 90 days, the highest strength is obtained when curing at 5˚C and the lowest at 40˚C. This is related to differences in the microstructural development as a similar degree of hydration and similar hydrates (C-S-H, AFm, AFt) are observed for all curing temperatures. The higher curing temperature (40°C) causes faster dissolution and precipitation reactions which in turn give rise to a more inhomogeneous distribution of the hydration products, leading to reduced mechanical properties.

No temperature inversion effect is observed on the compressive strength of the composite cements containing fly ash. Fly ash reacts differently at elevated curing temperature than OPC. Its reaction is accelerated over a longer time span, not only during the first couple of days. During the first days of hydration, the replacement of part of the OPC by fly ash gives rise to a more homogenous distribution of the hydration products as the fly ash serves as precipitation sides for hydration products and leads to an increase in the effective water to OPC ratio. At later ages, the pozzolanic hydration products fill the remaining porosity and thereby improve the compressive strength. Curing at 40˚C leads to higher compressive strength of the fly ash containing cements compared to OPC and OPC-L cements, after 7 days, while for curing at 20˚C the same effect is observed only after 90 days. At 5˚C, the dissolution of the glass phase of the fly ash is slow and the fly ash containing mortars are not able to catch up with the compressive strength observed for the OPC and OPC-L blends within the first 90 days of hydration.

The beneficial effect of limestone powder on the compressive strength, attributed to its impact on the AFm and AFt phases, is observed at all curing temperatures for both OPC and the fly ash blended cements. However, over time the effect is reduced for fly ash containing mortars cured at high temperatures due to either greater importance of the fly ash content as it is more reactive at higher temperatures or due to a slightly reduced ettringite content observed by XRD at 40°C.

Chapter 6 – Concluding remarks

A preliminary study showed that fly ash and limestone powder interact in a cementitious system. More water was bound relative to the fly ash content in the presence of limestone powder and the hydration products formed were proven to contain calcium carboaluminate hydrate.

A study on the effect of the fineness of the different components (OPC, fly ash and limestone) showed that the OPC fineness is the major factor regarding hydration both at early and later age. However, after 28 days the fineness of the fly ash also plays an important role as fly ash is activated by grinding. Varying the fineness of the limestone powder within the tested range did not affect the hydration of the cement considerably.

A synergetic effect between fly ash and limestone powder was observed in four independent sets of experiments in which different combinations of fly ash and limestone powder replaced 35%of the OPC. A considerable strength increase ranging between 8-13% was observed after 28 days when 5% of the fly ash is replaced by 5% of limestone powder in a 65%OPC + 35% fly ash. The effect has been documented up to 180 days, but diminishes with time after 28 days as more of the fly ash reacts. The effect of limestone powder appears to be more beneficial for fly ash blended cement than for OPC. In the case of OPC, a 5% limestone powder replacement results after 28 days of curing at 20°C in a slight strength decrease or a minor increase up to 4%.

The effect of small limestone powder additions on the compressive strength can be due to both a physical effect known as the filler effect, and/or a chemical effect.

To study the filler effect, equivalent mixes were prepared using crystalline quartz powder (considered chemically inert) instead of limestone powder, with a similar particle size distribution. The presence of limestone powder containing cements had higher compressive strength than their equivalents prepared with quartz. This indicates that the enhanced compressive strength observed upon limestone powder addition is partly due to a chemical interaction.

The reactivity of the clinker phases and the fly ash was not significantly altered by the presence of limestone powder. It was decided to determine the reactivity of the fly ash by SEM-IA, after different methods had been compared. The unreacted OPC was quantified by both SEM-IA and XRD-Rietveld,

The main impact of limestone powder on the hydration of OPC and fly ash blended cements seem to be due to changes in the nature of the hydration products. In the absence of limestone powder, ettringite decomposes to monosulphate. However, in the presence of limestone powder, the decomposition of ettringite to monosulphate is prevented as monosulphate is rendered unstable and instead calcium mono- or hemicarboaluminate are formed. This mechanism is predicted by thermodynamic modelling and confirmed with experimental data (TGA, XRD, EDX and pore solution analysis). The effect is more pronounced for the fly ash blended cements as the additional aluminates originating form the fly ash lower SO_3/Al_2O_3 ratio and thereby increase the AFm/AFt ratio. However, it should be noted that part of the aluminates liberated by fly ash also are incorporated in the C-S-H.

The stabilisation of ettringite and the formation of hemi-and monocarbonate, when limestone is present, leads to an increase in the volume of hydration products, which might result in a decrease in porosity and a subsequent increase in compressive strength. The stabilization of the ettringite and the increase of

the compressive strength have been confirmed experimentally. However, the experimental determination of the porosity of the cement paste did not show a clear difference between the blends with and without limestone powder. This might be due to either the relatively large error associated with the measurements, or the dehydration of the ettringite during the preparation of the samples.

Varying the curing temperature affects the hydration of OPC and fly ash blended cements in different ways. In the case of OPC with or without limestone powder, increasing the curing temperature results in an accelerated hydration of the OPC, but results in a decreased final compressive strength, due to an inhomogeneous distribution of the hydration products. The fly ash blended cements, on the other hand, demonstrate an increase in the final compressive strength with increasing curing temperature, as the fly ash reaction is activated by the elevated temperature and is able to contribute more to the compressive strength. The beneficial effect of fly ash when curing at elevated temperatures is twofold: the filler effect of the fly ash leads to a more homogeneous distribution of the hydration products at the early ages, additionally the formation of pozzolanic hydration products reduces the porosity of the matrix at later ages.

Replacing 5% of the OPC or fly ash with limestone powder has a beneficial effect on the compressive strength at all tested curing temperatures (5, 20 and 40°C). However, from 28 days on the effect is cancelled out for the fly ash blended cements cured at 40°C due to the activation of fly ash by the elevated temperature, rendering the fly ash content more important than the synergetic effect between fly ash and limestone powder.

Chapter 7 – Future research

Porosity measurements

There is one missing link in the thesis. The increase in compressive strength observed when 5% of OPC or fly ash is replaced by 5% limestone powder has been attributed to the stabilization of ettringite by limestone powder. This would increase the total volume of hydration products, which on its turn would reduce the porosity and cause an increase of the compressive strength. All of the steps of this reasoning have been confirmed except the porosity reduction. The problem is that ettringite ($3CaO{\cdot}Al_2O_3{\cdot}3CaSO_4{\cdot}32H_2O$) is a very water rich hydration product. Many techniques used to measure porosity require drying of the sample prior to analysis. In that case ettringite will loose most of its bound water and the pore filling effect of ettringite will be destroyed. Additionally, the effect of limestone powder on the porosity is relatively small and might therefore be within the error of many techniques.

One possible way to resolve this missing link could be the use of low temperature calorimetry which is a technique applied to compare the pore structure of different *saturated* samples (not dried) [47]. Unfortunately, only a few of these working instruments can be found in Europe.

Determining the reactivity of the limestone powder

The calcium carbonate content of a hydrated cement paste can be determined by X-ray diffraction (XRD) combined with Rietveld analysis, or by thermogravimetric analysis (TGA).

With XRD-Rietveld, the crystalline calcium carbonate content is determined. The problem is that only a couple percent of calcium carbonate relative to the total dry weight will react. In the case of XRD-Rietveld, the consumption of the calcium carbonate is not much larger than the error of measurement.

Using TGA, the calcium carbonate content is calculated from the weight loss in a temperature interval above 600°C where the carbonates decompose and CO_2 is emitted from the sample. In this case the problem is that the calcium carbonate bound in hydration products decomposes at slightly lower temperature interval than the unreacted calcium carbonate, but their intervals overlap.

A solution might be to deconvolute the DTG graphs in the area where the carbonates decompose or to find another technique.

Optimizing the gypsum content

Another point of interest is the optimal gypsum content of the Portland composite cement containing fly ash and limestone powder. Sulphates are added to the clinker mainly to regulate the setting, but their presence also influences the strength and the volumetric stability. In the presence of limestone, there will be the competition between carbonate and sulphate for the reaction with the aluminate. Limestone powder might therefore reduce the optimal gypsum content [48, 49], but how will the additional aluminates provided by the fly ash affect that?

Durability of the ternary composite cement

Limestone powder can enhance the sulphate resistance [50]. Fly ash on the other hand can reduce the chloride ingress and improve the resistance against alkali-silica reaction [20].

Over time thaumasite ($Ca_3Si(OH)_6(SO_4)(CO_3)\cdot 12H_2O$) may form in limestone containing cements when cured at lower temperatures (5-10°C) in humid conditions [39]. This can have a detrimental effect on the binding capacity of the cement paste. It should be noted that, no thaumasite was observed after ½ year of curing at 5°C submerged in saturated calcium hydroxide solution.

Hence, the study of the durability of concrete prepared with Portland composite cement containing both limestone powder and fly ash will be both complex and interesting.

References

[1] Cement industry energy and CO_2 performance - Getting the numbers right, in: World Business Council for Sustainable Development - The Cement Sustainability Initiative, 2009.
[2] E. Gartner, Industrially interesting approaches to "low-CO2" cements, Cement and Concrete Research, 34 (2004) 1489-1498.
[3] P. Purnell, L. Black, Embodied carbon of structural materials: the importance of the functional unit., in: L.M. Grover, M.P. Hofmann, H. Rossetto, A.M. Smith (Eds.) 30th Cement and Concrete Science Conference, Birmingham, 2010, pp. 141-144.
[4] J.S. Damtoft, J. Lukasik, D. Herfort, D. Sorrentino, E.M. Gartner, Sustainable development and climate change initiatives, Cement and Concrete Research, 38 (2008) 115-127.
[5] P.K. Mehta, Global concrete industry sustainability, Concrete International, 31 (2009) 45-48.
[6] F.W. Locher, Cement principles of production and use, Verlag Bau+Technik GmbH, Düsseldorf, 2005.
[7] Initiative progress report, in: World Business Council for Sustainable Development - The Cement Sustainability, 2005.
[8] R. Bertrandy, P. Poitevin, Limestone filler in concrete, French research in practice, in: R.N. Swamy (Ed.) Blended Cements in Construction, Elsevier, London, 1991, pp. 16-31.
[9] C. Müller, Cluster 2: Blended cements, European Construction in Service and Society (ECO-Serve), in: ECO-serve seminar - Challenge for sustainable construction; the concrete approach, Warszawa, Poland, 2006.
[10] R.S. Barneyback Jr, S. Diamond, Expression and analysis of pore fluids from hardened cement pastes and mortars, Cement and Concrete Research, 11 (1981) 279-285.
[11] G. Le Saout, T. Füllmann, V. Kocaba, K. Scrivener, Quantitative study of cementitous materials by X-ray diffraction/Rietveld analysis using an external standard, in: 12th International Congress on the Chemistry of Cement Montréal, Canada, 2007.
[12] R.L. Snyder, D.L. Bish, Quantitative analysis, in: D.L. Bish, J.E. Post (Eds.) Modern powder diffraction - Reviews in mineralogy 20, Mineralogical Society of America, 1989, pp. 101-144.
[13] D. Kulik, GEMS 2 software, in: http://gems.web.psi.ch/, PSI, Villingen, Switzerland, 2010.
[14] T. Thoenen, D. Kulik, Nagra/PSI chemical thermodynamic database 01/01 for GEMS-selektor (V.2-PSI) geochemical modeling code, in: http://gems.web.psi.ch/doc/pdf/TM-44-03-04-web.pdf, PSI, Villingen, 2003.
[15] W. Hummel, U. Berner, E. Curti, F.J. Pearson, T. Thoenen, Nagra/PSI chemical thermodynamic data base 01/01, in, Universal Publishers/uPUBLISH.com, USA also published as Nagra Tehcnical Report NTB 02-16, Wettingen, Switzerland
2002.
[16] B. Lothenbach, F. Winnefeld, Thermodynamic modelling of the hydration of Portland cement, Cement and Concrete Research, 36 (2006) 209-226.
[17] T. Matschei, B. Lothenbach, F.P. Glasser, Thermodynamic properties of Portland cement hydrates in the system CaO-Al_2O_3-SiO_2-$CaSO_4$-$CaCO_3$-H_2O, Cement and Concrete Research, 37 (2007) 1379-1410.
[18] B. Lothenbach, T. Matschei, G. Möschner, F.P. Glasser, Thermodynamic modelling of the effect of temperature on the hydration and porosity of Portland cement, Cement and Concrete Research, 38 (2008) 1-18.
[19] W. Kurdowski, Cement manufacture, in: J. Bensted, P. Barnes (Eds.) Structure and Performance of Cements, Spon Press, London, 2002, pp. 1-23.

[20] V.M. Malhotra, P.K. Mehta, High-Performance, High-Volume Fly-Ash Concrete: Materials, Mixture Proportioning, Properties, Construction practice and Case Histories, Supplementary Cementing Materials for Sustainable Development Inc., Ottawa, 2002.
[21] I. Soroka, N. Stern, Calcareous fillers and the compressive strength of portland cement, Cement and Concrete Research, 6 (1976) 367-376.
[22] Sjøvannets uheldige virkninger på betong, in: Aftenposten, Oslo, 27 June 1947, pp. 6.
[23] Kalcitt- og aktivittblanding i betong, in: Aftenposten, Oslo, 4 November 1952, pp. 9.
[24] Aktivitt-betong står hvor alminnelig betong snart går til grunne, in: Aftenposten, Oslo, 22 November 1955, pp. 2.
[25] Aktivittsak for å få Daniels' patent kjent delvis ugyldig, in: Aftenposter, Oslo, 21 June 1957, pp. 13.
[26] Ingeniør Arne Daniels 80 år, in: Aftenposten, Oslo, 30 May 1964, pp. 10.
[27] A.P. Barker, H.P. Cory, The early hydration of limestone-filled cement, in: R.N. Swamy (Ed.) Blended Cements in Construction, Elsevier, London, 1991, pp. 107-124.
[28] K.O. Kjellsen, B. Lagerblad, Influence of natural minerals in the filler fraction on hydration and properties of mortars, in: CBI report, Stockholm, 1995, pp. 41.
[29] J. Péra, S. Husson, B. Guilhot, Influence of finely ground limestone on cement hydration, Cement and Concrete Composites, 21 (1999) 99-105.
[30] G. Kakali, S. Tsivilis, E. Aggeli, M. Bati, Hydration products of C_3A, C_3S and Portland cement in the presence of $CaCO_3$, Cement and Concrete Research, 30 (2000) 1073-1077.
[31] V. Rahhal, R. Talero, Early hydration of portland cement with crystalline mineral additions, Cement and Concrete Research, 35 (2005) 1285-1291.
[32] T. Sato, J.J. Beaudoin, The effect of nano-sized $CaCO_3$ addition on the hydration of cement paste containing high volumes of fly ash, in: 12th ICCC, Montreal, 2007, pp. 1-12.
[33] D.P. Bentz, Modeling the influence of limestone filler on cement hydration using CEMHYD3D, Cement and Concrete Composites, 28 (2006) 124-129.
[34] H.J. Kuzel, H. Pöllmann, Hydration of C_3A in the presence of $Ca(OH)_2$, $CaSO_4 \cdot 2H_2O$ and $CaCO_3$, Cement and Concrete Research, 21 (1991) 885-895.
[35] V.L. Bonavetti, V.F. Rahhal, E.F. Irassar, Studies on the carboaluminate formation in limestone filler-blended cements, Cement and Concrete Research, 31 (2001) 853-859.
[36] T. Matschei, B. Lothenbach, F.P. Glasser, The role of calcium carbonate in cement hydration, Cement and Concrete Research, 37 (2007) 551-558.
[37] T. Matschei, B. Lothenbach, F.P. Glasser, The AFm phase in Portland cement, Cement and Concrete Research, 37 (2007) 118-130.
[38] B. Lothenbach, G. Le Saout, E. Gallucci, K. Scrivener, Influence of limestone on the hydration of Portland cements, Cement and Concrete Research, 38 (2008) 848-860.
[39] H.F.W. Taylor, Cement chemistry 2nd edition, Thomas Telford, London, 1997.
[40] I. Elkhadiri, A. Diouri, A. Boukhari, J. Aride, F. Puertas, Mechanical behaviour of various mortars made by combined fly ash and limestone in Moroccan Portland cement, Cement and Concrete Research, 32 (2002) 1597-1603.
[41] I. Elkhadiri, A. Diouri, A. Boukhari, Y. Benarchid, Morrocan composite cement with minor addition of fly ash, Journal of Materials Science, 40 (2005) 6195-6199.
[42] B. Yilmaz, A. Olgun, Studies on cement and mortar containing low-calcium fly ash, limestone, and dolomitic limestone, Cement and Concrete Composites, 30 (2008) 194-201.
[43] G. Menéndez, V. Bonavetti, E.F. Irassar, Strength development of ternary blended cement with limestone filler and blast-furnace slag, Cement and Concrete Composites, 25 (2003) 61-67.
[44] M.F. Carrasco, G. Menéndez, V. Bonavetti, E.F. Irassar, Strength optimization of "tailor-made cement" with limestone filler and blast furnace slag, Cement and Concrete Research, 35 (2005) 1324-1331.

[45] S. Hoshino, K. Yamada, H. Hirao, XRD/Rietveld analysis of the hydration and strength development of slag and limestone blended cement, Journal of Advanced Concrete Technology, 4 (2006) 357-367.
[46] M. Ghrici, S. Kenai, M. Said-Mansour, Mechanical properties and durability of mortar and concrete containing natural pozzolana and limestone blended cements, Cement and Concrete Composites, 29 (2007) 542-549.
[47] E.J. Sellevold, D.H. Bager, Low temperature calorimetry as a pore structure probe, in: 7th ICCC, Paris, 1980, pp. 395-399.
[48] A. Negro, G. Abbiati, Sur l'emploi du calcaire comme regulateur de prise du ciment, in: 8th ICCC, Rio de Janeiro, 1986, pp. 109-113.
[49] H. Hirao, K. Yamada, S. Hoshino, H. Yamashita, The effect of limestone addition on the optimum sulphate levels of cements having various Al_2O_3 contents, in: 12^{th} ICCC, Montreal, 2007.
[50] T. Schmidt, B. Lothenbach, M. Romer, J. Neuenschwander, K. Scrivener, Physical and microstructural aspects of sulfate attack on ordinary and limestone blended Portland cements, Cement and Concrete Research, 39 (2009) 1111-1121.

Paper I

Microstructure of binder from the pozzolanic reaction between lime and siliceous fly ash, and the effect of limestone addition.

De Weerdt K. & Justnes H.

Proceedings of the First International Conference on Microstructure Related Durability of Cementitious Composites, Ed. W. Sun, K. Van Breugel, C. Miao, G. Ye and H. Chen, 2008, Nanjing, RILEM PRO 61, Vol. 1 pp.107-116 (ISBN 978-2-35158-065-3, e-ISBN 978-2-35158-084-4).

MICROSTRUCTURE OF BINDER FROM THE POZZOLANIC REACTION BETWEEN LIME AND SILICEOUS FLY ASH, AND THE EFFECT OF LIMESTONE ADDITION

Klaartje De Weerdt [(1)], Harald Justnes [(1)]

(1) SINTEF Building and Infrastructure, Trondheim, Norway

Abstract

Currently, blended cements (CEM II) are the most commonly used cements in Europe. Most blended cements are binary, composed of clinker and one supplementary cementitious material (SCM). The clinker replacement level in blended cements may be increased by combining different SCM's. In this paper a preliminary study on the combination of fly ash (FA) and limestone and their interaction was conducted.

Cement-free pastes composed of lime/FA and lime/FA/limestone, respectively, were compared. Clinker was excluded to simplify the system. In stead an excess of calcium hydroxide ($Ca(OH)_2$) and alkaline mixing water (i.e. pH 13.2 and K/Na = 2:1) was used to simulate the conditions in a hydrating cement paste.

The mixes were cured at 5, 20, 38 and 80°C, and the reactions were stopped after 1, 3, 7, 28 and 88 days of curing. The microstructure of the hardened binder was investigated by thermogravimetry (TG), X-ray-diffraction (XRD) and scanning electron microscopy (SEM).

The addition of limestone resulted in a slight increase in the amount of chemically bound water relative to the amount of FA. FA also appeared to bind more water than what was provided by calcium hydroxide. The XRD patterns confirmed an interaction between the limestone and the FA, which resulted in the formation of calcium carboaluminate hydrates. At higher temperatures (80°C) the calcium carboaluminate phase appeared to be unstable and other hydration phases (e.g. hydrogarnet type phases) were observed.

1. INTRODUCTION

Nowadays blended cements are most often binary, containing only one supplementary cementitious material (SCM). Due to the rising environmental awareness and diminishing natural resources, there is a growing interest in all-round composite cements in which larger parts of the clinker are replaced by SCMs. At high replacement levels, the early strength development becomes an issue. A possible way to improve early hydration could be to replace

Corresponding author's e-mail: Klaartje.De.Weerdt@sintef.no
Corresponding author's fax: +47 735 97 136

the clinker with a combination of different materials, resulting in ternary and even quarternary systems. Some cement producers have added silica fume to cement containing larger amounts of fly ash or slag [1], in order to improve the early strength development. These cement types are far from common. As silica fume is becoming increasingly scarce, it might be interesting to look into more available products. One possible option can be finely ground limestone. The extra surface supplied by the small limestone particles provides extra nucleation sides for hydration products of the clinker and therefore accelerates its hydration. This effect is referred to as the filler effect.

When developing ternary cements, the chemical interaction between the different components is of great importance, in particular if it would lead to a denser binder. Besides the thorough studies of Bülent Yilmaz and Asim Olgun [2], and Taijiro Sato and James. J. Beaudoin [3] very little is published on ternary blends containing both limestone and fly ash. The few other studies only focus on the physical properties such as strength and heat development and omit the chemical interactions [4],[5]. This study on the chemical interactions will lead to a better understanding of the system, and will be of importance during the optimization of such ternary cements.

Fly ash is a pozzolan, when added to cement and water, it will react with the calcium hydroxide produced during clinker hydration. Reaction products such as calcium silicate hydrate (C-S-H), strätlingite and hydrogarnets may form.

The carbonate from the limestone, on the other hand, can react with the aluminate phase of the clinker. Due to the relatively low amounts of aluminate in clinker (5%), these interactions have been neglected by many researchers in the past, and limestone powder was often considered as inert.

There is generally a higher amount of aluminates in the fly ash, around 20%, than in clinker. This could render the interaction between the carbonates and the aluminates more important, in a blended cement containing fly ash.

In this paper pastes of calcium hydroxide (CH), siliceous fly ash (FA) and with/without limestone were prepared. Calcium hydroxide was in excess relative to the assumed pozzolanic reaction and alkaline water was used to simulate the conditions in cement paste. The reaction products and microstructure were analyzed with thermal analysis (TGA/SDTA), X-ray diffraction (XRD) and scanning electron microscopy (SEM).

2. MATERIALS

A commercial siliceous fly ash (FA) was provided by the Norwegian cement producer, Norcem. The FA composition determined by X-ray fluorescence analysis is shown in Table 1.

Table 1 : XRF results of the siliceous fly ash (FA) in %.

Oxide	Fe_2O_3	TiO_2	CaO	K_2O	P_2O_5	SiO_2	Al_2O_3	MgO	Na_2O	MnO	LOI
FA	6.66	1.28	6.31	1.82	0.91	53.83	23.45	1.82	0.62	0.1	4.96

The natural limestone filler was delivered by Franzefoss, Norway.

The pastes were prepared with alkaline water. The water had a K_2O/Na_2O ratio of 2:1 and a pH of 13.2, to simulate the water phase in a typical cement paste.

Corresponding author's e-mail: Klaartje.De.Weerdt@sintef.no
Corresponding author's fax: +47 735 97 136

3. EXPERIMENTAL

Two different pastes were prepared with recipes as given in Table 2.

Table 2 : Composition of the different blends (mass in g).

Notation	FA/L	FA
Fly ash	90	100
Limestone	10	-
$Ca(OH)_2$	100	100
Water	127	129

5g cerium oxide (CeO_2) was added to each blend in order to be able to quantify phases by XRD. Cerium oxide functions as a reference as it is inert in these high alkaline systems. The pastes were prepared in beakers and stirred by hand. The alkaline water was added until a castable mix was obtained. Several samples were taken of each blend. They were sealed in small glass vials with lids and stored in 5, 20, 38 and 80ºC rooms. After 0, 1, 3, 7, 28 and 88 days the reaction was stopped, as the samples were crushed fine and immersed in an excess of ethanol. Some larger fragments were kept separate in small glasses filled with ethanol. The ethanol was filtrated from the fine crushed samples, which were then dried at 105ºC for about 24 hours. The dried samples were then stored in glass vials with lids.

Simultaneous TGA/SDTA analyses were performed with a Mettler Toledo TGA/SDTA 851. Samples of about 300 mg were weighed into aluminium oxide crucibles. The tests were carried out with a heating rate of 10ºC/min going from 30ºC to 1,100ºC, while the samples were purged with N_2. The samples cured for 88 days at 20ºC and 80ºC were analysed by an AXS D8 focus X-ray diffractometer. The dry powders were submitted to an angular scan between 5 and 70º 2θ with a step size of 0.02º and a step time of 23.8 s. An AXS D8 focus and CuKα radiation was used. The larger fragments of samples cured for 88 days at 38ºC and 80ºC were investigated by a JEOL JXA-8500F Electron Probe Micro analyzer (EPMA), in order to detect certain hydrates. Interesting phases were analysed by an energy dispersive X-ray spectrometer (EDS).

4. RESULTS

4.1 Thermogravimetry

Fig. 1 and Fig. 2 show the results of the thermogravimetric (TG) analysis. The graphs on the left in both figures depict the weight loss due to the dehydration of reaction products such as calcium silicate hydrates (C-S-H), calcium aluminate hydrates (C-A-H) and calcium aluminosilicate hydrates (C-A-S-H). These reactions mainly take place in the temperature interval ranging from 105ºC up to the dehydration temperature of the reactant calcium hydroxide (about 450ºC). This last temperature is determined by the onset on the dehydration reaction which is clearly visible in the first derivative of the TG curve (DTG).

The graphs on the right of both Fig. 1 and Fig. 2 show how the weight loss due to dehydration of calcium hydroxide (CH) which is reduced with time due to consumption by the pozzolanic reaction. The temperature range for this reaction is determined for each sample

Corresponding author's e-mail: Klaartje.De.Weerdt@sintef.no
Corresponding author's fax: +47 735 97 136

from the DTG-curve in which this reaction results in a clear peak. The start and end temperatures vary around 400ºC and 550ºC, respectively.

The weight losses are expressed as a percentage of the amount of fly ash in the sample.

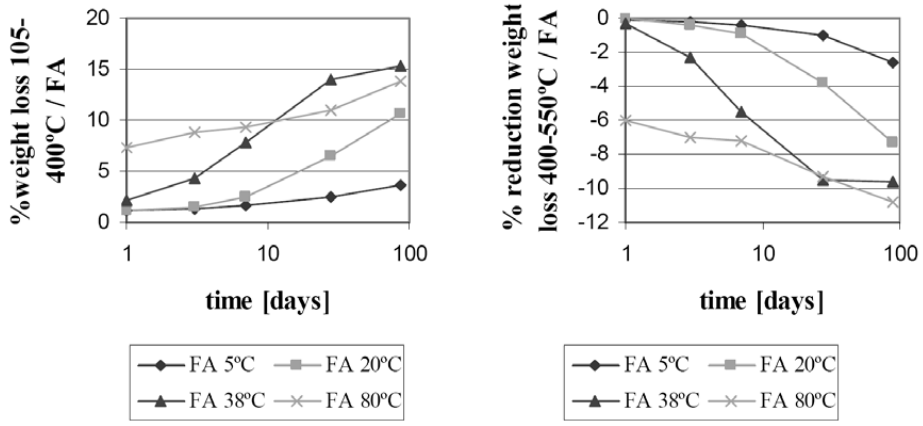

Fig. 1 : TGA results for the FA-blend. Left : weight loss due to dehydration of hydrates between 105ºC and about 400ºC. Right : reduction in the weight loss due to dehydration of calcium hydroxide between about 400ºC and 550ºC.

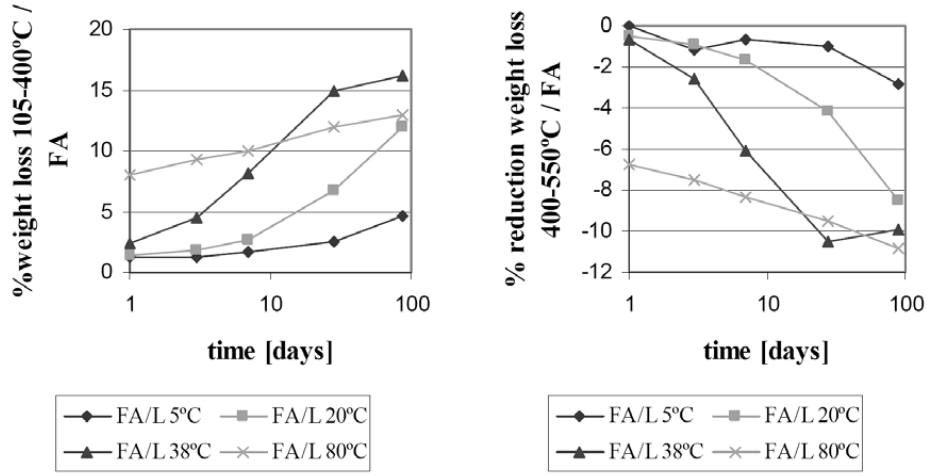

Fig. 2 : TGA results for the FA/L blend. Left : weight loss due to dehydration of hydrates between 105ºC and about 400ºC. Right : reduction in the weight loss due to dehydration of calcium hydroxide between about 400ºC and 550ºC.

In case of the samples cured at lower temperature, 5ºC, 20ºC and 38ºC, there is initially no great difference between both blends, FA and FA/L, as seen from Fig. 1 and Fig. 2 at early ages. But at later age, 28 and 88 days, the limestone containing samples seem to be able to bind slightly more water. This might be due to the formation of calcium carboaluminates.

Corresponding author's e-mail: Klaartje.De.Weerdt@sintef.no
Corresponding author's fax: +47 735 97 136

The samples cured at higher temperature are much more reactive in the beginning, but at longer curing times the amount of hydration products is lower than at lower curing temperatures (5ºC and 20ºC).

When comparing the left and right graph in Fig. 1and Fig. 2 it is clear that the reduction in the amount of calcium hydroxide is related to the amount of hydration products formed. This confirms the consumption of calcium hydroxide during the pozzolanic reaction of FA. The lower reduced mass loss of CH (solid water consumption) compared to the mass loss of hydration products, indicates that the pozzolanic reactions consumes liquid water in addition to what is inherent in CH. This is confirmed by showing that the increase in total mass loss of the dried paste increases as a function of time (relative to day 1) in Fig. 3.

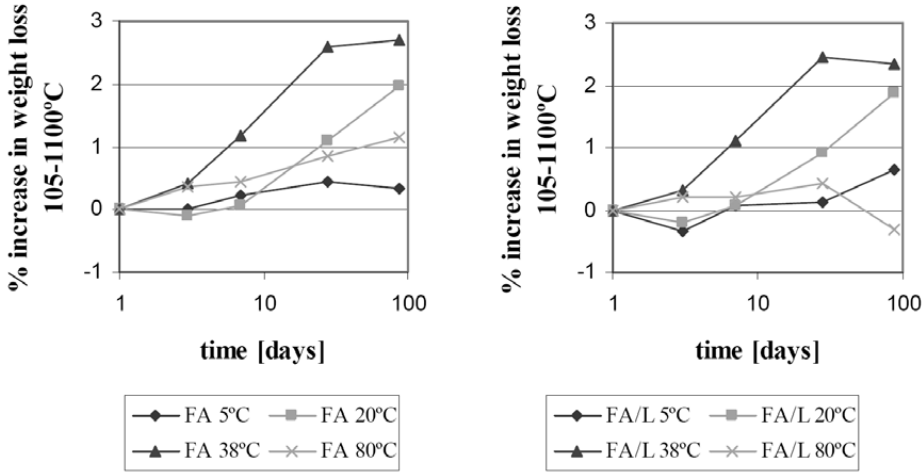

Fig. 3 : Increase in weight loss between 105ºC and 1100ºC relative to the weight loss at day 1. The graph at the left depicts the results for the FA samples cured at different temperatures, and in the graph at the right shows the results for the FA/L samples.

In Fig. 4, the first derivatives of the TG curves (DTG-curves) are depicted for FA- and FA/L-pastes cured at both 38ºC and 80ºC for 88 days. The weight losses in the temperature range 105ºC to about 400ºC are caused by the dehydration of phases such as calcium silicate hydrates (C-S-H), calcium aluminate hydrates (C-A-H) and calcium aluminosilicate hydrates (C-A-S-H), as mentioned before. The large peak at about 500ºC is related to the dehydration of CH. At higher temperatures weight losses are caused by decarbonation of carbonated phases or limestone.

Corresponding author's e-mail: Klaartje.De.Weerdt@sintef.no
Corresponding author's fax: +47 735 97 136

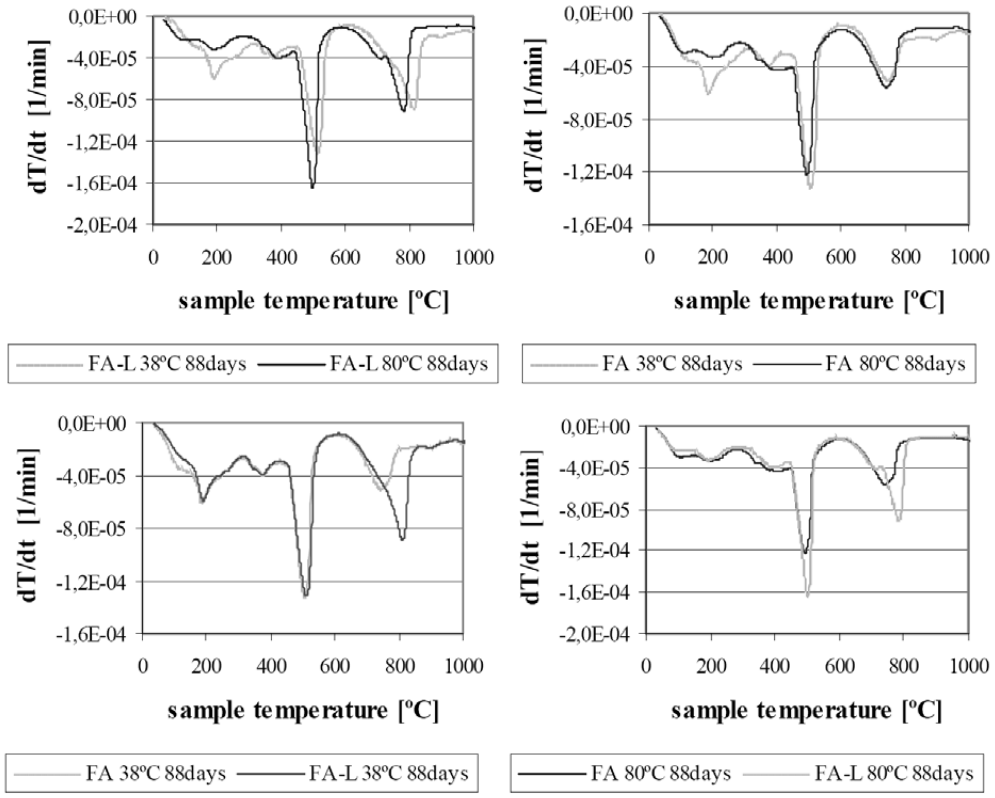

Fig. 4 : The first derivative of the TGA curves for FA- and FA/L-blends cured for 88 days at both 38ºC and 80ºC.

Changes in curing temperature result in clear changes in the DTG-graphs. The samples cured at 38ºC, both with and without limestone, exhibit a pronounced weight loss peak at about 190ºC. This peak is considerably smaller in the samples cured at 80ºC. According to Bushnell-Watson and Sharp [6], this peak is due to the dehydration of both C_2AH_8 and $C_4A\bar{C}H_{11}$. As the peaks of both phases overlap, one peak with a shoulder at lower temperature is formed.

The graphs for the pastes cured at 80ºC with and without limestone do not exert any large differences, except for the decarbonation peak of the limestone at about 800ºC in the limestone containing sample.

The fact that the peak around 190ºC disappears when the samples are cured at 80ºC instead of 38ºC, indicates that the particular phases, C_2AH_8 and $C_4A\bar{C}H_{11}$, are not stable at the higher temperatures such as 80ºC, which is in agreement with Fentiman [7] stating that these phases become unstable at 45ºC and 60ºC respectively.

Corresponding author's e-mail: Klaartje.De.Weerdt@sintef.no
Corresponding author's fax: +47 735 97 136

4.2 XRD

Fig. 5 and Fig. 6 depict the X-ray diffraction patterns of both the FA- and FA/L-pastes cured at both 20ºC and 80ºC. They clearly confirm the results of the thermal analysis.

In the samples cured at 20ºC calcium carboaluminate hydrate ($C_4A\bar{C}H_{11}$) has formed. The diffraction pattern of the sample containing limestone shows a larger and more defined diffraction peak at d ≈ 7.57 Å than for the sample without limestone.

The diffraction patterns of the samples cured at 80ºC, on the other hand, show no sign of the calcium carboaluminate phase. Instead a silicon-containing hydrogarnet phase (C_3ASH_4) has formed. Both the samples cured at 80ºC with and without limestone have very similar X-ray diffraction patterns (with exception of the $CaCO_3$), just like they had similar DTG curves.

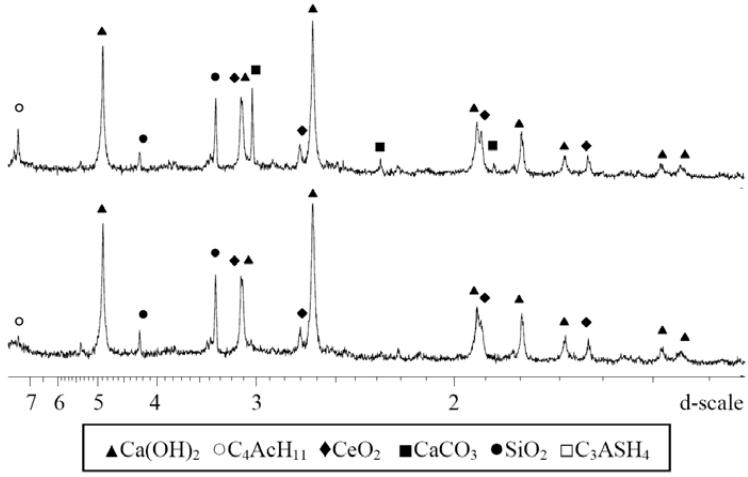

Fig. 5 : X-ray diffraction pattern of FA/L (upper) and FA (lower) pastes cured at 20ºC for 88 days.

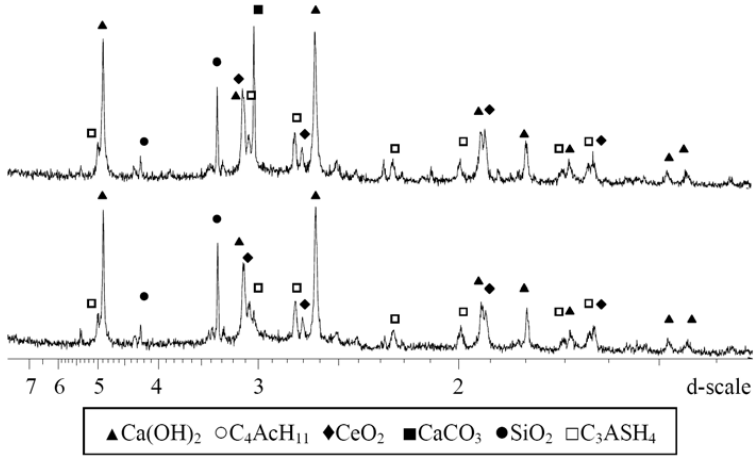

Fig. 6 : X-ray diffraction pattern of FA/L (upper) and FA (lower) pastes cured at 80ºC for 88 days.

Corresponding author's e-mail: Klaartje.De.Weerdt@sintef.no
Corresponding author's fax: +47 735 97 136

4.3 Microstructure

Samples of both FA- and FA/L-pastes cured at 20ºC and 80ºC for 88 days were analyzed by SEM equipped with energy dispersive X-ray spectrometer (EDS).

In the samples cured at 20ºC both with and without limestone, crystalline calcium aluminate hydrates were found (Fig. 7 and Fig. 8). Whether or not the hydration phases contain carbonates can not be determined by semi-quantitative EDS analysis. The EDS analyses however showed an atomic Ca/Al ratio of 1.4 to 1.5. This would comply with the presence of hydration phase of the hydrogarnet type. But no such phase was observed in the XRD diffraction patterns as the main peaks of both C_3ASH_4 and C_3AH_6, respectively at 2.74 and 3.26 Å, were absent. Calcium carboaluminate hydrate ($C_4A\bar{C}H_{11}$) and the calcium aluminate hydrate (C_2AH_8) would on the other hand result in an atomic Ca/Al ratios of 2 and 1, respectively, but this was not found by SEM/EDS. It is worth mentioning that these phases can not be distinguished visually as they both form hexagonal plate-like crystals [8],[9],[10].

Besides crystalline aluminate hydrates, also CSH-like hydration phases were found in the samples cured at 20ºC.

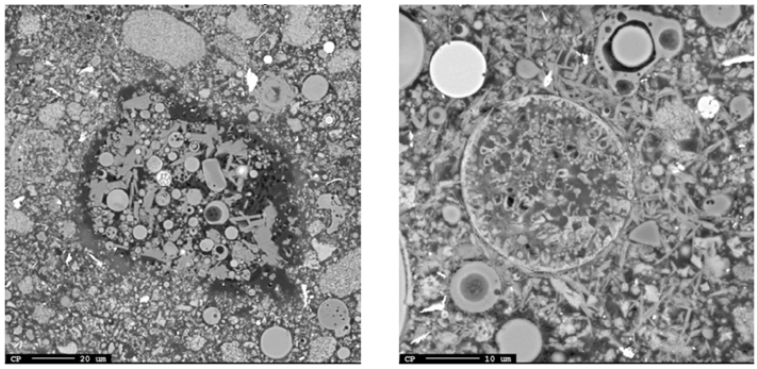

Fig. 7 : SEM image of the FA/L-blend cured at 20ºC for 88 days. Left: Plerosphere in which hydration products with atomic ratio Ca/Al =1.5 have formed. Right: Large fly ash particle surrounded by smaller particles and hydration products with atomic ratio Ca/Al = 1.4.

Corresponding author's e-mail: Klaartje.De.Weerdt@sintef.no
Corresponding author's fax: +47 735 97 136

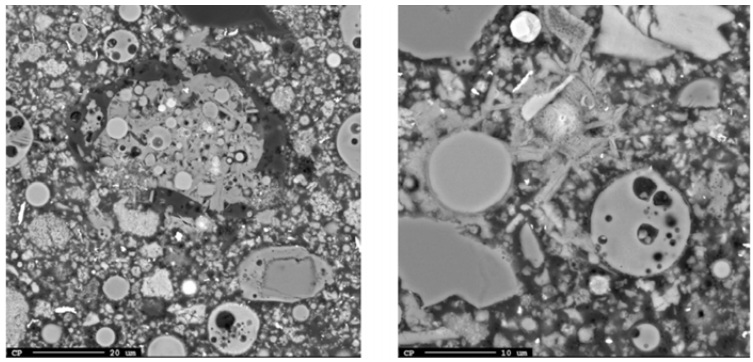

Fig. 8 : SEM image of the FA-blend cured at 20ºC for 88 days. Left: Plerosphere in which crystalline hydration products with atomic ratio Ca/Al = 1.4 have formed. Right: Mark of ion beam in hydration products with atomic ratio Ca/Al = 1.4.

In the samples cured at 80ºC no calcium aluminate hydrates were found by SEM/EDS. Instead calcium aluminosilicate hydrate was detected as bright phases in Fig. 9, while the darker phase is calcium silicate hydrate.

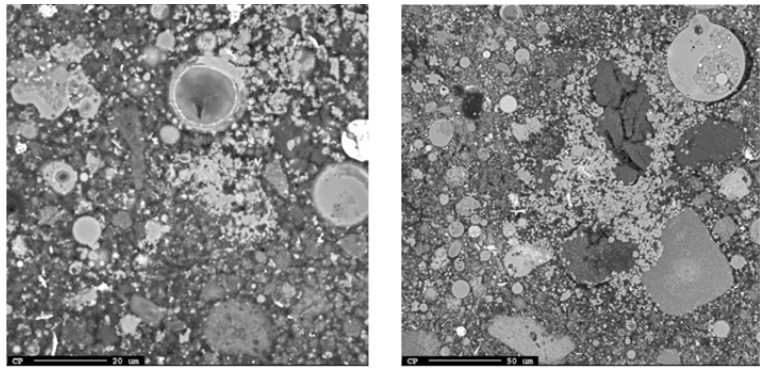

Fig. 9 : SEM image of the FA-blend cured at 80ºC for 88 days. Both images show bright (calcium aluminosilicate hydrate) and dark hydration phases (calcium silicate hydrate).

5. CONCLUSIONS

- The addition of limestone powder to the alkaline FA-CH blend resulted in a slight increase of chemically bound water relative to the amount of FA.
- Higher curing temperatures (38ºC and 80ºC) initially accelerate the pozzolanic reaction of fly ash. But at later age these higher curing temperatures seem to give rise to decrease in the amount of chemically bound water compare to lower curing temperatures.
- During the pozzolanic reaction of FA with CH more water was bound than the water inherent in CH. This effect is most pronounced at 20ºC and 38ºC.

Corresponding author's e-mail: Klaartje.De.Weerdt@sintef.no
Corresponding author's fax: +47 735 97 136

– XRD analysis confirmed the presence of calcium carboaluminate hydrate ($C_4A\bar{C}H_{11}$) in both FA and FA/L blends cured for 28 days at 38ºC. The minor presence in the former may be explained by carbonation. In the samples cured at 80ºC for 28 days calcium carboaluminates appeared to be unstable and instead a hydrogarnet phase had formed (C_3ASH_4).

ACKNOWLEDGEMENTS

The authors wish to acknowledge COIN (Concrete Innovation Centre, www.sintef.no/coin) with all its partners: the Research Council of Norway, SINTEF, NTNU, Norcem, Unicon, maxit Group, Borregaard, Spenncon, Rescon Mapei, The Norwegian Public Roads Administration, Veidekke, Skanska and Aker Solutions, for their support.

REFERENCES

[1] Thomas, M., Hopkins, D.S., Perreault, M. and Cail, K. 'Ternary cement in Canada', *Concrete International* **29**(7) (2007) 59-64.

[2] Yilmaz, B. and Olgun, A. 'Studies on cement and mortar containing low-calcium fly ash, limestone, and dolomitic limestone' *Cem. Concr. Comp*. **30**(3) (2008)194-201.

[3] Sato, T. and Beaudoin, J.J. 'The effect of nano-sized $CaCO_3$ addition on the hydration of cement paste containing high volumes of fly ash', *Proceeding of the 12th International Conference on the Chemistry of Cement*, Montreal, 2007.

[4] Elkhadir, I., Diouri, A., Boukhari, A., Aride, J. and Puertas, F. 'Mechanical behaviour of various mortars made by combined fly ash and limestone in Moroccan Portland cement', *Cem. Concr. Res*. **32**(10)(2002) 1597-1603.

[5] Härdtl, R., Dietermann, M. and Schmidt, K. 'Durability of blended cements with several main components', *Proceeding of the 12th International Conference on the Chemistry of Cement.* Montreal, 2007.

[6] Bushnell-Watson, S.M. and Sharp, J.H. 'The Detection of the carboaluminate phase in hydrated high alumina cements by differential thermal analysis', *Thermochim. Acta*, **93**(1985) 613-616.

[7] Fentiman, C.H. 'Hydration of carbo-aluminous cement at different temperatures', *Cem. Concr. Res.* **15**(4) (1985) 622-630.

[8] Ingram, K.D. and Daugherty, K.E. 'A review of limestone additions to Portland cement and concrete', *Cem. Concr. Comp.* **13**(3) (1991)165-170.

[9] Jambor, J. 'Influence of $3CaO.Al_2O_3.CaCO_3.nH_2O$ on the structure of cement paste', In: *Proceeding of the 7th International Conference on the Chemistry of Cement.* Paris: Editions Septima, 1980, Vol.IV:487-492.

[10] Gartner, E.M., Young, J.F., Damidot, D.A. and Jawed, I. 'Hydration of Portland cement', In: Bensted, J. and Barnes, P. (eds.), *Structure and Performance of Cements, Second Edition.* London: Spon Press, 2002, 57-113.

Corresponding author's e-mail: Klaartje.De.Weerdt@sintef.no
Corresponding author's fax: +47 735 97 136

Paper II

Fly ash-limestone ternary cements: effect of component fineness.
De Weerdt K., Sellevold E.J., Kjellsen K.O. & Justnes H.
Advances in Cement Research. Accepted.

Fly ash-limestone ternary cements: effect of component fineness.

K. De Weerdt[(1)], E. J.Sellevold[(1,2)], K.O. Kjellsen[(2,3)], H. Justnes[(1)],

[(1)] SINTEF Building and Infrastructure, 7465 Trondheim, Norway

[(2)] NTNU, Departement of Structural Engineering, 7465 Trondheim, Norway

[(3)] Norcem AS HeidelbergCement Group, 3991 Brevik, Norway

Abstract:

Composite cements in which the ordinary Portland cement (OPC) is party replaced by limestone powder and/or siliceous fly ash (FA) at levels up to 35% have been studied using three different finenesses for each material. The aim was to evaluate the influences of fineness and replacement level on the development of the compressive strength, the amount of bound water and calcium hydroxide and the heat of hydration of the composite cements.
Replacing up to 10 % of the fine OPC by fine limestone powder does not impair the compressive strength. Using 5% fine limestone powder instead of 5% fine FA in a cement containing 35% FA resulted, on the other hand, in a considerable strength increase of 13% at 28 days, indicating a synergetic effect between limestone powder and fly ash.
The OPC fineness is the major parameter regarding the early hydration. At 28 days the fineness of the fly ash also plays an important role due to its contribution to the pozzolanic reaction. Indeed, intensive grinding of the fly ash appears to render the fly ash more reactive. The fineness of the limestone powder within the tested range (362 – 812 m^2/kg) had no effect on the hydration of the OPC and the composite cement.

1 Introduction

Due to the rising environmental awareness and diminishing natural resources, there is a growing interest in composite cements in which considerable parts of the ordinary Portland cement (OPC) is replaced by supplementary cementing materials (SCM) such as slag, fly ash, metakaoline, silica fume or limestone powder. Of particular interest are the ternary cements consisting of OPC and a combination of two replacement materials. Combining them can make it possible to compensate for their individual shortcomings.

In this study we focus on siliceous class F fly ash and limestone powder. High replacement levels of clinker by fly ash result in lower early strength due to the slow pozzolanic reaction characteristic for siliceous fly ash (Malhotra and Mehta, 2002). Fine limestone powder, on the other hand, might accelerate the early hydration of the OPC due to its filler effect (Soroka and Stern, 1976, Soroka and Setter, 1977, Bonavetti et al., 2000, Bonavetti et al., 2003). At later age fly ash will contribute to the strength development through its pozzolanic reaction, whereas limestone powder is expected to be inert.

Another important reason for combining limestone powder and fly ash is an expected synergetic interaction between them (De Weerdt and Justnes, 2008). The calcium carbonate from the limestone powder is known to interact with the aluminate hydrates formed by hydrating OPC (Kuzel and Pöllmann, 1991, Kakali et al., 2000, Bonavetti et al., 2001, Matschei et al., 2007, Lothenbach et al., 2008). Monosulphate is unstable in the presence of calcium carbonate and instead mono- and hemicarboaluminate are formed. Adding limestone powder to the system will therefore prevent ettringite from decomposing partially to monosulphate, upon sulphate depletion. The stabilization of ettringite prevents a reduction of the total volume of hydration products, which might result in a decrease in porosity and a subsequent increase in strength. The effect of limestone powder on OPC is, however, restricted due to the limited amount of aluminate hydrates formed during the hydration

of OPC. Fly ash can introduce additional aluminates to the system through its pozzolanic reaction, causing a decrease in the sulphate:aluminate ratio and thereby amplifying the effect of the limestone powder (De Weerdt and Justnes, 2009).

The materials were ground separately, in order to have full control on the fineness of the different constituents. It is known that the reactivity of fly ash can be improved by grinding or classification (Schiessl and Härdtl, 1989, Payá et al., 1995, Eymael and Cornelissen, 1996, Bouzoubaâ et al., 1997, Erdogdu and Türker, 1998, Kiattikomol et al., 2001, Sekulic et al., 2004, Kumar et al., 2007, Justnes et al., 2007). A higher fineness of the OPC results also in a higher strength (Frigione and Marra, 1976, Schiller and Ellerbrock, 1992, Bentz and Haecker, 1999) and even limestone powder seems to be more "reactive" at higher finenesses (Soroka and Setter, 1977, Sato and Beaudoin, 2007). Grinding, however, is an energy craving process (Jankovic et al., 2004) and should therefore be limited.

The novelty of this study is the evaluation of the effect of the fineness of the individual components and their replacement level on the compressive strength, as also the attempt to assess the hydration of the ternary composite cement by determining the amount of bound water and calcium hydroxide, and the isothermal heat of hydration.

2 Materials and experiments

The materials used in this study are: ordinary Portland clinker, a class F siliceous fly ash (FA), limestone powder and natural gypsum. The chemical composition of the clinker, FA and limestone powder are given in Table 1. The clinker was interground with 3.7% of natural gypsum. The gypsum used contains 0.18% free water, and has a $CaSO_4 \cdot 2H_2O$ content of 91.4%. Additional properties of the fly ash are reported in (Ben Haha et al., 2010). The $CaCO_3$ content of limestone, determined by thermogravimetric analysis (TGA), is about 81%. The limestone powder and the fly ash were ground separately. The clinker interground with gypsum will be referred to as ordinary Portland cement (OPC). The materials were each ground to three different finenesses in a laboratory ball mill with a capacity of 9 kg. It should be noted that the materials develop a different particle size distribution (PSD) upon grinding in a laboratory mill than in a full-scale mill (Fredvik, 2005). The specific weight, the Blaine specific surface and the PSD of the materials were determined (see Table 2). The Rosin-Rammler-Sperling-Bennett (RRSB) parameters (Locher, 2005), x' and n, and the median diameter d_{50} are used to facilitate comparison of the PSD's. AccuPyc helium pycnometer from Micrometrics was used to determine the density. The PSD's of the powders were determined by laser diffraction using a Malvern Mastersizer.

The effect of replacing part of the clinker by the different limestone and/or fly ash combinations and the effect of the fineness of the different materials on the hydration, was studied using blended cements with different compositions. The experimental matrix is shown in Table 3 and can be subdivided into eight parts:

- mix 1 – 4: fine OPC was replaced by 0, 5, 10 and 15% fine limestone powder
- mix 5 – 8: combinations of fine fly ash (FF) and fine limestone (FL) + 65% fine OPC (FOPC)
- mix 3, 9 – 11: fineness and type of 10% limestone + 90% fine OPC (FOPC)
- mix 7, 12 – 14: fineness and type of 10% limestone + 65% fine OPC (FOPC) + 25% fine fly ash (FF)
- mix 1, 15, 16: fineness of 100% OPC
- mix 7, 17, 18: fineness of 65% OPC + 25% fine fly ash (FF) + 10% fine limestone (FL)
- mix 5, 19, 20: fineness of 35% fly ash + 65% fine OPC (FOPC)
- mix 7, 21, 22: fineness of 25% fly ash + 65% fine OPC (FOPC) + 10% fine limestone (FL)

Three mortar prisms of 40×40×160 mm, with water to binder ratio (w/b) of 0.50, were prepared for all the tested combinations for each testing age according to EN 196-1. The samples were cured in a

saturated $Ca(OH)_2$ solution at 20˚C. The compressive strength was tested after 1 and 28 days of curing and for some combination also after 3 days.

For all the combinations, cement pastes with w/b of 0.50 were prepared using a Braun MR5550CA high shear mixer. The paste was poured into 20 ml cylindrical glass vials and stored under sealed conditions at 20ºC. The hydration of the samples was stopped after 1 and 28 days of curing. To stop the hydration, the paste samples were crushed fine and immersed in ethanol for about 15 minutes.
Thermogravimetric analyses (TGA) was performed on the resulting slurries using a Mettler Toledo TGA/SDTA851. Samples of about 300 mg were weighed into aluminium oxide crucibles. Prior to the analysis the samples were dried under N_2-purging in the TG equipment at 40ºC to avoid carbonation while monitoring their mass. After drying, the samples were heated from 40ºC to 1,100ºC with a heating rate of 10ºC/min, while the oven was purged with N_2 at 50ml/min.
During the thermogravimetric analysis, the weight of the sample is monitored as a function of the temperature. The weight loss observed when the sample is heated from room temperature up to about 550ºC is due to the release of water from different hydrates and possibly some absorbed water. This weight loss will be referred to as the bound water (H). H is measured from 40ºC and not from about 100ºC as generally done, as the AFt phases and C-S-H already start to decompose at 100ºC. Between 400ºC and 550ºC, a sharp weight loss step occurs, due to the decomposition of calcium hydroxide (CH). Note that in the same temperature interval also other hydrates can decompose, therefore the weight loss due to CH is determined using the tangential method. At temperatures above about 550ºC, carbonates decompose and weight losses are registered as the sample releases CO_2. The sample weight at 550ºC is used as the dry weight, which is assumed to be constant during the hydration and equal to the initial binder weight. Using the sample weight at higher temperatures as dry weight could lead to an underestimation of the dry weight, as the calcium carbonate originating from the limestone powder decomposes. The amount of bound water (H) and calcium hydroxide (CH) are expressed both as % of the dry sample weight at 550ºC (w_{550}) and as % relative to the OPC content:

$$H = \frac{w_{40} - w_{550}}{w_{550}} \quad \text{and} \quad H/OPC = H \cdot \frac{100}{\%OPC} \tag{1}$$

$$CH = \frac{w_{450} - w_{550}}{w_{550}} \cdot \frac{74}{18} \text{ (*)} \quad \text{and} \quad CH/OPC = CH \cdot \frac{100}{\%OPC} \tag{2}$$

(*) $Ca(OH)_2$ (74 g/mol) → CaO + H_2O (18 g/mol) weight difference determined using tangential method

The standard deviation on three independent measurements at all tested ages is not larger than 0.1% for H and 0.2% for CH.

Of each mix 6 g of cement paste was prepared in glass vial (volume 15 ml) using a slow stirring IKA-WERKE RW16 mixer. After 1 minute of mixing the sample was sealed and loaded into TAM Air isothermal calorimeter from Thermometric AB. The isothermal heat of hydration as a function of time at 20ºC was measured for the first 24 hours after water addition. A typical heat of hydration curve of hydrating OPC consists of (Taylor, 1997): An initial peak caused by wetting and early stage reactions, observed during the first minutes. This period is referred to as the initial period, and is followed by the induction period with a low heat rate. The onset of the second, main peak (referred to as the hydration peak), is the start of the acceleration period. This peak is mainly associated with the hydration of C_3S. A gradually decreasing rate of hydration, after reaching a maximum, indicates the deceleration period. The hydration peak can have a shoulder, a superposed third peak, which is known to change when part of the OPC is replaced with different mineral additions and is generally associated with changes in AFt and/or AFm phases (Richardson et al., 1989).

3 Results

3.1 Isothermal calorimetry

Four important features of the isothermal calorimetry curves are compared: (1) the start of the acceleration period, indicating the acceleration or retardation of the cement hydration; (2) the maximum rate of heat generated during the hydration peak (q_{max}) and the time at which it is reached; (3) the cumulative heat generated during the first 24 hours, Q_{24h} (Table 3), corresponding to the area under the curve; (4) the shoulder on the hydration peak. The isothermal calorimetric curves are plotted per gram OPC to assess the changes in the OPC hydration.

Replacing fine OPC with fine limestone powder (FL) and/or fine fly ash (FF) results in an increase in q_{max} and Q_{24h} per OPC relative to the reference (100% FOPC) (Figure 1 A and B). Limestone powder reduces the induction period slightly whereas fly ash increases the induction period. The higher the limestone content, the higher is the q_{max} per OPC and the shorter is the induction period.

Changing the fineness of limestone powder or the type had little effect on the calorimetric curves both when replacing 10% of fine OPC (FOPC) and when 10% is combined with 65% fine OPC (FOPC) and 25% fine fly ash (FF) (Figure 1 C and D). However, the coarse limestone powder (CL) and laboratory grade $CaCO_3$ (P) tended to retard the hydration slightly and reduce the q_{max} per OPC.

Increasing the fineness of the fly ash, results in an increase of q_{max} per OPC and a slightly steeper slope of the hydration peak during the acceleration period (Figure 1 E and F). For the medium and coarse fly ash (MF and CF) the shoulder on the hydration peak appears to be delayed compared to the fine fly ash (FF).

The OPC fineness appears to be the most important parameter regarding the heat of hydration during the first 24 hours (Figure 1 G and H). The finer the OPC, the faster is the hydration, the higher is the maximum (q_{max}), the broader is the hydration peak and the higher is Q_{24h}. The fly ash and limestone powder substitution appear to accelerate the OPC hydration for medium and coarse OPC. The “third peak” or shoulder becomes larger relative to the main peak and appears later in time, as the OPC becomes coarser.

Replacing part of the OPC with fly ash and/or limestone powder, changes the effective water to OPC ratio : replacing 35% of the OPC in a paste with w/c of 0.50 results in an effective water to OPC ratio of 0.77. In order to isolate the effect of variations in the effective water to OPC ratio on the heat of hydration curves, some additional tests were preformed (see Figure 2).. Increasing the water to OPC ratio tends to slightly decrease and delay q_{max} , the Q_{24h}, however, does not appear to change.

3.2 TGA

Replacing up to 15% of the fine OPC with fine limestone powder increases the amount of bound water per OPC with increasing limestone powder content at both 1and 28 days (Figure 3 A). The calcium hydroxide (CH) content per OPC on the other hand tends to decrease when 5% of the OPC is replaced with limestone powder, but increases again when more limestone powder is included (10 and 15%).

Replacing 35% of fine OPC with different combinations of fine fly ash (FF) and fine limestone powder (FL) increases the amount of bound water and CH per OPC relative to the reference (100% FOPC) at 1 day regardless the combination (Figure 3 B). After 28 days, the amount of bound water per OPC is considerably higher than the reference for all tested combinations. It increases with increasing limestone content. While the CH content is lower than in the reference for the all combinations. A

clear decrease is observed when 5% of the fly ash is replaced with limestone powder. It increases again when more limestone powder is included.

Changing the fineness of the limestone powder does not influence the amount of bound water and CH after 1 and 28 days of hydration per OPC both when replacing 10% of fine OPC (FOPC) and when 10% is combined with 65% fine OPC (Figure 3 C) and 25% fine fly ash (Figure 3 D). The $CaCO_3$ increases the amount of bound water and CH at 1 day for fly ash containing composite cements, the reason for this is not clear. The effect disappears after 28 days.

The fineness of the fly ash did not influence the amount of bound water both at 1 and 28 days both for the fly ash blended cements (Figure 3 E) and the composite cements (Figure 3 F). The amount of CH on the other hand decreased considerably for the fine fly ash (FF) compared to the medium and coarse fly ash (MF and CF).

The fineness of the OPC did not change the CH content and the amount of bound water (H) after 1 and 28 days when tested without replacements (Figure 3 G). In combination with 25% fine fly ash and 10% fine limestone powder (Figure 3 H), a slightly decreasing trend can be observed in the amount of bound water with decreasing OPC fineness at 1 day. The CH content decreases as well except for the composite cement containing coarse OPC (COPC). This inconsistency between the amount of bound water and CH can not be explained at the moment. After 28 days the amount of CH and amount of bound water seems to be independent of the OPC fineness, except for the CH content in the composite cement containing fine OPC (FOPC), which is considerably lower compared to the others, again not readily explainable.

3.3 Strength

Up to 10% of fine OPC (FOPC) can be replaced with fine limestone powder (FL) without impairing the compressive strength, both at 1 and 28 days (Figure 4 A).

When replacing 35% of the fine OPC (FOPC) with different combinations of fine fly ash (FF) and fine limestone powder (FL) (see Figure 4 B), the compressive strength increases slightly with increasing limestone powder content after 1 day of curing. The tested composite cements containing both limestone powder and fly ash have higher strength than the blended cement containing only fly ash at all tested ages. After 28 days 65% FOPC+30% FF+5% FL appears to be the optimal combination with regard to strength strength; it has a higher strength than 65% FOPC+35% FF and a similar strength as the reference cement 100% FOPC.

The fineness of the limestone powder influences the 1 day compressive strength slightly, as the strength tends to increase with increasing fineness for both the limestone blended cements and the composite cements. After 3 and 28 days there is no significant difference between the tested limestone powders (Figure 4 C and D).

Increasing the fineness of the fly ash, results in a slightly higher compressive strength after 1 day and 3 days. The difference is however not larger than 2.5 MPa. Prolonged grinding of the fly ash (FF) resulted in a 20% compressive strength increase while short time grinding (MF) only gives a 4% increase compared to the coarse fly ash (CF) after 28 days, both in case of blended fly ash cement (Figure 4 E) and composite cement (Figure 4 F). The composite cements (65% FOPC+25% fly ash+10% FL) have about 8% higher compressive strength than the fly ash blended cements (65% FOPC+35% fly ash) independently of the fly ash fineness.

Increasing the OPC fineness increases the compressive strength for all tested combinations at all ages (see Figure 4 G and H).

4 Discussion

Limestone powder and fly ash both exert a filler effect on the OPC as they increase q_{max}, Q_{24h}, the amount of bound water and the CH content relative to the OPC content after 24 hours of hydration. This filler effect is generally attributed to the additional surface supplied by the powder replacing the OPC, serving as extra precipitation sites for hydration products of the OPC, and the increase of the effective water OPC ratio that accelerate the hydration reaction of the OPC (Ramachandran, 1988, Péra et al., 1999, Zhang and Zhang, 2008). The later does not appear to have a great impact in the tested water to OPC range as can be seen from Figure 2.

Fly ash and limestone powder however influence the OPC hydration in different ways. Limestone powder increases the maximum rate of heat per OPC (q_{max}) more than fly ash, and accelerates the OPC hydration whereas fly ash retards it. This results in a slightly higher compressive strength after 1 day when limestone powder is used instead of fly ash. These superior properties of limestone powder at early age have also been observed by others (Lagerblad and Kjellsen, 1996, Soroka and Stern, 1976).

By replacing part of the OPC with limestone or fly ash, the content of the main reactive component in the cement, namely the clinker, is reduced. This is known as the dilution effect. The filler effect of neither fly ash nor limestone powder is able to compensate for the dilution effect, as the reference (100% fine OPC) has the highest Q_{24h} of all tested combinations (per g of binder) and the highest compressive strength after 1 day (see Table 3).

However it should be noted that up to 10% of the fine OPC can be replaced with fine limestone powder without impairing the 1 and 28 day compressive strength. This is in agreement with the results of other studies (Soroka and Stern, 1976, Tsivilis et al., 1999). The TGA-results at 28 days of these combinations show some remarkable trends: replacing 5% of the OPC with limestone powder results in an increased amount of bound water per OPC, but a reduction in the amount of CH per OPC. One would expect the amount of CH to increase as the amount of bound water increases, assuming the hydration products remain the same (e.g. the hydration of the main clinker mineral alite (C_3S): $C_3S + 2.3\ H \rightarrow C_{1.7}SH + 1.3\ CH$). A decrease in the amount of CH and a corresponding increase of bound water indicates a change in the nature of the hydration products formed. In the absence of calcium carbonate, ettringite will react with the remaining aluminate and form calcium monosulphoaluminate hydrate (monosulphate), as the sulphate is depleted (Equation 3).

$$2\ C_3A + C_3A{\cdot}3CaSO_4{\cdot}32H_2O + 4\ H_2O \rightarrow 3\ C_3A{\cdot}CaSO_4{\cdot}12H_2O \quad (3)$$

However, in the presence of calcium carbonate, the main constituent of limestone powder, monosulphate is unstable and instead calcium mono- or hemicarboaluminate hydrates are formed.

$$C_3A + CaCO_3 + 11\ H_2O \rightarrow C_3A{\cdot}CaCO_3{\cdot}11H_2O \quad (4)$$
$$C_3A + 0.5\ CaCO_3 + 0.5\ Ca(OH)_2 + 12\ H_2O \rightarrow C_3A{\cdot}0.5CaCO_3{\cdot}0.5Ca(OH)_2{\cdot}12H_2O \quad (5)$$

In other words, the formation of hemicarboaluminate hydrate consumes CH, and this might explain the observed reduction in CH/OPC (Kakali et al., 2000, Bonavetti et al., 2001, Hoshino et al., 2006) (equation (5)).

From equation (3) it can be seen that ettringite is more water rich and therefore also more voluminous relative to the aluminate content than monosulphate. Stabilising the ettringite and preventing decomposition to monosulphate, upon sulphate depletion, will therefore lead to an increase in the total volume of the hydration products which might result in a reduction of the porosity and an improved compressive strength.

At higher limestone powder levels, the amount of CH per OPC increases again. This might be due to two reasons: first, at higher replacement levels the filler effect is greater and more CH is produced by promoting the clinker hydration than consumed by the formation of hemicarboaluminate, and secondly, monocarboaluminate, which does not consume CH, might have formed instead of hemicarboaluminate due to the higher limestone content and the lower aluminate content (OPC dilution).

A similar effect was observed for composite cements containing 65% fine OPC and 35% of a combination of fine fly ash and/or fine limestone powder. The composite cement containing 35% fly ash and no limestone powder had a higher CH content than the one with 30% fly ash and 5% limestone powder. One would expect that more CH is consumed when more fly ash is present. The explanation for this is similar to the one for minor additions of limestone powder to OPC, as mentioned earlier. The decrease in CH when 5% fly ash is replaced with 5% limestone powder could be due to the formation of hemicarboaluminate hydrate which consumes CH. The chemical interaction between the limestone powder and the aluminates phases (AFm and AFt) will be more important in the fly ash containing cements as fly ash will liberate additional aluminates during its pozzolanic reaction. This proposed synergetic effect between fly ash and limestone powder is supported by compressive strength results: replacing 5% of OPC with limestone resulted only in a 2% strength increase; whereas replacing 5% of fly ash with limestone in a fly ash blended cement (35% fly ash) resulted in a strength increase of 13%. Moreover, the composite cements (65% FOPC+25% fly ash+10% FL) have about 8% higher compressive strength than the fly ash blended cements (65% FOPC+35% fly ash) regardless the fly ash fineness.

The fineness of the limestone powder does not seem play any important role. Previous research has concluded the opposite (Sato and Beaudoin, 2007, Lagerblad and Kjellsen, 1996). It might be that the tested range of fineness (362 – 812 m^2/kg) was to narrow to see any effect. The purity of the limestone powder, tested by comparing it with laboratory grade $CaCO_3$, did not seem to influence the tested parameters either, except for the anomalous TGA results at 1day.

The fineness of the fly ash appeared to be more important. During the first day of hydration, a slight difference can be observed as the coarse and medium fly ash tend to retard the hardening slightly (decrease the slope of the hydration curve) and delays the shoulder on the hydration peak compared to the fine fly ash (FF), as also observed by (Kumar et al., 2007). After 28 days of hydration the difference between the different fly ash finenesses is clearer. The fly ash consumes CH during its pozzolanic reaction and the CH content per OPC for all composite cements containing fine fly ash (FF), is lower than for the corresponding combinations containing medium and coarse fly ash (MF and CF), indicating that the reaction of the fine ground fly ash is faster than the others, as expected.
When combining the TGA and compressive strength results of the fly ash blended cements (65% FOPC +35% fly ash) something interesting can be seen (Figure 3 and Figure 4). The blended cement containing fine fly ash (FF) has a higher compressive strength, but at the same time a similar amount of bound water after 28 days than the composite cements containing coarse and medium fly ash. This discrepancy between strength and bound water is not unexpected. A likely explanation is that when the fly ash reacts with the CH it will form hydration products which bind little water beyond that present in CH. These hydration products formed are expected to contribute more to the strength than the CH consumed.

The fineness of the OPC is the most important parameter during the first day of hydration. The length of the induction period, q_{max}, Q_{24h} and 1 day strength increase when using finer OPC. That higher OPC fineness results in superior compressive strength is common knowledge (Frigione and Marra, 1976, Schiller and Ellerbrock, 1992, Bentz and Haecker, 1999). It should be noted that at 1

day, the relative strength gain is greater than at 28 days. From the TGA results, however, the effects of OPC fineness are smaller and less consistent as discussed already.

The correlations between the different tested parameters: compressive strength, heat of hydration and bound water after 1 day of hydration are depicted in Figure 5 and Figure 6. The parameters appear to correlate well at 1 day. After 28 days (see Figure 7) the correlation between strength and the amount of bound water changes for the blends containing FA (indicated by an ellipse) due to formation of the pozzolanic reaction products as mentioned before.

5 Conclusions

Limestone powder and fly ash both display a filler effect when they replace OPC in a 1:1 ratio, but they influence the OPC hydration in different ways. Limestone powder accelerates the OPC hydration whereas fly ash retards it. This results in a slightly higher compressive strength after 1 day when limestone powder compared to fly ash. The filler effect of neither fly ash nor limestone powder appears to be able to compensate for the *dilution effect*. However up to 10% of the fine OPC can be replaced by fine limestone without impairing the compressive strength after 1 and 28 days. A decrease in the amount of CH and a corresponding increase of bound water indicate a change in the nature hydration products formed, namely calcium mono- or hemicarboaluminate hydrates are formed instead of calcium monosulphoaluminate. This is suggested to cause the observed compressive strength increase.

A similar but stronger effect was observed when replacing 5% of the fly ash with limestone powder in a composite cement containing 65% fine OPC and 35% fly ash. A 5% limestone replacement in OPC cement resulted only in a 2% strength increase whereas for fly ash blended cement (35% fly ash versus 30% fly ash and 5% limestone) it resulted in a strength increase of 13%. This synergetic effect between fly ash and limestone powder is believed to be due to the additional aluminates provided by the fly ash during its pozzolanic reaction which amplify the chemical interaction between the limestone powder and the aluminate phases (AFm and AFt).
The fineness of the limestone powder in the tested range (362 – 812 m^2/kg) does not seem play an important role.
The fineness of the OPC is the most important parameter during the early stage of hydration.
The fineness of the fly ash becomes important at 28 days as fine grinding accelerates the pozzolanic reaction of the fly ash.

6 Acknowledgements

The authors would like to acknowledge COIN, the COncrete INnovation centre (www.coinweb.no) for the financial support.

7 References

Ben Haha, M., De Weerdt, K. & Lothenbach, B. (2010) Quantification of the degree of reaction of fly ash. *Cement and Concrete Research (in review)*.

Bentz, D. P. & Haecker, C. J. (1999) An argument for using coarse cements in high-performance concretes. *Cement and Concrete Research,* 29**,** 615-618.

Bonavetti, V., Donza, H., Menéndez, G., Cabrera, O. & Irassar, E. F. (2003) Limestone filler cement in low w/c concrete: A rational use of energy. *Cement and Concrete Research,* 33**,** 865-871.

Bonavetti, V., Donza, H., Rahhal, V. & Irassar, E. (2000) Influence of initial curing on the properties of concrete containing limestone blended cement. *Cement and Concrete Research,* 30**,** 703-708.

Bonavetti, V. L., Rahhal, V. F. & Irassar, E. F. (2001) Studies on the carboaluminate formation in limestone filler-blended cements. *Cement and Concrete Research,* 31**,** 853-859.

Bouzoubaâ, N., Zhang, M. H., Bilodeau, A. & Malhotra, V. M. (1997) The effect of grinding on the physical properties of fly ashes and a portland cement clinker. *Cement and Concrete Research,* 27**,** 1861-1874.

De Weerdt, K. & Justnes, H. (2008) Microstructure of binder from the pozzolanic reaction between lime and siliceous fly ash and the effect of limestone addition. IN SUN, W., VAN BREUGEL, K., MIAO, C., YE, G. & CHEN, H. (Eds.) *Microstructure Related Durability of Cementitious Composites* Nanjing.

De Weerdt, K. & Justnes, H. (2009) Synergic Reactions in Triple Blended Cements. *11th NCB International Seminar on Cement and Building Materials.* New Delhi.

Erdogdu, K. & Türker, P. (1998) Effects of fly ash particle size on strength of portland cement fly ash mortars. *Cement and Concrete Research,* 28**,** 1217-1222.

Eymael, M. M. T. & Cornelissen, H. A. W. (1996) Processed pulverized fuel ash for high-performance concrete. *Waste Management,* 16**,** 237-242.

Fredvik, T. I. (2005) Initial strength development of fly ash and limestone blended cements at various temperatures predicted by ultrasonic pulse velocity. *Department of Structural Engineering.* Trondheim, NTNU.

Frigione, G. & Marra, S. (1976) Relationship between particle size distribution and compressive strength in portland cement. *Cement and Concrete Research,* 6**,** 113-127.

Hoshino, S., Yamada, K. & Hirao, H. (2006) XRD/Rietveld Analysis of the Hydration and Strength Development of Slag and Limestone Blended Cement. *Journal of Advanced Concrete Technology,* 4**,** 357-367.

Jankovic, A., Valery, W. & Davis, E. (2004) Cement grinding optimisation. *Minerals Engineering,* 17**,** 1075-1081.

Justnes, H., Ronin, V., Jonasson, J. E. & Elfgren, L. (2007) Mechanochemical technology: synthesis of energetically modified cements (EMC) with high volume fly ash content. *12th ICCC.* Montreal.

Kakali, G., Tsivilis, S., Aggeli, E. & Bati, M. (2000) Hydration products of C3A, C3S and Portland cement in the presence of CaCO3. *Cement and Concrete Research,* 30**,** 1073-1077.

Kiattikomol, K., Jaturapitakkul, C., Songpiriyakij, S. & Chutubtim, S. (2001) A study of ground coarse fly ashes with different finenesses from various sources as pozzolanic materials. *Cement and Concrete Composites,* 23**,** 335-343.

Kumar, R., Kumar, S. & Mehrotra, S. P. (2007) Towards sustainable solutions for fly ash through mechanical activation. *Resources, Conservation and Recycling,* 52**,** 157-179.

Kuzel, H. J. & Pöllmann, H. (1991) Hydration of C3A in the presence of Ca(OH)2, CaSO4·2H2O and CaCO3. *Cement and Concrete Research,* 21**,** 885-895.

Lagerblad, B. & Kjellsen, K. O. (1996) Effect of Mineralogy of Fillers on the Cement Hydration. IN JENNINGS, H., KROPP, J. & SCRIVENER, K. (Eds.) *The Modelling of Microstructure and Its Potential for Studying Transport Properties and Durability.* Netherlands, Kluwer Academic Publisher.

Locher, F. W. (2005) *Cement principles of production and use,* Düsseldorf, Verlag Bau+Technik GmbH.

Lothenbach, B., Le Saout, G., Gallucci, E. & Scrivener, K. (2008) Influence of limestone on the hydration of Portland cements. *Cement and Concrete Research,* 38**,** 848-860.

Malhotra, V. M. & Mehta, P. K. (2002) *High-Performance, High-Volume Fly-Ash Concrete: Materials, Mixture Proportioning, Properties, Construction practice and Case Histories,* Ottawa, Supplementary Cementing Materials for Sustainable Development Inc.

Matschei, T., Lothenbach, B. & Glasser, F. P. (2007) The AFm phase in Portland cement. *Cement and Concrete Research,* 37**,** 118-130.

Payá, J., Monzó, J., Borrachero, M. V. & Peris-Mora, E. (1995) Mechanical treatment of fly ashes. Part I: Physico-chemical characterization of ground fly ashes. *Cement and Concrete Research,* 25**,** 1469-1479.

Péra, J., Husson, S. & Guilhot, B. (1999) Influence of finely ground limestone on cement hydration. *Cement and Concrete Composites,* 21**,** 99-105.

Ramachandran, V. S. (1988) Thermal analyses of cement components hydrated in the presence of calcium carbonate. *Thermochimica Acta,* 127**,** 385-394.

Richardson, I. G., Wilding, C. R. & Dickson, M. J. (1989) The hydration of blastfurnace slag cements. *Advances in Cement Research,* 2**,** 14-157.

Sato, T. & Beaudoin, J. J. (2007) The effect of nano-sized $CaCO_3$ addition on the hydration of cement paste containing high volumes of fly ash. *12th ICCC.* Montreal.

Schiessl, P. & Härdtl, R. (1989) Alkali activated slag - fly ash cements. *3th International Conference on fly ash, silica fume, slag and natural pozzolans.* Trondheim.

Schiller, B. & Ellerbrock, H.-G. (1992) Mahlung und Eigenschaften von Zementen mit mehreren Hauptbestandteilen. *ZKG International,* 9**,** 10.

Sekulic, Z., Petrov, M. & Zivanovic, D. (2004) Mechanical activation of various cements. *International Journal of Mineral Processing,* 74**,** S355-S363.

Soroka, I. & Setter, N. (1977) The effect of fillers on strength of cement mortars. *Cement and Concrete Research,* 7**,** 449-456.

Soroka, I. & Stern, N. (1976) Calcareous fillers and the compressive strength of portland cement. *Cement and Concrete Research,* 6**,** 367-376.

Taylor, H. F. W. (1997) *Cement chemistry 2nd edition,* London, Thomas Telford.

Tsivilis, S., Chaniotakis, E., Badogiannis, E., Pahoulas, G. & Ilias, A. (1999) A study on the parameters affecting the properties of Portland limestone cements. *Cement and Concrete Composites,* 21**,** 107-116.

Zhang, Y. & Zhang, X. (2008) Research on effect of limestone and gypsum on C3A, C3S and PC clinker system. *Construction and Building Materials,* 22**,** 1634-1642.

List of Tables:

Table 1: Chemical composition of the clinker, fly ash and limestone in % 12
Table 2: Different materials used, their short notation, grinding time, Blaine specific surface, specific density, RRSB parameters (x',n) and the median diameter (d_{50})..... 12
Table 3: Experimental matrix with the compressive strength (σ), amount of bound water (H) and calcium hydroxide (CH) per OPC, and the cumulative heat of hydration emitted per g binder and g OPC during the first 24 hours of hydration (Q_{24h}). 13

List of Figures:

Figure 1: Isothermal calorimetric curves for cement paste expressed per g OPC, varying (A) OPC replacement level with limestone; (B) different combinations of fine limestone and fine fly ash replacing 35% of OPC; (C) and (D) limestone fineness; (E) and (F) fly ash fineness; (G) and (H) OPC fineness..... 14
Figure 2: Isothermal calorimetric curves for cement paste expressed per g OPC with varying w/c ratio all with a Q_{24h} of about 240±2 J/g OPC. 15
Figure 3: The amount of bound water (H) and calcium hydroxide (CH) per OPC after 1 day (dark) and 28 days (bright) for (A) OPC replacement level with limestone; (B) different combinations of fine limestone and fine fly ash replacing 35% of OPC; (C) and (D) varying limestone fineness; (E) and (F) fly ash fineness; (G) and (H) OPC fineness. 16
Figure 4: Compressive strength (σ) after 1, 3 and 28 days (from bright to dark) for (A) OPC replacement level with limestone; (B) different combinations of fine limestone and fine fly ash replacing 35% of OPC; (C) and (D) varying limestone fineness; (E) and (F) fly ash fineness; (G) and (H) OPC fineness..... 17
Figure 5: Correlation between the cumulative heat (Q_{24h}) and the compressive strength (σ) after 1 day. 18
Figure 6: Correlation between the amount of bound water (H) and the compressive strength after 1 day not taking into account the bright points (mix 14 and mix 15). 18
Figure 7: Correlation between the amount of bound water (H) and the compressive strength after 1 day (bright) and 28 days (dark); the spheres represent the fly ash containing blends and the triangles the blends containing OPC and limestone. 18

Table 1: Chemical composition of the clinker, fly ash and limestone in %

	Clinker	Fly ash	Limestone
SiO_2	20.8	50.0	12.8
Al_2O_3	5.6	23.9	2.7
Fe_2O_3	3.2	6.0	2.0
CaO	63.0	6.3	42.3
MgO	3.0	2.1	1.8
SO_3	1.5	0.4	-
P_2O_5	0.1	1.1	-
K_2O	1.3	1.4	0.6
Na_2O	0.5	0.6	0.5
Na_2O Eq.	1.4	1.6	
LOI	0.3	3.6	37.7
Carbon	-	3.1	-
Chloride	0.05	-	-
Free CaO	1.9	-	-

Table 2: Different materials used, their short notation, grinding time, Blaine specific surface, specific density, RRSB parameters (x',n) and the median diameter (d_{50}).

		Short notation	Grinding time [minutes]	Blaine surface [m^2/kg]	Density [kg/dm^3]	x' [µm]	n	d_{50} [µm]
OPC	fine	FOPC	180	557	3.15	9	1.1	7
	medium	MOPC	100	453	3.15	16	1.0	11
	coarse	COPC	55	358	3.15	20	1.0	16
limestone	fine	FL	90	812	2.74	11	0.9	4
	medium	ML	30	658	2.74	14	1.0	7
	coarse	CL	0	362	2.74	28	1.0	18
fly ash	fine	FF	120	675	2.6	8	1.6	6
	medium	MF	15	449	2.49	18	1.3	14
	coarse	CF	0	357	2.34	28	1.1	18
$CaCO_3$		P	-	-	2.71	-	-	-

Table 3: Experimental matrix with the compressive strength (σ), amount of bound water (H) and calcium hydroxide (CH) per OPC, and the cumulative heat of hydration emitted per g binder and g OPC during the first 24 hours of hydration (Q_{24h}).

Mix	Cement composition										σ [MPa]			H/OPC [%]		CH/OPC [%]		Q_{24h} [J/g]	
	FOPC	MOPC	COPC	FL	ML	CL	P	FF	MF	CF	1 d	3 d	28 d	1 d	28 d	1 d	28 d	/g	/OPC
1	100										26.8	36.4	52.9	10.3	19.3	12.9	21.6	239	239
2	95			5							27.4	-	54.0	10.2	20.5	12.6	20.4	232	244
3	90			10							25.9	-	52.7	11.1	21.2	12.7	20.8	226	251
4	85			15							25.4	-	51.0	11.2	22.2	13.3	21.4	220	259
5	65							35			16.0	25.7	47.2	12.7	24.9	14.4	21.3	183	281
6	65			5				30			17.3	29.5	53.5	12.4	25.9	14.3	19.8	185	284
7	65			10				25			17.6	29.2	50.9	12.5	26.3	14.2	20.0	186	285
8	65			15				20			18.0	28.9	48.9	12.9	27.2	14.5	20.7	187	288
9	90				10						26.0	-	53.4	11.2	21.0	13.1	20.8	223	248
10	90					10					24.1	-	52.0	10.6	21.8	13.1	21.0	222	247
11	90						10				23.4	-	51.8	10.6	21.7	13.1	21.1	222	247
12	65				10			25			17.0	28.3	50.5	12.5	26.5	14.5	19.7	190	293
13	65					10		25			16.6	28.1	50.2	12.5	27.2	14.5	20.2	187	287
14	65						10	25			15.7	28.3	49.2	14.9	26.7	17.5	20.4	185	285
15		100									22.4	-	49.0	10.9	19.4	11.8	21.0	210	210
16			100								20.3	-	46.5	9.3	18.7	13.2	21.0	195	195
17		65		10				25			14.5	26.1	47.4	12.0	27.1	13.4	25.3	166	255
18			65	10				25			12.1	23.9	43.7	10.7	27.0	16.5	25.1	152	233
19	65								35		14.9	23.7	41.0	12.6	25.9	18.3	29.3	181	279
20	65									35	14.0	23.2	39.4	12.0	25.6	17.7	30.8	178	274
21	65			10					25		17.1	27.9	44.4	12.4	27.1	17.7	27.7	186	287
22	65			10						25	16.2	27.2	42.8	11.8	27.1	17.3	27.9	184	284

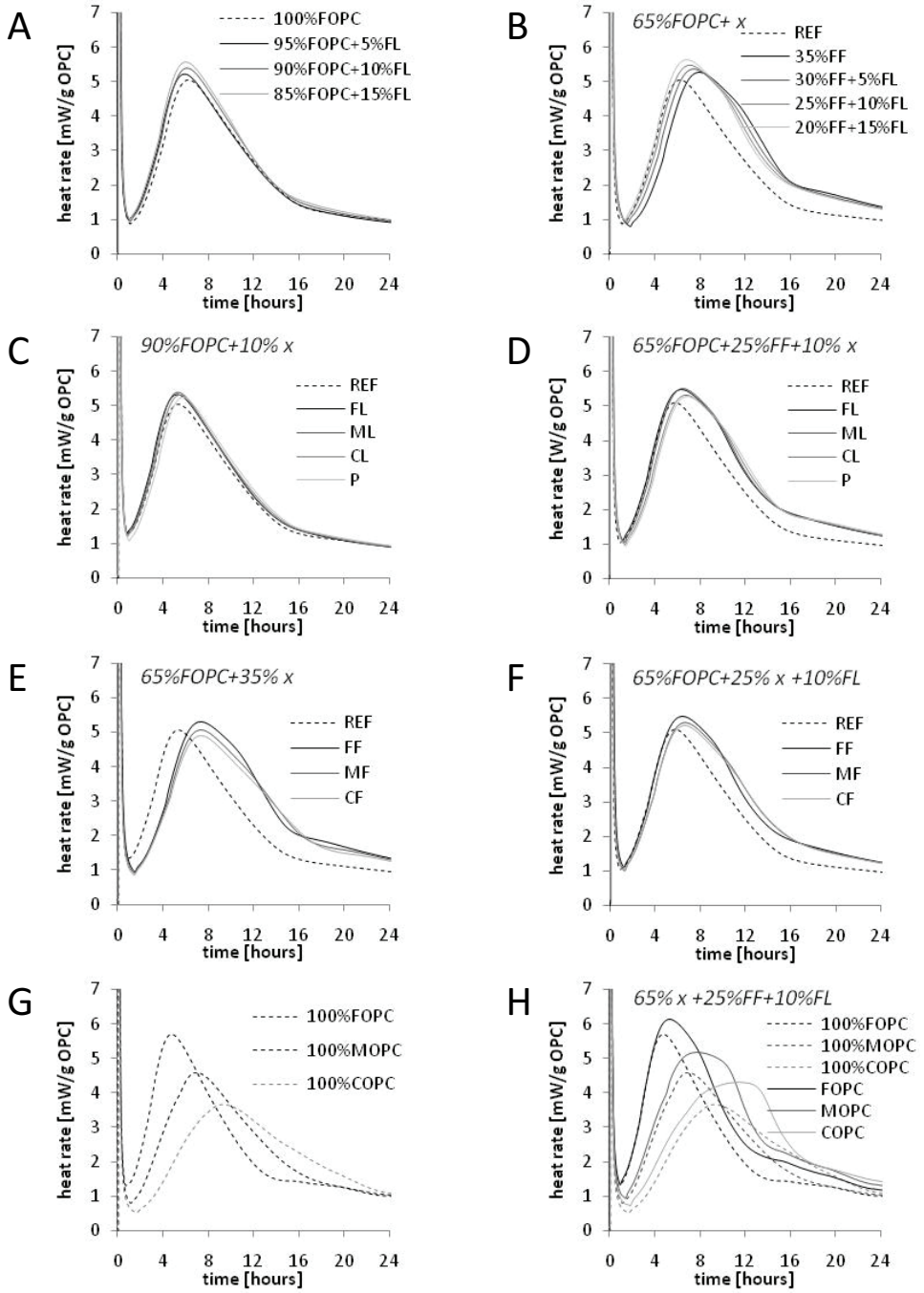

Figure 1: Isothermal calorimetric curves for cement paste expressed per g OPC, varying (A) OPC replacement level with limestone; (B) different combinations of fine limestone and fine fly ash replacing 35% of OPC; (C) and (D) limestone fineness; (E) and (F) fly ash fineness; (G) and (H) OPC fineness.

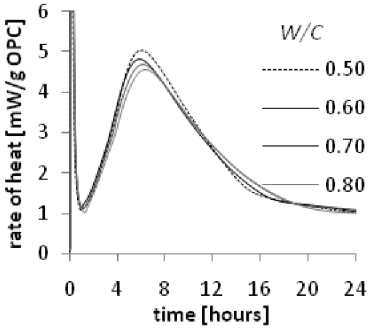

Figure 2: Isothermal calorimetric curves for cement paste expressed per g OPC with varying w/c ratio all with a Q_{24h} of about 240±2 J/g OPC.

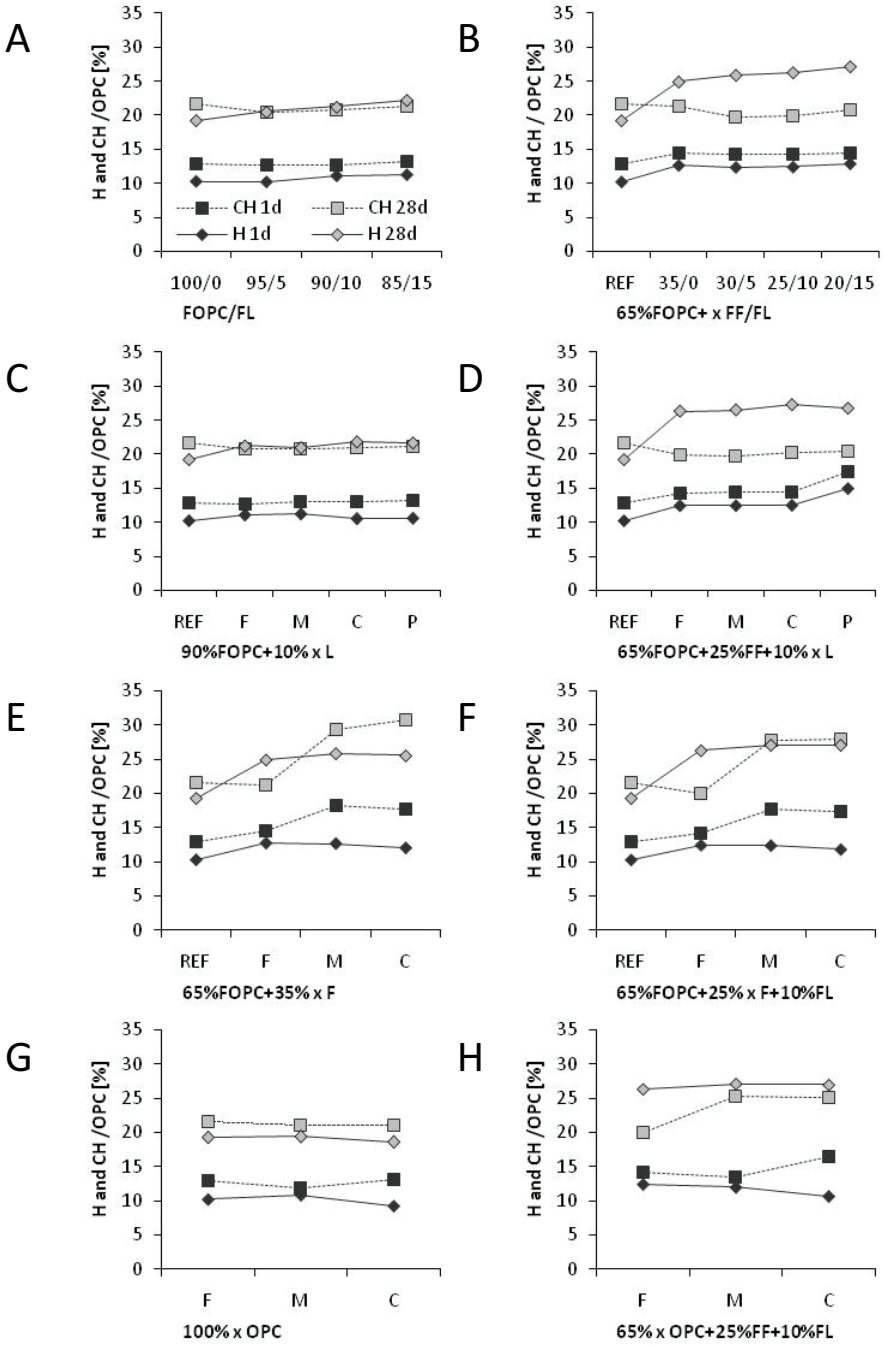

Figure 3: The amount of bound water (H) and calcium hydroxide (CH) per OPC after 1 day (dark) and 28 days (bright) for (A) OPC replacement level with limestone; (B) different combinations of fine limestone and fine fly ash replacing 35% of OPC; (C) and (D) varying limestone fineness; (E) and (F) fly ash fineness; (G) and (H) OPC fineness.

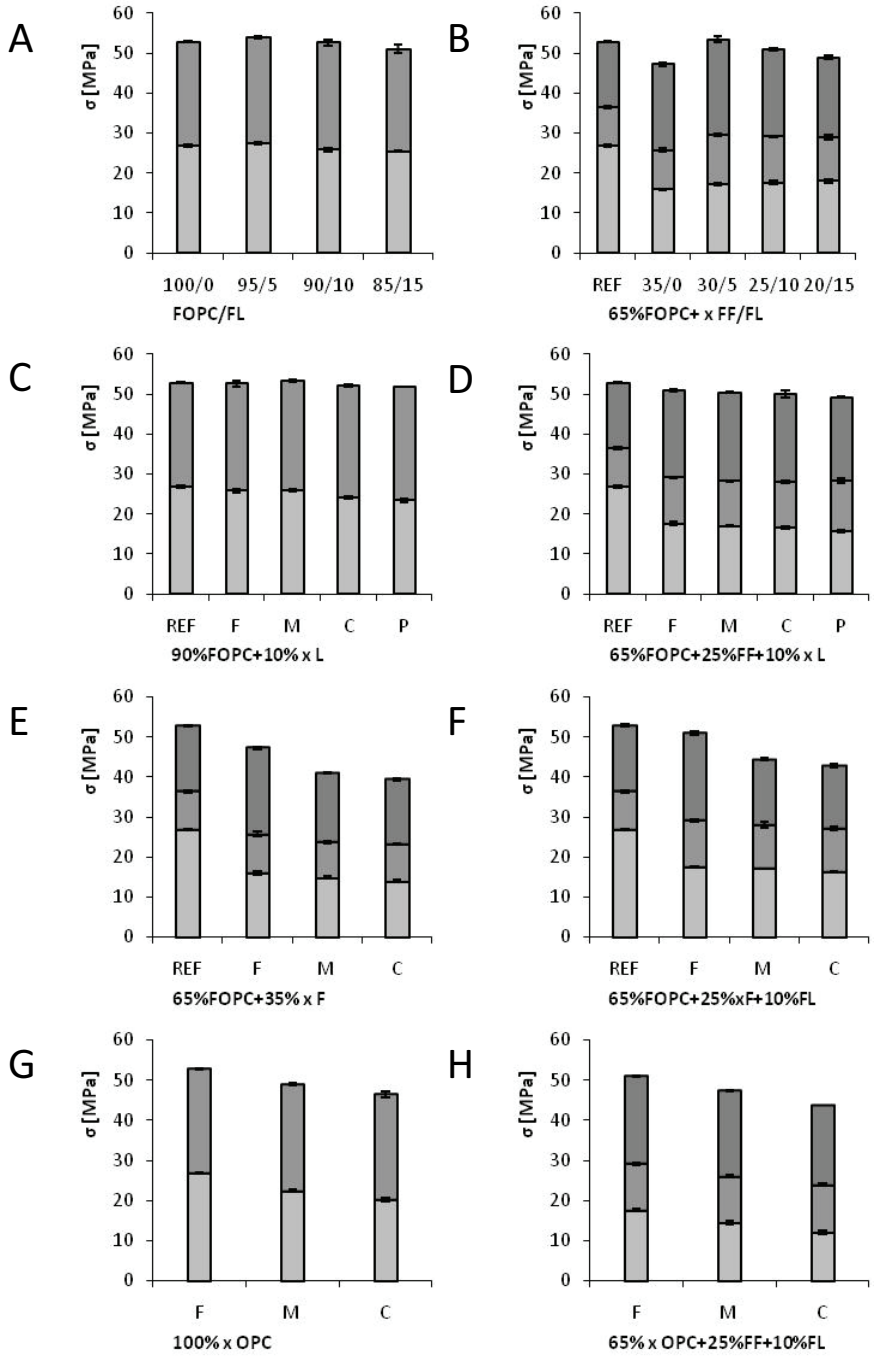

Figure 4: Compressive strength (σ) after 1, 3 and 28 days (from bright to dark) for (A) OPC replacement level with limestone; (B) different combinations of fine limestone and fine fly ash replacing 35% of OPC; (C) and (D) varying limestone fineness; (E) and (F) fly ash fineness; (G) and (H) OPC fineness.

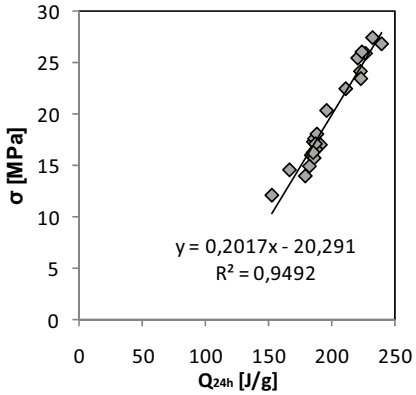

Figure 5: Correlation between the cumulative heat (Q_{24h}) and the compressive strength (σ) after 1 day.

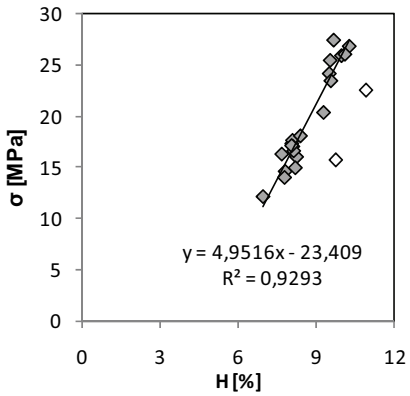

Figure 6: Correlation between the amount of bound water (H) and the compressive strength after 1 day not taking into account the bright points (mix 14 and mix 15).

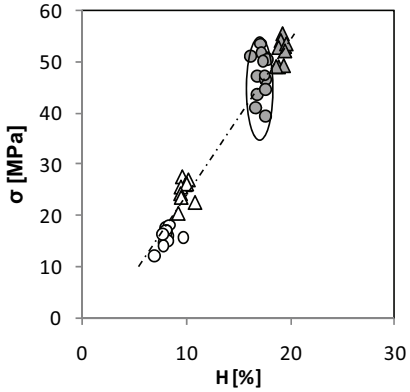

Figure 7: Correlation between the amount of bound water (H) and the compressive strength after 1 day (bright) and 28 days (dark); the spheres represent the fly ash containing blends and the triangles the blends containing OPC and limestone.

Paper III

Fly ash -limestone ternary composite cements: synergetic effect at 28 days.
De Weerdt K., Justnes H., Kjellsen K.O. & Sellevold E.J.
Nordic Concrete Research, 2010, Vol.42 (2) pp. 51-70

Fly ash-limestone ternary composite cements: synergetic effect at 28 days.

Klaartje De Weerdt
M.Sc., Ph.D.-student
SINTEF Building and Infrastructure
NO-7465 Trondheim
E-mail: klaartje.de.weerdt@sintef.no

Harald Justnes
Ph.D., Adjunct Professor NTNU
SINTEF Building and Infrastructure
NO-7465 Trondheim
E-mail: harald.justnes@sintef.no

Knut O. Kjellsen
Ph.D., Adjunct Professor NTNU
Norcem Heidelberg Cement
NO-3908 Brevik
E-mail: knut.kjellsen@norcem.no

Erik J. Sellevold
Professor NTNU
Departement of Structural Engineering
NO-7491 Trondheim
Email: erik.sellevold@bygg.ntnu.no

ABSTRACT

Composite cements containing OPC, fly ash and limestone powder were tested in paste and mortar after 28 days of curing at 20°C to verify a postulate claiming that calcium aluminate hydrates produced by the pozzolanic reaction of fly ash would react further with limestone to form calcium carboaluminate hydrates and thereby increase the total amount of hydrates and consequently strength. Thermogravimetric tests indicated indeed a change in hydration products when limestone powder was included in the system. This was also confirmed by X-ray diffraction showing the formation of calcium carboaluminate hydrates. It was demonstrated that this synergetic interaction between fly ash and limestone increases the compressive strength more than cement replacement by limestone or fly ash alone.

Key words:

ternary cement, fly ash, limestone, carboaluminate hydrate

1 INTRODUCTION

During cement production large amounts of CO_2 are emitted. In 2000, about 0.87 ton CO_2 per ton clinker was emitted on average, about 40% coming from fuel combustion, grinding and other operations, and 60% from the de-carbonation of limestone to form the clinker phases [1]. In order to reduce these emissions, cement factories have switched over to larger fractions of alternative fuels, optimized energy consumption (e.g. regeneration of heat, optimized the clinker with mineralisers, etc) [2].

The fact that, in the future, emitting CO_2 will come at a price, gives the cement producers a new incentive to reduce the emissions even more. One way of doing that on a short term is by replacing part of the clinker with other materials such as slag, limestone powder, fly ash, silica fume, natural pozzolans etc [3]. The type of replacement materials used depends on their availability (amount available, price, transportation …) and is therefore dependent on the geographical location of the cement plant.

The aim of this study is to contribute to the development of a novel all-round Portland composite cement for the Norwegian market. Currently the cements produced at the Norwegian cement plants are: CEM I [4] Portland cements containing up to 5% limestone powder and CEM II/A-V [4] Portland fly ash cements containing up to 20% fly ash but no limestone powder. In this study, the effect of increasing the replacement levels of the ordinary Portland cement (OPC) (up to 35%), and combining fly ash and limestone powder to replace OPC are investigated.

Limestone powder is known to accelerate the hydration of cement, especially the C_3S phase, by acting as nucleation surface for portlandite and CSH precipitation [5-7]. The accelerating effect can give rise to a slightly higher compressive strength at early age at moderate OPC replacements (<10%). At later age, replacing part of the OPC with limestone powder may result in a strength reduction, due to the replacement of the more reactive component, OPC, with less or non reactive one [8]. This effect is referred to as the dilution effect. Besides this physical effect, the calcium carbonate of the limestone powder is also known to interact with the aluminate phases of OPC [7, 9-13]. In the presence of small amounts of limestone powder, monosulphoaluminate hydrate is replaced by mono- or hemicarboaluminate hydrate and more ettringite. Due to this change in hydration products the volume of the hydration products formed can increase slightly [12-14]. This can in its turn lead to a slight increase in strength and a decrease in permeability. The effect is however limited due to the small amount of aluminate present in the OPC.

ASTM Class F fly ash [15] is a slow reacting pozzolan. It can take up to several weeks before it starts to react significantly at 20°C. The fly ash will not react noticeably during the so-called “incubation period” the length of which is believed to depend mainly on the alkalinity of the pore water [16, 17] and therefore also on the type of cement used [18]. Fly ash reduces early strength due to the dilution effect. However, it can contribute to a higher long-term strength, due to its pozzolanic reaction.

When combining limestone powder and fly ash, a synergetic effect between the two is expected to take place. Fly ash is an aluminate rich pozzolan, as it reacts it will introduce additional aluminates to the system, thereby decreasing the SO_3/Al_2O_3 ratio and amplifying the impact of the limestone powder on the hydration products. The increase of bound water and compressive strength gain resulting from a minor limestone powder addition is therefore is expected to be

greater for fly ash containing cements than for OPC. This was first postulated in the COIN application in 2005 (www.coinweb.no). The goal of the study is to validate this postulate concerning the synergetic effect between limestone powder and fly ash.

A preliminary study on fly ash-limestone-calcium hydroxide-alkaline solution [19]: showed a clear interaction between fly ash and limestone powder. More water was bound relative to the fly ash content and the hydration products formed were proven to contain calcium carboaluminate hydrate.

In literature many studies can be found on composite cements containing limestone powder and slag [20, 21], limestone powder and natural pozzolans [22] and even limestone powder and fly ash [23-26] have been investigated. However, these studies focused on heat of hydration, strength and durability, whereas the chemical interaction between the different components was not studied [24]. An exception is Hoshino at al. [27] who studied the addition of limestone powder to slag cements and linked the changes in the hydration phases observed by XRD with the increase in compressive strength. To the author's knowledge, the hydration mechanisms of composite cements containing both limestone powder and fly ash have not been fully investigated yet.

2 EXPERIMENTAL

2.1 Materials

The materials used in this project were: CEM I clinker, siliceous fly ash, limestone powder and natural gypsum. The composition of clinker, fly ash and limestone used as well as their density and specific surface are listed in Table 1. Table 2 gives the mineral composition of the clinker determined by Rietveld analysis. The clinker was interground with 3.7% of gypsum to form OPC, so that the total SO_3 content would be about 3% including the sulphates of the clinker. The gypsum contained 0.18% free water, and had a $CaSO_4 \cdot 2H_2O$ content of 91.39%. The particle size distribution of the different materials was determined with a Mastersizer from Malvern. The results are shown in Figure 1.

Table 1: Chemical composition, density and Blaine specific surface of the clinker, fly ash and limestone powder

	Clinker	Fly ash	Limestone
SiO_2	20.8	50.0	12.9
Al_2O_3	5.6	23.9	2.7
Fe_2O_3	3.2	6.0	2.0
CaO	63.0	6.3	42.3
MgO	3.0	2.1	1.8
SO_3	1.5	0.4	-
P_2O_5	0.1	1.1	-
K_2O	1.3	1.4	0.6
Na_2O	0.5	0.6	0.5
Na_2O Eq.	1.4	1.6	
LOI	0.3	3.6	37.7
Carbon	-	3.1	-
Chloride	0.05	-	-
Free CaO	1.9	-	-
Density [kg/m^3]	3150*	2740	2490
Blaine specific surface [m^2/kg]	500*	470	810

* for OPC = clinker + gypsum

Table 2: Mineral composition of the clinker determined by Rietveld analysis

Minerals	%
C_2S	19
C_3S	54
C_3A	11
C_4AF	8

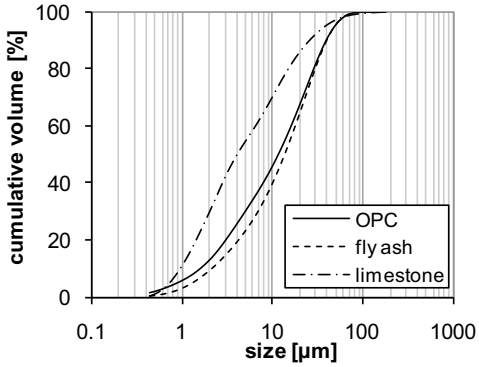

Figure 1: The particle size distribution of the materials used in this study determined by laser diffraction.

2.2 Testing

Table 3 shows the different composite cements which were tested. The experimental matrix can be divided into three main groups, together with the reference (mix 1). In the first group, OPC is gradually replaced by limestone powder, starting at 5% up to 35% in steps of 5% (mix 2 to mix 8). In the second group OPC is similarly replaced with fly ash (mix 9 to mix 15). In the third group different limestone powder and fly ash combinations were tested (mix 16 – mix 21) at a constant OPC replacement level of 35%, which is the potential replacement level for future commercial cements produced in Norway.

Table 3: Composite cement combinations tested (replacement by mass)

mix	OPC	fly ash	limestone
1	100	/	0
2	95	/	5
3	90	/	10
4	85	/	15
5	80	/	20
6	75	/	25
7	70	/	30
8	65	/	35
9	95	5	/
10	90	10	/
11	85	15	/
12	80	20	/
13	75	25	/
14	70	30	/
15	65	35	/
16	65	30	5
17	65	25	10
18	65	20	15
19	65	15	20
20	65	10	25
21	65	5	30

The replacements are done by mass as this is most relevant for cement production. The aim of the study is to develop an all-round Portland composite cement which will be used at fixed w/c ratio's. Furthermore, additional tests showed little difference in compressive and flexural strength when OPC was replaced with crystalline quartz (considered inert material) either by mass or by volume (see Figure 2).

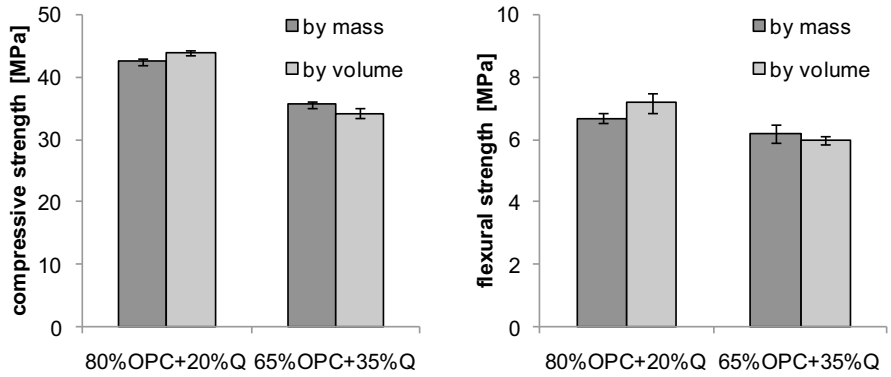

Figure 2: Comparison of the effect of replacement by mass and by volume on 28 day compressive and flexural strength results for two different combinations of OPC and crystalline quartz, Q (density 2700kg/m^3).

Three mortar prisms of 40×40×160 mm were prepared for all the tested combinations according to NS-EN 196-1 (water-to-powder ratio 0.50, powder : sand = 1:3). The flexural and compressive strength was determined after 28 days of curing submerged in saturated lime water.

The volume of air voids in the mortars was determined according to [28]. The mortar samples are first dried in an oven at 105ºC for 1 week. Then their dry mass is determined. After this the samples are submerged in water for a week. When weighing the samples after this, the amount of water taken up due to capillary suction can be determined. During the last step of the procedure the samples are put into a pressure tank at 50 MPa for 2 days. From the mass of the samples weighed immediately after removing them from the pressure tank, one can calculate the volume of air voids in the samples assuming that the air voids fill under pressure, but can not fill by capillary suction due to their large radius.

The volume of air voids of the mortar samples was determined in order to take into account their effect on the compressive strength. The rule of thumb applied, is that a 1% increase in air void volume will lead to a 5% decrease in compressive strength [29]. The results were corrected relative to the average air porosity.

For all tested combinations, 300 ml of paste was made with a water-powder ratio of 0.50. The mixing water was distilled water. No admixtures were used, as all pastes were stable and mixable at this water-to- powder ratio. The pastes were mixed with a Braun MR5550CA high shear mixer. The mixing procedure consisted of mixing for half a minute, resting for five minutes and mixing again for one minute. The paste was poured into 15 ml glass vials and was stored under sealed conditions at 20°C.
To stop the hydration after 28 days, a sample of paste was crushed and washed twice with 150 ml ethanol. The suspension was filtrated. The remaining wet slurry was then poured into a glass vial which was sealed with a plastic lid to avoid evaporation of the ethanol.

Simultaneous TGA/SDTA analyses were performed on these wet slurries with a Mettler Toledo TGA/SDTA851. Samples of about 200mg were weighed into aluminium oxide crucibles. The samples were first dried inside the TGA/SDTA by purging them with N_2 for about 2 hours at 40ºC. The weight of the sample was monitored during drying and the analysis was started when

approximately constant weight was reached. This is however not a defined equilibrium condition. One might prefer to dry the samples at a certain RH until equilibrium is reached, but this might lead to carbonation during the handling the samples. By drying the samples in the TGA apparatus, carbonation could be limited to a minimum.

After this the samples were heated from 40ºC to 1,100ºC at a heating rate of 10ºC/min. During the analysis the oven was purged with N_2 at 50ml/min.

During a thermogravimetric analysis (TGA), the weight of the sample is monitored as a function of the temperature. The weight loss observed when the sample is heated from room temperature up to about 600ºC is due to the release of water bound in hydrates (H). Between 450ºC and 550ºC, a sharp weight loss step occurs. This is due to the decomposition of calcium hydroxide (CH). At temperatures above 600ºC carbonates decompose and weight losses are registered as the sample releases CO_2. The carbonates can originate from limestone powder if the sample contained limestone, any dehydrated calcium carboaluminate hydrate formed and/or carbonates which could have formed due to carbonation of the sample.

The weight losses were determined in two different temperature intervals. The weight loss due to the decomposition of CH, ranging from about 450ºC to 550ºC, and the weight loss corresponding to the release of bound water (H), measured between 50°C and about 550-600°C. The start and ending of each temperature interval is determined for each sample based on the DTG-curve.

The standard deviation for the thermogravimetric measurements are 0.3% for the H measurements and 0.05% for the CH measurements. This data is based on the results of three independent experiments.

The weight losses are expressed as a % of the “dry sample mass” or OPC content. The “dry sample mass” is the weight at 600°C.

For some mixes of particular interest small amounts were dried gently over $CaCl_2$ in order to analyse them with an AXS D8 focus X-ray diffractometer. The diffractometer had a CuKα source and a 0.2 mm slit was used. An angular scan was performed for diffraction angles between 5 and 75° 2θ with an increment of 0.04° 2θ and a scanning speed of 0.3 s/step. The XRD-spectra give a qualitative idea of the crystalline hydration products formed, not a quantitative. The spectra are given as a function of the characteristic lattice distance, d.

3 RESULTS AND DISCUSSION

In Table 4 the compressive and flexural strength, the air porosity and the corrected compressive strength for all tested combinations are given. One can see that fly ash containing cements have a tendency to lower the air content in the mortars. For limestone powder the opposite seems to be the case. This might be due to the effect of these materials on the compactibility of the mortars. Round fly ash particles are known to improve workability and fine limestone powder is known to stabilize and thicken mortars and concretes. By correcting the compressive strength for the air voids, the strength of the fly ash containing mixes is slightly reduced and the limestone containing blends is slightly increased. The trends observed in the results however do

not change whether or not the compressive strength is correct for the air content. For the following discussion the not-corrected results will be used.

Table 4: The mean value and standard deviation of the compressive and flexural strength, the air porosity and the corrected compressive strength for all tested combinations after 28 days of curing at 20°C.

mix	C	F	L	flexural	compressive	air porosity	compressive difference	corrected
	[%]			[MPa]	[MPa]	[%]	[%]	[MPa]
1	100	0	0	7.1 ± 0.3	48.3 ± 0.7	2.6 ± 0.2	3.4	49.9
2	95	0	5	7.7 ± 0.1	49.7 ± 0.3	2.7 ± 0.0	4.1	51.8
3	90	0	10	7.7 ± 0.3	48.8 ± 0.4	2.4 ± 0.1	2.5	50.0
4	85	0	15	7.8 ± 0.2	48.1 ± 0.4	2.2 ± 0.2	1.7	48.9
5	80	0	20	7.3 ± 0.1	46.1 ± 0.3	2.1 ± 0.1	0.8	46.5
6	75	0	25	6.8 ± 0.2	42.9 ± 0.3	2.6 ± 0.1	3.4	44.3
7	70	0	30	7.1 ± 0.2	40.7 ± 0.4	2.4 ± 0.1	2.6	41.7
8	65	0	35	6.6 ± 0.2	37.6 ± 0.4	2.5 ± 0.1	2.8	38.6
9	95	5	0	8.0 ± 0.1	49.7 ± 0.8	1.8 ± 0.2	-0.3	49.6
10	90	10	0	7.9 ± 0.2	49.2 ± 1.0	1.5 ± 0.1	-2.3	48.1
11	85	15	0	7.8 ± 0.3	46.5 ± 0.6	1.4 ± 0.1	-2.4	45.3
12	80	20	0	7.6 ± 0.2	45.2 ± 0.4	1.4 ± 0.1	-2.4	44.1
13	75	25	0	7.1 ± 0.5	42.9 ± 1.0	1.4 ± 0.1	-2.4	41.8
14	70	30	0	7.0 ± 0.3	41.2 ± 1.0	1.5 ± 0.2	-1.9	40.4
15	65	35	0	6.2 ± 0.4	38.8 ± 0.7	1.4 ± 0.1	-2.7	37.8
16	65	30	5	7.3 ± 0.1	42.4 ± 0.7	1.6 ± 0.1	-1.3	41.8
17	65	25	10	7.3 ± 0.2	41.3 ± 0.5	1.6 ± 0.0	-1.4	40.7
18	65	20	15	7.3 ± 0.2	40.7 ± 0.4	1.7 ± 0.0	-1.1	40.3
19	65	15	20	6.6 ± 0.2	39.9 ± 0.5	1.6 ± 0.1	-1.6	39.2
20	65	10	25	6.8 ± 0.2	39.2 ± 0.4	1.8 ± 0.0	-0.7	39.0
21	65	5	30	6.3 ± 0.1	38.2 ± 0.4	1.8 ± 0.1	-0.6	38.0

In Figure 3 the compressive strength of cements containing different amounts of either fly ash or limestone powder are given. It can be seen that part of the OPC can be replaced with limestone powder without impairing the compressive strength after 28 days of hydration (up to 15%). Replacing 5% of the OPC by limestone even increases the compressive strength. A similar effect is observed for the fly ash. This might partly be due to better compaction properties of the mortars contain fly ash as the strength increase disappears when the strength is corrected for the air content. It seems as if fly ash has not reacted that much since the compressive strength of the mortars containing fly ash is similar to the ones containing limestone powder.

The flexural strengths of cements containing different amounts of either fly ash or limestone powder are given in Figure 4. The relative standard deviations of the results are large, up to 7%. Even so it can be seen that replacing part of the OPC with limestone powder or fly ash improves the flexural strength up to replacement levels of about 20%.

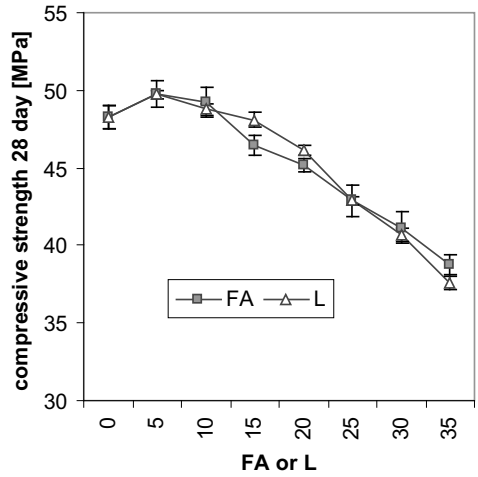

Figure 3: The 28 day compressive strength not-corrected for the air content for cements in which OPC is replaced by fly ash and limestone powder up to 35%.

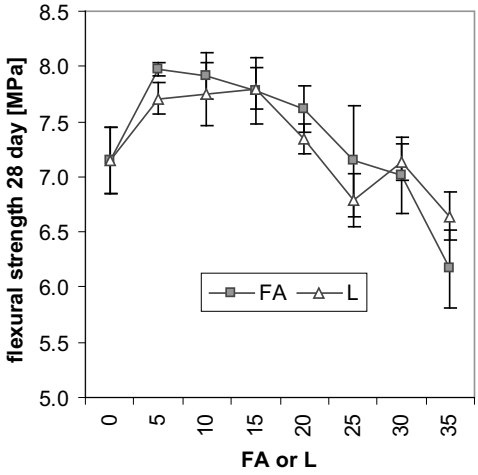

Figure 4: The 28 day flexural strength for cements in which OPC is replaced by fly ash and limestone powder up to 35%.

Figure 5 shows the compressive strength of composite cements in which 35% of the OPC is replaced by different combinations of fly ash and limestone powder. A significant compressive strength increase can be observed when instead of 35% fly ash, a combination of 5% limestone and 30% fly ash is used. This strength increase is about 4 MPa, which is approximately a 10% increase in compressive strength. This indicates that the postulated chemical synergic effect between fly ash and limestone plays a significant role. This beneficial effect on the compressive strength decreases with further increasing limestone powder content. In the corresponding flexural strength results a similar trend can be observed (see Figure 6).

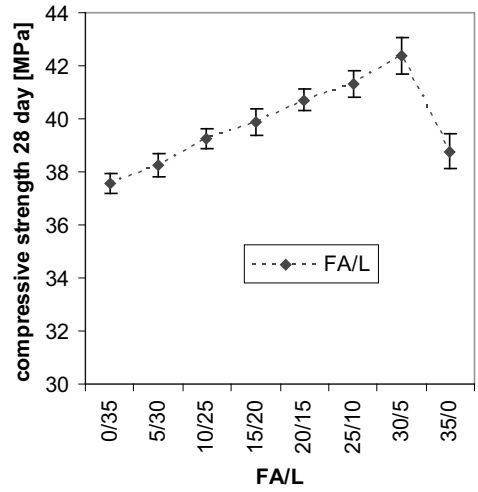

Figure 5: The 28 day compressive strength for composite cements containing 65% OPC and different combination of fly ash and limestone powder.

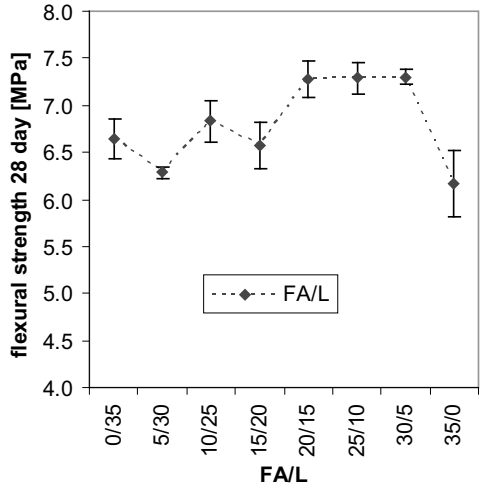

Figure 6: The 28 day flexural strength for composite cements containing 65% OPC and different combination of fly ash and limestone powder.

The compressive strength results of the cements with only fly ash are compared with those of the composite cements containing different combinations of fly ash and limestone powder in Figure 7.

The fly ash curve with filled squares (FA) represents the compressive strength results for cements in which the OPC is replaced only by fly ash. The replacement levels go from 0% in the left of the graph to 35% in the right side in steps of 5%. The dotted with black diamonds (FA+L) represents cements containing 65%OPC and 35% of different combination of fly ash and limestone.

An interesting result is the fact that cement containing 30% fly ash and 70% OPC has a slightly lower compressive strength after 28 days than a cement containing 30% fly ash, 5% limestone and 65% OPC. This means that in this case replacing 5% of the OPC with 5% limestone powder results in a slightly higher compressive strength after 28 days. This result shows that the cement producers could burn 5% less clinker and instead add limestone powder. This is both economically and environmentally beneficial, as less energy is needed and less CO_2 will be emitted.

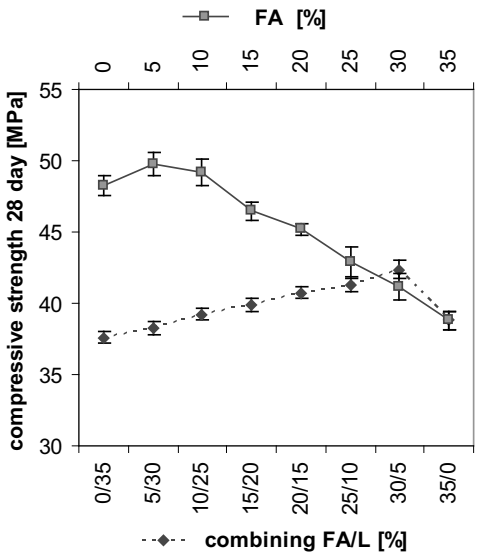

Figure 7: Comparing the 28 day compressive strength of the composite cements with different combination of fly ash and limestone powder and 65% OPC (lower abscissa), and the cements in which OPC is gradually replaced by fly ash (upper abscissa). Different abscissae were used to be able to compare cements with different OPC content and evaluate whether part of the OPC can be replaced by limestone powder without impairing the strength.

In Figure 8 the compressive strength results are compared with the thermogravimetric (TG) results for different replacement levels of OPC with limestone powder.

The decrease in calcium hydroxide per *dry content*, when the OPC is increasingly replaced by limestone powder, is due to the dilution effect. OPC is the major reactive component, and as the amount of OPC decreases in the sample the amount of reaction products, such as CSH and CH, will also decrease.

More interesting is the observation that the amount of CH per *OPC content* decreases slightly when 5% and even 10% of OPC is replaced by limestone powder. Due to the filler effect of the limestone powder one would expect that the amount of CH would increase, but the amount of produced CH only starts to increase when 15% or more of the OPC is replaced by limestone powder.

When 5% of OPC is replaced by limestone powder, the amount of bound water (H) per OPC and the compressive strength increases, but the CH content decreases. A strength increase should correspond to an increase in hydration products formed (H). Assuming the following reaction for the hydration of the main OPC mineral alite (C_3S):

$$C_3S + 2.3\ H \rightarrow C_{1.7}SH + 1.3\ CH \qquad (1)$$

According to equation 1, a strength increase caused by an increase of hydration products like CSH would also implicate an increase in CH if the C/S of CSH remains constant. A decrease in the amount of CH and a corresponding increase in strength can only be explained by either the formation of CSH with a higher C/S ratio or the formation of other hydration products (e.g. alumina or iron rich hydration products) consuming CH.

The decrease in calcium hydroxide can be explained by the formation of calcium hemicarboaluminate hydrate ($C_3A{\cdot}0.5CaCO_3{\cdot}0.5Ca(OH)_2{\cdot}11.5H_2O$) that in accordance with the formula will consume half a mole $Ca(OH)_2$ per mole $CaCO_3$ [7, 11, 27].

The amount of chemically bound water gives an indication about the degree of hydration, and therefore also for the strength development for a given cement. The compressive strength and amount of chemically bound water follow the same trend as they both increase when 5% of the OPC is replaced by limestone powder. For higher replacement levels (>5%) both properties decrease steadily (see Figure 8).

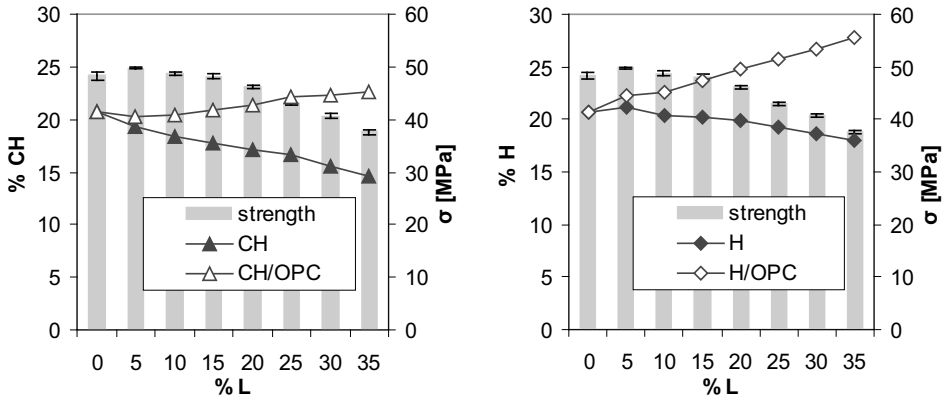

Figure 8: Comparison between the compressive strength and the amount of calcium hydroxide (CH) and bound water (H) both relative to the dry samples mass and the OPC content for limestone cements after 28 days of curing at 20°C.

In Figure 9 the compressive strength results are compared with the thermogravimetric (TG) results for different replacement levels of OPC with fly ash.

The amount of calcium hydroxide (CH) is given both relative to the dry sample mass and to the OPC content. The amount of CH relative to the dry sample mass, decreases due to the dilution effect. The amount of CH relative to the OPC content on the other hand increases due to the filler effect. Fly ash can react with the CH in a pozzolanic reaction and form hydration products similar to the ones of OPC. From the compressive strength results, it appeared that fly ash had

not reacted that much after 28 days of curing at 20°C. The strength of the fly ash cements was similar to the corresponding limestone cements. The amount of CH relative to the OPC content flattens out at replacement levels above 15% and even decreases a bit at 35%. This might indicate that the fly ash has reacted somewhat. As more fly ash is present some more CH has been consumed.

The compressive strength is compared with the amount of bound water in Figure 9. The results correlate quite well as both the compressive strength and amount of chemically bound water are quite similar for the reference up to the one containing 10% fly ash but then decrease with increasing replacement level. The decreasing trend is due to the dilution effect. The filler effect on the other hand is visible when the amount of chemically bound water is expressed relative to the amount of OPC. The amount of chemically bound water relative to the OPC content increases with increasing OPC replacement.

In Figure 10 and Figure 11 the compressive strength results are compared with the thermogravimetric (TG) results for different combinations of fly ash and limestone powder replacing 35% of the OPC.

When 5% to 15% of the fly ash is replaced by limestone, the amount of CH decreases compared to the cement with 35% fly ash. Initially one would expect the opposite as the fly ash should consume CH during its pozzolanic reaction. Therefore a higher amount of fly ash should lead to less CH. The amount of produced CH starts to increase only when 20% of the limestone powder or more is included in the system. The decrease in CH is accompanied by an increase in compressive strength. The reason is probably, as described for OPC/limestone, that calcium hemicarboaluminate hydrate is formed.

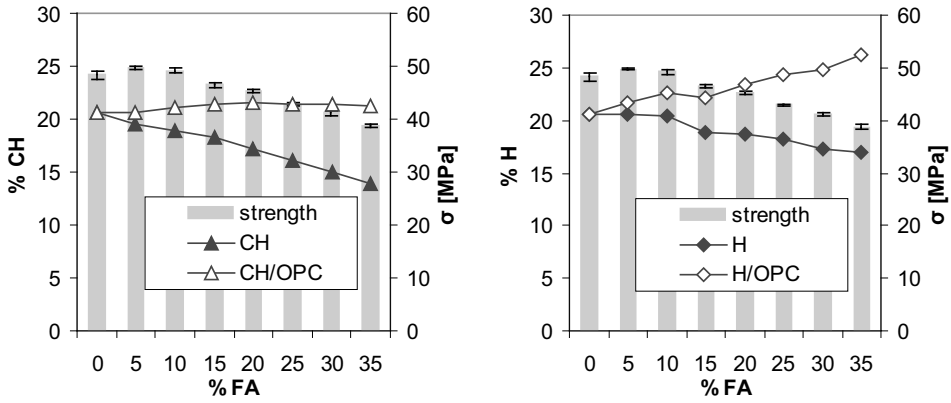

Figure 9: Comparison between the compressive strength and the amount of calcium hydroxide (CH) and bound water (H) both relative to the dry samples mass and the OPC content for fly ash cements after 28 days of curing at 20°C.

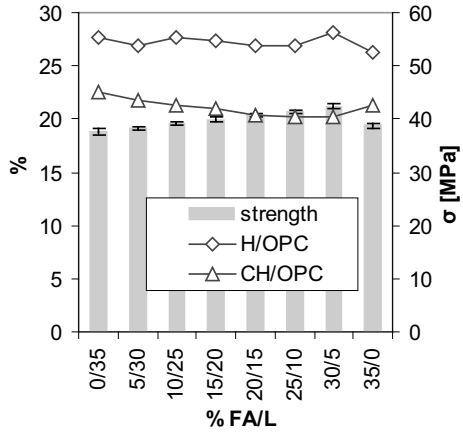

Figure 10: Comparison between the compressive strength and the amount of calcium hydroxide (CH) and bound water (H) relative to the OPC content for composite cements containing 65% OPC and a combination of fly ash and limestone powder after 28 days of curing at 20°C.

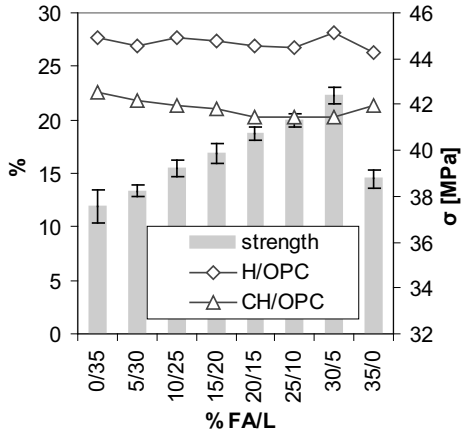

Figure 11: Magnification of the ordinate in Figure 10 in order to visualize the synergetic effect better.

From the previous results it can be concluded that an interesting phenomenon occurs when small amounts of limestone are used to replace both ordinary Portland cement and fly ash cement. The amount of CH decreases and the compressive strength increases. The effect on the fly ash cement seemed to be stronger than on the OPC, although the fly ash had not react that much. The thermogravimetric curves (TG-curves) and the differential thermogravimetric curves (DTG-curves) of some interesting combinations were compared in order to understand this phenomenon better. In Figure 12 the TG and DTG are depicted for 100%OPC cement and 100%OPC+5%L. Figure 13 shows the corresponding curves for 65%OPC+35%FA and 65%OPC+30%FA+5%L.

From Figure 12 it can be seen that the limestone containing cement binds about the same amount of water than the reference, as they reach about the same total weight loss at about

600°C. Some differences can be seen between the DTG-curves of the two cements. First there is the peak just above 100°C. This peak is partly due to the decomposition of ettringite. Limestone powder seems to stabilize the ettringite as expected. This peak should however always be interpreted with care as it is very sensitive to the preparation of the samples and the pre-drying. Secondly there is dissimilarity between 600°C and 800°C. This is due to the decomposition of the $CaCO_3$ present in the limestone powder. A remarkable difference between the two curves is the double peak for the reference around 180°C, which turns into a single peak when limestone is included in the system. The curves are also different between 200 and 400°C. The differences indicate that there is a change in hydration products when limestone powder is included in the system.

From Figure 13 it can be seen that when 5% of the fly ash is replaced by limestone powder more water is bound, as the total weight loss at about 600°C is larger. The DTG curves are fairly similar to the once shown in Figure 12, except for the weight changes at 750°C and higher, caused by the fly ash present in the system and the lower content of calcium hydroxide (between 400 and 500°C) due to the both dilution effect and slight pozzolanic reaction of the fly ash. Once more, the double peak around 180°C shown for the fly ash cement without limestone powder, turns into a single peak when limestone is included in the system and the ettringite appears to be stabilized.

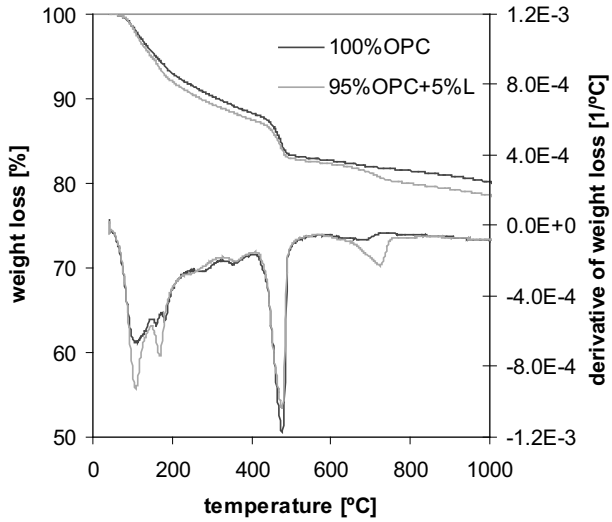

Figure 12: Thermogravimetric curves (TG) and differential thermogravimetric curves (DTG) for the reference (100% OPC) and a limestone cement (5% limestone powder + 95% OPC hydrated for 28 days).

In order to try to understand this change in hydration products X-ray diffraction analysis were performed. The cements tested were:

- 100% OPC (reference)
- 95% OPC + 5% limestone powder
- 65% OPC + 35% fly ash
- 65% OPC + 30% fly ash + 5% limestone powder

The pastes had hydrated for 28 days at 20°C when they were analysed.

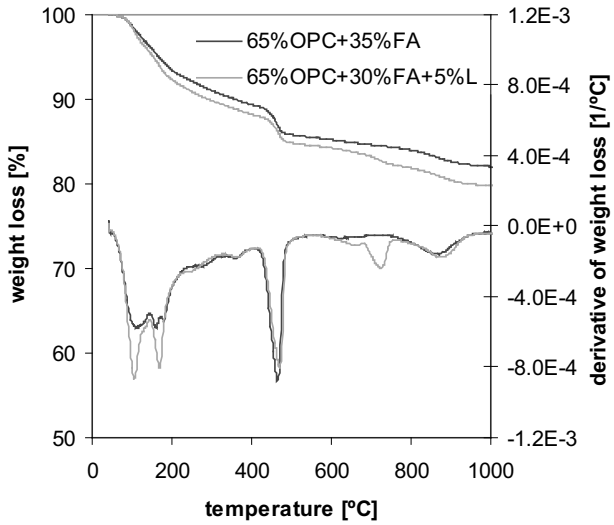

Figure 13: Thermogravimetric curves (TG) and differential thermogravimetric curves (DTG) for a fly ash cement containing 65% OPC and 35% fly ash and a composite cement containing 65% OPC, 5% limestone powder and 30% fly ash hydrated for 28 days.

In Figure 14 the XRD spectra of the tested cements are shown. The d-range of particular interest was enlarged and is shown in Figure 15. The main crystalline phases were:

•	CH	portlandite	$Ca(OH)_2$
•	Q	quartz	SiO_2
•	C$\underline{C}$	calcium carbonate	$CaCO_3$
•	E	ettringite	$C_3A{\cdot}3CaSO_4{\cdot}32H_2O$
•	MS	calcium monosulphoaluminate hydrate	$C_3A{\cdot}CaSO_4{\cdot}12H_2O$
•	M$\underline{C}$	calcium monocarboaluminate hydrate	$C_3A{\cdot}CaCO_3{\cdot}11H_2O$
•	H$\underline{C}$	calcium hemicarboaluminate hydrate	$C_3A{\cdot}0.5CaCO_3{\cdot}0.5Ca(OH)_2{\cdot}11.5H_2O$

It can be seen that when limestone powder is present the calcium monosulphate hydrate disappears and instead ettringite, calcium monocarbonate hydrate and calcium hemicarbonate hydrate are formed.

The effect of small additions of limestone powder seemed to be more pronounced for the fly ash cements than for the ordinary Portland cement. This might be due to the liberation of additional aluminates by the fly ash. They cause a decrease of the sulphate/aluminate ratio of the system. Therefore relatively more calcium monosulphate hydrate than ettringite will form in the fly ash

blended cement. The presence of limestone will then have a larger impact as more calcium monosulphate hydrate will shift to ettringite in a fly ash containing cement as calcium monocarboaluminate hydrate and calcium hemicarboaluminate hydrate are formed. This process will lead to relatively more bound water and higher total volume of hydrates, which in turn will decrease porosity and increase strength even more in the case of fly ash blended cements compared to OPC. The chemistry of this synergy was recently elaborated by De Weerdt and Justnes [30] .

The applicability of this study is proven by a pilot project recently launched by the Norwegian cement manufacturer Norcem using a "low carbon", environmentally friendly cement containing 65%OPC, 30% fly ash and 5% limestone [31] .

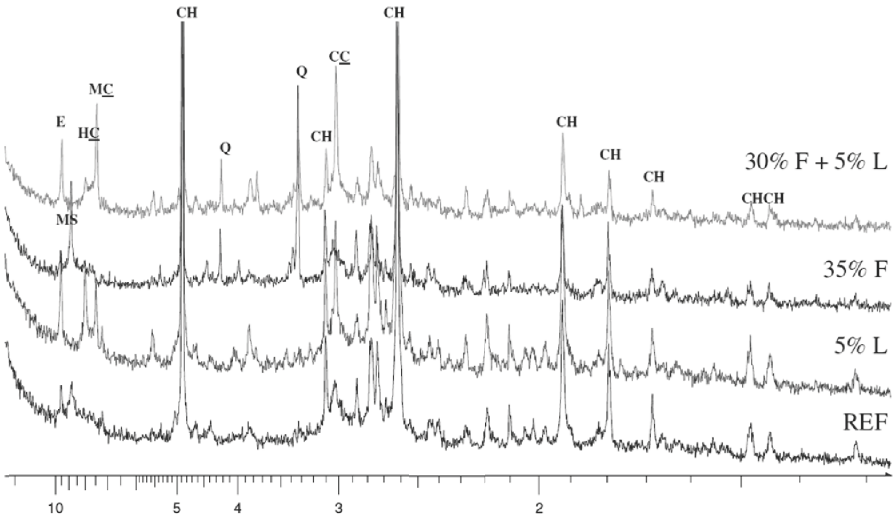

Figure 14: X-ray spectra for 100% OPC (REF), 95% OPC and 5% L (5% L), 65% OPC and 35% FA (35% F), and 65% OPC, 30% FA and 5% L (30% F + 5% L) all hydrated for 28 days at 20°C.

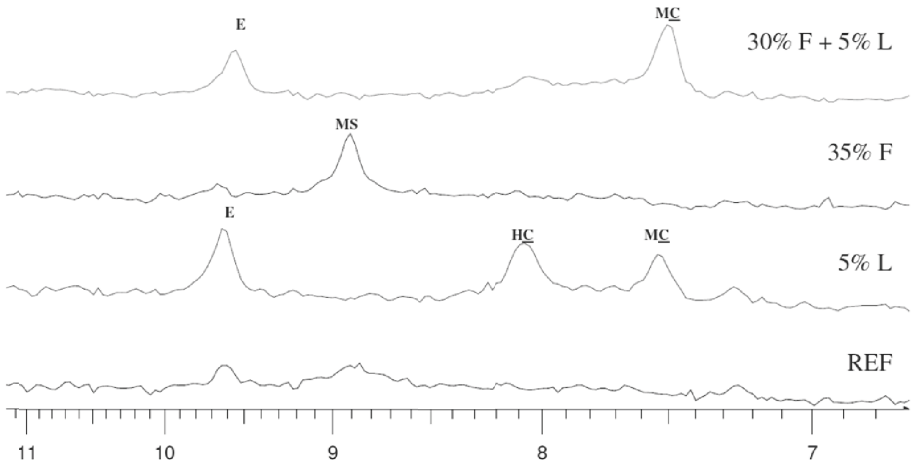

Figure 15: Zoomed in on the X-ray spectra for 100% OPC (REF), 95% OPC and 5% L (5% L), 65% OPC and 35% FA (35% F), and 65% OPC, 30% FA and 5% L (30% F + 5% L) all hydrated for 28 days at 20°C.

4 CONCLUSION

The compressive strength results at 28 days indicated a synergetic interaction between fly ash and limestone powder. Replacing 5% of fly ash with 5% of limestone powder in the 65% OPC + 35% FA cement resulted in a strength increase of about 10% (from 38 MPa to 42 MPa). The replacement of 5% OPC with limestone powder only resulted in a strength increase of about 4% (from 49.9 MPa to 51.8 MPa). Moreover, the combination 65% OPC + 30% FA + 5% L had a higher compressive strength after 28 days than the cement prepared with 70% OPC + 30% FA (41 MPa). This means that in this case it would be more beneficial to use 5% of limestone instead of 5% of OPC.

The thermogravimetric results showed that the hydration products change when limestone powder is included in the system. Moreover small additions of limestone resulted in a slight decrease of calcium hydroxide, indicating a possible formation of calcium hemicarboaluminate hydrate.

The X-ray diffraction results showed a change in crystalline hydration products. Calcium monosulphoaluminate hydrate disappears when limestone powder is present and instead ettringite, calcium monocarboaluminate hydrate and calcium hemicarboaluminate hydrate form.

It can be concluded that minor additions of limestone powder can have a beneficial effect on the strength development of Portland cement after 28 days of hydration most likely related to the interaction with the AFm and AFt phases. For fly ash containing cements this effect seems to be even greater.

Further research should be done to further explain this phenomenon. For example figuring out whether this is a pure chemical interaction or are there as well some physical effects playing a role in this, quantifying the chemical and physical effect etc. It is also important to look at how the interaction between fly ash and limestone powder evolves over time and how it will affect creep, shrinkage, durability, etc.

5 Acknowledgements

The authors would like to acknowledge COIN, the COncrete INnovation centre (www.coinweb.no) for the financial support.

REFERENCES

[1] Damtoft JS, Lukasik J, Herfort D, Sorrentino D, Gartner EM. Sustainable development and climate change initiatives. Cement and Concrete Research. 2008;38(2):115-127.

[2] Justnes H. Principles of making cement with reduced CO_2 emission. COIN State of the art report, wwwcoinwebno; 2007.

[3] Justnes H. Making cements with less clinker content. COIN State of the art report, wwwcoinwebno; 2007.

[4] EN 197.1: 2000+A1. Part 1: Composition, specifications and conformity criteria for commen cements 2005.

[5] Ramachandran VS. Thermal analyses of cement components hydrated in the presence of calcium carbonate. Thermochimica Acta. 1988;127:385-394.

[6] Péra J, Husson S, Guilhot B. Influence of finely ground limestone on cement hydration. Cement and Concrete Composites. 1999;21(2):99-105.

[7] Kakali G, Tsivilis S, Aggeli E, Bati M. Hydration products of C_3A, C_3S and Portland cement in the presence of $CaCO_3$. Cement and Concrete Research. 2000;30(7):1073-1077.

[8] Soroka I, Stern N. Calcareous fillers and the compressive strength of portland cement. Cement and Concrete Research. 1976;6(3):367-376.

[9] Kuzel HJ, Pöllmann H. Hydration of C_3A in the presence of $Ca(OH)_2$, $CaSO_4 \cdot 2H_2O$ and $CaCO_3$. Cement and Concrete Research. 1991;21(5):885-895.

[10] Vernet C, Noworyta G. Mechanisms of limestone fillers reactions in the system {C3A-CSH2-CH-CC-H}: Competition between calcium monocarbo- and monosulpho-aluminate hydrates formation. 9th ICCC. New Delhi, India; 1992. p. 430-436.

[11] Bonavetti VL, Rahhal VF, Irassar EF. Studies on the carboaluminate formation in limestone filler-blended cements. Cement and Concrete Research. 2001;31(6):853-859.

[12] Matschei T, Lothenbach B, Glasser FP. The AFm phase in Portland cement. Cement and Concrete Research. 2007;37(2):118-130.

[13] Lothenbach B, Le Saout G, Gallucci E, Scrivener K. Influence of limestone on the hydration of Portland cements. Cement and Concrete Research. 2008;38(6):848-860.

[14] Hirao H, Yamada K, Hoshino S, Yamashita H. The effect of limestone addition on the optimum sulphate levels of cements having various Al_2O_3 contents. 12th ICCC. Montreal; 2007.

[15] ASTM C618-08a. Standard specification for coal fly ash and raw or calcined natural pozzolan for use in concrete. In: ASTM International WC, PA, 2008, DOI: 10.1520/C0618-08 editor.

[16] Fraay ALA, Bijen JM, de Haan YM. The reaction of fly ash in concrete a critical examination. Cement and Concrete Research. 1989;19(2):235-246.

[17] Fraay A, Bijen JM, Vogelaar P. Cement-stabilized fly ash base courses. Cement and Concrete Composites. 1990;12(4):279-291.

[18] Pietersen HS. The reactivity of fly ash in cement geochemistry. Delft: TU Delft; 1993. p. 271.

[19] De Weerdt K, Justnes H. Microstructure of binder from the pozzolanic reaction between lime and siliceous fly ash and the effect of limestone addition. In: Sun W, van Breugel K, Miao C, Ye G, Chen H, editors. Microstructure Related Durability of Cementitious Composites Nanjing; 2008. p. 107-116.

[20] Menéndez G, Bonavetti V, Irassar EF. Strength development of ternary blended cement with limestone filler and blast-furnace slag. Cement and Concrete Composites. 2003;25(1):61-67.
[21] Carrasco MF, Menéndez G, Bonavetti V, Irassar EF. Strength optimization of "tailor-made cement" with limestone filler and blast furnace slag. Cement and Concrete Research. 2005;35(7):1324-1331.
[22] Ghrici M, Kenai S, Said-Mansour M. Mechanical properties and durability of mortar and concrete containing natural pozzolana and limestone blended cements. Cement and Concrete Composites. 2007;29(7):542-549.
[23] Elkhadiri I, Diouri A, Boukhari A, Aride J, Puertas F. Mechanical behaviour of various mortars made by combined fly ash and limestone in Moroccan Portland cement. Cement and Concrete Research. 2002;32(10):1597-1603.
[24] Yilmaz B, Olgun A. Studies on cement and mortar containing low-calcium fly ash, limestone, and dolomitic limestone. Cement and Concrete Composites. 2008;30(3):194-201.
[25] Sato T, Beaudoin JJ. The effect of nano-sized $CaCO_3$ addition on the hydration of cement paste containing high volumes of fly ash. 12th ICCC. Montreal; 2007. p. 1-12.
[26] Härdtl R, Dietermann M, Schmidt K. Durability of blended cements with several main components. 12th ICCC. Montréal; 2007.
[27] Hoshino S, Yamada K, Hirao H. XRD/Rietveld analysis of the hydration and strength development of slag and limestone blended cement. Journal of Advanced Concrete Technology. 2006;4(3):357-367.
[28] Sellevold EJ, Farstad T. The PF-method - A simple was to estimate the w/c-ratio and air content of hardened concrete. ConMat'05. Vancouver, Canada; 2005. p. 10.
[29] Neville AM. Properties of concrete - Fourth edition. Prentice Hall, Pearson Education Limited, 2000.
[30] De Weerdt K, Justnes H. Synergic reactions in triple blended cements. 11th NCB International Seminar on Cement and Building Materials. New Delhi; 2009. p. 257-261.
[31] Mathisen E. Green cement for the house of the future (in Norwegian). Cement Nå. Oslo, Norway: Norcem HeidelbergCement Group 2009. p. 3-6.

Paper IV

Synergy between fly ash and limestone powder in ternary cements
De Weerdt K., Kjellsen K.O., Sellevold E.J. & Justnes H.
Cement and Concrete Composites, 2011, Vol.33 (1) pp. 30-38.
doi:10.1016/j.cemconcomp.2010.09.006

Cement & Concrete Composites 33 (2011) 30–38

Contents lists available at ScienceDirect

Cement & Concrete Composites

journal homepage: www.elsevier.com/locate/cemconcomp

Synergy between fly ash and limestone powder in ternary cements

K. De Weerdt [a,*], K.O. Kjellsen [b,c], E. Sellevold [a,b], H. Justnes [a]

[a] SINTEF Building and Infrastructure, 7465 Trondheim, Norway
[b] NTNU, Department of Structural Engineering, 7491 Trondheim, Norway
[c] Norcem AS, Heidelberg Cement Group, Setreveien 2, 3991 Brevik, Norway

ARTICLE INFO

Article history:
Received 17 June 2010
Received in revised form 2 September 2010
Accepted 7 September 2010
Available online 16 September 2010

Keywords:
Cement
Fly ash
Limestone
AFm
Ternary
Calcium carboaluminate hydrates

ABSTRACT

The interaction between limestone powder and fly ash in ternary composite cement is investigated. Limestone powder interacts with the AFm and AFt hydration phases, leading to the formation of carboaluminates at the expense of monosulphate and thereby stabilizing the ettringite. The effect of limestone powder on OPC may be restricted due to the limited amount of aluminate hydrates formed by the hydration of OPC. The additional aluminates brought into the system by fly ash during its pozzolanic reaction amplify the mentioned effect of limestone powder. This synergistic effect between limestone powder and fly ash in ternary cements is confirmed in this study and it translates to improved mechanical properties that persist over time.

1. Introduction

It is estimated that cement production is responsible for about 5% of the global man-made CO_2 emissions [1]. This fact, together with the still increasing volume of cement produced worldwide renders the cement industry an important contributor to the global CO_2 emission. For each ton of cement produced on average 0.87 tons of CO_2 is emitted [1]. The cement industry is putting huge efforts into reducing the emission during cement manufacturing, for example by using alternative fuels and by optimising the heat transfer in the production of clinker. An additional option widely adopted is the use of blended cements in which part of the clinker is replaced by "supplementary cementing materials" (SCM) or fillers. Supplementary cementing materials such as silica fume, fly ash, ground granulated blast furnace slag and natural pozzolans have been used for many years. As the pressure to reduce emissions is rising, research is being directed towards increasing the replacement levels of clinker and optimising different combinations of supplementary materials.

In this study ternary cements containing ordinary Portland cement (OPC) and different replacement levels of limestone powder and siliceous class F fly ash are investigated. The effect of limestone powder on OPC is twofold. Fine limestone powder exerts a physical filler effect on the OPC hydration. Replacing part of the OPC with limestone will increase the effective water to OPC ratio, and provide additional surface for precipitation of hydration products, thereby promoting the early age hydration of the OPC [2–5]. Besides the filler effect, there is also a chemical effect: the calcium carbonate of the limestone powder can interact with the aluminate hydrates formed by OPC hydration [6–9]. Calcium monosulphoaluminate hydrate is unstable in the presence of calcium carbonate, and instead calcium mono- and hemicarboaluminate hydrate will form. This leads to the stabilisation of the ettringite and will result in an increase in the total volume of the hydration products [9–12], which potentially might result in a decrease in porosity and thus an increase in strength. The effect of this chemical interaction in an OPC–limestone system is, however, not so pronounced due to the limited aluminate content in the anhydrous clinker. In an ordinary Portland cement the limestone filler is therefore often considered inert. Additional calcium aluminate hydrates may be produced by supplementary cementitious materials (SCM's) containing aluminates (e.g. slag, fly ash, metakaolin). The chemical interaction between calcium aluminate hydrates and calcium carbonate might therefore be of greater importance in cements containing fly ash or other aluminates containing SCMs [13].

A clear demonstration of interaction between fly ash and limestone powder was observed when studying fly ash–limestone–calcium hydroxide mixes prepared with a high alkaline solution (pH = 13.2) [14]. More water was bound relative to the fly ash content, and the hydration products formed were altered when limestone was included in the system. The calcium aluminate hydrates formed during the pozzolanic reaction reacted with the calcium

* Corresponding author. Address: Richard Birkelandsvei 3, 7465 Trondheim, Norway. Tel.: +47 73594866.
E-mail address: klaartje.de.weerdt@sintef.no (K. De Weerdt).

0958-9465/$ - see front matter © 2010 Elsevier Ltd. All rights reserved.
doi:10.1016/j.cemconcomp.2010.09.006

carbonate of the limestone powder, and formed calcium carboaluminate hydrates.

In a study evaluating the effect of fineness of the different materials in a ternary composite cement, a substantial strength increase was observed after 28 days of curing when combining fly ash and limestone powder compared to only using fly ash [15]. However the tests were only performed on very fine ground materials. Subsequently, a series of mortar and paste mixes were prepared with ternary cements containing OPC, limestone powder and fly ash, but from an industrial point of view, more realistic finenesses [16,17]. The samples were tested after 28 days of curing at 20 °C. A similar strength increase was observed when a small part of the fly ash was replaced by limestone powder as in [15].

The aim of this study is to investigate the interaction between limestone powder and fly ash in ternary composite cements after longer times, up to 140 days of hydration. Both compressive and flexural strength of mortars have been measured. In addition, thermogravimetric analysis (TGA) was used to determine the content of bound water and calcium hydroxide and X-ray diffraction (XRD) was applied to identify the AFm and AFt phases.

2. Materials and experimental

The materials used in this study were: ordinary Portland clinker, a class F ASTM siliceous fly ash (FA), limestone powder and natural gypsum. The chemical composition of the ordinary Portland clinker, fly ash and limestone powder are given in Table 1. The natural gypsum contained 0.2% free water, and had a $CaSO_4{\cdot}2H_2O$ content of 91.4%. Additional properties of the fly ash are found in [18]. The $CaCO_3$ content of the limestone as determined by TGA was about 81%.

The materials were ground in a laboratory ball mill with a capacity of about 9 kg. Fly ash and limestone powder were ground separately. The clinker interground with 3.7% of gypsum by mass is referred to as OPC. The Blaine specific surface and density are given in Table 1. The finenesses of the different materials were selected based on the results found in a previous study [15]. The fly ash was ground for 15 min in order to crush the largest particles. This corresponds to common practice in Portland fly ash cement manufacturing, where the fly ash is added in the air separator at the end of the cement mill. In that case, the largest particles will be returned to the ball mill and be crushed.

Table 2 shows the different composite cements which were tested. The experimental matrix can be divided into three main groups and the reference, 100% OPC (mix 1). In the first group, OPC is gradually replaced by limestone powder, in steps of 5% up to 35% (mix 2–8). In the second group OPC is similarly replaced with fly ash (mix 9–15). In the third group different limestone powder and fly ash combinations were tested (mix 16–21), all at a total OPC replacement level of 35% by mass.

Table 1
Chemical composition and physical characteristics of the clinker, fly ash and limestone.

	Clinker	Fly ash	Limestone
SiO_2	20.8	50.0	12.9
Al_2O_3	5.6	23.9	2.7
Fe_2O_3	3.2	6.0	2.0
CaO	63.0	6.3	42.3
MgO	3.0	2.1	1.8
SO_3	1.5	0.4	–
P_2O_5	0.1	1.1	–
K_2O	1.3	1.4	0.6
Na_2O	0.5	0.6	0.5
Na_2O Eq.	1.4	1.6	
LOI	0.3	3.6	37.7
Carbon	0.1	3.1	–
Chloride	0.05	0.0	–
Free CaO	1.9	–	–
Blaine surface (m^2/kg)	500*	470	810
Density (kg/m^3)	3150*	2490	2740

* For OPC = clinker + gypsum.

Table 2
Experimental matrix.

Mix	Composition		
	OPC (%)	FA	L
1	100	0	0
2	95	0	5
3	90	0	10
4	85	0	15
5	80	0	20
6	75	0	25
7	70	0	30
8	65	0	35
9	95	5	0
10	90	10	0
11	85	15	0
12	80	20	0
13	75	25	0
14	70	30	0
15	65	35	0
16	65	30	5
17	65	25	10
18	65	20	15
19	65	15	20
20	65	10	25
21	65	5	30

Three mortar prisms ($40 \times 40 \times 160$ mm) were prepared for each testing age and material combination, according to EN 196-1 (water-to-binder ratio 0.50, binder:sand = 1:3). The samples were cured at 20 °C, submerged in a saturated $Ca(OH)_2$ solution.

For all the mortar mixes, corresponding cement pastes with water-to-binder ratio of 0.5 were prepared using a vacuum mixer from Renfert. The pastes were poured into 20 ml cylindrical plastic bottles and stored under sealed conditions at 20 °C. The hydration of the samples was stopped after 1, 28, 90 and 140 days of curing via solvent exchange using isopropanol and ether. The samples were stored for about 2–3 h in a desiccator over silica gel, prior to analysis, to let the remaining ether evaporate. Simultaneous TGA/SDTA analyses were performed on the dried powders using a Mettler Toledo TGA/SDTA851. Samples of about 50 mg were weighed into aluminium oxide crucibles. The samples were heated from 30 °C to 980 °C at a heating rate of 20 °C/min. During the analysis the oven was purged with N_2 at 50 ml/min. During a thermogravimetric analysis (TGA), the weight of the sample is monitored as a function of the temperature. The amount of bound water (H) and calcium hydroxide (CH) are determined as described in [15]. Both are expressed as a % of the dry sample weight and as a % of OPC content in the sample. The standard deviation on three independent measurements at all tested ages is not larger than 0.1% for H and 0.2% for CH.

In order to focus on the effects of small limestone replacements in both ordinary Portland cement and fly ash cement, thermogravimetric curves and X-ray diffraction patterns of the four following mixes of particular interest were studied:

- 100% OPC (reference)
- 95% OPC + 5% limestone powder
- 65% OPC + 35% fly ash
- 65% OPC + 30% fly ash + 5% limestone powder

For the X-ray diffraction (XRD), larger paste samples of about 60 ml were prepared for each combination. After 1, 28, 90 and

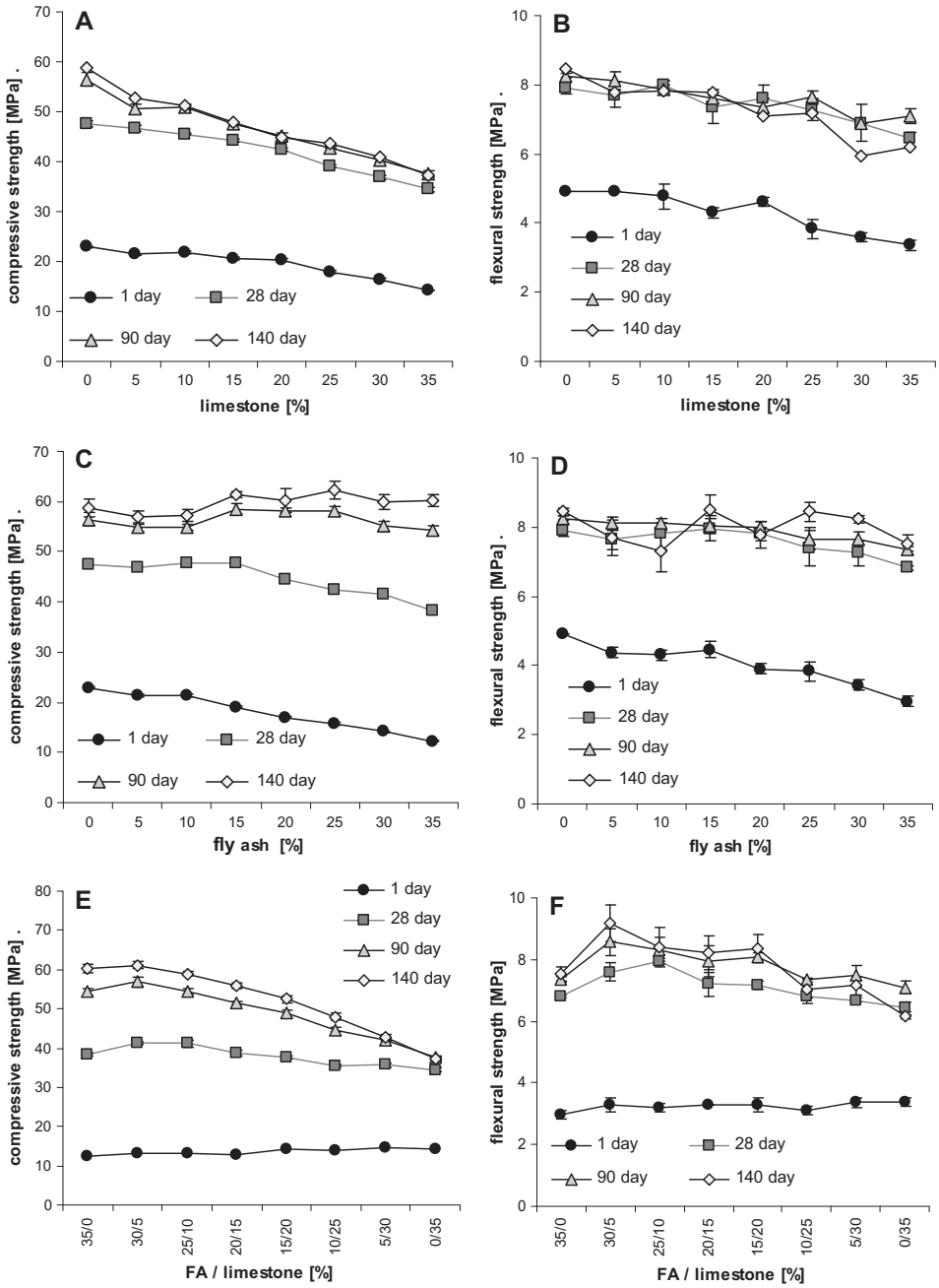

Fig. 1. The compressive and flexural strength with standard deviation (bars) after 1, 28, 90 and 140 days of curing for: (A) and (B) limestone blended cements, (C) and (D) fly ash blended cements, and (E) and (F) composite cements containing both fly ash and limestone.

140 days of sealed curing at 20 °C, discs with a diameter of about 30 mm and a thickness of 3–5 mm were cut from the paste samples using a water lubricated saw and the top layer was removed using fine sand paper. The discs were analysed using a PANalytical X'Pert Pro MPD diffractometer in a $\theta - 2\theta$ configuration with an incident beam monochromator and Cu Kα radiation (λ = 1.54 Å).

Table 3
Compressive (σ_{comp}) and flexural strength (σ_{flex}) after 1, 28, 90 and 140 days of curing, of all tested combinations.

Mix	Composition			1 day		28 days		90 days		140 days	
	OPC (%)	FA	L	σ_{comp} (MPa)	σ_{flex}	σ_{comp} (MPa)	σ_{flex}	σ_{comp} (MPa)	σ_{flex}	σ_{comp} (MPa)	σ_{flex}
1	100	0	0	22.9	4.9	47.5	7.9	56.5	8.3	58.7	8.4
2	95	0	5	21.4	4.9	46.6	7.7	50.6	8.1	52.7	7.8
3	90	0	10	21.7	4.8	45.5	8.0	50.9	7.9	51.1	7.8
4	85	0	15	20.6	4.3	44.3	7.4	47.7	7.6	47.8	7.8
5	80	0	20	20.3	4.6	42.5	7.6	45.1	7.4	44.9	7.1
6	75	0	25	18.0	3.8	39.1	7.3	42.8	7.6	43.6	7.2
7	70	0	30	16.3	3.6	36.9	6.9	40.4	6.9	40.9	5.9
8	65	0	35	14.2	3.4	34.4	6.4	37.5	7.1	37.2	6.2
9	95	5	0	21.2	4.4	46.9	7.6	54.9	8.1	56.8	7.7
10	90	10	0	21.4	4.3	47.6	7.8	54.9	8.1	57.2	7.3
11	85	15	0	19.1	4.5	47.8	8.0	58.4	8.0	61.4	8.5
12	80	20	0	17.0	3.9	44.6	7.8	58.2	8.0	60.2	7.8
13	75	25	0	15.8	3.8	42.6	7.4	58.2	7.7	62.3	8.5
14	70	30	0	14.1	3.4	41.4	7.3	55.1	7.7	59.9	8.2
15	65	35	0	12.3	3.0	38.3	6.8	54.4	7.4	60.2	7.5
16	65	30	5	13.2	3.3	41.2	7.6	56.9	8.6	61.1	9.2
17	65	25	10	13.3	3.2	41.2	7.9	54.5	8.3	59.0	8.4
18	65	20	15	12.9	3.3	38.6	7.2	51.4	7.9	55.8	8.2
19	65	15	20	14.2	3.3	37.5	7.2	48.9	8.1	52.5	8.4
20	65	10	25	13.9	3.1	35.4	6.8	44.7	7.3	48.0	7.1
21	65	5	30	14.6	3.4	35.7	6.7	42.1	7.5	42.7	7.2

3. Results

3.1. Flexural and compressive strength

The compressive and flexural strength of the *limestone blended cements* decrease with increasing limestone powder replacement at all ages from 1 to 140 days (Fig. 1A and B). The main compressive and flexural strength gain takes place during the first 28 days of curing as might be expected. The flexural strength and the compressive strength do not seem to change after 28 and 90 days of curing, respectively.

The compressive and flexural strength after 1 day of curing decreases with increasing fly ash replacement for the *fly ash blended cements* (Fig. 1C and D). The fly ash blended cements containing up to 15% fly ash obtain a similar compressive strength as the OPC reference after 28 days, while higher replacement levels lead to a reduction in compressive strength. After 90 and 140 days of curing, all tested fly ash blended cements reach compressive and flexural strength levels equal to the OPC reference regardless of the fly ash content. The main strength development occurs during the first 28 days. However, there is still a considerable strength increase between 28 and 90, and 90 and 140 days especially for the mixes containing large volumes of fly ash (>15%). The flexural strength, on the other hand, does not change greatly after 28 days of curing.

Table 3 shows the compressive and flexural strength results of the different tested combinations. It can be seen that at the same replacement level the limestone blended cements (mix 2–8) develop a slightly higher strength than the fly ash blended cements (mix 9–15) after 1 day. After 28 days, however, the fly ash blended cements surpass the limestone blended cements and at 90 and 140 days the gap between the two increases with increasing replacement level.

The compressive and flexural strength results for the *composite cements containing 65% OPC and 35% of a combination of limestone powder and fly ash* are shown in Fig. 1E and F. After 1 day of curing, limestone powder seems to promote the early age hydration more than fly ash as the compressive strength tends to increase as limestone replaces fly ash. After 28 days, on the other hand, the blend with 35% limestone powder has an average compressive strength of 34.4 MPa and the one with 35% fly ash 38.3 MPa (Table 3).

The maximum 28 day compressive strength is obtained for the mixes containing 30% fly ash and 5% limestone (41.2 MPa) or 25% fly ash and 10% limestone powder (41.2 MPa). Up to 15% limestone powder (38.6 ± 0.8 MPa) can be used instead of fly ash without impairing the strength at 28 days relative to the 65% OPC and 35% FA blend (38.3 ± 0.4 MPa). A compressive strength increase of about 8% was obtained at 28 days when replacing 5% fly ash by 5% limestone in the 35% fly ash mix. This is comparable to the about 10% compressive strength increase reported after 28 days of curing in our preceding study [15] for a parallel series of the same mixes. After 90 days of curing a similar but slightly smaller strength increase when replacing a small part of the fly ash with limestone powder in the composite cements can be observed (Fig. 3E, Table 3). A strength increase of 5% is obtained (54.4 MPa versus 56.9 MPa). The effect is further reduced at 140 days. At this age similar strength performances are obtained for the 35% fly ash and 30% fly ash and 5% limestone blends (60.2 MPa versus 61.1 MPa). Replacing 5–10% of the fly ash with limestone appears also to be beneficial for the flexural strength after 28, 90 and 140 days. The main compressive and flexural strength development occurs during the first 28 days. After 28 and even 90 days there is considerable compressive and flexural strength increase for the mixes with high fly ash content. When comparing mix 14 (70% OPC and 30% fly ash) and mix 16 (65% OPC, 5% limestone and 30% fly ash), it can be seen that they develop about the same compressive strength at all tested ages, indicating that 5% of OPC can be replaced by limestone powder in a Portland fly ash cement without impairing the strength.

3.2. Amount of bound water (H) and calcium hydroxide (CH)

Fig. 2 shows the amount of bound water (H) relative to the dry content and the OPC content.

Both for the *limestone and fly ash blended cements*, the amount of bound water per dry content decreases (Fig. 2A and C), and the amount of bound water relative to the OPC content increases (Fig. 2B and D), with increasing replacement level, except for the 5% replacement of the OPC with limestone powder that shows no reduction in the amount of bound water relative to the dry content.

The amount of bound water for the *composite cements containing 65% OPC and 35% of a combination of fly ash and limestone powder* (Fig. 2E) is similar for all tested combinations after 1 day of curing. However, the amount of bound water increases as limestone powder and fly ash are combined instead of just using one of them after

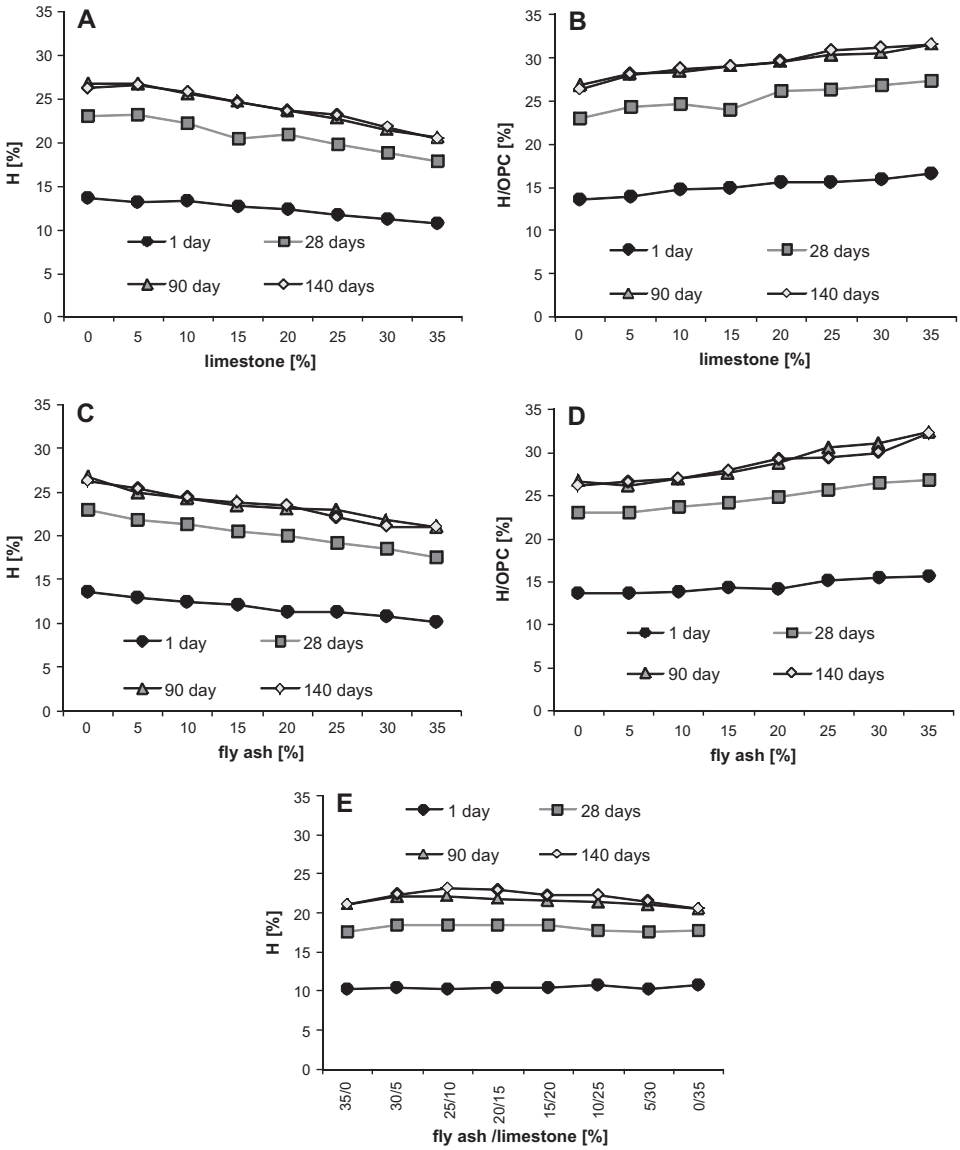

Fig. 2. The amount of bound water (H) per dry content and per OPC after 1, 28, 90 and 140 days of curing for: (A) and (B) limestone blended cements, (C) and (D) fly ash blended cements, and (E) composite cements containing both fly ash and limestone.

28, 90 and 140 days. The maximum amount is obtained for 25% fly ash and 10% limestone powder after 90 and 140 days.

The main part of the bound water is bound during the first day and the following 28 days. The amount of bound water increases slightly up to 90 days, but generally does not change thereafter.

Fig. 3 depicts the calcium hydroxide content (CH) both relative to the dry content and the OPC content.

The CH content per dry content decreases with increasing limestone or fly ash replacement for the *fly ash and limestone blended cements* (Fig. 3A and C). The CH content per OPC increases with increasing limestone or fly ash replacement at 1 day (Fig. 3B and D). However at later ages, different trends are observed for limestone and fly ash blended cements. For the *limestone blended cements* there is a decreasing trend in the CH content per OPC at 5–10% limestone, but the amount tends to increase again at higher replacement levels. For the *fly ash blended cements* with high fly ash content ($\geqslant$20%) a decrease in CH content can be observed after 28 days. The higher the fly ash content, the more prominent is the CH reduction.

The CH content for the *composite cements containing 65% OPC and 35% of a combination of fly ash and limestone powder* is similar for all tested combinations after 1 day (Fig. 3E). At later ages, the

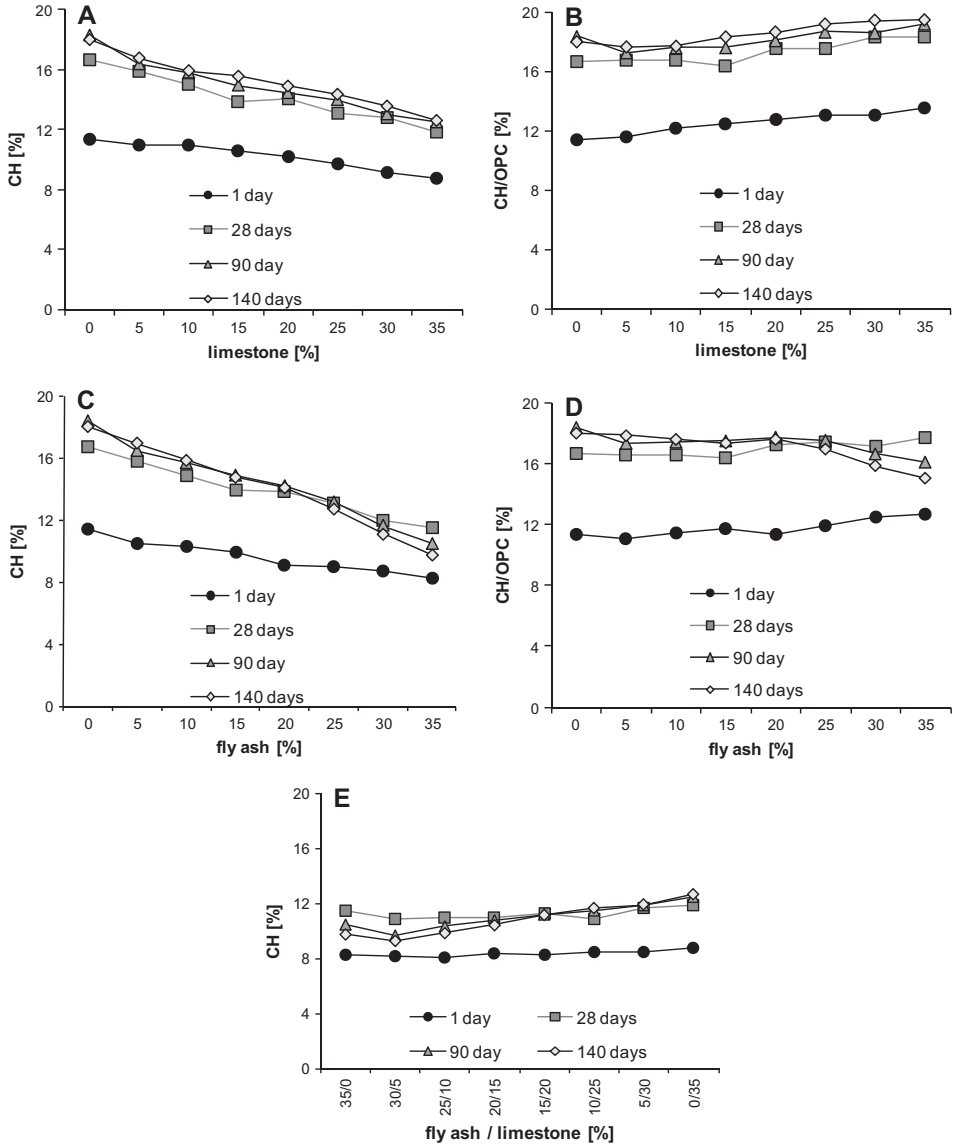

Fig. 3. The calcium hydroxide content (CH) per dry content and per OPC after 1, 28, 90 and 140 days of curing for: (A) and (B) limestone blended cements, (C) and (D) fly ash blended cements, and (E) composite cements containing both fly ash and limestone.

CH content tends to decrease with increasing fly ash content. However, the combination containing 35% fly ash does not show the minimum CH content. Interestingly, the minimum is reached for the combination containing 30% fly ash and 5% limestone.

3.3. Changes in the hydration products

Fig. 4 depicts the thermogravimetric curves (TG-curves) and the differential thermogravimetric curves (DTG-curves) for 100% OPC cement and 100% OPC + 5% L after 28 and 140 days of hydration. Fig. 5 shows the corresponding curves for 65% OPC + 35% fly ash and 65% OPC + 30% fly ash + 5% limestone. The dark curves represent the combinations without limestone powder and the brighter curves those containing 5% limestone powder. From Fig. 4 it can be seen that the limestone containing cement (95% OPC + 5% limestone) binds about the same amount of water as the reference (100% OPC) after both 28 and 140 days of curing, as their total weight loss at about 550 °C is similar. Some differences can be observed between the DTG-curves of the two cements. The peak above 100 °C, partially due to the decomposition of ettringite

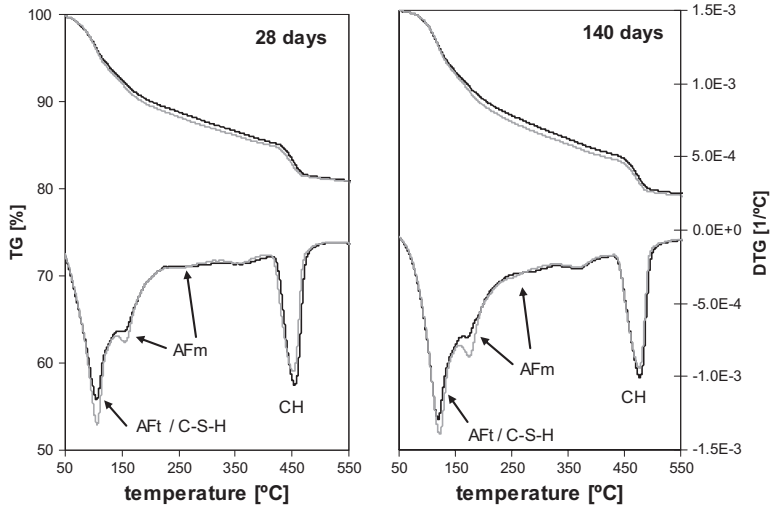

Fig. 4. The thermogravimetric (TG) and differential thermogravimetric (DTG) results for 100% OPC (dark) and 95% OPC + 5% L (bright) after 28 and 140 days of sealed curing.

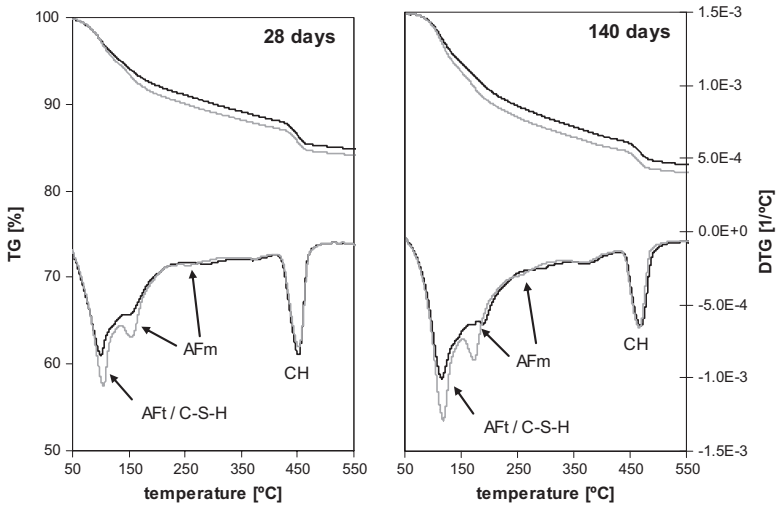

Fig. 5. The thermogravimetric (TG) and differential thermogravimetric (DTG) results for 65% OPC + 35% FA (dark) and 65% OPC + 30% FA + 5% L (bright) after 28 and 140 days of sealed curing.

(AFt), is larger in the presence of limestone, showing that limestone powder seems to stabilize the ettringite as expected [8,9,11,13,17]. The limestone containing cement has a clear single peak at about 180 °C whereas the reference develops a smaller peak with a slight shoulder at higher temperatures. These peaks are associated with the decomposition of AFm phases such as monosulphate, mono- and hemicarbonate [19].

From Fig. 5 it can be seen that when 5% fly ash is replaced by 5% limestone powder slightly more water is bound. When the DTG-curves of the two cements are compared, similar observations can be made as for Fig. 4, except that the effect tends to be more pronounced.

In Fig. 6 the X-ray diffraction patterns at low angle (8–13°2θ) for the different tested combinations cured for 1, 28, 90 and 140 days are shown. After 1 day of hydration the diffraction pattern of the different tested mixes are quite similar, as they all contain ettringite (9.1 2θ) and some hemicarbonate (10.8 2θ).

At later ages (28, 90 and 140 days), ettringite, calcium monocarbonate hydrate (11.7 2θ) and calcium hemicarbonate hydrate are formed in the mixes containing limestone powder. In the absence of limestone only calcium monosulphate hydrate and ettringite are observed. Two types of monosulphate were observed: monosulpoaluminate (Ms, 9.9 2θ) and hydroxyl-AFm type solid solution (Ms*, 10.4 2θ) in which part of sulphate is substituted by hydrox-

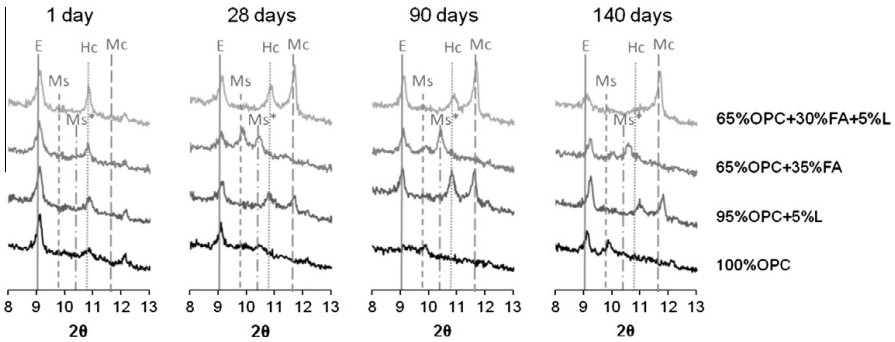

Fig. 6. X-ray diffraction patterns at low diffraction angle (8–13°2θ) for 100% OPC, 95% OPC + 5% L, 65% OPC + 35% FA and 65% OPC + 30% FA + 5% L after 1, 28, 90 and 140 days of sealed curing (E = ettringite, Ms = monosulphate, Ms* = hydroxyl-AFm, Hc = hemicarbonate, Mc = monocarbonate).

ides [9,11]. Note that these results were not interpreted quantitatively. The AFm and AFt phases were found to be very sensitive and tended to decompose upon handling, as can be seen from 100% OPC mix at 90 days in which all of the AFt and AFm phases have disappeared.

4. Discussion

The compressive strength of *limestone blended cement* decreases with increasing OPC replacement at all tested ages. In a previous study [17], up to 15% of the OPC could be replaced by limestone powder without impairing the compressive strength after 28 days of curing under the same curing conditions. Similar results were also obtained by others [2,20]. However, no strength increase was observed at low replacement levels in this study. It should be noted that the effect of limestone powder on the compressive strength is likely to be more pronounced at lower w/b ratios [21].

According to the thermogravimetric results (H and CH), two mechanisms can be distinguished: the *filler effect* related to the increase of the amount of bound water (H) and calcium hydroxide (CH) relative to the OPC content with increasing replacement of OPC with limestone (Figs. 2B and 3B). Indeed, replacing OPC with limestone raises the effective water to OPC ratio, and the limestone powder provides additional surface for the precipitation of hydrates; both effects promote clinker hydration. And the *dilution effect* is caused by the reduction in the amount of the most reactive component, OPC, in the system. At replacement levels larger than 5%, the H and CH per dry content and the compressive strength decrease with increasing replacement of OPC by limestone indicating that the filler effect can not compensate for the dilution effect at all tested ages (Figs. 2A and 3A).

At low limestone replacement (up to 10%) of the OPC, the amount of bound water per OPC increases (Fig. 2B), but at the same time the amount of CH per OPC decreases after 28, 90 and 140 days (Fig. 3B). During the hydration of OPC, an increase in the amount of CH is generally accompanied by an increase in the amount of H, such as during the hydration of the main clinker mineral alite (C_3S): $C_3S + 2.3\ H \rightarrow C_{1.7}SH + 1.3\ CH$. The decrease in CH therefore indicates a change in the nature of the hydration products formed, which is confirmed by the changes in the TG and DTG (see Fig. 4). The presence of limestone leads to the formation of carboaluminate hydrates, as observed with XRD (Fig. 6). This reaction might cause the decrease in CH as reported in previous studies [8,9,11,13,17]. The increase of the amount of CH per OPC for higher replacement (>10%) can be related to a larger filler effect promoting the CH production which compensates for the consumption of CH by the hemicarbonate formation [7], or the formation of monocarboaluminate instead of hemicarboaluminate, which does not consume CH [6,9,11].

For the *fly ash blended cement* it was observed that fly ash, similar to the limestone powder, exerts a filler effect on the OPC hydration which does not compensate for the dilution effect after 1 day: increasing H and CH per OPC, but decreasing it per dry content, as well as decreasing the compressive and flexural strength with increasing OPC replacement. At later ages, the pozzolanic reaction of the fly ash plays an important role for the fly ash blended cements. Contrary to the limestone blended cements, there is still a considerable strength increase after 28 days with higher replacement levels as expected. The extent of the fly ash reaction is recently documented in [18]. The amount of CH gives an indication for the pozzolanic reactivity of the fly ash, as fly ash consumes CH during its pozzolanic reaction. Care should be taken when interpreting these results as the filler effect of the fly ash initially increases the CH/OPC content with increasing fly ash content. However, after 28 days a consumption of CH can be observed for the fly ash blended cements with high fly ash content (>20%) (Fig. 3D). Furthermore, the dissolved species from the fly ash may also react directly with the C–S–H gel [22–24]. The latter reaction mechanism would lower the Ca/Si ratio and possibly increase the Al/Si ratio in the C–S–H gel.

An OPC or a limestone containing cement shows an almost linear trend between compressive strength and the amount of bound water (H) (Figs. 1C and 2C) [15]. However, this relation is not valid in the case of FA blended cements due to two major facts: curing conditions and the nature of the pozzolanic reaction products. The mortars were stored in saturated CH solution, whereas the paste samples were cured under sealed conditions. The pozzolanic reaction might in the case of the mortar samples have been altered due to the continuous access to water and CH and a possible leaching of alkali (pH solution 12.5, pH mortar 13.5). The pozzolanic reaction products of the fly ash were found to enhance the mechanical properties without necessarily binding more water than what is inherent in the CH.

At all tested ages, 5% of the fly ash in the blended fly ash cement (65% OPC + 35% fly ash) can be replaced with limestone powder (resulting in 65% OPC + 30% fly ash + 5% limestone) without impairing the compressive and flexural strength (Fig. 1E and F). At 28 days a compressive strength increase of 8% is observed, however the effect diminishes over time: 5% increase at 90 and 2% at 140 days. The increasing contribution of the pozzolanic reaction of fly ash to the compressive strength, probably explains the reduc-

tion of the effect over time. Also 5% OPC in the 70% OPC + 30% fly ash blend can be replaced by 5% limestone powder resulting in the combination 65% OPC + 30% fly ash + 5% limestone powder without reducing the compressive and flexural strength at all tested ages (Table 3).

Both observations are important for the cement manufacturers producing fly ash blended cements. As limestone powder is the main raw material for OPC, it is always available in abundance at cement plants. Fly ash on the other hand has to be carefully selected and purchased from coal fired power plants and transported to the cement plant. In the future good quality fly ash can also be scarce as the demand increases as blended cements gain popularity. Being able to replace part of the fly ash with limestone powder renders the cement production less dependent on the fly ash supply and is economically beneficial. Being able to replace 5% of the OPC with limestone powder results in a reduction of costs and emissions related to the clinkerization.

Replacing 5% of the fly ash with limestone powder in a 65% OPC + 35% fly ash cement in addition to producing a strength increase, also results in a decrease in CH content at 28, 90 and 140 days (Fig. 3E). The CH content normally decreases with increasing fly ash content. The observed decrease in CH with less fly ash therefore indicates a similar reaction to the one observed for minor additions of limestone powder to OPC: the formation of hemicarbonate (Fig. 6), with calcium being supplied by OPC as opposed to the fly ash, due to its higher CaO content (Table 1).

The effect of the presence of 5% limestone powder seems to be more pronounced for the fly ash cements than for the ordinary Portland cement (Figs. 4 and 5). As the fly ash reacts, aluminates are liberated by dissolution of fly ash, thereby decreasing the sulphate/aluminate ratio. Therefore more ettringite will decompose after sulphate depletion and react with the additional aluminates to form calcium monosulphate hydrate. The presence of limestone will then have a larger impact as this will stabilize the ettringite by reacting with the additional aluminates provided by the fly ash to form calcium carboaluminate hydrates. The net result is more ettringite, more chemically bound water and a larger volume of hydrates leading to less porosity and thereby higher strength, i.e. a true synergistic effect exists and can be used to advantage. The chemistry of this synergy was recently elaborated in [16].

5. Conclusions

The key observation in this study is the confirmation of the synergetic interaction between limestone powder and fly ash and its persistence over time. The presence of limestone leads to the formation of mono- or hemicarboaluminate hydrates instead of monosulphoaluminate hydrate and stabilizes thereby the ettringite. This leads to an increase in the volume of hydrates and a subsequent decrease in porosity and an increase in strength. Fly ash, on the other hand, can provide additional aluminates which will lower the sulphate/aluminate ratio and thereby amplify the impact of the limestone.

Replacing 5% of the OPC with limestone powder at a water-to-binder ratio of 0.5 resulted in a reduction in compressive and flexural strength, whereas replacing 5% of the OPC with limestone powder in a fly ash blended cement with 30% fly ash and 70% OPC produced no strength loss. The composite cements consisting of 65% OPC, 30% fly ash and 5% limestone powder have a slightly higher or similar strength compared to the 65% OPC and 35% fly ash and the 70% OPC and 30% fly ash blends at 28, 90 and 140 days. This means that, 5% of OPC or 5% of fly ash can be replaced with 5% limestone powder in this system, without impairing the compressive and flexural strength. The TGA and XRD results confirmed the change in the hydration products when limestone is included in the system.

Acknowledgements

The authors would like to acknowledge COIN, the COncrete INnovation centre (www.coinweb.no) for the financial support; and the team from EMPA, Dübendorf Switzerland in particular: Barbara Lothenbach, Mohsen Ben Haha and Gwenn Le Saout for their helpful discussions and Walter Trindler, Luigi Brunetti and Angela Steffen for their help with the experimental work.

References

[1] Damtoft JS, Lukasik J, Herfort D, Sorrentino D, Gartner EM. Sustainable development and climate change initiatives. Cem Concr Res 2008;38(2):115–27.
[2] Soroka I, Stern N. Calcareous fillers and the compressive strength of Portland cement. Cem Concr Res 1976;6(3):367–76.
[3] Soroka I, Setter N. The effect of fillers on strength of cement mortars. Cem Concr Res 1977;7(4):449–56.
[4] Bonavetti V, Donza H, Rahhal V, Irassar E. Influence of initial curing on the properties of concrete containing limestone blended cement. Cem Concr Res 2000;30(5):703–8.
[5] Bonavetti V, Donza H, Menéndez G, Cabrera O, Irassar EF. Limestone filler cement in low w/c concrete: a rational use of energy. Cem Concr Res 2003;33(6):865–71.
[6] Kuzel HJ, Pöllmann H. Hydration of C_3A in the presence of $Ca(OH)_2$, $CaSO_4{\cdot}2H_2O$ and $CaCO_3$. Cem Concr Res 1991;21(5):885–95.
[7] Kakali G, Tsivilis S, Aggeli E, Bati M. Hydration products of C_3A, C_3S and Portland cement in the presence of $CaCO_3$. Cem Concr Res 2000;30(7):1073–7.
[8] Bonavetti VL, Rahhal VF, Irassar EF. Studies on the carboaluminate formation in limestone filler-blended cements. Cem Concr Res 2001;31(6):853–9.
[9] Lothenbach B, Le Saout G, Gallucci E, Scrivener K. Influence of limestone on the hydration of Portland cements. Cem Concr Res 2008;38(6):848–60.
[10] Hirao H, Yamada K, Hoshino S, Yamashita H. The effect of limestone addition on the optimum sulphate levels of cements having various Al_2O_3 contents. In: 12th ICCC, Montreal; 2007.
[11] Matschei T, Lothenbach B, Glasser FP. The AFm phase in Portland cement. Cem Concr Res 2007;37(2):118–30.
[12] Matschei T, Lothenbach B, Glasser FP. The role of calcium carbonate in cement hydration. Cem Concr Res 2007;37(4):551–8.
[13] Hoshino S, Yamada K, Hirao H. XRD/Rietveld analysis of the hydration and strength development of slag and limestone blended cement. J Adv Concr Technol 2006;4(3):357–67.
[14] De Weerdt K, Justnes H. Microstructure of binder from the pozzolanic reaction between lime and siliceous fly ash and the effect of limestone addition. In: Sun W, van Breugel K, Miao C, Ye G, Chen H, editors. Microstructure related durability of cementitious composites. Nanjing; 2008. p. 107–16.
[15] De Weerdt K, Justnes H, Kjellsen KO. Fly ash–limestone ternary Portland cements: effect of component fineness. Adv Cem Res, accepted for publication.
[16] De Weerdt K, Justnes H. Synergic reactions in triple blended cements. In: 11th NCB international seminar on cement and building materials. New Delhi; 2009. p. 257–61.
[17] De Weerdt K, Justnes H, Kjellsen KO. Fly ash–limestone ternary composite cements: synergetic effect at 28 days. Nordic Concr Res 2010;42(2):20.
[18] Ben Haha M, De Weerdt K, Lothenbach B. Quantification of the degree of reaction of fly ash. Cem Concr Res 2010;40(11):1620–9.
[19] Ramachandran VS. Thermal analyses of cement components hydrated in the presence of calcium carbonate. Thermochim Acta 1988;127:385–94.
[20] Tsivilis S, Chaniotakis E, Badogiannis E, Pahoulas G, Ilias A. A study on the parameters affecting the properties of Portland limestone cements. Cem Concr Compos 1999;21(2):107–16.
[21] Bentz DP. Modeling the influence of limestone filler on cement hydration using CEMHYD3D. Cem Concr Compos 2006;28(2):124–9.
[22] Rayment PL. The effect of pulverised-fuel ash on the c/s molar ratio and alkali content of calcium silicate hydrates in cement. Cem Concr Res 1982;12(2):133–40.
[23] Taylor HFW, Mohan K, Moir GK. Analytical study of pure and extended Portland cement pastes: II, fly ash- and slag-cement pastes. J Am Ceram Soc 1985;68(12):685–90.
[24] Pietersen HS. The reactivity of fly ash in cement geochemistry. Delft: TU Delft; 1993. p. 271.

Paper V

Quantification of the degree of reaction of fly ash
Ben Haha M., De Weerdt K. & Lothenbach B.
Cement and Concrete Research, 2010, Vol. 40 (11) pp.1620-9.
doi:10.1016/j.cemconres.2010.07.004

Cement and Concrete Research 40 (2010) 1620–1629

Contents lists available at ScienceDirect

Cement and Concrete Research

journal homepage: http://ees.elsevier.com/CEMCON/default.asp

Quantification of the degree of reaction of fly ash

M. Ben Haha [a,*], K. De Weerdt [b,*], B. Lothenbach [a]

[a] Empa, Swiss Federal Laboratory for Materials Testing and Research, Laboratory for Concrete and Construction Chemistry, 8600 Dübendorf, Switzerland
[b] SINTEF Building and Infrastructure, 7465 Trondheim, Norway

ARTICLE INFO

Article history:
Received 23 April 2010
Accepted 16 July 2010

Keywords:
Blended cements
Chemical dissolution
Scanning electron microscopy (SEM)
Image analysis (IA)
Degree of reaction

ABSTRACT

The quantification of the fly ash (FA) in FA blended cements is an important parameter to understand the effect of the fly ash on the hydration of OPC and on the microstructural development. The FA reaction in two different blended OPC-FA systems was studied using a selective dissolution technique based on EDTA/NaOH, diluted NaOH solution, the portlandite content and by backscattered electron image analysis.
The amount of FA determined by selective dissolution using EDTA/NaOH is found to be associated with a significant possible error as different assumptions lead to large differences in the estimate of FA reacted. In addition, at longer hydration times, the reaction of the FA is underestimated by this method due to the presence of non-dissolved hydrates and MgO rich particles. The dissolution of FA in diluted NaOH solution agreed during the first days well with the dissolution as observed by image analysis. At 28 days and longer, the formation of hydrates in the diluted solutions leads to an underestimation. Image analysis appears to give consistent results and to be most reliable technique studied.

1. Introduction

The development of new materials and technologies utilizing waste and bi-products of industrial processes is an important task for the cement industry in their quest to reduce CO_2 emissions. Fly ash (FA) is a commonly used pozzolanic material in concrete, and many researchers have investigated its effect on the microstructure of concrete. Commercial fly ash blended cements in Europe can contain up to 35% of fly ash (CEM II). Due to regulations on CO_2 emissions cement producers are interested in replacing even larger parts of the Portland cement with fly ash. This gives new incentives to study high volume fly ash cements.

When combined with ordinary Portland cement, SiO_2 and Al_2O_3 originating from the glass phase of the FA will partly dissolve due to the high pH of the pore solution and will react with $Ca(OH)_2$ to form hydration products similar to the ones formed by ordinary Portland cement [1]. The determination of the amount of reacted as a function of time in fly ash blended cements enables to link the progress of the reaction of the different components (OPC, fly ash) and the subsequent changes.

FA gives a very broad X-ray peak which makes a quantification of unhydrated fly ash by XRD in the presence of other amorphous phases rather imprecise. Methods reported in literature to determine the amount of fly ash reacted include (i) selective dissolution methods, (ii) consumption of portlandite, and (iii) determination of fly ash reactivity in highly diluted solution.

Selective dissolution methods are commonly used techniques and aim at dissolving the hydrates and the unhydrated clinkers without dissolving the unreacted fly ash. This allows a direct determination of the amount of unreacted fly ash in a hardened cement paste as the unreacted fly ash remains as residue and can be quantified. A number of different methods have been reported in literature, generally based on the use of either acids or complexing agents.

Among all the acids reported in literature, picric acid appears to be the most promising for selective dissolution of hydrates and clinkers [2,3]. The method has been originally tested for a fly ash–gypsum–$Ca(OH)_2$ systems [2] and for hydrated cement pastes containing fly ash [3]. In the meantime the method has been employed in several studies [4–7]. In other studies, salicylic acid has been used as a dissolving agent as it is known to dissolve the silicates phases in OPC [8]. The technique appeared to be suitable when applied to a C_3S–fly ash systems [9,10]. However, when used in cementitious composite systems, it dissolved hydrates and interstitial (aluminates and ferrites) unreacted OPC phases insufficiently [2,11]. NaOH and sugar are known to dissolve the interstitial phases in unreacted OPC [8]. NaOH and sugar have been therefore combined with salicylic acid to study the fly ash reaction in blended cements [12]. The fraction of glass in fly ash reacted did not increase and agreed with the results found in previous studies [9,10]. Salicylic acid has also been tested in combination with hydrochloric acid (HCl) [11,13]. However, HCl was found to be too aggressive and to dissolve parts of the fly ash [2]. Acid conditions can also result in silica gel precipitation [11].

A frequently used complexing agent for selective dissolution of blended cements is ethylene diamine tetra acetic acid (EDTA) combined

* Corresponding authors. Haha is to be contacted at Tel.: +41 44 823 49 47; fax: +41 44 823 40 35. De Weerdt, Tel.: +47 73 59 48 66; fax: +47 73 59 71 36.
E-mail addresses: mohsen.ben-haha@empa.ch (M.B. Haha), klaartje.de.weerdt@sintef.no (K. De Weerdt).

0008-8846/$ – see front matter © 2010 Elsevier Ltd. All rights reserved.
doi:10.1016/j.cemconres.2010.07.004

with triethanolamine (TEA). It was first tried on slag blended cements [11] and later tested in a slightly adapted version on fly ash blended cements [14]. The EDTA method was not able to dissolve hydrotalcite and siliceous hydrogarnet-like phases and might have led to precipitation of amorphous silica [14]. The application of the EDTA/TEA method on fly ash was not a success [14].

In this study, different selective dissolution methods are compared on a hydrated fly ash cement pastes as previously reported comparative studies had been performed on "ideal systems" such as gypsum–$Ca(OH)_2$ [2] or on slag blended cements [11].

The pozzolanic reaction of the fly ash consumes $Ca(OH)_2$ to produce C–S–H. Thus the consumption of $Ca(OH)_2$ has been used as a measure for the degree of reaction of the fly ash [14]. The $Ca(OH)_2$ content in the hydrated OPC cement paste without fly ash is compared to the $Ca(OH)_2$ content in a corresponding paste containing fly ash. These results are difficult to interpret as not only the pozzolanic reaction influences the $Ca(OH)_2$ content but the fly ash also promotes clinker hydration due to the filler effect. Portland cement blended with fly ash shows initially a higher degree of reaction resulting in the presence of more portlandite than cement without fly ash [12]. This complicates the evaluation as it is difficult to assess where the filler effect ends and the pozzolanic reaction starts. Furthermore, there is the possibility that the dissolved silicate from the fly ash reacts directly with already formed C–S–H gel [15–17] rather than to precipitate in reaction with portlandite. This reaction mechanism will lead to lower Ca/Si ratio of the C–S–H instead of a decrease of the portlandite content.

A more theoretical approach to study the reactivity of fly ash is to investigate strongly diluted suspension of fly ash at high pH values [15]. The solution has been analyzed for Si, Al and K as a function of time and the obtained values are compared with Si, Al and K content of the glass phase in the FA. The fly ash was found to dissolve congruently; the difference in pH appeared to be more important than the difference in fly ash chemistry [15].

Backscattered electrons (BSE) images coupled with image analysis are a further possibility to quantify the reaction of fly ash in blended cements. BSE coupled with images analysis has been successfully used to quantify the reaction of Portland cement clinkers [18–20] and of blast furnace slags [21] and to study the extent of alkali aggregate reaction in concrete samples [22]. In this study the SEM-BSE images were analyzed quantitatively to get volume fractions of hydrated and unhydrated phases in the blended cement pastes. The segmentation of the unreacted fly ash particles was obtained using a combination of image analysis techniques such as grey-level threshold, and specific morphological filtering.

In this study different techniques of quantification of FA reaction in FA blended cements are evaluated and compared critically.

2. Materials and methods

2.1. Materials

The chemical composition of the Portland cement clinker, type F siliceous fly ash (FA) and limestone powder used in this study are given in Table 1. The $CaCO_3$ content of limestone determined by TGA is about 81%. The clinker has been interground with 3.7% of natural gypsum to obtain a total SO_3 content of 3% in the Portland cement. The used gypsum contained 0.2% free water, and had a $CaSO_4 \cdot 2H_2O$ content of 91.4%. The XRD-Rietveld of the FA indicates the presence of 18 wt.% mullite, 12 wt.% quartz and an amorphous content of 68 wt.% (Table 2). The amorphous content includes besides the glass phase, 3% of amorphous carbon. The composition of the glass phase given in Table 3 was calculated by subtracting the oxides present in the crystalline phases of FA (determined by XRD-Rietveld) from the total amount of oxides present in the FA as determined by XRF.

Table 1
Chemical composition of the clinker, fly ash and limestone in wt.%.

	Clinker	Fly ash	Limestone
SiO_2	20.8	50.0	12.9
Al_2O_3	5.6	23.9	2.7
Fe_2O_3	3.2	6.0	2.0
CaO	63.0	6.3	42.3
MgO	3.0	2.1	1.8
SO_3	1.5	0.4	–
P_2O_5	0.1	1.1	–
K_2O	1.3	1.4	0.6
Na_2O	0.5	0.6	0.5
Na_2O Eq.	1.4	1.6	
LOI	0.3	3.6	37.7
Carbon	–	3.1	–
Chloride	0.051	–	–
Free CaO	1.85	–	–
Blaine surface [m^2/kg]	310	450	900
Density [kg/m^3]	3150	2740	2490

2.2. Assessment of the degree of reaction

2.2.1. Selective dissolution

In this study, six different selective dissolution methods based on salicylic acid, hydrochloric acid (HCl), EDTA or picric acid have been tested and compared (see Table 4). The materials subjected to the selective dissolution experiments are:

- unhydrated OPC
- unreacted FA
- reacted OPC-FA = hydrated paste (80% OPC + 20% FA with w/b = 0.5 hydrated for 90 days at 20 °C)
- 80% reacted OPC-FA + 20% unreacted FA

The selective dissolution methods aim to dissolve selectively the hydrates and the unhydrated clinkers without dissolving the unreacted fly ash. The residue after dissolution is compared with the original sample mass to calculate the degree of reaction of the FA. The effectiveness of the different selective dissolution techniques were tested on the raw materials, unreacted FA and unhydrated OPC in order to identify techniques that dissolve all unhydrated clinker and hydrates without affecting the unreacted FA.

To study the efficiency of different dissolution techniques, on the "reacted OPC-FA", consisting of the hydrated 80% OPC + 20% FA cured for 90 days at 20 °C: the residues after dissolution were examined using SEM techniques. To check for systematic errors, a fourth combination was tested, consisting of 80% reacted OPC-FA to which 20% unreacted FA was added. The weight difference of the residues between reacted OPC-FA and 80% reacted OPC-FA + 20% unreacted FA should be the weight corresponding to 20% FA considering the amount of residue not dissolved by the different dissolution techniques.

The unreacted FA and OPC were used as received for the selective dissolution. The hydrated pastes were treated prior to the selective dissolution with isopropanol and ether to stop hydration, ground to pass a 63 μm sieve and stored in a dessicator over silica gel. The powder was added to the solvent and stirred for the required time (Table 4). After mixing, the suspension was filtrated through a dried

Table 2
XRD-Rietveld analyses of the FA (wt.%).

	[g/100 g]
Quartz	12.3
Calcite	0.4
Hematite	0.6
Anhydrite	0.4
Mullite	18.3
Amorphous*	68.0

* glass and 3% amorphous carbon.

Table 3
Glass composition FA.

Glass*	[g/100 g]
SiO_2	54.1
Al_2O_3	17.9
Fe_2O_3	9.1
CaO	9.8
MgO	3.5
K_2O	2.4
Na_2O	1.0

*Glass composition calculated from XRF and Rietveld-XRD data.

and weighted Whatman GF/C filter (minimum particle size retained 1.2 μm). The residue was washed with distilled water, ethanol or methanol (see Table 4). The filter and residue were dried at 40 °C until a constant weight was reached. The weight of the samples was corrected for the water uptake during hydration using the dry weight as determined by TGA at 600 ° C.

2.2.2. Diluted alkaline solutions

The reaction of FA can be followed by measuring the dissolution of FA in a diluted alkaline solution [15] that has the same pH as observed in the pore solution of the cement paste (pH 13.6 for 65% OPC/ + 35% FA). The measured dissolved concentrations of Si and Al can be used to calculate the amount of dissolved glass of the FA.

0.050 g of FA was added to 50 ml 0.1, 0.2 and 0.5 mol/l NaOH solutions corresponding to a pH of 13.1, 13.3 and 13.7 respectively. After 1, 2, 3, 7, 14 and 28 days the Si content of the solution was analysed by a Dionex Ion Chromatography system (ICS) 3000 using Si standards from Fluka as reference. The Al content was only determined for the 0.5 mol/l NaOH solution using a simultaneous ICP-OES Varian Vista Pro.

To calculate the reaction of the FA, the dissolved quantities of Al and Si are compared to the glass composition as given in Table 3.

2.2.3. Scanning electron microscopy

An ESEM Philips FEG-XL30 microscope was used. The accelerating voltage of the beam was 15KV to provide a good compromise between spatial resolution and adequate excitation of the FeKα peak.

Table 4
Description of the different selective dissolution methods tested.

Methods	Chemicals needed/1 g sample	References
Salicylic acid	6 g salicylic acid 40 ml methanol *methanol**	[2,8–11]
Hydrochloric and salicylic acid	5 g salicylic acid 4.2 ml hydrochloric acid fill to 100 ml with methanol *methanol**	[13]
Hydrochloric acid	250 ml (1:20) hydrochloric acid *distilled water**	[30] [31]
EDTA/DEA	25 ml triethanolamine 9.3 g disodium EDTA*$2H_2O$ 17.3 ml diethylamine (DEA) fill to 100 ml with distilled water 1600 ml distilled water *distilled water**	[21,32]
EDTA/NaOH	500 ml disodium EDTA*$2H_2O$ (0.05 M) in NaOH (0.1 M) 500 ml distilled water 50 ml (1:1) triethanolamine:water 125 ml NaOH (1 M) to adjust pH *distilled water and ethanol**	[11,14,33]
Picric acid	11 g picric acid 60 ml methanol 40 ml distilled water methanol* 500 ml distilled water at 40 °C*	[2,3]

*Rinse solution.

2.2.3.1. Residues of selective dissolution. Polished sections of the residues of the different selective dissolution techniques were studied using both backscattered electron (BSE) imaging and energy dispersive X-ray spectroscopy (EDS) to check the nature of the elements present in the residues.

2.2.3.2. Reaction of the FA. To study the reaction of FA, a slice was cut from the hydrated paste samples at different hydration times. The slices were immersed in isopropanol for 30 min to stop hydration and then dried in an oven for 1 day at 40 °C. After drying, the slices were vacuum impregnated with low viscosity resin and gradually polished down to 0.1 μm using diamond pastes. The drying and impregnation procedure did not induce any significant cracks. Backscattered electron (BSE) images of the polished sections were acquired using the ESEM. For the BSE imaging, the spot size was chosen to have a good resolution of the images. To avoid the charging effect, all specimens were coated with a thin film of carbon (around 5 nm). A typical BSE image and its corresponding grey level histogram are given in Fig. 1.

Image analysis of backscattered electron (BSE) images was carried applying different filters to the BSE images to get the volume fraction of unhydrated FA. The SEM-BSE images can be analysed to get volume fractions of phases in concrete, based on application of segmentation methods. The area fractions obtained from a 2D cross-section are equal to volume fractions from the 3D real structure when materials have a random and isotropic nature. The microstructure of cement paste can be considered to satisfy those stereological conditions [23].

As cementitious materials are heterogeneous, phase quantification by image analysis is usually done on a large number of fields in order to take into account the variations from one field to the other. Some

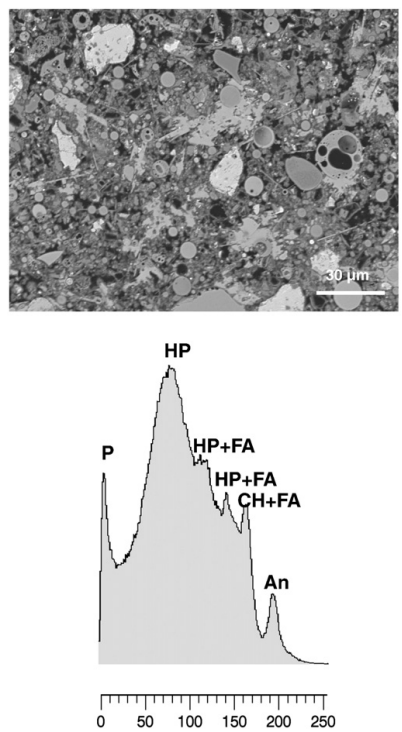

Fig. 1. Backscattered image of a FA blended cement at 28 days and its corresponding grey level histogram (P: porosity, HP: hydration products other than Portlandite, CH: Portlandite, An: unreacted clinker particle, FA: fly ash).

authors have tried to optimise the number of images to be taken, as a function of the magnification, to achieve the lowest standard error on the quantified phases [20,22,24]. At a magnification of 1600×, 60 images are found to be sufficient to include more than 20,000 FA particles which are large enough to ensure that the results are statistically relevant.

Concerning the BSE images of FA blended cements, there are many small FA particles. Omitting the small particles in the images could lead to great underestimation in volume fraction of unreacted FA in the pastes. Therefore, all images for the quantification are acquired with 1024×800 pixels at a magnification of 1600. The pixel size at this magnification is 0.14 μm. This is however not the minimum size measured as the threshold for any species involves an averaging effect whereby some pixels counted for the different species present in the images in fact contain some other species and vice versa corresponding to a threshold of approximately 1 μm. The result will remain always within the error of measurement of the technique. The magnification used offers the possibility to capture more than 97% of the starting material, as about 3% of the unreacted FA is smaller than 1 μm (see Fig. 2).

3. Assessment of the efficiency of selective dissolution methods

3.1. Mass differences

A comparison of the different selective dissolution methods is shown in the Table 5. The residue R is calculated by subtracting the weight of the filter, w_F, from the weight of the treated sample (TS) and the filter (F) after drying at 40 °C, w_{TS+F}. This value is reported relative to the dry weight of the hydrated sample (DS), obtained by TGA at 600 °C, $w_{DS}=w_{S,600\ °C}$:

$$R_S = \frac{w_{TS+F}-w_F}{w_{DS}}$$

An efficient technique should dissolve all unreacted OPC; the residue after selective dissolution should be close to zero. Comparing the residue of unreacted OPC in Table 5, it is clear that the method using salicylic acid is ineffective as 36% of the OPC remains undissolved after 3 h. If salicylic acid is used together with HCl or just HCl was used, more OPC is dissolved but if the samples are kept longer than 1 h in the solution, glassy particles have been observed to precipitate, most likely silica gel. The use of EDTA/DEA, EDTA/NaOH and picric acid resulted in a nearly complete reaction of the OPC (residue of about 2 wt.%).

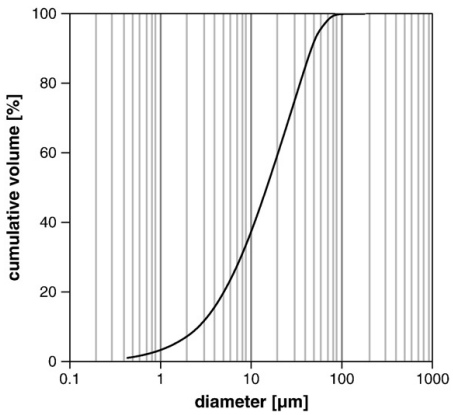

Fig. 2. Particle size distribution of FA obtained by laser granulometry.

Table 5
Assessment of the selective dissolution results: residue (R) as a % of the initial mass.

Method	Salicylic acid	Salicylic acid + HCl			HCl	EDTA/DEA	EDTA/NaOH	picric acid
Time	3 h	30 min	1 h	2 h	3 h	3 h	2 h	1 h	40 min
OPC	36.6	10.0	7.9	7.2	6.6	4.3	1.9	2.2	1.7
FA	96.9	93.4					90.7	92.2	82.5
reacted OPC-FA	47.2	22.2					15.8	17.2	12.2
% FA reacted	3.0	16.7					20.0	14.6	31.9
80%reacted OPC-FA + 20% FA	61.5	35.7					28.2	33.8	28.8
Expected	*57.1*	*36.4*					*30.7*	*32.2*	*26.2*

The ideal method should also leave the unreacted fly ash undissolved, resulting in a residue close to 100%. Comparing the results of the different applied selective dissolution techniques (Table 5), it can be seen that salicylic acid dissolves the least of the unreacted FA (3%) and picric acid the most (18%). The EDTA methods dissolve about 10% of the fly ash. The fact that the residue of the pure fly ash is not 100% could be explained by the dissolution of the finest and/or most reactive fly ash particles or the passing of the finest particles through the filter.

The percentage of fly ash reacted is calculated as follows:

$$\%FA = \left(\frac{R_{UP}-R_{HP}}{R_{UP}}\right)\times 100$$

$R_{UP}=R_{OPC}\times\%OPC+R_{FA}\times\%FA+R_L\times\%L$ with $\%OPC+\%FA+\%L=100\%$ where R_{UP} is the calculated residue of the unhydrated blended paste which is the sum of the residues of the unreacted components (R_{OPC}, R_{FA} and R_L) and R_{HP} is the residue of the hydrated blended paste.

In the hydrated sample (reacted OPC-FA) a part of the FA should have reacted after 90 days. The residue should therefore be lower than the initial 20% FA content used. All methods, if the amount of unreacted OPC is considered, achieve this requirement. The calculated degree of FA reaction, however, varies from 3 to 32% with an error of measurement of ±1.0%, as the balance records with a sensitivity of 0.0001 g.

A good selective dissolution method is expected to be able to determine the amount of unreacted FA correctly. The residue of the hydrated sample (reacted OPC-FA) containing additional 20% of unhydrated FA should be close to the expected value, that is the sum of 80% of the residue of hydrated sample (reacted OPC-FA) and 20% of the residue of FA (the unreacted fly ash). Based on these results (see Table 5) all the methods perform about equally well.

3.2. Microscopic evaluation

The residues of the hydrated fly ash cement paste (reacted OPC-FA) were impregnated with epoxy resin and examined with SEM by backscattered (BSE) imaging coupled to energy-dispersive X-ray spectroscopy (EDS), see Fig. 3.

After extraction with salicylic acid, unreacted FA particles, hydration phases and certain parts of the unreacted OPC phases are still present (Fig. 3 A). The EDS point analyses show the presence of aluminium and sulphur rich phases as well as some silicate hydrates in the remaining hydration products. The presence of these hydration phases as well as unreacted OPC phases in the residue explains the high amount of residue found after the treatment (Table 5). In the unreacted clinker grains the silicate phases are dissolved and the iron and aluminum rich phases, C_3A and C_4AF, remain. These results are in agreement with the findings of Gutteridge [8] using the same method on unreacted cement. This method is thus not suitable for the determination of the degree of reaction of the fly ash.

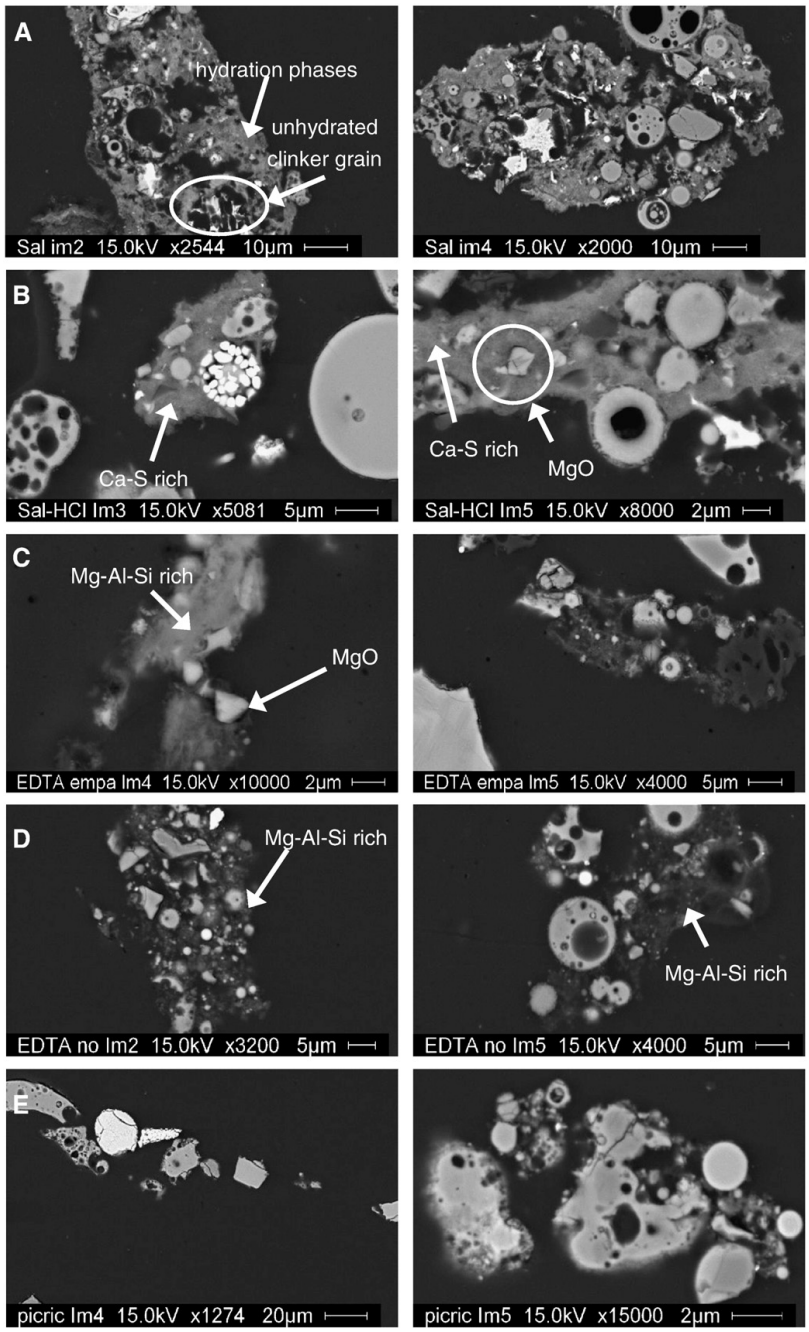

Fig. 3. Backscattered electron (BSE) image of the residues of OPC-FA reacted for 90 days after selective dissolution with A) salicylic, B) salicylic acid and hydrochloric acid, C) EDTA and DEA, D) EDTA and NaOH and E) picric acid.

The residues after the selective dissolution using both salicylic acid and hydrochloric acid contain besides unreacted fly ash particles and MgO particles, parts of the hydrated phases (Fig. 3 B). These parts are rich in calcium and sulfur with some traces of aluminium. This is in agreement with the previous reported results [13] that find that using this dissolution method only 1/3 of the gypsum dissolves. The

presence of these Ca–S-phases might lead to a not neglectable residue due to the initial volume of the gypsum in the OPC.

After treating the hydrated paste with the EDTA and DEA (Fig. 3 C) a residue rich in Mg, Al and Si is found between the fly ash particles. The residue consists of unreacted fly ash particles and MgO particles and an amorphous phase rich in Mg, Al and Si.

The residue after treating the hydrated paste with the EDTA and NaOH method is found to be similar to the one found after treatment with EDTA and DEA (Fig. 3 D). Some pure MgO particles are embedded in this residue. The residue of a 65% OPC + 35% FA blended cement hydrated for 140 day examined by TGA exhibits a weight loss of 4% (50–600 °C), indicating the presence of hydration phases. The profile of the weight loss curve shows similarities to the weight loss pattern of hydrotalcite confirming the findings of the ESEM observation on the residue. Many clusters of fine fly ash particles are spotted when studying the residue. This might indicate that this method is not too aggressive towards finer fly ash particles.

Using picric acid, no hydration products are found in the residue (Fig. 3 E). Most remaining fly ash particles appear to be quite large. Only few clusters of finer particles can be observed when compared to the residues from the other techniques. This might indicate that treatment with picric acid dissolves a part of the smaller fly ash particles.

3.3. Comparison of the selective dissolution techniques

From both the evaluation of the mass of the different residues and the examination of the residues with SEM it can be concluded that salicylic acid is not suitable for the purpose of determining the degree of reaction of FA as it does not dissolve the hydration phases and certain unreacted OPC phases (C_3A and C_4AF). The performance of the selective dissolution improves when salicylic acid is combined with hydrochloric acid. No unhydrated clinker phases were found, but still an amorphous residue of hydration phases rich in Ca and S is detected. This introduces errors in the determination of the degree of reaction of the fly ash. Selective dissolution using picric acid results in the smallest residue for the hydrated paste. The residue consists only of not too small unreacted fly ash particles. No residues of hydration phases or unreacted clinker grains are found, but 18% of the unhydrated FA has dissolved. This method seems to be rather too harsh for determining the degree of reaction of the fly ash. In addition, picric acid can be explosive upon drying [25,26]. Thus this method is not recommended. The two EDTA selective dissolution techniques using DEA or NaOH lead to similar results. The residue after the selective dissolution consists of unreacted fly ash particles, Mg-rich particles and a Mg–Al–Si rich amorphous phases. The presence of these amorphous phases in the residue leads to an error in the determination of the degree of reaction of the fly ash in fly ash blended cements. By comparing the systematic error, the ability to determine the amount of unhydrated FA correctly (Table 5), user-friendliness and the residues, it can be concluded that the EDTA with NaOH appears to be the most suitable selective dissolution method to determine the degree of reaction of the fly ash in hydrated FA blended cement pastes.

4. Determination of FA reaction in blended systems

The degree of reaction of FA over time was determined in two different FA blended cement systems containing 65% OPC + 35% FA and 65% OPC + 30% FA + 5% L, respectively. Cement pastes with water to binder ratio of 0.5 were prepared using a vacuum mixer from Renfert. The paste was poured in to 60 ml cylindrical plastic bottles and stored under sealed conditions at 20 °C.

4.1. EDTA with NaOH

The results of the selective dissolution with EDTA and NaOH are given in the Table 6; 92% of the unreacted FA, 2% of the OPC and 17% of the limestone remain after treatment. The 2% residue of the OPC might be related to the MgO particles present in the OPC which do not dissolve by the EDTA and NaOH treatment, as shown by the ESEM and TGA investigation of the residues. The 17% residue of the limestone corresponds to the quantity of impurities present (Table 1). The 8% of FA which disappears during the EDTA treatment might either slip through the filter or is due to the dissolution of readily soluble small particles or phases present in the FA. To check the importance of the passing size, a finer filter (0.7 μm) was used. However, no differences in the residues are observed.

Table 6
Reaction of FA in cement pastes containing 65% OPC + 35% FA and 65% OPC + 30% FA + 5% L determined by dissolution in diluted alkaline solution (DA), image analysis (IA) and selective dissolution (with EDTA/NaOH).

		DA		*IA*	Selective dissolution		
	Time				% FA reacted		Residue*
	[day]	Si	Al		min	max	
100% FA							*92*
100% L							*17*
100% OPC							*2*
65% OPC	0	0	0	–	0	9	*33*
+ 35% FA	1	1	3	2	−2	7	*34*
	7	5	12	8	0	9	*33*
	28	10	22	21	3	12	*32*
	90	14	32	30	9	18	*30*
	140	–	–	35	11	19	*30*
65% OPC	0	0	0	–	0	8	*30*
+ 30% FA	1	1	3	1	−3	5	*31*
+ 5% L	7	5	12	6	0	8	*30*
	28	10	22	22	3	12	*29*
	90	14	32	29	9	17	*27*
	140	–	–	35	12	20	*26*

*Residues from the selective dissolution used for the calculations.

The residues are calculated as described in the Section 3.1. Those of the hydrated pastes are corrected for residues of the raw materials (FA, limestone and OPC). Concerning OPC and L, their residues have only a minor effect on the calculated % of reacted FA. However, the residue of FA has a significant impact (up to 8%). Omitting the later correction leads to an overestimation of the amount of FA reacted at early age, but it might be more accurate at later age as the part of the unreacted FA that dissolves in the selective dissolution (small reactive particles), might have reacted anyway during hydration.

Minimal and maximal values are reported in Table 6 and Fig. 4 as different assumptions can be made for the calculations. At early reaction times, it might be appropriate to use the measured residue of the unhydrated OPC and FA, to calculate the degree of reaction (minimal value). At later ages, however, all the small particles originally present in the FA might have reacted completely, so that this correction is no longer adequate but better the theoretical amount of FA (35% or 30% FA) is used (maximal value). The difference between the two assumptions is significant (up to 8% of difference in % reacted FA), see Table 6.

The reproducibility of the selective dissolution is high; a standard deviation of 0.2% on a 32.1% residue was obtained on triplicate samples, an error which is very small compared to the error introduced by the assumptions needed to calculate the amount of FA reacted. These assumptions are a major cause of errors, rendering this method inadequate for quantifying the degree of reaction of FA.

The percentage of FA reacted determined with the three different methods for the 65% OPC + 35% FA and 65% OPC + 30% FA + 5% L blends are compared in Fig. 4. The percentage of FA reacted determined by selective dissolution is generally lower than the values obtained by other methods. This underestimation is probably due to the presence of hydrates in the residue (in TGA a weight loss of the residue of up to 4 wt.% is observed).

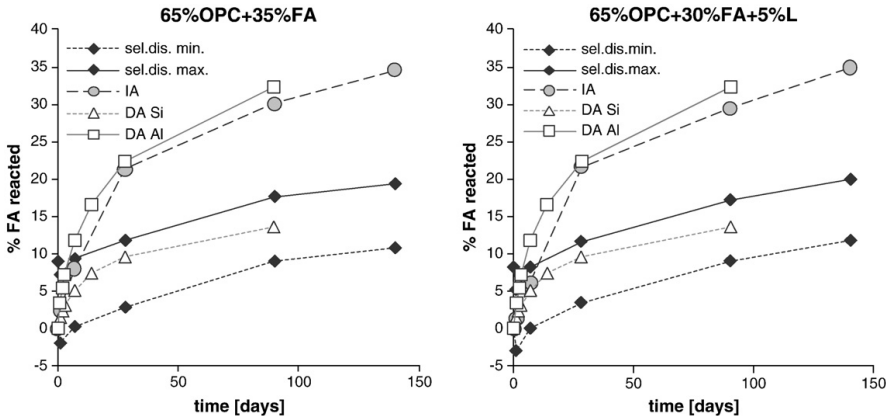

Fig. 4. The % of FA reacted in the two tested mixes determined by image analysis (IA), FA dissolution in 0.5 mol/l NaOH (DA) and selective dissolution using EDTA/NaOH (sel.dis. min./max.).

4.2. Diluted alkaline solutions

The dissolution of FA can be determined in alkaline solutions by measuring silicate or aluminium concentration as a function of time and comparing it with the SiO_2 or Al_2O_3 content in the glass of the FA [15].

$$\%FA\ reacted = \frac{[X_{meas}]}{[X_{tot}]} \times 100;$$

where X is the measured species (Al or Si), $[X_{meas}]$ is the measured concentration and $[X_{tot}]$ is the total concentration assuming a total dissolution of the amorphous part of the FA.

The FA dissolves faster at higher NaOH concentrations (Fig. 5). The pH in the FA cements during the first 90 days has been determined to be 13.6, close to the pH 13.7 of the 0.5 mol/l NaOH solution. The Al concentration in the solution is considerably higher than the Si concentration relative to their initial amount in the glass composition (Fig. 5) indicating an inhomogeneous glass dissolution, due probably to a preferential dissolution of Al from FA glass or to the precipitation of the Si in a gel. The FA still present after 28 days is conglomerated indicating the formation of reaction products.

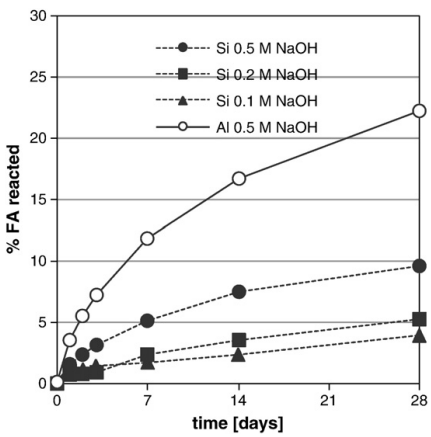

Fig. 5. % FA reacted calculated based on measured Al and Si concentrations resulting from FA dissolution in different NaOH solutions.

The amount of FA reacted based on the Al concentration in the 0.5 M NaOH solution is comparable to the results obtained by image analysis (IA) (see Fig. 4). The degree of reaction of FA calculated from the Si concentration results in a lower degree of dissolution from 7 days when compared to both IA and Al concentrations.

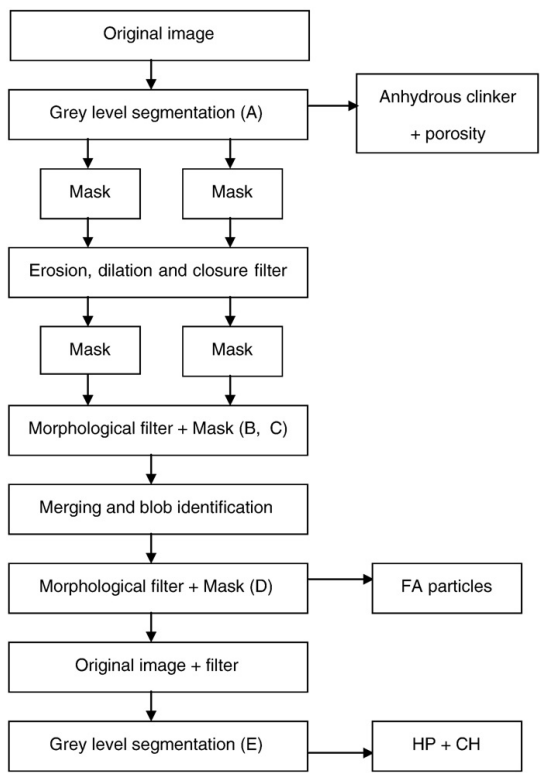

Fig. 6. Image processing sequence. Letters (A, B, C, D and E) refer to the steps shown in Fig. 7.

4.3. Image analysis

Backscattered electron imaging provides image contrast as a function of element composition [23]. The grey level of BSE image is directly proportional to the backscattered coefficient which is related to the atomic weight. Accordingly, the higher the average atomic number, the brighter it is in the backscattered image. Since the images are acquired in 8 bits, 256 grey level values are included in the image, ranging from 0, black (porosity) to 255, white. The BSE image and grey level histogram of FA blended cement hydrated for 28 days are given in the Fig. 1. Typical constituents of a hydrated OPC can be distinguished by their grey levels: unreacted OPC phases appear bright, calcium hydroxide (CH) light grey, other hydration products grey and porosity black [19]. However, for blended fly ash cements it turns more complicated as the FA particles have different grey levels depending on their chemical composition. Their grey level is within the range of C–S–H and CH. The challenge in this approach is therefore to correctly distinguish the FA from the cement matrix.

In this paper a new method is proposed for quantitative measurements of the reaction degree of FA in hardened cement paste using image analysis (IA) techniques applied on BSE images. The method developed for the segmentation of the unreacted FA particles is similar to the procedure reported in the literature [22,27] for the segmentation of aggregates from a concrete matrix. It is not possible to segment the FA purely on the basis of grey level due to the overlap. Therefore various morphological filters are applied in different steps of the segmentation as described in the Fig. 6.

Morphological operations apply a structuring element. A 3×3 element is used for this study. Setting the size of the structuring element is similar to setting the observation scale and setting the criterion to differentiate image objects or features according to size. In general, smaller structuring elements preserve finer details within an image than larger elements. The operation compares the element to the underlying image and generates an output pixel based upon the function of the morphological operation. The size and shape of the structuring element determines what is extracted or deleted from an

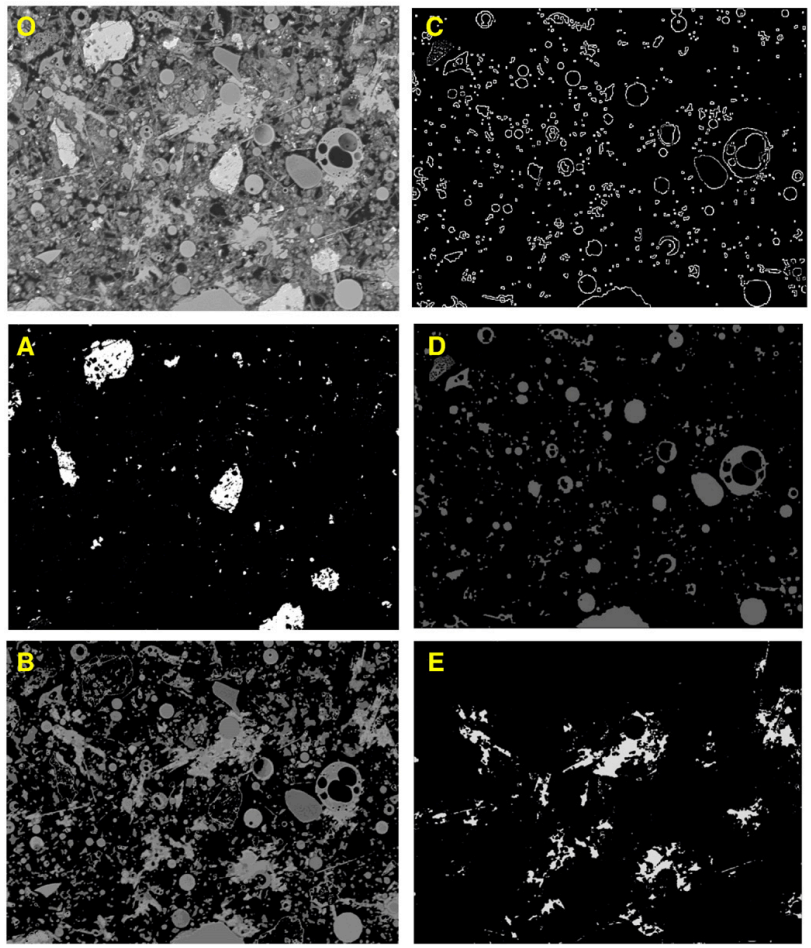

Fig. 7. Original BSE image (O) of Fig. 1 and different steps of segmentation leading to A (anhydrous clinker), D (anhydrous FA) and E (calcium hydroxide CH) obtained by the application of proposed image analysis procedure.

image. When applying morphological operations to a greyscale level, each pixel value is compared to the neighbourhood minimum or maximum value (as required by the morphological process).

The blob filter is used after segmentation to group pixels in some meaningful way into blobs of a single color with black pixels being the background [28,29]. When the image is grouped into blobs, the mask filters are used to remove the pixels remaining in the image that are not wanted.

In order to follow the reaction over time of FA particles, well polished thin sections of pastes at different ages of reaction are required. A good polishing is a key factor for a good image analysis. The application of the morphological filter to get out the FA particles could miss edges of the particles in not well polished surfaces presenting sharp edges. However, this error involves only the contours of FA particles these are estimated to 2.5% of the total volume of FA. This value will contribute to the systematic error of the method in not well polished samples.

The threshold of 1 μm could lead to an overestimation of the FA reaction. Nevertheless, this overestimation is controlled by comparing the original and segmented images. The results obtained at 1 day using SEM-IA (around 2% of FA reacted for both systems) show that these error are fairly low for the FA investigated.

The BSE-IA technique enables the quantification of the content of unreacted FA particles. Additionally, the total volumes of unreacted cement, CH, other hydrates or capillary porosity is obtained (see Fig. 7). However, in this paper we focus on quantifying the FA.

The degree of reaction of FA is obtained by subtracting the content of unreacted FA determined by IA from the initial FA content and dividing it by the initial FA content.

$$\%FA\ reacted = \left(1 - \frac{V_{meas}}{V_{ini}}\right) \times 100;$$

where V_{meas} is the volume of FA obtained from the IA and V_{ini} is the initial volume of FA in the mix proportions.

The data as shown in Table 6 and Fig. 4 indicate little reaction during the first day (≤2%) confirming that at least 98% of the FA particles are visible by IA. The FA continues to react at a rather steady rate during the first 28 days (Fig. 4), at longer hydration times the reaction rate of FA slows down, resulting in a total reaction of the FA of 35% after 140 days.

The SEM image analysis is a direct method for the calculation of the degree of reaction. Indeed, from the segmented images the different phase assemblages could be controlled visually in order to verify whether the segmentation process is accurate or not. A combination of filters and grey level thresholding was applied to distinguish between the unreacted FA and the hydrated phases. The results at early age show no overestimation of the reaction degree of FA, indicating accurate quantification of these phases. The results of the IA during the first week are comparable to the reaction determined in diluted alkaline solutions (Fig. 4). However, at later ages the results of the diluted solution diverges between Al and Si and some precipitates are observed. In the diluted solution method, a nearly infinite medium is available around FA particles: 0.05 g of FA in 50 ml of the solvent, which does not represent the situation in concrete. Additionally, other ions that may interact with FA particles to enhance or retard its dissolution are missed. The use of SEM-IA for quantifying the reactivity of the FA particles in the FA blended cements is a relatively simple and reliable method even if it requires advanced equipment and it is time consuming.

5. Conclusions

Different methods to determine the degree of reaction of FA in blended cement were evaluated and compared: selective dissolution, dissolution of FA in a diluted alkaline solution and image analysis. The techniques use different approaches: selective dissolution uses the weight fraction of phases; the dissolution rate is based on the concentration values in the solution, while the SEM image analysis is calculated from the volume change of unreacted FA.

Selective dissolution, 0.5 NaOH diluted solution and IA indicate that in both the OPC–FA and the OPC–FA–L mixture all the FA reacts significantly during the first 28 days and the reaction slows down later.

During the first 90 days, the degree of reaction of the FA measured by SEM-IA agrees well with the degree of reaction determined by Al-dissolution in alkaline solution even if the conditions are different (cementitious environment and alkaline solution). The Si concentration underestimate the FA reaction. After 28 days, conglomerates were observed in the alkaline solution, which lead to an underestimation of the degree of reaction of FA using the dilution method.

The difference in the degree of reaction between the maximum values of selective dissolution and SEM-IA starts to be very significant after 28 days, due to the presence of hydrates in the residues of the selective dissolution (Fig. 3D) leading to an underestimation of the FA reaction for the selective dissolution method. The different assumptions and corrections as well as to the presence of hydration products in the residues as observed by SEM and TGA introduce a large error in the degree of reaction determined by selective dissolution.

The SEM image analysis technique gave the most reliable and consistent results of the degree of reaction of FA in FA blended cements.

Acknowledgements

The authors would like to acknowledge COIN, the COncrete INnovation centre (http://www.coinweb.no) for facilitating the cooperation and the financial support; Frank Winnefeld and Florian Deschner for their helpful discussions of the experimental setup and the results; Harald Justnes for his helpful comments; Zajac Maciej for his contribution concerning the dissolution techniques; Gwenn Le Saout for the Rietveld analysis of FA; Boris Ingold for the excellent preparation of the polished SEM samples and Luigi Brunetti for his help on the selective dissolution experiments.

References

[1] H.F.W. Taylor, Cement chemistry, Thomas Telford publishing, London, 1997.
[2] S. Ohsawa, K. Asaga, S. Goto, M. Daimon, Quantitative determination of fly ash in the hydrated fly ash — $CaSO_4 \cdot 2H_2O$–$Ca(OH)_2$ system, Cement and Concrete Research 15 (1985) 357–366.
[3] S. Li, D.M. Roy, A. Kumar, Quantitative determination of pozzolanas in hydrated systems of cement or Ca(OH)2 with fly ash or silica fume, Cement and Concrete Research 15 (1985) 1079–1086.
[4] S.K. Antiohos, A. Papageorgiou, V.G. Papadakis, S. Tsimas, Influence of quicklime addition on the mechanical properties and hydration degree of blended cements containing different fly ashes, Construction and Building Materials 22 (2008) 1191–1200.
[5] G. Baert, Physico-chemical interactions in Portland cement — (high volume) fly ash binders, PhD, Faculty of Engineering, Ghent University, , 2009.
[6] L. Lam, Y.L. Wong, C.S. Poon, Degree of hydration and gel/space ratio of high-volume fly ash/cement systems, Cement and Concrete Research 30 (2000) 747–756.
[7] Y.M. Zhang, W. Sun, H.D. Yan, Hydration of high-volume fly ash cement pastes, Cement and Concrete Composites 22 (2000) 445–452.
[8] W.A. Gutteridge, On the dissolution of the interstitial phases in Portland cement, Cement and Concrete Research 9 (1979) 319–324.
[9] K. Mohan, H.F.W. Taylor, Pastes of tricalcium silicate with fly ash — analytical, electron microscopy, trimethylsilylation and other studies, Material Research Society, Annual Meeting (1981) 54–59.
[10] K. Ogawa, H. Uchikawa, K. Takemoto, I. Yasui, The mechanism of the hydration in the system C3S-pozzolana, Cement and Concrete Research 10 (1980) 683–696.
[11] K. Luke, F.P. Glasser, Selective dissolution of hydrated blast furnace slag cements, Cement and Concrete Research 17 (1987) 273–282.
[12] J.A. Dalziel, W.A. Gutteridge, The influence of pulverized fuel ash upon the hydration characteristics and certain physical properties of a Portland cement paste, Cement and Concrete Association, technical report 560, 1986, 28 pages.
[13] B.A. Suprenant, G. Papadopoulos, Selective dissolution of Portland Fly Ash cements, Journal of Materials and Civil Engineering 3 (1991).
[14] K. Luke, F.P. Glasser, Internal chemical evolution of the constitution of blended cements, Cement and Concrete Research 18 (1988) 495–502.
[15] H.S. Pietersen, The reactivity of fly ash in cement, PhD thesis, TU Delft, (1993).

[16] P.L. Rayment, The effect of pulverised-fuel ash on the c/s molar ratio and alkali content of calcium silicate hydrates in cement, Cement and Concrete Research 12 (1982) 133–140.
[17] H.F.W. Taylor, K. Mohan, G.K. Moir, Analytical study of pure and extended Portland cement pastes: II, fly ash- and slag-cement pastes, Journal of the American Ceramic Society 68 (1985) 685–690.
[18] M. Mouret, A. Bascoul, G. Escadeillas, Study of the degree of hydration of concrete by means of image analysis and chemically bound water, Advanced Cement Based Materials 6 (1997) 109–115.
[19] K.L. Scrivener, Backscattered electron imaging of cementitious microstructures: understanding and quantification, Cement and Concrete Composites 26 (2004) 935–945.
[20] K.L. Scrivener, H.H. Patel, P.L. Pratt, L.J. Parrott, Analysis of phases in cement paste using backscattered electron images, methanol adsorption and thermogravimetric analysis, Proceeding Material Research Society Symposium, Microstructural Development During the Hydration of Cement (1986) 67–76.
[21] A. Gruskovnjak, B. Lothenbach, F. Winnefeld, B. Münch, R. Rigi, S. Ko, M. Adler, U. Mäder, Quantification of hydration phases in supersulphated cements : review and new approaches, Advances in cement research, (Submitted).
[22] M. Ben Haha, E. Gallucci, A. Guidoum, K.L. Scrivener, Relation of expansion due to alkali silica reaction to the degree of reaction measured by SEM image analysis, Cement and Concrete Research 37 (2007) 1206–1214.
[23] K.L. Scrivener, T. Füllmann, E. Gallucci, G. Walenta, E. Bermejo, Quantitative study of Portland cement hydration by X-ray diffraction/Rietveld analysis and independent methods, Cement and Concrete Research 34 (2004) 1541–1547.
[24] M. Mouret, E. Ringot, A. Bascoul, Image analysis: a tool for the characterisation of hydration of cement in concrete — metrological aspects of magnification on measurement, Cement and Concrete Composites 23 (2001) 201–206.
[25] P.C. Ashbrook, T.A. Houts, Picric acid, Chemical Health and Safety 10 (2003) 27–???.
[26] G. Lunn, E.B. Sansone, Destruction of hazardous chemicals in the laboratory, John Wiley & Sons, New York, 1990, pp. 219–221.
[27] R. Yang, N.R. Buenfeld, Binary segmentation of aggregate in SEM image analysis of concrete, Cement and Concrete Research 31 (2001) 437–441.
[28] T. Jiang, M.B. Merickel, Identification and boundary extraction of blobs in complex imagery, Computerized Medical Imaging and Graphics 13 (1989) 369–382.
[29] D. Marr, E. Hildreth, Theory of edge detection, Proceedings of the Royal Society of London Series B, Biological Sciences 207 (1980) 187–217.
[30] A. Fernández-Jiménez, A.G. de la Torre, A. Palomo, G. López-Olmo, M.M. Alonso, M.A.G. Aranda, Quantitative determination of phases in the alkaline activation of fly ash. Part II: degree of reaction, Fuel 85 (2006) 1960–1969.
[31] K. Dombrowski, A. Buchwald, M. Weil, The influence of calcium content on the structure and thermal performance of fly ash based geopolymers, Journal of Materials Science 42 (2007) 3033–3043.
[32] J.S. Lumley, R.S. Gollop, G.K. Moir, H.F.W. Taylor, Degrees of reaction of the slag in some blends with Portland cements, Cement and Concrete Research 26 (1996) 139–151.
[33] H.M. Dyson, I.G. Richardson, A.R. Brough, A combined [29]Si MAS NMR and selective dissolution technique for the quantitative evaluation of hydrated blast furnace slag cement blends, Blackwell, Malden, MA, ETATS-UNIS, 2007.

Paper VI

Hydration mechanisms of ternary Portland cements containing limestone powder and fly ash
De Weerdt K., Ben Haha M., Le Saout G., Kjellsen K.O., Justnes H. & Lothenbach B.
Cement and Concrete Research, 2010, in press,
doi:10.1016/j.cemconres.2010.11.014

Cement and Concrete Research xxx (2010) xxx–xxx

Contents lists available at ScienceDirect

Cement and Concrete Research

journal homepage: http://ees.elsevier.com/CEMCON/default.asp

Hydration mechanisms of ternary Portland cements containing limestone powder and fly ash

K. De Weerdt [a,*], M. Ben Haha [b], G. Le Saout [b], K.O. Kjellsen [c,d], H. Justnes [a], B. Lothenbach [b]

[a] SINTEF Building and Infrastructure, 7465 Trondheim, Norway
[b] EMPA, Swiss Federal Laboratories for Material Science and Technology, Laboratory for Concrete and Construction chemistry, 8600 Dübendorf, Switzerland
[c] NTNU, Department of Structural Engineering, 7491 Trondheim, Norway
[d] Norcem AS HeidelbergCement, Setreveien 2, 3991 Brevik, Norway

ARTICLE INFO

Article history:
Received 30 August 2010
Accepted 19 November 2010
Available online xxxx

Keywords:
Pore solution (B)
SEM (B)
X-ray diffraction (B)
Thermodynamic calculations (B)
Compressive strength (C)

ABSTRACT

The effect of minor additions of limestone powder on the properties of fly ash blended cements was investigated in this study using isothermal calorimetry, thermogravimetry (TGA), X-ray diffraction (XRD), scanning electron microscopy (SEM) techniques, and pore solution analysis. The presence of limestone powder led to the formation of hemi- and monocarbonate and to a stabilisation of ettringite compared to the limestone-free cements, where a part of the ettringite converted to monosulphate. Thus, the presence of 5% of limestone led to an increase of the volume of the hydrates, as visible in the increase in chemical shrinkage, and an increase in compressive strength. This effect was amplified for the fly ash/limestone blended cements due to the additional alumina provided by the fly ash reaction.

1. Introduction

Adding 5% limestone powder to Portland cement has been a point of discussions in the past. Proponents put forward energy savings during production, without impairing the quality of the cement and concrete properties. Whereas the opponents claim that limestone powder is merely an adulterant, leading to a reduction in quality [1,2]. One of the first incentives to allow carbonate additions to Portland cement was given by the oil shortage in the 1970's–1980's. This led to an adaption of the Canadian standard CAN3-A5-M83 permitting 5% limestone powder in Portland cement since 1983, followed by the Brazilian norm NBR-5732 adapted in 1988. The rising focus on greenhouse-gasses in the 1990's added to the motivation and in 2000 the proposal for the European standard EN 197-1 (CEN 2000) was accepted, followed by the ASTM C150 in 2004 and the AASHTO M85 in 2007.

A thorough review on the use of limestone powder in Portland cement is given by Hawkins et al. [3]. The effect of 5% limestone powder addition on short and long term macroscopical properties is generally small. Regarding the compressive strength, both enhanced strength and reduced strength have been reported upon limestone addition. A benefit of the addition of small amounts of carbonate is a reduction of the expansion observed upon sulphate attack, which is most prominent for cements with high C_3A-content [3,4]. It also leads to a reduction of the optimal gypsum content, which may result in a reduction of raw material costs. Some of the beneficial effects of limestone powder are attributed to its filler effect. Some researchers report an acceleration of the C_3S and an incorporation of the calcium carbonate into the C–S–H [5,6]. Additionally, limestone is known to interact with AFm and AFt phases. In an ordinary Portland cement without limestone powder, the C_3A and at a slower rate also the C_4AF will react with the calcium sulphate to form ettringite ($C_3(A,F)\cdot 3CaSO_4\cdot 32H_2O$). Upon depletion of the sulphates, the remaining C_3A and C_4AF will react with the ettringite to form monosulphate ($C_3(A,F)\cdot CaSO_4\cdot 12H_2O$) or hydroxy-AFm solid solution. In the presence of limestone, the AFm-carbonate equivalents such as monocarbonate ($C_3(A,F)\cdot CaCO_3\cdot 11H_2O$) are formed rather than the sulphate containing AFm phases. The AFt-carbonate equivalent has been observed by some researchers [7], but it is unlikely to form in a significant amount at ambient temperatures in a hydrating cements as it is less stable than the AFm phases [8,9]. The decomposition of ettringite to monosulphate when reacting with the remaining C_3A and C_4AF upon sulphate depletion is prevented as monosulphate is less stable than monocarbonate in the presence of limestone. The stabilisation of the voluminous, water rich ettringite instead of the less voluminous monosulphate, gives rise to an increase of the total volume of hydration products [10–13]. If some of the beneficial macroscopic effects observed for limestone additions up to 5%, are due to this chemical interaction, it is obvious that the impact will be greater for cements with a high C_3A and C_4AF content as observed by previous investigations [2].

The previous statements and observations brought the idea to investigate the effect of limestone powder additions on blended fly ash cements. Fly ash has generally higher alumina content than OPC. The reaction of fly ash brings additional alumina, which reduce the

* Corresponding author. Tel.: +47 73594866.
E-mail address: klaartje.de.weerdt@sintef.no (K. De Weerdt).

0008-8846/$ – see front matter © 2010 Published by Elsevier Ltd.
doi:10.1016/j.cemconres.2010.11.014

sulphate to alumina ratio and therefore increases the impact of limestone powder. Previous studies have documented a beneficial effect on the strength development when a small amount of limestone powder is combined with either fly ash [14], natural pozzolans [15] or slag [11,16,17]. Up to 90 days, the ternary Portland cements containing pozzolans or slag, and limestone had a higher strength than their equivalent composite cements without limestone. The underlying reasons for this effect have not been investigated, except by Hoshino et al. [11] who attributed the observed interaction between slag and limestone powder to changes in the AFm and AFt phases, using XRD-Rietveld analysis.

Several series of experiments investigating ternary Portland cements containing fly ash and limestone powder have been performed to study the effect of OPC or fly ash replacement by limestone powder in respectively OPC and fly ash blended cement [18–23]. Minor replacements of fly ash by limestone powder appeared to have a beneficial effect on the strength development of the tested ternary blended cements. A similar effect was observed for the tested OPC but the effect appeared to be less pronounced [21,22] and in some cases replacing 5% of OPC by limestone powder resulted even in a loss of strength [23].

The aim of this paper is to find out how exactly minor additions of limestone powder affect the hydration of OPC and blended fly ash cement. In order to investigate the effect quantitatively, a multi-method approach was adopted on the four following mixes: 100% OPC, 95% OPC + 5% limestone, 65% OPC + 35% fly ash and 65% OPC + 30% fly ash + 5% limestone.

2. Materials

The materials used in this study are: ordinary Portland clinker, class F siliceous fly ash (FA), limestone powder (L), natural gypsum and crystalline quartz (Q). The chemical composition determined by XRF and the physical properties of the clinker, fly ash, limestone and quartz are given in Table 1. The clinker was interground with 3.7% of natural gypsum and is further referred to as ordinary Portland cement (OPC). The gypsum used has a $CaSO_4 \cdot 2H_2O$ content of 91.4%. The mineral composition of the OPC and the fly ash determined by Rietveld analysis are given in Tables 2 and 3. The $CaCO_3$ content of the limestone, determined by thermogravimetric analysis (TGA), is about 81%. The limestone powder and the fly ash were ground separately in a laboratory ball mill with a capacity of 9 kg. The particle size distribution of OPC, fly ash and limestone powder determined by laser granulometry using a Malvern Mastersizer are given in Fig. 1.

The experimental matrix is given in Table 4. Some additional combinations were tested using quartz powder instead of limestone powder. The crystalline quartz was assumed to be chemically inert and was therefore used to study the filler effect. The quartz powder was obtained by combining 3 different powders, resulting in a particle size distribution similar to the one of limestone powder (Fig. 1).

Table 1
Chemical composition (wt.%) and the physical characteristics of the clinker, fly ash and limestone powder.

	Clinker	Fly ash	Limestone	Quartz
SiO_2	20.0	50.0	12.9	99.4
Al_2O_3	5.4	23.9	2.7	0.3
Fe_2O_3	3.1	6.0	2.0	0.04
CaO	60.6	6.3	42.3	0.02
MgO	2.9	2.1	1.8	–
SO_3	1.5	0.4	–	–
P_2O_5	0.1	1.1	–	–
K_2O	1.2	1.4	0.6	0.04
Na_2O	0.5	0.6	0.5	–
LOI	0.3	3.6	37.7	–
Carbon	–	3.1	–	–
Chloride	0.05	0.0	–	–
Free CaO	1.85	–	–	–
Gypsum	3.7	–	–	–
Blaine surface [m^2/kg]	450*	450	810	–
Density [kg/m^3]	3150*	2490	2740	2650
D_{50} [μm]	11*	14	4	5

* For OPC = clinker + gyspum.

Table 2
Mineral composition of the clinker determined by XRD-Rietveld analysis.

Minerals	[wt.%]
C_2S	19
C_3S	54
C_3A	11
C_4AF	8

Table 3
Mineral composition of the fly ash determined by XRD-Rietveld analysis.

Minerals	[wt.%]
quartz	12.3
calcite	0.4
hematite	0.6
anhydrite	0.4
mullite	18.3
amorphous*	68.0

* Glass and 3% amorphous carbon.

3. Methods

Mortar prisms (40 × 40 × 160 mm) with cement–sand–water proportions of (1/3/0.5) were prepared. The samples were cured in $Ca(OH)_2$ saturated solution at 20 °C. The *compressive and flexural strength* were determined on two mortar prisms for each testing age according to EN 196-1.

About 6 g of paste with water to binder ratio of 0.5 was prepared in a glass vial using a slow stirring IKA-WERKE RW16 mixer. The vial was sealed and loaded into a TAM Air isothermal calorimeter in order to determine the *rate of heat of hydration* during the first 24 h at 20 °C.

Chemical shrinkage at 20 °C was assessed using the method described by Geiker et al. [24].

Cement paste samples were prepared with water to binder ratio of 0.5 and stored at 20 °C in 20 ml sealed plastic vessels for thermogravimetric analysis (TGA), X-ray diffraction (XRD) and scanning electron microscopy (SEM) studies, and 500 ml sealed plastic bottles for pore solution analysis. The samples, used for thermogravimetric

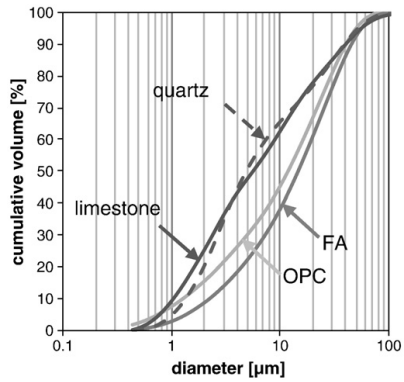

Fig. 1. The particle size distribution of OPC, FA, limestone and quartz determined by laser diffractometry.

Please cite this article as: K. De Weerdt, et al., Hydration mechanisms of ternary Portland cements containing limestone powder and fly ash, Cem. Concr. Res. (2010), doi:10.1016/j.cemconres.2010.11.014

Table 4
Experimental matrix in wt.%.

Name	OPC	FA	L
OPC	100	–	–
OPC-L	95	–	5
OPC-FA	65	35	–
OPC-FA-L	65	30	5

analysis and X-ray diffraction, were crushed (<63 μm). The hydration was stopped by solvent exchange using isopropanol during 15 min and flushing with ether.

Thermogravimetric analysis was performed on about 50 mg of the resulting powder by monitoring the weight while heating up from 30 to 980 °C at 20 °C/min and purging with N_2, in a Mettler Toledo TGA/SDTA851. The amount of hydrate water (H) and calcium hydroxide (CH) are expressed as% of the dry sample weight at 550 °C (w_{550}):

$$H = \frac{w_{40} - w_{550}}{w_{550}} \quad (1)$$

and

$$CH = \frac{w_{450} - w_{550}}{w_{550}} \cdot \frac{74}{18}(*) \quad (2)$$

(*) $Ca(OH)_2$ (74g/mol) → CaO + H_2O (18g/mol) weight difference determined using stepwise method.

The exact boundaries for the temperature intervals were read from the derivative curve (DTG). The standard deviation on three independent measurements at all tested ages is not larger than 0.1% for H and 0.2% for CH.

About 3 g of the powder was analysed by *X-ray diffraction* (XRD) using a PANalytical X'Pert Pro MPD diffractometer in a θ–2θ configuration with an incident beam monochromator and CuKα radiation (λ = 1.54 Å). The samples were scanned between 5° and 70° with the X'celerator detector. The *Rietveld analysis* was performed using an external CaF_2 standard according to the method described by Le Saout et al. [25].

Slices of hydrated cement paste samples were cut using a water lubricated saw. They were immediately immersed in isopropanol, kept in it for 30 min and subsequently dried at 40 °C for 24 h. The outer layer of the slice was removed using sand paper. A piece of the slices of the hydrated paste was impregnated using low viscosity epoxy resin, polished down to 0.25 μm, coated with carbon (few nm) and examined using a Philips ESEM FEG XL 30 scanning electron microscopy (SEM). *Backscattered electron images* (BSE) were analysed quantitatively using *image analysis* (IA) to determine the coarse capillary porosity and the degree of reaction of OPC and fly ash [26] by monitoring the changes in their vol.% over time. Sixty images were taken per sample at a magnification of 1600. The minimum pore radius measured corresponds to 0.17 μm. Hence, the coarse porosity measured by this method is only a fraction of the total porosity. *Energy dispersive X-ray spectroscopy* (EDX) was applied to determine the element compositions of the matrix. The Ca/Si ratios, as well as the Al incorporation in the C–S–H, were determined. The analyses were carried out using an accelerating voltage of 15 kV to ensure a good compromise between spatial resolution and adequate excitation of the FeKα peak.

The pore solution was extracted using the steel die method [27]. Immediately after extraction, the solution was filtrated using a 0.45 μm nylon filter. The pH of the pore solution was analysed with a *pH* electrode, calibrated with known KOH concentrations. The concentration of Na, K, S, Ca, Si and Al in the *pore solution* was determined using a Dionex Ion Chromatography system (ICS) 3000 using standards from Fluka.

The hydration of the tested cements was modelled using the Gibbs free energy minimization program, GEMS [28]. The thermodynamic data from the PSI-GEMS database [29,30] was supplemented with cement specific data [31–33]. GEMS computes the equilibrium phase assemblage in a multi-component system based on the bulk composition of the materials. For the sake of simplicity, the part of limestone which is not $CaCO_3$ is considered inert as well as the crystalline part of the fly ash, and the glass phase of the fly ash [26] is assumed to dissolve uniformly.

To check whether the crystalline quartz behaves as an inert material, 50 g of quartz powder was mixed with 50 g of $Ca(OH)_2$ and 100 ml alkaline solution with a pH of 13.5 and KOH:NaOH ratio of 2:1. A small portion of the paste was taken immediately after mixing and the reaction was stopped by solvent exchange using isopropanol and flushing with ether. The rest of the paste was stored under sealed conditions at 20 °C and after 28 days the reaction of the paste was stopped. Both the sample taken immediately after mixing (0 day) and the 28 day old sample were analysed by TGA (see Fig. 2). The quartz seems to be slightly reactive as water was bound in hydration products (increased weight loss up to 350 °C) and calcium hydroxide was consumed (16% decrease in weight loss between 350 and 500 °C). This indicates that the "inert" quartz filler was not completely inert.

4. Results and discussions

4.1. General

Limestone replacement seems to influence the compressive strength of the OPC and OPC-FA mortars. Indeed, the *compressive strength* tends to increase slightly when 5% of respectively OPC or fly ash is replaced by 5% limestone powder from 3 days and onwards, but not after 1 day (Table 5 and Fig. 3). The increase in strength in the presence of 5% limestone is more pronounced for the OPC-FA than for the OPC sample. Replacing part of the OPC by fly ash, results in a slower strength development up to 28 days (Fig. 3). The impact of the replacement with limestone on the *flexural strength* (Table 5) was within the variations of the results.

The effect of limestone and fly ash replacement on the amount of hydrate water (H) and the amount of calcium hydroxide (CH) is determined by TGA analyses. The results (Table 5 and Fig. 4) show that replacing 5% of OPC with limestone powder does not influence the *amount of hydrate water* per OPC but tends to decrease the *CH content* per OPC from 7 days. Replacing 5% of fly ash by 5% of limestone

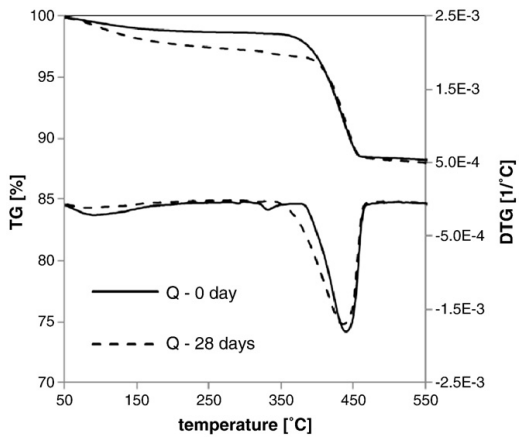

Fig. 2. Weight loss (TG) and derivative weight loss (DTG) curves for 50:50 $Ca(OH)_2$: quartz (Q) mix.

Please cite this article as: K. De Weerdt, et al., Hydration mechanisms of ternary Portland cements containing limestone powder and fly ash, Cem. Concr. Res. (2010), doi:10.1016/j.cemconres.2010.11.014

Table 5
The compressive (σ_{comp}) and flexural strength (σ_{flex}), and the amount of hydrate water (H) and calcium hydroxide (CH).

Time [days]	σ_{comp} [MPa]	σ_{flex} [MPa]	H [wt.%]	CH [wt.%]
OPC				
1	22.1	5.3	15.1	12.3
3	31.6	7.2	–	–
7	36.1	7.7	21.9	18.6
28	45.6	7.1	24.1	20.1
90	48.0	6.9	26.3	22.6
180	–	–	28.2	23.4
OPC-L				
1	21.9	5.0	14.6	11.9
3	32.8	7.0	–	–
7	38.1	7.4	21.0	16.3
28	43.9	7.4	23.4	17.9
90	51.5	7.5	25.0	19.3
180	–	–	27.3	20.5
OPC-FA				
1	12.1	3.1	11.2	9.1
3	21.5	4.7	–	–
7	25.7	5.2	16.0	13.1
28	37.8	7.0	18.2	13.5
90	52.3	6.8	19.8	12.5
180	–	–	22.1	12.1
OPC-FA-L				
1	12.4	3.2	11.4	9.6
3	23.8	4.8	–	–
7	28.8	5.7	17.0	12.9
28	39.8	6.0	19.4	12.7
90	55.3	8.5	21.1	11.9
180	–	–	22.9	11.4

powder in OPC-FA however increases the amount of hydrate water per OPC after 7 days and decreases the CH content per OPC after 28 days. The observed decrease in CH when limestone powder is present indicates the formation of hydration products which consume CH e.g. calcium hemicarboaluminate hydrate.

The CH content and the amount of hydrate water per OPC of the fly ash containing cements are initially higher than the OPC and OPC-L cements (Fig. 4), due to the filler effect of the fly ash. Replacing OPC with fly ash increases the effective water to OPC ratio and the fly ash provides additional surface for hydration products to precipitate on, thereby stimulating the OPC reaction. However, the amount of hydrate water relative to the dry binder however decreases, indicating that the filler effect does not compensate for the replacement of the OPC. From 7 to 28 days, the CH content per OPC starts to decrease in the fly ash containing cements as it is consumed by the pozzolanic reaction of the fly ash. The amount of CH was also determined by XRD-Rietveld. The results of both techniques correlated well (±1 wt.% error on both techniques).

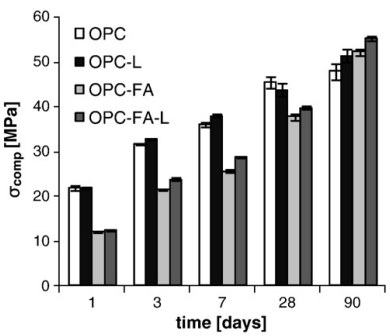

Fig. 3. The compressive strength of mortar samples.

Isothermal calorimetry shows that there is hardly any difference between the heat of hydration per gram OPC evolved during the hydration of OPC or OPC-FA and their limestone containing equivalents during the first 24 h (Fig. 5), which is in agreement with other findings [13]. However, it should be noted that the effect of limestone powder on the heat of hydration emitted depends on the water-to-cement ratio used [34] and the fineness of the limestone powder [35]. The replacement of OPC by fly ash results in an increase and a delay of the maximum *rate of heat of hydration* relative to the OPC content. The shape of the heat evolution curves is also influenced by the presence of the fly ash confirming previous investigations [21]. The cumulative heat per binder emitted during the first 24 h is decreased with the replacement of 35% of OPC with fly ash and/or limestone, (230 → 180 J/g binder). However, the cumulative heat per OPC content increases due to filler effect (230 → 280 J/g OPC) of both limestone and fly ash.

Coupling the previous observations, limestone powder has clearly an effect on the hydration of OPC and OPC-FA reflected by the increase of the compressive strength and amount of bound water and the decrease of calcium hydroxide. However, this effect is not clearly shown from the one day results (e.g. calorimetry and strength), but only prevails later. Microstructural investigations are performed to define qualitatively and quantitatively the effect of limestone powder on the hydrates of both OPC and OPC-FA blended systems.

4.2. Physical or chemical effect?

In order to investigate whether the effect of limestone powder on the hydration of OPC and fly ash blended cements is only physical (additional nucleation sites and higher effective water to cement ratio) or whether there is also chemical effect; limestone powder was replaced with crystalline quartz powder with similar particle size distribution to simulate the physical effect of the limestone.

A new series of experiments including compressive and flexural strength as well as TGA experiments were performed using a different batch of the clinker interground with gypsum. The compressive and flexural strength as well as the amount of hydrate water (H) and calcium hydroxide (CH) after 1 and 28 days of curing at 20 °C, are shown in Table 6 for OPC and fly ash blended cements in which the same amounts of limestone powder and quartz were used. The obtained results are similar to those shown in Table 5.

There is no clear difference between limestone and quartz replacement (5 and 10% of the OPC) in *OPC systems* after 1 day of hydration as shown by both compressive strengths and TGA measurements. Using limestone powder instead of quartz resulted in all cases in a higher compressive strength (about 3–5%) after 28 days of hydration (Table 6). The TGA results after 28 days shows slightly more hydrate water for the limestone powder containing blends (Table 6). The slightly reduced CH content for the quartz containing blends compared to the limestone containing ones is most likely caused by the slight reactivity of the quartz powder (Fig. 2).

For the *fly ash blended cements*, an increase in compressive (8%) and flexural (10%) strength is observed when 5 and 10% of the fly ash is replaced with limestone powder at 28 days (Table 6). Fly ash can be substituted with quartz without impairing the early age compressive and flexural strength. After 28 days more water was bound and slightly less CH was present in the fly ash cements containing limestone powder than in the pure fly ash blended cements, as observed also in Table 5 and Fig. 4. When quartz is used instead of limestone powder in the fly ash blended cements the amount of hydrate water and CH is lower.

The *chemical shrinkage* relative to the OPC content for some of the composite cements containing limestone or quartz is shown in Fig. 6.

Please cite this article as: K. De Weerdt, et al., Hydration mechanisms of ternary Portland cements containing limestone powder and fly ash, Cem. Concr. Res. (2010), doi:10.1016/j.cemconres.2010.11.014

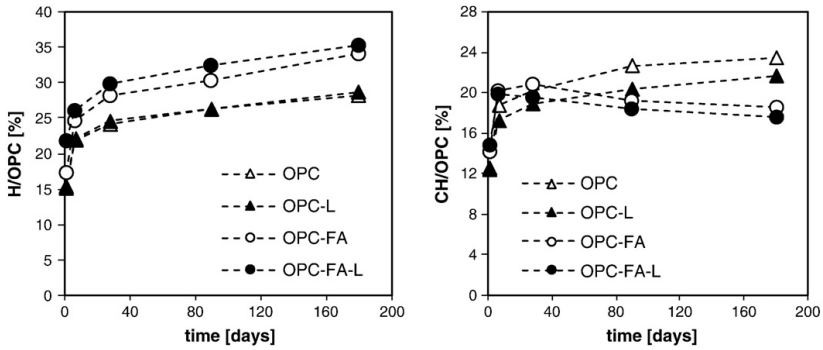

Fig. 4. The amount of hydrate water (H) and calcium hydroxide (CH) relative to the OPC content.

During cement hydration the cement paste exerts chemical shrinkage as the volume of hydration products is smaller than the volume of the reactants. OPC-L and OPC-FA-L have a slightly higher chemical shrinkage per OPC than their limestone free equivalents, OPC and OPC-FA (Fig. 6), indicating that when limestone is present more hydration products are formed, or alternatively different hydrates are formed with even less volume relative to the reactants than the usual hydrates. The fly ash containing cements have a higher total chemical shrinkage per OPC partly caused by the filler effect of the fly ash and partly by the pozzolanic reaction of the fly ash which progresses with time. The quartz (Q) seems to react over time as the slope of the curve after about 12 days is steeper than the ones of 100% OPC and 95% OPC + 5% L. The chemical shrinkage per OPC for the 65% OPC + 30% FA + 5% L and 65% OPC + 30% FA + 5% Q is similar. The fact that the chemical shrinkage of 65% OPC + 35% FA is slightly higher than 65% OPC + 35% Q indicates that the fly ash is more reactive than the quartz.

4.3. Hydration

4.3.1. Anhydrous phases

In order to investigate whether the observed effect of the limestone powder on the mechanical properties of the OPC and the fly ash blended cements is due to a promotion of the clinker hydration, the hydration of clinker phases was monitored by XRD-Rietveld analysis at 0, 1, 7, 28, 90 and 180 days.

The evolution of the anhydrous clinker phases over time is shown in Table 7. *Alite* appears to react fast: more than 70% has reacted after 1 day and more than 90% after 7 days for all tested combinations. The faster reaction of the clinker phases observed in the presence of FA can be attributed to the filler effect of fly ash [36–39]. There is no large difference between OPC-FA and OPC-FA-L concerning the alite hydration, which could explain the observed effect on the compressive strength, bound water and CH of limestone powder on the blended fly ash cement. The content of the aluminate and ferrite phases in the pastes are rather low and their relative error is large, rendering the interpretation of these results difficult. The trends indicate a faster reaction of aluminate and ferrite in the FA containing mixtures. From 28 days, the fly ash tends to retard the reaction of belite in the FA blended pastes confirming the previous reported results [37,39,40]. The overall % of OPC reacted as function of time is similar for all tested combinations.

The degree of hydration of the clinker was also determined by SEM-IA (Fig. 7). Compared to the results from XRD-Rietveld analysis (Table 7), SEM-IA slightly overestimates the degree of reaction of the OPC at early age compared to XRD-Rietveld analysis, possibly due to the omission of small anhydrous grains not detected by SEM-IA. Overall, there is a reasonable agreement between two techniques.

The observed enhancing effect of limestone on the strength, TGA weight loss and chemical shrinkage of the OPC-FA cement might also be caused by a promotion of the fly ash reaction. The degree of

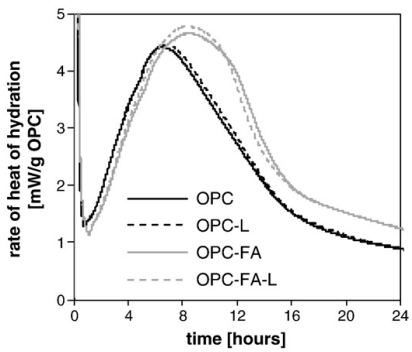

Fig. 5. The rate of heat of hydration relative to the OPC content.

Table 6
Comparing compressive (σ_{comp}) and flexural strength (σ_{flex}), hydrate water (H) and calcium hydroxide (CH) when replacing limestone powder with crystalline quartz.

	Time [days]	σ_{comp} [MPa]	σ_{flex} [MPa]	H [wt.%]	CH [wt.%]
LIMESTONE (L)					
100OPC	1	22.9	4.9	13.6	13.7
	28	47.5	7.9	22.9	21.2
95OPC-5L	1	21.4	4.9	13.2	13.2
	28	46.6	7.7	23.1	20.0
90OPC-10L	1	21.7	4.8	13.3	13.3
	28	45.5	8.0	22.2	19.1
65OPC-35FA	1	12.3	3.0	10.2	10.6
	28	38.3	6.8	17.4	15.0
65OPC-30FA-5L	1	13.2	3.3	10.5	10.6
	28	41.2	7.6	18.5	14.4
65OPC-25FA-10L	1	13.3	3.2	10.3	10.5
	28	41.2	7.9	18.5	14.5
QUARTZ (Q)					
95OPC-5Q	1	20.6	4.8	13.6	13.5
	28	44.4	7.6	22.5	19.4
90OPC-10Q	1	20.8	5.0	13.4	13.2
	28	44.0	7.6	21.6	18.6
65OPC-30FA-5Q	1	12.7	3.4	11.2	11.3
	28	38.5	6.7	18.1	13.9
65OPC-25FA-10Q	1	12.8	3.2	10.4	10.5
	28	38.7	6.8	16.5	12.2

Please cite this article as: K. De Weerdt, et al., Hydration mechanisms of ternary Portland cements containing limestone powder and fly ash, Cem. Concr. Res. (2010), doi:10.1016/j.cemconres.2010.11.014

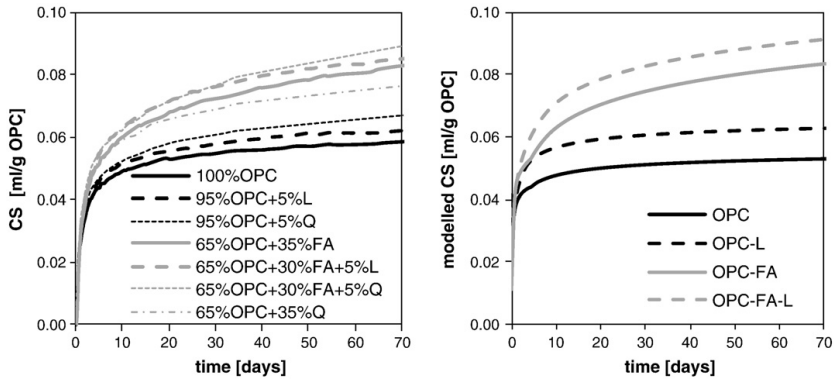

Fig. 6. The measured and modelled chemical shrinkage (CS) relative to the OPC content.

reaction of the fly ash was quantified using SEM-IA as reported in a previous study [26]. Limestone powder does not seem to accelerate the fly ash reaction; the fly ash degree of reaction is similar in both OPC-FA and OPC-FA-L (see Fig. 7).

4.3.2. Hydration products

In order to study the difference in hydration products formed by the tested composite cements, their XRD patterns are compared. The main difference in the XRD-patterns can be seen at low angles, where the main peaks of the AFm and AFt phases are found (Fig. 8). After 1 day of hydration, the patterns are similar for all tested cements: ettringite (9.1° 2θ) and ferrite (12.2° 2θ) are observed. In the absence of limestone powder, the remaining aluminates react with the ettringite to form monosulphate (Ms 9.8° 2θ) [41] after all gypsum is consumed according to:

$$2\ C_3A + C_6A\underline{S}_3H_{32} + 4\ H \rightarrow 3\ C_4A\underline{S}H_{12} \quad (3)$$

Table 7
Content of calcium hydroxide (CH), ettringite, amorphous phases, anhydrous clinker phases relative to the dry content in wt.% determined by XRD-Rietveld analysis.

	Time [days]	CH	Ettringite	Amorphous*	C_3S [wt.%]	C_2S	C_3A	C_4AF	%OPC reacted
OPC	0	–	–	–	55.3	18.9	10.7	8.1	–
	1	12.6	9.8	46.2	15.3	17.8	5.9	5.9	51.7
	7	18.9	10.1	61.3	6.5	17.1	2.5	3.7	68.0
	28	19.0	9.1	71.9	4.5	15.5	1.5	2.5	74.3
	90	21.8	7.4	77.2	2.0	8.2	1.5	2.5	84.7
	180	21.9	8.8	79.6	1.4	6.5	1.5	2.7	87.1
OPC-L	0	–	–	–	52.5	18.0	10.2	7.7	–
	1	11.5	9.0	48.4	13.0	16.7	5.5	5.5	54.0
	7	18.0	9.6	57.1	6.1	15.5	1.8	3.5	69.6
	28	18.3	10.4	62.0	2.9	13.4	1.3	2.5	77.3
	90	18.8	9.9	68.7	2.2	7.8	1.4	2.2	84.5
	180	21.0	11.0	67.9	1.6	5.8	1.4	2.2	87.6
OPC-FA	0	–	–	23.8	33.2	12.2	7.0	5.2	–
	1	8.7	9.0	52.4	9.2	12.2	3.8	4.0	49.1
	7	14.0	7.4	62.6	2.4	11.6	0.8	2.5	69.8
	28	13.7	7.5	69.3	–	10.6	–	1.6	79.0
	90	12.5	6.6	71.2	–	7.8	–	1.5	84.0
	180	11.3	6.6	76.5	–	7.1	–	–	87.6
OPC-FA-L	0	–	–	20.4	33.2	12.2	7.0	5.2	–
	1	8.8	9.3	49.5	8.8	12.0	3.8	3.8	50.8
	7	13.5	9.2	58.4	1.8	11.6	0.7	2.1	71.6
	28	12.8	9.5	67.3	0.6	9.3	–	–	82.8
	90	12.2	10.5	63.0	–	7.3	–	–	87.4
	180	10.8	10.9	69.5	–	6.1	–	–	89.5

* Amorphous = C–S–H + AFm + amorphous content fly ash.

Thus less ettringite is observed in the blends without limestone (Fig. 8). Additionally, another broad peak is observed between Ms and Hc, which might be associated with a carbonate and sulphate containing hydroxy-AFm (AFm*) [13,41].

From 7 days on, AFm* is observed in OPC and OPC-FA. In the OPC-FA blend monosulfate is (Ms) is clearly visible after 28 days.

For the limestone containing combinations, the remaining aluminates will react with calcium carbonate to form a combination of mono- and hemicarbonate (Mc at 11.7° 2θ and Hc at 10.8° 2θ) as observed in Fig. 8 for OPC-L and OPC-FA-L. In this case ettringite does not decompose in reaction with C_3A (Eq. 3):

$$C_3A + C\underline{C} + 11\ H \rightarrow C_4A\underline{C}H_{11} \quad (4)$$

$$C_3A + 0.5\ C\underline{C} + 0.5\ CH + 11.5\ H \rightarrow C_4AC_{0.5}H_{12} \quad (5)$$

After 7 days and longer a relatively large peak for hemicarbonate is observed, which decreases with time as monocarbonate forms instead in the OPC-L and OPC-FA-L blends. This might be due to the limited solubility/slow dissolution of the limestone powder.

It should be noted that the calcium hydroxide is consumed during the formation of hemicarbonate (Eq. (5)) which is in line with the observed relative decrease in CH determined by TGA when 5% of the OPC or fly ash is replaced by 5% limestone powder.

SEM-EDX and TGA measurements shown in Fig. 9 confirm the changes in the AFm phases: when limestone is present Mc and Hc are formed instead of Ms, which is in agreement with XRD data discussed previously.

The fly ash blended cements have higher amount of AFm phases relative to the OPC content due to the additional alumina provided by the reaction of the fly ash and to a smaller extent due to the acceleration of the hydration of the aluminate phase of the OPC (Fig. 8).

Rietveld analysis was used to quantify the portlandite, ettringite and the amount of amorphous phases (Table 7). AFm phases are not quantified due to their ill-crystalline structure, their relatively low amount and the lack of data concerning some structures such as hemicarbonate or hydroxyl AFm. Somewhat more ettringite and slightly less portlandite were observed in the samples containing limestone. The presence of FA increased the amount of ettringite per g OPC and decreased the amount of portlandite over time.

The composition of the C–S–H is characterised by SEM-EDX. The Ca/Si ratio and Al/Si ratio of OPC and OPC-L are constant over time with a mean Ca/Si ≈ 1.8 ± 0.1 and Al/Si ≈ 0.06 ± 0.01. For OPC-FA and OPC-FA-L the ratios change with time: the Ca/Si ratio decreases from ≈1.7 at 1 day to ≈1.4 at 140 days, and the Al/Si ratio increases

Please cite this article as: K. De Weerdt, et al., Hydration mechanisms of ternary Portland cements containing limestone powder and fly ash, Cem. Concr. Res. (2010), doi:10.1016/j.cemconres.2010.11.014

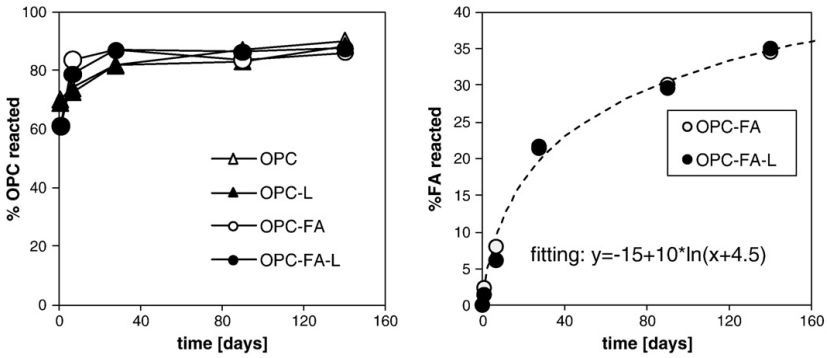

Fig. 7. Percentage of OPC and FA reacted as a function of time both determined by SEM-IA.

respectively from ≈0.06 to ≈0.13 indicating the formation of a more Si rich C–S–H which incorporates more aluminium. The lower Ca/Si and higher Al/Si ratios in the presence of fly ash after longer reaction times agree well with the values found in literature [36,42,43]. The C–S–H present in the OPC-FA blends shows a significant variation in the composition. EDX analysis indicates a large spread of the Ca/Si ratio of the C–S–H from 1.2 to 2.2. This agrees with the findings of other studies, where an inhomogeneous microstructure with large differences in the hydrates and the C–S–H composition are found near fly ash particles, in the outer product or in the inner products near the clinker grains [43–45].

4.3.3. Pore solution

The *pore solution* of the different tested cements was analysed after 1, 28, 90 and 140 days of curing. The different concentrations are given in Table 8. The sulphate concentration and the pH are plotted as a function of time in Fig. 10. For OPC and OPC-L, the Na and K concentration and the pH values increase over time. The pore solution of the fly ash containing cements have lower pH and alkali concentrations than OPC and OPC-L mixes, as reported by previous studies [43,46–48]. Initially, this is due to the dilution of OPC by fly ash. However, after more than 28 days, the alkali concentrations decrease for the fly ash containing combinations indicating an incorporation of alkali in the hydration products formed by the fly ash [43,48,49]. The Ca, Si and Al of both OPC and OPC-L are not significantly different. The Ca-concentration in the pore solution of the OPC-FA and OPC-FA-L mixes, on the other hand, shows a clear decrease, most likely associated with the calcium hydroxide consumption during the pozzolanic reaction of the fly ash observed by TGA and XRD-Rietveld (Fig. 4 and Table 7). The Si and Al concentrations are rather low and are thereby limited in accuracy; however a slight increasing trend with time might be observed for the fly ash containing cements as observed previously [43].

The main difference in pore solution composition between OPC and OPC-FA, and the limestone containing equivalents is the sulphate concentration (Fig. 10). After 7 days the concentration is almost twice as high in the limestone containing mixes than in the ones without limestone, indicating a change in the sulphate containing AFm and AFt phases. The same observations on OPC systems were reported previously [13]. Replacing OPC with fly ash considerably lowers sulphate concentrations, more than what would be expected from the OPC dilution. The chemical reasons for that observed strong decrease of sulphate concentrations are not clear. Possibly, the increase of the total Al_2O_3/SO_3 ratio in the fly ash containing blends is responsible for the observed lower sulphate concentrations in the pore solutions.

Based on the measured concentrations, saturation indices (SI) were calculated. The use of saturation indices can be misleading when comparing phases which dissociate into a different number of ions, thus "effective" saturation indices were calculated by dividing the saturation indices by the number of ions participating in the reactions to form the solids as described by Lothenbach et al. [13]. A positive saturation index implies oversaturation and thereby possible precipitation of the solid; a negative value indicates undersaturation, meaning that the solid cannot form or dissolves. The effective SI for hemi- and monocarbonate has been calculated assuming saturation of the pore solutions with respect to calcite. The effective SI's for

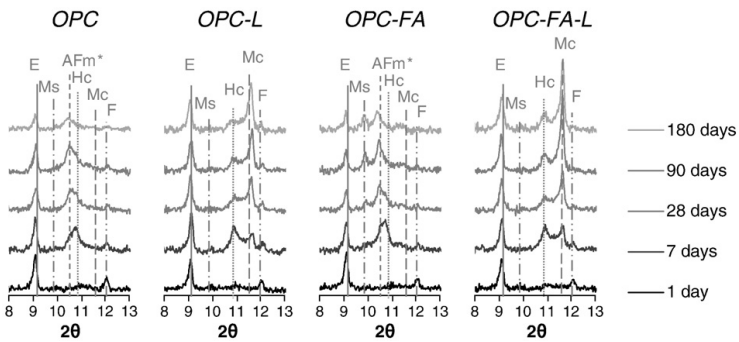

Fig. 8. XRD-patterns for the different tested blends at 1, 7, 28, 90 and 180 days. The main peaks of ettringite (E), monosulphate (Ms), possibly a sulphate and carbonate containing hydroxy-AFm(AFm*), hemicarbonate (Hc), monocarbonate (Mc) and ferrite (F) are indicated.

Please cite this article as: K. De Weerdt, et al., Hydration mechanisms of ternary Portland cements containing limestone powder and fly ash, Cem. Concr. Res. (2010), doi:10.1016/j.cemconres.2010.11.014

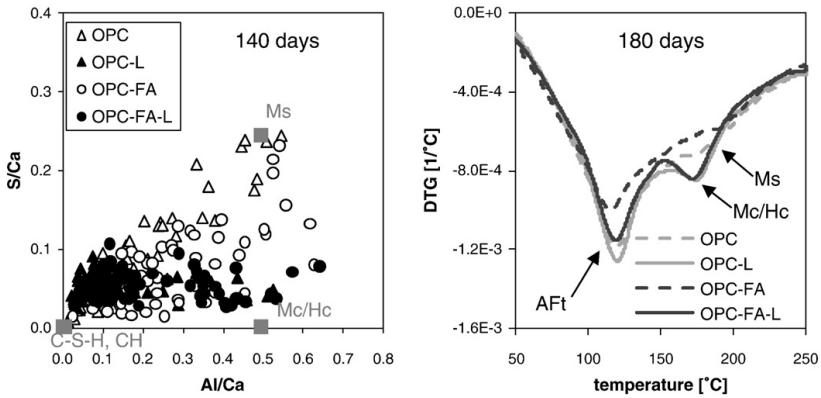

Fig. 9. EDX and TGA analysis of respectively 140 and 180 day old paste samples indicating changes in the composition of the AFm phases.

portlandite, gypsum, ettringite, monosulphate, monocarbonate and hemicarbonate at 1, 7, 28, 90 and 140 days are given in Table 8. Gypsum is under-saturated for all tested combinations. After 28 days and longer portlandite is under-saturated in the fly ash containing blends, due to its consumption by the pozzolanic reaction of the fly ash. This under-saturation is consistent with the slow dissolution of portlandite in the FA containing samples as observed by TGA and XRD (Fig. 4 and Table 7). Ettringite is over-saturated at all times for the OPC, OPC-L and OPC-FA-L samples. Ettringite is under-saturated in the OPC-FA (without limestone) after more than 28 days indicating that ettringite slowly dissolves in this blend. Generally, the effective SI of ettringite is higher in the limestone containing samples. Monosulphate is near saturation for all blends. Mono- and hemicarbonate are near saturation for both limestone containing combinations (except for hemicarbonate for the OPC-FA-L blend at 90 and 140 days).

The pore solution analysis indicates the presence of ettringite and AFm phases as well as the consumption of portlandite in the FA containing blends due to the pozzolanic reaction with the fly ash.

4.3.4. Porosity

The *porosity of the cement paste* has been found to be lower when a small amount of limestone powder is added to OPC [50]. Relative to the aluminate content, ettringite ($C_6A\underline{S}_3H_{32}$) is more voluminous than monosulphate ($C_4A\underline{S}H_{12}$): 707 cm^3/mol versus 309 cm^3/mol at 25 °C [33]. As limestone powder stabilizes the ettringite and prevents the transformation to monosulphate, the total volume of hydration products relative to the OPC content will increase. This volume increase of the hydration products might lead to a reduction in porosity that more than compensates the replacement of OPC by limestone powder.

Table 8
Composition pore solution and effective saturation indices for calcium hydroxide (CH), gypsum, ettringite (Ett), monosulphate (Ms), monocarbonate (Mc) and hemicarbonate (Hc).

Time [days]	Concentration in pore solution [mmol/l]								Effective saturation index					
	Na	K	Ca	S	Si	Al	OH^-	pH	CH	Gypsum	Ett	Ms	Mc	Hc
OPC														
1	131	315	1.1	4.2	0.43	0.22	653	13.7	0.05	−1.35	0.11	0.03	–	–
7	196	417	1.5	6.3	0.37	0.17	699	13.8	0.16	−1.27	0.17	0.09	–	–
28	244	495	1.0	9.3	0.33	0.17	675	13.7	0.14	−1.31	0.13	0.05	–	–
90	274	534	1.4	10.9	0.34	0.23	699	13.8	0.20	−1.23	0.20	0.12	–	–
140	302	565	1.0	13.0	0.30	0.33	627	13.7	0.15	−1.3	0.17	0.10	–	–
OPC-L														
1	258	443	1.5	6.3	0.37	0.21	589	13.7	0.18	−1.31	0.17	0.10	0.19	0.27
7	244	497	1.8	12.8	0.31	0.25	653	13.7	0.22	−1.12	0.28	0.18	0.24	0.36
28	258	515	0.9	17.1	0.29	0.23	631	13.7	0.12	−1.21	0.17	0.07	0.15	0.18
90	274	537	1.2	25.1	0.30	0.21	631	13.7	0.16	−1.09	0.23	0.12	0.17	0.22
140	279	532	1.2	27.6	0.29	0.31	677	13.7	0.17	−1.05	0.28	0.16	0.21	0.30
OPC-FA														
1	223	310	2.0	1.2	0.22	0.16	459	13.6	0.19	−1.51	0.10	0.07	–	–
7	223	303	1.6	1.3	0.16	0.13	493	13.6	0.15	−1.54	0.05	0.02	–	–
28	228	271	1.2	1.6	0.26	0.10	459	13.6	0.09	−1.55	0.00	−0.05	–	–
90	165	241	0.5	2.6	0.48	0.15	368	13.5	−0.08	−1.59	−0.08	−0.14	–	–
140	151	227	0.7	2.6	0.53	0.27	303	13.4	−0.07	−1.53	−0.01	−0.07	–	–
OPC-FA-L														
1	158	313	2.2	1.7	0.21	0.14	442	13.5	0.18	−1.38	0.15	0.09	0.19	0.28
7	184	336	1.9	4.1	0.17	0.13	475	13.6	0.17	−1.25	0.19	0.10	0.18	0.24
28	193	297	1.2	5.9	0.28	0.16	426	13.5	0.08	−1.27	0.14	0.04	0.12	0.12
90	176	251	0.7	7.2	0.45	0.16	368	13.5	−0.04	−1.32	0.06	−0.06	0.04	−0.06
140	151	235	0.6	6.5	0.42	0.22	278	13.3	−0.07	−1.34	0.06	−0.05	0.05	−0.06

Please cite this article as: K. De Weerdt, et al., Hydration mechanisms of ternary Portland cements containing limestone powder and fly ash, Cem. Concr. Res. (2010), doi:10.1016/j.cemconres.2010.11.014

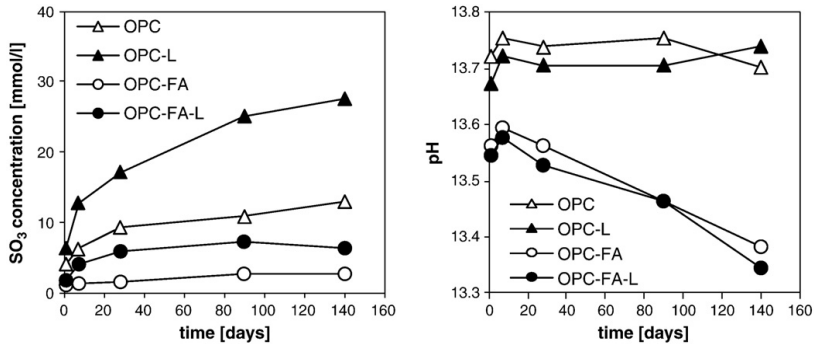

Fig. 10. SO_3 concentration and the pH in the pore solution a function of time.

Image analysis (IA) of backscattered electron (BSE) images taken by a scanning electron microscope (SEM) is used to study the changes of the coarse porosity (Fig. 11). Based on the magnification applied, only coarser pores >0.17 μm are included. In the case of OPC and OPC-L the porosity reduces up to 28 days after which it stays approximately constant, indicating that most of the OPC has reacted within the first 28 days. The initial coarse porosity in the OPC-FA and OPC-FA-L blend is higher and decreases more slowly up to 90 days to values slightly lower than observed for the OPC samples. The coarse porosity does not change significantly between the 90 and 140 days in the FA blended systems.

The relationship between compressive strength and coarse porosity for all tested mixes is presented in Fig. 12 indicating a clear negative correlation between porosity and compressive strength. This suggests that the coarse porosity dominates the compressive strength, independent of the mix designs, which is in agreement with the previous observations [51]. The presence of limestone or FA does not alter the relation between coarse porosity and compressive strength.

4.4. Thermodynamic modelling

4.4.1. Hydrate assemblage

The changes in the hydrate assemblage were calculated based on the observed dissolution of the anhydrous phases. The dissolution of the clinker phases was mathematically described using the Parrot and Killoh equations [52]. The parameters of the equations were adapted to fit the XRD-Rietveld results. The fly ash reaction was expressed using a function fitted to the data obtained in a previous study [26] shown in Fig. 7. Hence, the composition of the hydrate assemblage was predicted based on the degree of reaction of the OPC and the fly ash as a function of the time assuming thermodynamic equilibrium at each stage of the hydration. Some assumptions were introduced while modelling:

- The glassy phase of the fly ash was assumed to dissolve uniformly.
- In the model the formation of monocarbonate was predicted, while by XRD the formation of hemicarbonate instead of monocarbonate was observed at early hydration times (Fig. 8). It is unclear whether the formation of moncarbonate is slower than the formation of hemicarbonate or whether the dissolution of the limestone powder is too slow.
- The EDX results show that the Al-incorporation and the Ca/Si ratio of the C–S–H changes over time for the fly ash containing cements as mentioned before. However, the composition of the C–S–H is kept constant over time. For C–S–H in OPC-FA and OPC-FA-L an Al/Si ratio of 0.13 was used.

The predicted hydrates include C–S–H, CH, AFt and AFm phases including a small amount of hydrotalcite-like phases as shown in Fig. 13. When comparing OPC and OPC-FA with their limestone containing equivalents, the presence of limestone leads to the formation of monocarbonate thus indirectly stabilising ettringite. In the absence of limestone the formation of monosulphate is predicted and a reduction of the amount of ettringite with time (Fig. 13). In the OPC-FA in addition the formation of hydrogarnet is predicted after longer hydration times. Qualitatively these results agree well with experimental results shown in Fig. 8.

In the OPC-FA and OPC-FA-L blends a considerable part of the OPC is replaced by fly ash. OPC reacts faster than the fly ash (Fig. 7), so

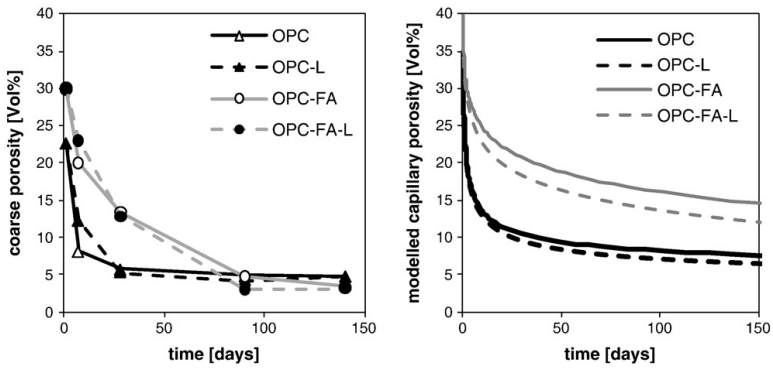

Fig. 11. Coarse porosity determined by SEM-IA (error<2–3%) and modelled capillary porosity.

Please cite this article as: K. De Weerdt, et al., Hydration mechanisms of ternary Portland cements containing limestone powder and fly ash, Cem. Concr. Res. (2010), doi:10.1016/j.cemconres.2010.11.014

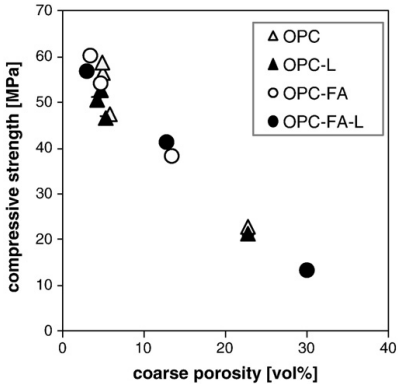

Fig. 12. Relation between compressive strength (error<2%) and coarse porosity determined by SEM-IA (error<2–3%).

initially fly ash acts as an adulterant for OPC. As the fly ash reacts over time, it will introduce additional silicates and alumina to the system. The silicates will react with the portlandite and form additional C–S–H. The alumina will partly be incorporated in the C–S–H and partly in AFm and AFt phases.

The total gypsum content is lower in OPC-FA and OPC-FA-L as gypsum is part of the OPC. The additional alumina provided by the fly ash will therefore lower the SO_3-alumina ratio. Hence, relatively more AFm than AFt phases are formed over time in the fly ash containing blends (see Fig. 13). This amplifies the effect of the limestone powder on the system as limestone interacts with the AFm phases, thereby giving rise to a larger increase in solid volume.

The mass percentage of ettringite, amorphous hydrates and CH determined by Rietveld analysis are compared with the predicted ones (Fig. 14). In the case of OPC and OPC-L, the *CH content* was overestimated by the model, most likely due to differences between the real (Ca/Si = 1.8) and the modelled (Ca/Si = 1.6) C–S–H composition. The model slightly underestimates the CH content for OPC-FA and OPC-FA-L at 28 and 90 days, as:

i) The C–S–H in the OPC-FA(-L) samples shows a lower Ca/Si of 1.4 than the modelled C–S–H (Ca/Si = 1.6). The C–S–H formed in the OPC-FA (−L) blends shows a significant variation in the composition, low Ca/Si C–S–H forms near the FA particles while in other places portlandite is still present. In contrast to these experimental observations, the modelled C–S–H has a constant Ca/Si ratio of 1.6 as the model calculates only bulk properties. The presence of even small quantities of portlandite leads to the stabilisation of high Ca/Si C–S–H.
ii) The dissolution of portlandite may proceed more slowly than the reaction of the FA. The pore solution after 90 and 140 days is undersaturated with respect to portlandite (Table 8), indicating only a slow portlandite dissolution. Due to the inhomogeneous distribution of the C–S–H and the portlandite in the cement matrix, portlandite does persist in some parts of the microstructure while in other areas a low Ca/Si C–S–H is formed.

The *amorphous content* is slightly overestimated for all tested combinations, mainly due to the difference between the modelled and

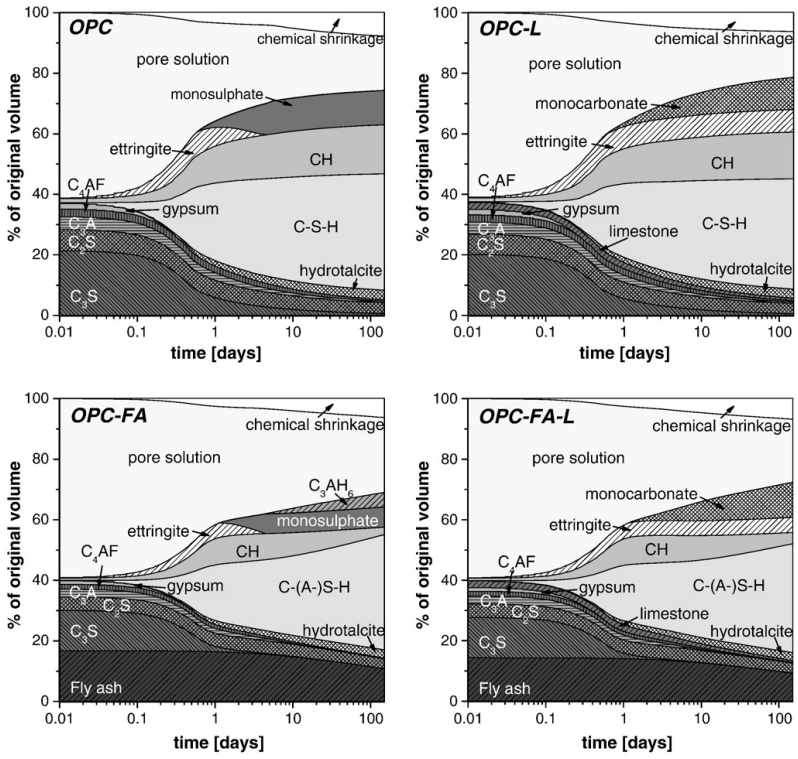

Fig. 13. The volume of the different phases as function of time in hydrating cement pastes modelled by GEMS.

Please cite this article as: K. De Weerdt, et al., Hydration mechanisms of ternary Portland cements containing limestone powder and fly ash, Cem. Concr. Res. (2010), doi:10.1016/j.cemconres.2010.11.014

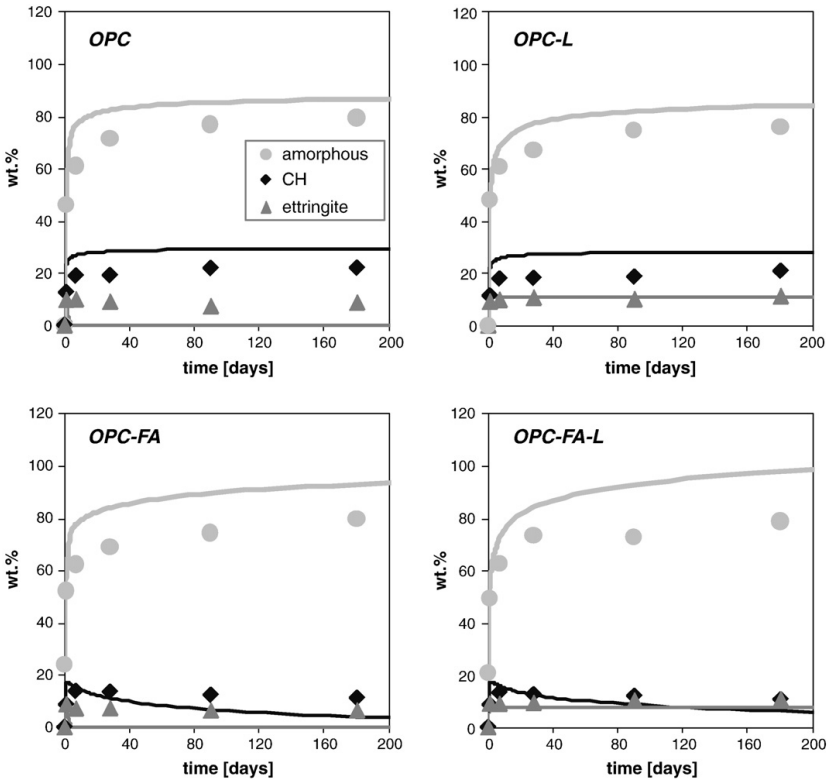

Fig. 14. Comparing XRD-Rietveld (data points) with results calculated by thermodynamic modelling (solid lines) in wt.%, for details see text. Amorphous includes different hydrates (C–S–H, AFm or hydrotalcite-like phases) and the amorphous fly ash.

real C–S–H. The difference is larger for the fly ash containing blends as their C–S–H deviates even more from the one used in the modelled.

Ettringite is predicted to disappear in both the OPC and OPC-FA blend during the first few days of hydration, however ettringite was observed up to 140 days (Fig. 14); instead traces of hydrogarnet were observed by XRD in the pastes older than 28 days. The persistence of ettringite in the experiments is most likely due to slow kinetics of the decomposition of ettringite to monosulphate and differences in local equilibria. The similar solubility of ettringite and monosulphate in cement systems, as visible in the similar effective saturation index (SI) of monosulphate and ettringite (Table 8), confirms the observed slow kinetics.

For the limestone containing blends, OPC-L and OPC-FA-L, the ettringite content is well predicted (Fig. 14). The model predicts only the formation of monocarbonate after 2 to 3 days (Fig. 13) whereas by XRD hemicarbonate was also observed (Fig. 8). This may be attributed to the slow dissolution kinetics of the limestone powder or to the slower formation of monocarbonate than of hemicarbonate.

4.4.2. Chemical shrinkage and porosity

Based on the predicted volume of unhydrated cement and the hydration products (Fig. 13), the chemical shrinkage (CS_t) and the total porosity (P_t) can be calculated (see Figs. 6 and 11).

$$CS_t = \left(V_{OPC+FA+L,t=0} + V_{solution,t=0}\right) - \left(V_{OPC+FA+L,t} + V_{solution,t} + V_{hydrates,t}\right) \quad (6)$$

$$P_t = \frac{\left(V_{OPC+FA+L,t=0} + V_{solution,t=0}\right) - \left(V_{OPC+FA+L,t} + V_{hydrates,t}\right)}{V_{OPC+FA+L,t=0} + V_{solution,t=0}} \quad (7)$$

CS_t is expressed in cm^3 or ml per g OPC, with $V_{OPC+FA+L,t=0}$ is the initial volume of dry material and $V_{solution,\,t=0}$ the initial amount of water added to the system. $V_{OPC+FA+L,t}$ is the remaining volume of anhydrous material at time t, $V_{solution,\,t}$ the remaining solution and $V_{hydrate,\,t}$ the volume of hydrates formed. The total porosity P_t is expressed as a% of the total volume which is assumed to remain constant over time; shrinkage of the sample is not taken into account. The porosity corresponds roughly to the sum of the capillary pores, thereby not including cracks or air voids [33].

The changes in hydration products result in a difference in chemical shrinkage (Fig. 6). The chemical shrinkage (CS) relative to the OPC content tends to increase when limestone is present. This can be attributed to the fact that more free water is bound in ettringite. The modelled chemical shrinkage shows similar trends as the experimental data (Fig. 6), however the observed effect is somewhat smaller than the modelled one. The modelled porosity as a function of hydration time (Fig. 11) indicates that the effect of limestone powder on OPC-FA cement is larger than on OPC cement, which is in line with previous observations. Note that the coarse porosity as measured by SEM-IA represents only a fraction of the capillary porosity.

5. Conclusions

Five percent of limestone powder can have a beneficial effect on the compressive strength of OPC [13]. This study confirms this and

Please cite this article as: K. De Weerdt, et al., Hydration mechanisms of ternary Portland cements containing limestone powder and fly ash, Cem. Concr. Res. (2010), doi:10.1016/j.cemconres.2010.11.014

shows that the effect is even more pronounced for the inclusion of 5% limestone powder in fly ash blended cements. The beneficial effect of the limestone powder cannot be solely attributed to a physical effect due to the presence of 5% limestone (additional nucleation sites and higher effective water to cement ratio), as after longer hydration times, no significant differences in the amount of clinker or fly ash reacted were observed between limestone containing and limestone free blends. Additionally, the presence of 5% limestone increases relative to blends containing the same amount of crystalline quartz powder, the amount of bound water and the compressive strength.

The effect of limestone powder on the hydration of OPC and OPC-FA systems tested in this study, therefore, appears to be mainly due to its interaction with the hydration products formed. At 1 day the hydrates formed are similar for all tested combinations: C–S–H, portlandite, ettringite. But after more than 1 day, when the reaction of the clinkers continues while the gypsum has been depleted, the kind and amount of AFm and AFt phases start to differ between the limestone containing and limestone-free OPC and OPC-FA blends. In the absence of limestone powder, ettringite decomposes to monosulphate. However, in the presence of calcium carbonate, the main constituent of limestone powder, the decomposition of ettringite to monosulphate is prevented as monosulphate is rendered unstable and instead calcium mono- or hemicarboaluminate are formed as observed experimentally and predicted by the thermodynamic modelling. The changes in AFm phases are reflected in the sulphur concentrations of pore solution. This effect is well known for OPC, however, this study proofs that the effect is more pronounced for the fly ash blended cement due to a lower SO_3/Al_2O_3 ratio caused by replacing part of the OPC with fly ash which as it reacts introduces additional alumina to the system. As predicted by the thermodynamic modelling, the XRD patterns show a larger amount of AFm and AFt phases when fly ash is present. However, aluminates liberated by fly ash do not go only into AFm and AFt phases as part of it is also incorporated in the C–S–H gel as observed by the increase of the Al/Si ratio of the C–S–H.

The stabilisation of ettringite, when limestone is present, leads to an increase in the volume of hydration products, as can be deduced from the chemical shrinkage results, to a decrease in porosity and thus to an increase in compressive strength. While a clear increase in strength was observed, the experimental determination of the porosity of the cement paste did not show a clear difference between the blends with and without limestone powder, due the relatively large error associated with the measurements.

Acknowledgement

The authors would like to acknowledge COIN, the COncrete INnovation centre (http://www.coinweb.no) for the financial support.

References

[1] L.L. Mayfield, Limestone additions to Portland cement — an old controversy revisited, Cement, Concrete and Aggregates 10 (1988) 3–8.
[2] K.D. Ingram, K.E. Daugherty, A review of limestone additions to Portland cement and concrete, Cement and Concrete Composites 13 (1991) 165–170.
[3] P. Hawkins, P. Tennis, R. Detwiler, The use of limestone in Portland cement: a state-of-the-art review, EB227, Portland Cement Association, Skokie, Illinois, USA, 2003, p. 44.
[4] T. Schmidt, B. Lothenbach, M. Romer, J. Neuenschwander, K. Scrivener, Physical and microstructural aspects of sulfate attack on ordinary and limestone blended Portland cements, Cement and Concrete Research 39 (2009) 1111–1121.
[5] V.S. Ramachandran, Thermal analyses of cement components hydrated in the presence of calcium carbonate, Thermochimica Acta 127 (1988) 385–394.
[6] G. Kakali, S. Tsivilis, E. Aggeli, M. Bati, Hydration products of C_3A, C_3S and Portland cement in the presence of $CaCO_3$, Cement and Concrete Research 30 (2000) 1073–1077.
[7] J. Bensted, Further hydration investigations involving Portland cement and the substitution of limestone for gypsum, World Cement 14 (1983) 383–392.
[8] W. Klemm, L. Adams, An investigation on the formation of carboaluminate, in: P. Klieger, D. Hooton (Eds.), ASTM Spec Tech Publ, 1064, 1990.
[9] T. Matschei, F.P. Glasser, Temperature dependence, 0 to 40 °C, of the mineralogy of Portland cement paste in the presence of calcium carbonate, Cement and Concrete Research 40 (2010) 763–777.
[10] H.J. Kuzel, H. Pöllmann, Hydration of C_3A in the presence of $Ca(OH)_2$, $CaSO_4 \cdot 2H_2O$ and $CaCO_3$, Cement and Concrete Research 21 (1991) 885–895.
[11] S. Hoshino, K. Yamada, H. Hirao, XRD/Rietveld analysis of the hydration and strength development of slag and limestone blended cement, Journal of Advanced Concrete Technology 4 (2006) 357–367.
[12] T. Matschei, B. Lothenbach, F.P. Glasser, The role of calcium carbonate in cement hydration, Cement and Concrete Research 37 (2007) 551–558.
[13] B. Lothenbach, G. Le Saout, E. Gallucci, K. Scrivener, Influence of limestone on the hydration of Portland cements, Cement and Concrete Research 38 (2008) 848–860.
[14] B. Yilmaz, A. Olgun, Studies on cement and mortar containing low-calcium fly ash, limestone, and dolomitic limestone, Cement and Concrete Composites 30 (2008) 194–201.
[15] M. Ghrici, S. Kenai, M. Said-Mansour, Mechanical properties and durability of mortar and concrete containing natural pozzolana and limestone blended cements, Cement and Concrete Composites 29 (2007) 542–549.
[16] G. Menéndez, V. Bonavetti, E.F. Irassar, Strength development of ternary blended cement with limestone filler and blast-furnace slag, Cement and Concrete Composites 25 (2003) 61–67.
[17] M.F. Carrasco, G. Menéndez, V. Bonavetti, E.F. Irassar, Strength optimization of "tailor-made cement" with limestone filler and blast furnace slag, Cement and Concrete Research 35 (2005) 1324–1331.
[18] K. De Weerdt, H. Justnes, Microstructure of binder from the pozzolanic reaction between lime and siliceous fly ash and the effect of limestone addition, in: W. Sun, K. van Breugel, C. Miao, G. Ye, H. Chen (Eds.), Microstructure Related Durability of Cementitious Composites Nanjing, 2008, pp. 107–116.
[19] K. De Weerdt, H. Justnes, Synergic reactions in triple blended cements, 11th NCB International Seminar on Cement and Building Materials, New Delhi, 2009, pp. 257–261.
[20] K. De Weerdt, H. Justnes, Synergy in ternary cements — the interaction between limestone powder and fly ash, in: L. Black, P. Purnell (Eds.), 29th Cement and Concrete Science Conference, Leeds, UK, 2009, pp. 153–156.
[21] K. De Weerdt, E.J. Sellevold, H. Justnes, K.O. Kjellsen, Fly ash-limestone ternary cements: effect of component fineness., Advances in cement research (accepted), (2010).
[22] K. De Weerdt, H. Justnes, K.O. Kjellsen, E. Sellevold, Fly ash - limestone ternary composite cements: synergetic effect at 28 days, Nordic Concrete Research 42 (2010).
[23] K. De Weerdt, K.O. Kjellsen, E.J. Sellevold, H. Justnes, Synergistic effect between fly ash and limestone powder in ternary cements, Cement and Concrete Composites 33 (2011) 30–38.
[24] M. Geiker, Studies of Portland cement hydration: measurements of chemical shrinkage and a systematic evaluation of hydration curves by means of the dispersion model. Ph.D Thesis, in, Technical University of Denmark, Copenhagen, 1983.
[25] G. Le Saout, T. Füllmann, V. Kocaba, K. Scrivener, Quantitative study of cementitous materials by X-ray diffraction/Rietveld analysis using an external standard, 12th International Congress on the Chemistry of Cement Montréal, Canada, 2007, 2007.
[26] M. Ben Haha, K. De Weerdt, B. Lothenbach, Quantification of the degree of reaction of fly ash, Cement and Concrete Research 40 (2010) 1620–1629.
[27] R.S. Barneyback Jr., S. Diamond, Expression and analysis of pore fluids from hardened cement pastes and mortars, Cement and Concrete Research 11 (1981) 279–285.
[28] D. Kulik, GEMS 2 software, http://gems.web.psi.ch/ PSI, Villingen, Switzerland, 2010.
[29] T. Thoenen, D. Kulik, Nagra/PSI chemical thermodynamic database 01/01 for GEMS-selektor (V.2-PSI) geochemical modeling code, http://gems.web.psi.ch/doc/pdf/TM-44-03-04-web.pdf PSI, Villingen, 2003.
[30] W. Hummel, U. Berner, E. Curti, F.J. Pearson, T. Thoenen, Nagra/PSI chemical thermodynamic data base 01/01, Universal Publishers/uPUBLISH.com, USA also published as Nagra Tehcnical Report NTB 02-16, Wettingen, Switzerland 2002, 2002.
[31] B. Lothenbach, F. Winnefeld, Thermodynamic modelling of the hydration of Portland cement, Cement and Concrete Research 36 (2006) 209–226.
[32] T. Matschei, B. Lothenbach, F.P. Glasser, Thermodynamic properties of Portland cement hydrates in the system $CaO–Al_2O_3–SiO_2–CaSO_4–CaCO_3–H_2O$, Cement and Concrete Research 37 (2007) 1379–1410.
[33] B. Lothenbach, T. Matschei, G. Möschner, F.P. Glasser, Thermodynamic modelling of the effect of temperature on the hydration and porosity of Portland cement, Cement and Concrete Research 38 (2008) 1–18.
[34] D.P. Bentz, Modeling the influence of limestone filler on cement hydration using CEMHYD3D, Cement and Concrete Composites 28 (2006) 124–129.
[35] T. Sato, J.J. Beaudoin, The effect of nano-sized $CaCO_3$ addition on the hydration of cement paste containing high volumes of fly ash, 12th ICCC, Montreal, 2007, pp. 1–12.
[36] H.F.W. Taylor, K. Mohan, G.K. Moir, Analytical study of pure and extended Portland cement pastes: II, fly ash- and slag-cement pastes, Journal of the American Ceramic Society 68 (1985) 685–690.
[37] W. Lukas, The influence of an Austrian fly ash on the reaction processes in the clinker phases of Portland cements, Materials and Structures 9 (1976) 331–337.
[38] K. Ogawa, H. Uchikawa, K. Takemoto, I. Yasui, The mechanism of the hydration in the system C_3S-pozzolana, Cement and Concrete Research 10 (1980) 683–696.

Please cite this article as: K. De Weerdt, et al., Hydration mechanisms of ternary Portland cements containing limestone powder and fly ash, Cem. Concr. Res. (2010), doi:10.1016/j.cemconres.2010.11.014

[39] E. Sakai, S. Miyahara, S. Ohsawa, S.-H. Lee, M. Daimon, Hydration of fly ash cement, Cement and Concrete Research 35 (2005) 1135–1140.
[40] J.A. Dalziel, W.A. Gutteridge, The influence of pulverized-fuel ash upon the hydration characteristics and certain physical properties of a Portland cement paste, Cement and Concrete Association: Technical Report, Wexham Springs, 1986, p. 28.
[41] T. Matschei, B. Lothenbach, F.P. Glasser, The AFm phase in Portland cement, Cement and Concrete Research 37 (2007) 118–130.
[42] P.L. Rayment, The effect of pulverised-fuel ash on the C/S molar ratio and alkali content of calcium silicate hydrates in cement, Cement and Concrete Research 12 (1982) 133–140.
[43] K. Luke, E. Lachowski, Internal composition of 20-year-old fly ash and slag-blended ordinary Portland cement pastes, Journal of the American Ceramic Society 91 (2008) 4084–4092.
[44] J.I. Escalante-Garcia, J.H. Sharp, The chemical composition and microstructure of hydration products in blended cements, Cement and Concrete Composites 26 (2004) 967–976.
[45] A.M. Harrisson, N.B. Winter, H.F.W. Taylor, An examination some pure and composite Portland cement pastes using scanning electron microscopy with X-ray analytical capability, 8th ICCC, Rio de Janeiro, Brasil, 1986, pp. 170–175.
[46] I. Canham, C.L. Page, P.J. Nixon, Aspects of the pore solution chemistry of blended cements related to the control of alkali silica reaction, Cement and Concrete Research 17 (1987) 839–844.
[47] F.P. Glasser, K. Luke, M.J. Angus, Modification of cement pore fluid compositions by pozzolanic additives, Cement and Concrete Research 18 (1988) 165–178.
[48] S. Diamond, Effects of two Danish flyashes on alkali contents of pore solutions of cement-flyash pastes, Cement and Concrete Research 11 (1981) 383–394.
[49] M.H. Shehata, M.D.A. Thomas, R.F. Bleszynski, The effects of fly ash composition on the chemistry of pore solution in hydrated cement pastes, Cement and Concrete Research 29 (1999) 1915–1920.
[50] D. Herfort, Relationship between strength, porosity and cement composition, Nanocem workshop on “the relation between microstructure and mechanical properties”, Czech Technical University, Prague, 2004.
[51] S. Igarashi, M. Kawamura, A. Watanabe, Analysis of cement pastes and mortars by a combination of backscatter-based SEM image analysis and calculations based on the Powers model, Cement and Concrete Composites 26 (2004) 977–985.
[52] L.J. Parrot, D.C. Killoh, Prediction of cement hydration, British Ceramic Proceedings 35 (1984) 41–53.

Please cite this article as: K. De Weerdt, et al., Hydration mechanisms of ternary Portland cements containing limestone powder and fly ash, Cem. Concr. Res. (2010), doi:10.1016/j.cemconres.2010.11.014

Paper VII

The effect of limestone powder additions on strength and microstructure of fly ash blended cements

De Weerdt K., Justnes H., Ben Haha M. & Lothenbach B.

13th International Congress on the Chemistry of Cement, 2011, Madrid, in review.

The effect of limestone powder additions on strength and microstructure of fly ash blended cements

[1]De Weerdt K[1]*, [1]Justnes H
[1] *SINTEF Building and Infrastructure Trondheim, Norway*
[2]Lothenbach B, [2]Ben Haha M
[2] *EMPA, Swiss Federal Laboratories for Material Testing and Research, Dübendorf, Switzerland*

Abstract
Limestone powder additions influence the hydration products in an OPC system. The calcium carbonate present in the limestone powder interacts with the calcium aluminate hydrates (AFm), forming calcium monocarboaluminate hydrate instead of calcium monosulphoaluminate hydrate, thereby stabilizing the ettringite (AFt) and increasing the amount of bound water. This could in turn lead to lower porosity and subsequently higher strength.

The idea was that the effect of limestone powder might be more pronounced in fly ash blended cement than in OPC. This would be due to the higher amount of calcium aluminate hydrates generated in the fly ash containing system, compared to the limited amounts generated by OPC.

A systematic study of several mixes containing different combination of ASTM class F fly ash and limestone powder, replacing 35% percent of the OPC has been carried out. The aim was to relate microstructural properties such as the degree of reaction, nature of hydration phases and capillary porosity to compressive strength.

In order to understand the effect of limestone powder in this system, X-ray diffraction (XRD), thermogravimetric analysis (TGA) and quantitative microstructural analysis were performed on paste samples using scanning electron microscopy (SEM) with image analysis (IA). These experimental results were then compared with the output of a thermodynamic model. The model predicts the hydration assemblage at equilibrium for a given composition of raw materials. The results of the model can be used to investigate the sensitivity of the system for certain parameters e.g. the degree of hydration of the FA, the limestone or gypsum content.

The compressive strength results showed a strength decrease when OPC is replaced with limestone powder alone, whereas a strength increase occurred when 5% of fly ash was replaced with limestone powder. The increase in compressive strength appears to correspond to the changes in the AFm and AFt hydration phases and the subsequent increase in total volume of hydration products. The effect of limestone powder additions was greater in the case of the fly ash blended cement than for the OPC and the effect increases with increasing degree of reaction of the fly ash. Thus the initial hypothesis was confirmed.

Originality
In this study a multi method approach, including compressive strength, quantitative and qualitative microstructural analysis and thermodynamic modeling was used to investigate the system OPC - fly ash - limestone powder.

The thermodynamic model is used to understand and illustrate the effect of limestone powder on the composition of the hydration products. It enables us to interpolate between certain combinations, investigate the sensibility of the system for certain parameters.

Chief contributions
It is known that 5-10% of an OPC can be replaced by limestone powder without altering the macro-properties to a great extend. Whether this is also valid for fly ash blended cements is investigated in this study.
A combination of techniques was applied to understanding the interaction between the different components in the OPC - fly ash - limestone powder system.
The use of the thermodynamic model for the prediction of the composition of hydration products for composite cements was investigated and discussed.

Keywords: *limestone, fly ash, modeling*

[1] Corresponding author: Email klaartje.de.weerdt@sintef.no Tel +4773594866

Introduction

The effect of limestone powder on the hydration of ordinary Portland cement (OPC) or specific clinker phases has been studied thoroughly (Soroka et al. 1976; Kuzel et al. 1991; Bonavetti et al. 2001; Matschei et al. 2007; Lothenbach et al. 2008). The aim of this study is to investigate the impact of limestone powder on the hydration of fly ash blended cements.
The effect on the compressive strength of gradual replacement of OPC with limestone powder (up to 35%) and the replacement of fly ash by limestone powder in fly ash blended cement (fixed OPC content of 65%) has been evaluated. Additional tests have been performed on four combinations of interest: 100%OPC (OPC), 95%OPC+5%L (OPC-L), 65%OPC+35%FA (OPC-FA) and 65%OPC+30%FA+5%L (OPC-FA-L).

Materials

The materials used in this study are: ordinary Portland clinker, a class F siliceous fly ash (FA), limestone powder (L), and natural gypsum. The chemical composition determined by XRF and the physical properties of the clinker, fly ash, and limestone are given in Table 1. The clinker was interground with 3.7% of natural gypsum and is further referred to as ordinary Portland cement (OPC). The gypsum used contains 0.18% free water, and has a $CaSO_4 \cdot 2H_2O$ content of 91.4%. The $CaCO_3$ content of the limestone, determined by thermogravimetric analysis (TGA), is about 81%.

Table 1: Chemical composition and the physical characteristics of the clinker, fly ash and limestone powder

	Clinker	Fly ash	Limestone
SiO_2	20.0	50.0	12.9
Al_2O_3	5.4	23.9	2.7
Fe_2O_3	3.1	6.0	2.0
CaO	60.6	6.3	42.3
MgO	2.9	2.1	1.8
SO_3	1.5	0.4	-
P_2O_5	0.1	1.1	-
K_2O	1.2	1.4	0.6
Na_2O	0.5	0.6	0.5
LOI	0.3	3.6	37.7
Carbon	-	3.1	-
Chloride	0.05	0.0	-
Free CaO	1.85	-	-
Gypsum	3.7	-	-
Blaine surface [m^2/kg]	450*	450	810
Density [kg/m^3]	3150*	2490	2740
d_{50} [µm]	11*	14	4

* For OPC = clinker + gypsum

Methods

The compressive strength was tested on three mortar prisms (40×40×160 mm) prepared with a water-to-binder weight ratio of 0.50 and binder-to-sand weight ratio of 1:3. The samples were cured at 20ºC, in a saturated $Ca(OH)_2$ solution.

Paste samples of 4 mixes: OPC, OPC-L, OPC-FA and OPC-FA-L were prepared with a water-to-binder ratio of 0.50. The pastes were stored under sealed conditions at 20ºC. At the age of testing the samples were crushed and the hydration was stopped by solvent exchange using isopropanol and ether. The resulting powders were examined by thermogravimetric analysis (TGA) using a Mettler Toledo

TGA/SDTA851 and by X-ray diffraction (XRD), using a PANalytical X'Pert Pro MPD diffractometer in a θ-2θ configuration with an incident beam monochromator and CuKα radiation (λ=1.54Å).

A piece of the hydrated paste was impregnated using low viscosity epoxy resin, polished down to ¼ μm, coated with carbon (few nm) and examined using a Philips ESEM FEG XL 30 scanning electron microscopy (SEM). Backscattered electron images (BSE) were analysed quantitatively using image analysis (IA) to determine the coarse porosity and the degree of reaction of OPC and fly ash as described in previous study (Ben Haha et al. 2010).

The hydration of the tested cements was modelled using the Gibbs free energy minimization program, GEMS (Kulik 2010). The thermodynamic data from the PSI-GEMS database (Hummel et al. 2002; Thoenen et al. 2003) was supplemented with cement specific data (Lothenbach et al. 2006; Matschei et al. 2007; Lothenbach et al. 2008). GEMS computes the equilibrium phase assemblage in a multi-component system based on the bulk composition of the materials. The aluminium uptake in the C-S-H used for the calculation was based on energy dispersive X-ray spectroscopy (EDX) results which are presented in (De Weerdt et al. 2010).

Results

1. Compressive strength

Replacing part of the OPC with limestone powder results in a decrease in compressive strength (see Figure 1), whereas, up to 10% of the fly ash can be replaced by limestone powder in the blended systems without impairing the strength. The beneficial effect of limestone powder on the compressive strength of the fly ash blended cements is most prominent at small dosages of limestone powder. Therefore additional tests were performed in an attempt to explain this phenomenon on 4 mixes as mentioned in the introduction.

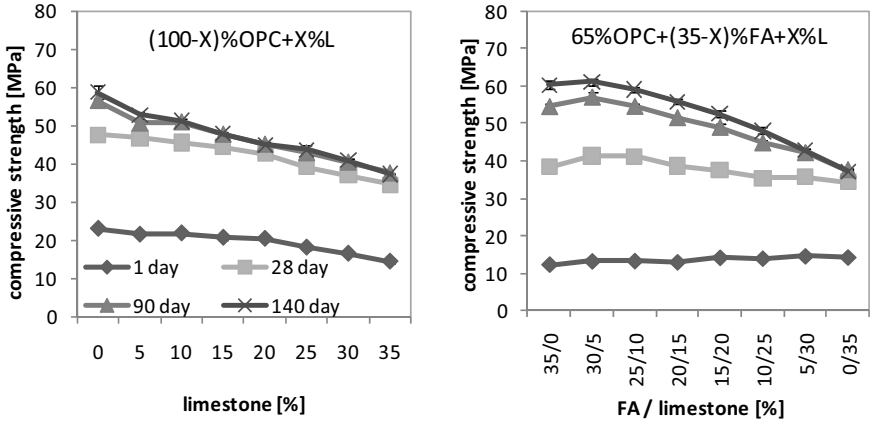

Figure 1: Compressive strength of mortar prisms in which OPC is replaced by limestone and in which fly ash is replaced by limestone after 1, 28, 90 and 140 days (De Weerdt et al. 2010).

2. Degree of hydration

One possible explanation for the beneficial effect of limestone powder might be the promotion of either the hydration of OPC or the reaction of fly ash. However, Figure 2 indicates that this limestone powder does not affect either of them significantly.

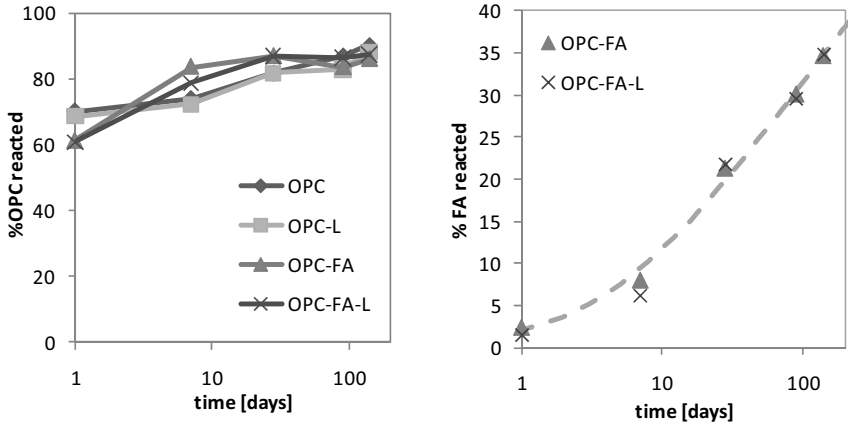

Figure 2: % OPC and % FA reacted using SEM-IA (Ben Haha et al. 2010; De Weerdt et al. 2010).

3. Hydration products

The nature of the hydration products formed is affected by the presence of limestone powder. When limestone powder is part of the system, the derivative of the thermogravimetric curves (Figure 3, left) show an increase in the weight loss at about 120˚C which is the temperatures range in which amongst others ettringite dehydrates and additionally some changes are observed around 180˚C which is in the dehydration range of the AFm phases. These changes are confirmed by the XRD-spectra (Figure 3, right). In the absence of limestone powder, ettringite, monosulphate and a phase, possibly a carbonate and sulfate containing hydroxy-AFm (broad peak between Ms and Hc) are observed. Whereas in the presence of limestone, monocarboaluminate hydrate forms, but no monosulphate. Preventing monosulphate to form, leads to a stabilization of ettringite. Furthermore, the effect seems to be more pronounced for the fly ash containing cements.

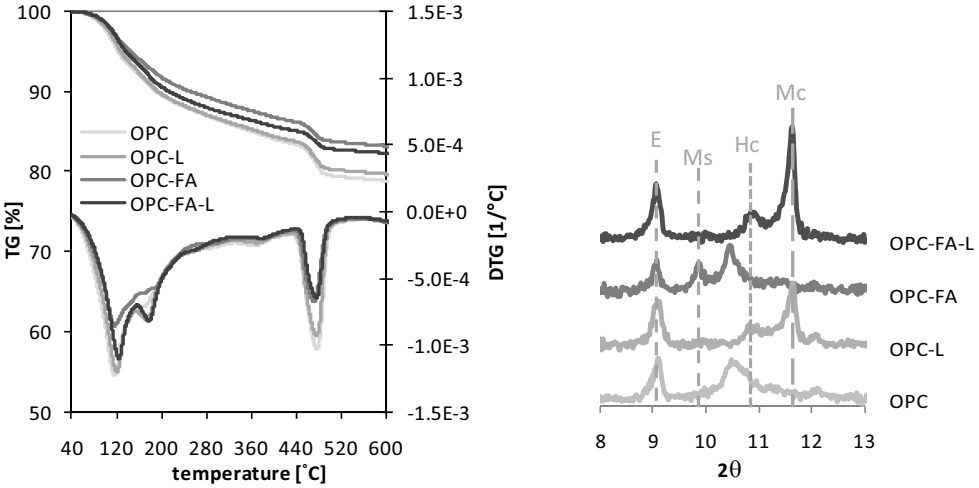

Figure 3: Left: Thermogravimetric (TG) curves and their derivatives (DTG) for pastes cured for 90 days at 20˚C. Right: XRD spectrum for pastes cured for 90 days with E=ettringite, Ms = monosulphate, Hc = hemicarbonate and Mc = monocarbonate.

4. Porosity

One of the major parameters influencing the strength of mortar or hardened cement paste is its porosity. The limestone powder does not appear to influence significantly the coarse porosity (> 0.17μm) determined by image analysis of BSE images (see Figure 4). This might be due to fact that limestone powder affects smaller pores not measured by this technique, or that the effect of the limestone powder is within the error of the measurement. Replacing part of OPC with fly ash, on the other hand, results in an increased coarse porosity up to 90 days. This is attributed to the slow reaction of the fly ash which steadily fills up the porosity of the matrix.

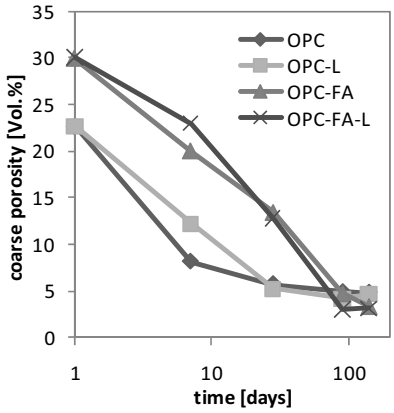

Figure 4: The coarse porosity determined by image analysis of backscattering images.

5. Model

The impact of the limestone powder on the assemblage of hydration products of OPC and fly ash blended cements is investigated using a simplified model. The assumptions made for the modelling are: (1) OPC has 100% reacted; (2) FA has 30% reacted; (3) L has a 81% $CaCO_3$ content, the rest is considered inert; (4) Al incorporation in C-S-H for fly ash blended cement corresponds to Al/Si = 0.15 and for OPC Al/Si = 0.10; (5) all calcium carbonate of the limestone powder can react.

From Figure 5, it can be seen that the presence of limestone powder results in the formation of hemi- and monocarboaluminate hydrate instead of monosulphate and hydrogarnet, thereby stabilizing the ettringite. This is in agreement with the XRD-patterns shown in Figure 3. The transformation of monosulphate to ettringite upon limestone powder addition results in an increase of the volume of the hydrates as ettringite has a lower density than monosulphate, 1.77 vs. 2.01 g/cm^3 (Taylor 1997). The opposite is observed for the transformation of hemicarboaluminate to monocarboaluminate as the former has a slightly lower density than the latter, 1.98 vs. 2.17 g/cm^3 (Taylor 1997). These two mechanisms result in a maximum solid volume predicted for limestone powder additions around to be around 2-3% for both tested cements. Upon further replacement of OPC or fly ash with limestone powder, the total solid volume starts to decline again, as the additional limestone does no longer react and therefore acts as filler replacing the reactive components, OPC and fly ash.

The limestone addition has a larger impact on the total volume of solids in the case of fly ash blended cement compared to OPC (see Figure 5). The volume increases with 3 cm^3/100g blended cement or 4.5% at the maximum relative to the volume without limestone addition for the fly ash cement. In case of the OPC the volume increases with 1.6 cm^3/100g cement or 2.1%. It should also be noted that the optimal limestone content is higher for the fly ash cement than for the OPC, respectively 2% and 1% assuming all limestone powder reacts.

The reason for this slightly higher effect of limestone powder on the fly ash blended cements is due to the additional aluminates provided by the dissolution of the fly ash, leading to a decrease in the SO_3/Al_2O_3 ratio and a subsequent decrease in the AFt/AFm ratio. The impact of the limestone powder is thus enhanced as it is able to convert relatively to the aluminates content more monosulphate to ettringite and more hemi- to monocarboaluminate.

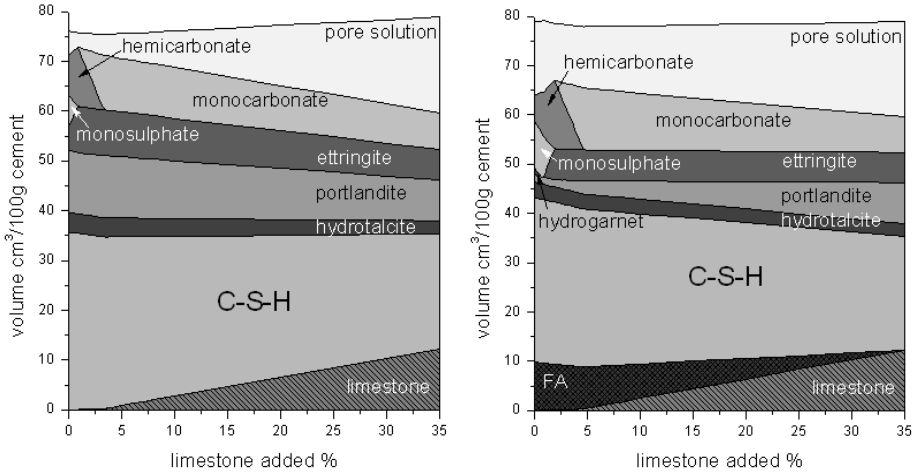

Figure 5: Right: (100-X)%OPC+X%L; Left: 65%OPC+(35-X)%FA+X%L both with OPC 100% reacted, FA 30% reacted and the limestone which can react has reacted.

By using the model, the effect of certain parameters can be predicted as shown in Figure 6. The effect of the limestone powder becomes greater as more fly ash has reacted (see Figure 6 left). At the same time the optimal level of limestone replacement increases with increasing percentage of fly ash reacted.

In the previous modelling results, the calcium carbonate part of the limestone powder is assumed to be able to react fully. This may however not be the case in reality. The graph in the right of Figure 6 shows that as more of the limestone powder reacts, the limestone content at which the maximum solid volume is obtained shifts to the left.

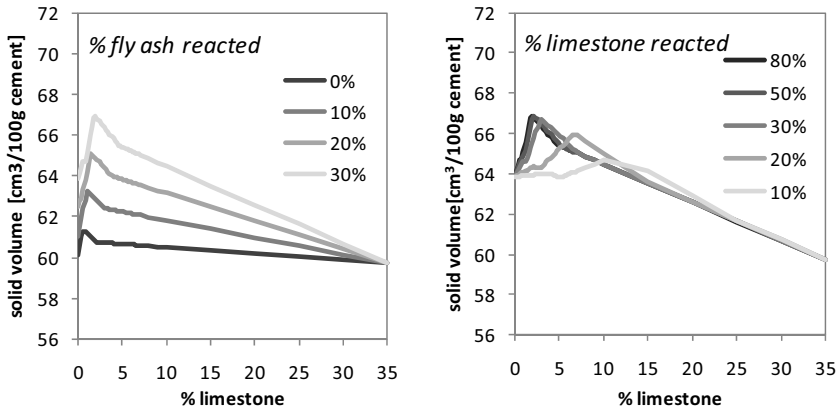

Figure 6: The effect of limestone on cement containing 65%OPC+(35%-X%)FA+X%L with OPC 100% reacted Left: FA 0-30% reacted and L 100% reacted; Right: FA 30% reacted and L 10-80% reacted.

Conclusions

Limestone powder affects the hydration of OPC and fly ash cement by changing the hydrate assemblage. For minor limestone powder additions, an increase in total solid volume is predicted which on its turn might lead to a decrease in porosity and an increase in strength. However, the porosity measurements by image analysis do not show a significant difference in coarser porosity when limestone powder is included in the system.
Limestone powder tends to have a larger impact on fly ash blended cements than on OPC. This is attributed to the additional aluminates supplied over time to the system by the reacting fly ash.
The model applied in this study can be used to predict the impact of changes in the composition when studying similar systems.

Acknowledgements

The authors would like to acknowledge COIN, the COncrete INnovation centre (http://www.coinweb.no) for the financial support, and Gwenn Le Saoût and Knut O. Kjellsen for helpful discussions.

References

- Ben Haha, M., K. De Weerdt and B. Lothenbach (2010). Quantification of the degree of reaction of fly ash. *Cement and Concrete Research* 40(11): 1620-1629.
- Bonavetti, V. L., V. F. Rahhal and E. F. Irassar (2001). Studies on the carboaluminate formation in limestone filler-blended cements. *Cement and Concrete Research* 31(6): 853-859.
- De Weerdt, K., M. Ben Haha, G. Le Saout, K. O. Kjellsen, H. Justnes and B. Lothenbach (2010). Hydration mechanisms of ternary Portland cements containing limestone powder and fly ash. *Cement and Concrete Research* In review.
- De Weerdt, K., K. O. Kjellsen, E. J. Sellevold and H. Justnes (2010). Synergistic effect between fly ash and limestone powder in ternary cements. *Cement and Concrete Composites*(Accepted).
- Hummel, W., U. Berner, E. Curti, F. J. Pearson and T. Thoenen (2002). Nagra/PSI chemical thermodynamic data base 01/01, Universal Publishers/uPUBLISH.com, USA also published as Nagra Tehcnical Report NTB 02-16, Wettingen, Switzerland
- Kulik, D. (2010) "GEMS 2 software." http://gems.web.psi.ch/.
- Kuzel, H. J. and H. Pöllmann (1991). Hydration of C_3A in the presence of $Ca(OH)_2$, $CaSO_4 \cdot 2H_2O$ and $CaCO_3$. *Cement and Concrete Research* 21(5): 885-895.
- Lothenbach, B., G. Le Saout, E. Gallucci and K. Scrivener (2008). Influence of limestone on the hydration of Portland cements. *Cement and Concrete Research* 38(6): 848-860.
- Lothenbach, B., T. Matschei, G. Möschner and F. P. Glasser (2008). Thermodynamic modelling of the effect of temperature on the hydration and porosity of Portland cement. *Cement and Concrete Research* 38(1): 1-18.
- Lothenbach, B. and F. Winnefeld (2006). Thermodynamic modelling of the hydration of Portland cement. *Cement and Concrete Research* 36(2): 209-226.
- Matschei, T., B. Lothenbach and F. P. Glasser (2007). The role of calcium carbonate in cement hydration. *Cement and Concrete Research* 37(4): 551-558.
- Matschei, T., B. Lothenbach and F. P. Glasser (2007). Thermodynamic properties of Portland cement hydrates in the system CaO-Al2O3-SiO2-CaSO4-CaCO3-H2O. *Cement and Concrete Research* 37(10): 1379-1410.
- Soroka, I. and N. Stern (1976). Calcareous fillers and the compressive strength of portland cement. *Cement and Concrete Research* 6(3): 367-376.
- Taylor, H. F. W. (1997). Cement chemistry 2nd edition. London, Thomas Telford.
- Thoenen, T. and D. Kulik (2003) "Nagra/PSI chemical thermodynamic database 01/01 for GEMS-selektor (V.2-PSI) geochemical modeling code." http://gems.web.psi.ch/doc/pdf/TM-44-03-04-web.pdf.

Paper VIII

The effect of temperature on the hydration of Portland composite cements containing limestone powder and fly ash

De Weerdt K., Ben Haha M., Le Saout G., Kjellsen K.O., Justnes H. & Lothenbach B.
Materials and Structures, 2010, in review.

The effect of temperature on the hydration of composite cements containing limestone powder and fly ash

K. De Weerdt[1,*], M. Ben Haha[2], G. Le Saout[2], K.O. Kjellsen[3,4], H. Justnes[1], B. Lothenbach[2]

[1] SINTEF Building and Infrastructure, 7465 Trondheim, Norway

[2] EMPA, Swiss Federal Laboratories for Material Science and Technology, Laboratory for Concrete and Construction chemistry, 8600 Dübendorf, Switzerland

[3] NTNU, Department of Structural Engineering, 7491 Trondheim, Norway

[4] Norcem AS HeidelbergCement, Setreveien 2, 3991 Brevik, Norway

[*] Corresponding author. E-mail address: klaartje.de.weerdt@sintef.no; Tel: +47 73 59 48 66; Fax: +47 73 59 71 36

Abstract

The aim of this study is to investigate the effect of temperature (5, 20 and 40°C) on the degree of hydration, amount of bound water and calcium hydroxide, porosity and mechanical properties of pastes and mortars prepared with fly ash-limestone Portland composite cements. Increasing the curing temperature for ordinary Portland cement leads to a more inhomogeneous distribution of hydration products, resulting in an increased coarse porosity and therefore a lower compressive strength after 7 days and longer. In contrast, the fly ash containing mortars showed higher compressive strength with increasing curing temperature up to 90 days. The reaction of the fly ash is increased at 40°C and strongly retarded at 5°C. At 20 and 40°C, fly ash reduces the porosity at later ages. The replacement of 5% of the OPC or fly ash by limestone powder did not impair the strength at 5 and 20˚C, but lowered strength slightly at 40˚C for the fly ash blended cements. The porosity appears to be the dominating factor regarding the compressive strength, independent of whether part of the OPC is replaced by fly ash and limestone powder or not.

Keywords: Blended cements; Temperature; Microstructure; Degree of reaction; Fly Ash; Limestone

1. Introduction

The effect of the curing temperature on the development of the microstructure, the hydrates assemblage and the mechanical properties of hydrated OPC pastes and concrete has been a research area of interest during the last decades [1-8]. Studies on ordinary Portland cement (OPC) showed that raising the temperature results in an accelerated hydration during first couple of days [1, 2], thereby enhancing the early strength development. However, at later ages, the strength tends to decrease with increasing curing temperature [1, 2]. This temperature inversion effect, being initially beneficial for strength development and after a while detrimental, has been related to the microstructural development of the cementitious matrix [3-6]. Indeed, curing at elevated temperatures gives rise to a non-uniform distribution of hydration products. A dense rim of inner-product is observed around the anhydrous cement grains and a more porous outer-product for pastes cured at 50˚C, whereas a more homogenous microstructure had formed at 5˚C. The dense inner product formed at higher temperatures resulted in a larger pore volume both measured by mercury intrusion porosimetry (MIP) and image analysis (IA) of backscattered electron (BSE) images [6, 8].

Blended cements containing fly ash react differently on variations of the curing temperature [9-12]. The pozzolanic reaction of the fly ash is accelerated by raising the curing temperature, however in a different way than the OPC. The FA reaction is accelerated over longer time span, whereas, the acceleration of the OPC mainly takes place during the first week of hydration.

The evaluation of the hydration of Portland composite cements containing both fly ash and limestone powder cured at 20˚C has been reported previously [13-16]. Replacing 5% of fly ash with 5% limestone powder in a 65% OPC+35% FA cement resulted in enhanced mechanical properties. This is attributed to the additional aluminates provided by the fly ash which amplify the beneficial effect of limestone powder forming calcium carboaluminate hydrates [17].

This study focuses on the effect of the curing temperature on the hydration Portland composite cement containing both fly ash and limestone powder. Samples were cured at 5, 20 and 40˚C. Additionally, by including the neat OPC in the experimental matrix, the influence of the pozzolanic reaction of the fly ash and the effect of the limestone are examined at these different curing temperatures. A quantitative multi-method approach is adopted in this study using: thermogravimetric analysis (TGA), X-ray diffraction (XRD) combined with Rietveld analysis, and BSE-IA.

2. Materials

The following materials were used: ordinary Portland clinker interground with 3.7% of natural gypsum (referred to as OPC), class F siliceous fly ash (FA) and limestone powder (L). Their chemical composition, together with the specific Blaine surface and the density are given in Table 1. Table 2 shows the mineral composition of the OPC determined by Rietveld analysis. The fly ash has a glass content of 65%, and the limestone powder contains 81% $CaCO_3$.

The hydration of five different cements (see Table 3) at three different curing temperatures 5, 20 and 40˚C was monitored up to 180 days.

3. Methods

The compressive and flexural strength were tested on mortar prisms (40×40×160 mm) with cement – sand – water proportions of 1 – 3 – 0.5. The ingredients were stored sealed at 5, 20 and 40˚C for 24 hours prior to mixing. For the first 24 hours after mixing the samples were stored in closed plastic bags, after demoulding, curing continued submerged in $Ca(OH)_2$ saturated solution at the respective temperatures.

Cement paste samples were prepared with water to binder ratio of 0.5 and stored in 20 ml sealed plastic vessels cured at 5, 20 and 40˚C. Prior to examination with thermogravimetric analysis and X-ray diffraction, part of the sample was crushed (< 63 μm) and the hydration was stopped by solvent exchange using isopropanol during 15 minutes and flushing with ether.

The amount of bound water (H) and calcium hydroxide (CH) are determined by thermogravimetric analysis using a Mettler Toledo TGA/SDTA851 by measuring the weight loss of a 50 mg sample in the temperature intervals 40-550˚C for bound water and 450-550˚C for CH. The exact boundaries for the temperature interval of CH are adapted based on the derivative curve (DTG). The values are expressed as %wt. of the dry sample at 550˚C.

The crystalline anhydrous and hydrous phases were identified, and if possible quantified applying X-ray diffraction (XRD) combined with Rietveld analysis using a PANalytical X'Pert Pro MPD diffractometer in a θ-2θ configuration with a CuKα source (λ=1.54Å) equipped with an incident beam monochromator. The back-loaded powder samples of about 3 g were scanned between 5° and 70° with the X'celerator detector. An external CaF_2 standard was measured for each test series to facilitate quantitative Rietveld analysis [18].

The degree of hydration of OPC and fly ash, and the coarse porosity were determined using image analysis (IA) [19-21] applied on backscattered electron (BSE) images taken by a Philips ESEM FEG XL 30 of a epoxy resin impregnated, polished and carbon coated piece of hydrated cement paste. Over sixty images were taken per sample at a magnification of 1600. The minimum pore radius measured corresponds to 0.17 µm. The analyses were carried out using an accelerating voltage of 15 kV to ensure a good compromise between spatial resolution and adequate excitation of the FeKα peak. The content of unreacted FA and OPC in the hydrated paste samples is determined from BSE images using image analysis as described in previous investigation [21]. The percentage of FA and OPC reacted is calculated by dividing the volume of anhydrous materials in the hydrated sample with the theoretical content in the unhydrated sample.

4. Results and discussion

4.1. Compressive and flexural strength

For all tested combinations the early age compressive and flexural strengths increase with increasing curing temperature (Table 4 and Figure 1). After 7 days and longer, however, curing at elevated temperatures (40°C) appears to be detrimental for the strength development of the OPC and OPC-L mortars. The OPC and OPC-L mortars cured at 5°C show the highest strengths. This temperature "inversion effect" on the compressive strength of neat OPC cements has been observed in several other studies [1, 2, 4, 11, 22].

Increased curing temperature resulted in a higher strength up to 28 days for the fly ash containing blends. At 90 days the mortars cured at 20˚C and 40˚C reach a similar strength, but which is still higher than the one obtained by curing at 5˚C. Similar observations have been made in the past for cements containing 20-30% fly ash [11, 22, 23]. An inversion effect is not observed for the fly ash containing blends in this study in the temperature interval of 5 to 40˚C up to 90 days (Table 4), but it might occur after longer hydration times. Temperature inversion for OPC-fly ash has been reported within 180 days for samples cured at relatively higher temperatures (60 and 80°C) than the one used for the current study [11, 23].

Blended cements containing fly ash appear to be more sensitive to low curing temperature than the OPC and OPC-L cements. Curing at 5˚C tends to slow down the strength development for fly ash blended cements, so that even after 90 days of curing, the mortars only reach about 2/3 of the strength obtained by plain OPC, similar findings have been reported before for curing at 8˚C [9]. At 20˚C the compressive strength of the fly ash containing cements surpasses that of the neat cements after 28 days. Increasing the curing temperature to 40˚C increases the strength development of fly ash blended cements considerably. Hence, the fly ash containing cements surpass their fly ash free equivalents cured at 40˚C already after 7 days.

Generally about 5% of OPC can be replaced by limestone powder without impairing the compressive strength [16, 24, 25]. The results in Table 4 show that varying the temperature does not seem to change that. A similar observation can be made for the fly ash containing cements at 20˚C and 40˚C (comparing

OPC-FA* and OPC-FA-L). However, at 5˚C, substituting 5% of the OPC with limestone powder results in a decrease of compressive strength at all tested ages.

Replacing 5% of fly ash with 5% of limestone powder (comparing OPC-FA and OPC-FA-L) has been shown to be beneficial for the compressive strength at 20˚C in [14-16, 26]. The results presented in Table 4 confirm this for all tested ages when cured at 5˚C or 20˚C. However, at 40˚C, the fly ash seems to be activated by the elevated temperature, therefore the higher fly ash content overrules the beneficial effect of the limestone addition.

4.2. **Reaction of the anhydrous phases**

4.2.1. **Reaction of the OPC**

The effect of the curing temperature on the hydration of the different clinker phases is studied using XRD-Rietveld and BSE-IA. The percentages of the anhydrous phases relative to the OPC content present after 1, 7, 28, 90 and 180 days of hydration for the different curing temperatures tested are given in Table 5.

The reaction of alite, aluminate and ferrite is accelerated by increasing the curing temperature up to 7 days. The belite reaction, on the other hand, only starts to be accelerated after 7 days. After 180 days, alite has reacted nearly completely at all curing temperatures. Only approx. 30% of the belite has reacted at 5°C and about 70% at 20 and 40°C after 180 days. For aluminate and ferrite a slight temperature inversion effect can be observed; the final degree of reaction tends to be slightly higher at the lower curing temperatures. In previous studies [1, 10], a similar temperature inversion was reported for ferrite. The reaction of OPC as a whole is accelerated by increasing the curing temperature, but after 90 days the clinker have reacted to a similar level independent of the temperature (Table 5, Table 6 and Figure 2).

The presence of fly ash tends to accelerate the alite hydration after 1 day, and slows down the belite reaction at 20˚C and 40˚C which is in line with the findings of other studies [27-30]. At 5˚C, the alite reaction tends to be retarded by the presence of fly ash. The hydration of the aluminate and ferrite phases is not affected considerably by the fly ash, except for the slight increase in the final degree of hydration of theses phases which is consistent with observations reported in other studies [28]. The overall reaction of the OPC is accelerated by the filler effect of the fly ash and the increase in effective water to OPC ratio at 20 and 40°C (Table 5, Table 6 and Figure 2), which is in agreement with observations reported in literature [27, 29-31]. However at 5˚C, fly ash tends to retard the OPC reaction during the first day of hydration. The reason for this might be that as OPC reacts, heat is produced and temporarily the curing temperature of the sample will increase somewhat, thereby it accelerates its own hydration. Replacing OPC with fly ash will reduce the produced heat and therefore lead to a relative retardation of the hydration during the first day.

4.2.2. **Reaction of the fly ash**

Increasing the curing temperature accelerates the fly ash reaction as shown in Figure 3. After 180 days, the degree of reaction of the fly ash is similar for the samples cured at 20 and 40°C, whereas the fly ash cured at 5°C only reaches about 1/3 of this. The slow reacting fly ash is more sensitive to the curing temperature than the relatively fast reacting clinker. Similar sensitivity to the curing temperature has previously been reported for the reaction of silica fume, geothermal silica and for slag [32-35]. The slow reaction of fly ash at 5°C is mirrored in the inferior mechanical properties observed for the fly ash containing blended cements at this temperature (Figure 1 and Table 4).

The reactivity of the fly ash is not influenced by the presence of limestone powder neither by the fly ash content and is similar for OPC-FA*, OPC-FA and OPC-FA-L at a given temperature, which is in agreement with results previously reported for 20°C [16].

4.3. **Effect on Portlandite and total bound water**

The amount of bound water (H) (water loss from 40 to 550°C) and calcium hydroxide (CH) (by mass loss from 450 to 550°C) increase initially with increasing curing temperature for all tested combinations (Table 7 and Figure 4). After 90 and 180 days, the Portlandite content was similar for all temperatures. In contrast, the amount of bound water starts to decrease with increasing curing temperature for the OPC and OPC-L pastes. The XRD-Rietveld and BSE-IA results obtained indicate a similar degree of hydration for the OPC at 180 days independent of the temperature (Table 5 and Table 6). The results in Figure 5 indicate that at higher curing temperatures, less water is bound per OPC reacted. This is in contrast with previous observations where a similar water content was observed in this temperature range [2, 36, 37], but it agrees with the findings of Zhang [8] who observed a lower water content at higher curing temperatures for OPC. The differences in amount of bound water could be due to the relatively high belite content (19%) of the cement used in this study, with belite being more sensitive to curing temperature than alite. Alternatively, the presence of less ettringite at higher temperatures (Figure 6) [2, 38], and the formation of a C-S-H containing less water at higher temperatures [8] could be the reason for the observed lower water content at higher curing temperature.

This shows the limitations concerning the use of the amount of bound water to evaluate the degree of reaction of the OPC when varying the curing temperature.

For the fly ash containing pastes, the H is similar at all tested temperatures from 28 days on, except for a small relative decrease after 90 days at 40˚C (Table 7 and Figure 4). They have generally a lower H and CH content than their fly ash free equivalents at all tested ages. This might be partly due to the replacement of OPC with fly ash, the dilution effect. Moreover, the pozzolanic hydration products might not bind much water in addition to the water inherent to the CH it reacts with, as also reported by Escalante-Garcia [37].

From 7 to 28 days on, the CH content in the fly ash containing pastes decreases with increasing curing temperature as reported in previous studies [39]. The elevated temperature promotes the pozzolanic reaction of the fly ash and thereby the CH consumption. Furthermore, the maximum CH concentration is observed at earlier times as the curing temperature increases. Indeed, the maximum at 5, 20 and 40˚C occurs at respectively ≥ 180 days, ≈28 days and 1-7 days which is in agreement with previous findings reported in the literature [9, 10].

Replacing 5% of OPC with 5% of limestone powder, results in a decrease in CH and H at all tested temperatures and ages. In case of the fly ash containing pastes (comparing OPC-FA* with OPC-FA-L) the H is similar or slightly higher and CH content is lower (Table 7). The difference in CH between the two mixes can not be caused by the pozzolanic reaction as both mixes have the same fly ash content which has reacted to the same extent (Figure 3). It is most likely due to a change in hydration products caused by the presence of limestone powder e.g. the formation of hemicarboaluminate hydrate and more ettringite as observed in previous studies [40-42].

Replacing 5% of fly ash with 5% of limestone powder (comparing OPC-FA and OPC-FA-L) results in a slight increase in H and a similar CH content at all tested ages and temperatures. This might also indicate the formation of carboaluminate hydrates and the stabilization of ettringite when limestone is present, leading to an increase in H and a decrease in CH. Therefore, no lower CH content was observed for the OPC-FA blend, even though it has higher fly ash content.

The CH content was also determined by XRD-Rietveld. The values obtained with both techniques, TGA and XRD-Rietveld, correlated well.

4.4. **Porosity**

For OPC and OPC-L, the coarse porosity at 1 day decreases with increasing curing temperature (Figure 7) as the reaction of the OPC is accelerated at higher temperatures. At 7 days, the OPC and OPC-L pastes reach a similar level of coarse porosity independent of the curing temperature. Upon further curing an opposite trend is observed; the coarse porosity is reduced at lower curing temperatures. A similar inversion effect has been reported in previous studies [6]. It should be noted that after 90 days the degree of reaction of OPC is similar regardless the curing temperature. The changes in coarse porosity at that age therefore must originate from differences in hydration products regarding composition and distribution throughout the matrix.

For the fly ash containing combinations, the trends observed at 1 day are similar as for their fly ash free equivalents: the higher the curing temperature the lower is the porosity. At 1 day OPC is the dominating factor, however, upon further curing, fly ash plays an important role. At 5˚C the reactivity of the fly ash is limited and is therefore not able to compensate for the dilution effect due to the replacement of the OPC. Nevertheless, a gradual reduction in coarse porosity can be observed between 28 and 180 days, most likely caused by the pozzolanic reaction of the fly ash filling up part of the porosity since most of the OPC has reacted by 28 days. At 20 and 40˚C the supplementary volume of hydration products resulting from the FA reaction are able to fill the coarse porosity and compensate for the dilution effect visible at early age.

4.5. **Microstructure**

Figure 8 shows the BSE image of OPC cured for 90 days at 5 and 40˚C. At both temperatures, remaining anhydrous phases, most likely belite, are observed. At 40˚C, clear zones of brighter inner-product can be seen around the anhydrous clinker grains. At 5˚C, on the other hand, hardly any inner-product is observed and C-S-H seems to have precipitated more homogenously in the matrix. In addition, a few Hadley grains are found for samples cured at 5˚C. A similar temperature dependency of the microstructure has been reported by Kjellsen et al. [3, 4]. The bright colour of the inner-product compare to the outer-product is not attributed to changes in composition, but to a lower content of micro-porosity and bound water [43]. The homogenous distribution of the hydration products at lower curing temperatures results in a finer pore structure (except for the Hadley grains) relative to the sample cured at 40˚C which favour the formation of a denser inner-product and a more porous outer-product. This is confirmed by the quantification of the total coarse porosity by image analysis of the BSE images (Figure 8).

For the systems containing fly ash, the matrix development during the first days is mainly due to the OPC reaction. Even though fly ash does not react considerably the first days, it does influence the microstructure due to its filler effect: the surface of the fly ash particles serves as precipitation surface for the hydration

products, and the effective water-to-cement ratio is increased, thereby resulting in a more homogenous filling of the microstructure. Figure 9 shows the BSE images for OPC-FA* hydrated at 5 and 40˚C for 90 days. At 5˚C the dissolution of fly ash is restricted, leading to a more porous microstructure for fly ash blended cements compared to the neat OPC cured at 5˚C (Figure 8). At 40°C, on the other hand, the pozzolanic reaction products contribute to fill the matrix and reduce the coarse porosity.

Additionally, it can be seen from Figure 9 that the inner-product is hardly distinguishable from the outer-product in the fly ash blended cement cured at 40°C compared to the neat OPC. This indicates that the high final strengths obtained with the fly ash blended cement cured at 40˚C are not only due to additional filling of voids by pozzolanic reaction products, but also by a more even distribution of the hydration products due to the filler effect of the fly ash.

For both neat and blended cements (Figure 8 and Figure 9), the morphology of the calcium hydroxide seems to depend on the curing temperature, as reported in previous studies [3, 4]. At 5˚C more lamellar and elongated calcium hydroxide is observed most likely resulting form the cross section of platelets, whereas at 40˚C it is denser and more irregular shaped.

5. Factors influencing compressive strength

Figure 10 presents the compressive strength versus bound water and degree of reaction of OPC and FA, and the coarse porosity, for the OPC and OPC-FA-L samples cured for 1, 7, 28 and 90 days at 5, 20 and 40°C.

The fly ash containing cement tends to bind less water than the OPC, for the same level of compressive strength. Little additional water seems to be bound after 28 days of curing in the fly ash cements even though a considerable strength increase is observed. This indicates that the fly ash mainly binds the water inherent to the calcium hydroxide in its hydration products and only little additional water.

The degree of reaction of OPC does not correlate well with its compressive strength for samples cured at different temperatures. For a similar degree of reaction, a lower strength is reached at higher curing temperatures. This can be attributed to the inhomogeneous distribution of the hydration products at higher curing temperatures, as mentioned above in the discussion of the microstructure. For the ternary cements the correlation is better as exemplified for OPC-FA-L in Figure 10. At early ages, the filler effect of the fly ash results in a better distribution of the hydration products and at later ages the hydration products from the fly ash makes the matrix denser. It should, however, be noted that at the same total percentage of OPC and fly ash reacted, compressive strength is much lower for the neat OPC than for the fly ash containing mixtures. This could indicate that fly ash contributes relatively more to the compressive strength than OPC, by converting calcium hydroxide to C-S-H which has a higher binding capacity.

The coarse porosity correlates best with the compressive strength from all of factors presented in Figure 10. The correlation appears to be independent of whether part of the OPC is replaced by fly ash and limestone powder or not.

6. Conclusion

After the first day of hydration, the curing temperature accelerates significantly the OPC hydration and thus increases the compressive and flexural strength and the amount of bound water and portlandite. After about 7 days of hydration, the compressive strength of OPC and OPC-L cements exhibit a crossover. The

higher curing temperature, initially yielding higher strength and more bound water, turns out to be detrimental from 7 days and onwards. After 90 days, the highest strength is obtained when curing at 5˚C and the lowest at 40˚C. This is related to the formation of a denser C-S-H containing less water (Figure 5) and the resulting coarser porosity (Figure 8) at higher temperatures and to the formation of less ettringite at higher temperatures (Figure 6), as a similar degree of hydration is observed after 28 days and longer at all curing temperatures.

No temperature inversion effect was observed for the compressive strength of the composite cements containing fly ash. Fly ash reacts differently at elevated curing temperature than OPC. During the first days of hydration, replacing part of the OPC by fly ash gives rise to a more homogenous distribution of the hydration products as the fly ash serves as precipitation sites for hydration products and leads to an increase in the effective water to OPC ratio. At later ages, the pozzolanic hydration products further fill the coarse porosity and thereby improve the compressive strength. Hence, the fly ash containing cements cured at 20 and 40˚C reach a higher final compressive strength than their fly ash free equivalents. However at 5˚C, the dissolution of the glass phase of the fly ash is very slow and the fly ash containing mortars are not able to catch up with the compressive strength observed of the OPC and OPC-L blends within the first 90 days of hydration.

An evaluation of the factors influencing the compressive strength revealed that to reach the same strength level, fly ash blended cement bind less water than OPC. In the case of neat cement, the percentage of OPC reacted is not a good indication for the strength when the samples are cured at different temperatures. In contrast, for fly ash containing cements, the total amount of OPC and fly ash reacted correlates rather well with strength. Additionally, less OPC plus fly ash has to react than OPC in the neat cement to reach the same compressive strength. Finally, the coarse porosity appears to be the dominating factor regarding the compressive strength, independent of whether part of the OPC is replaced by fly ash and limestone powder or not.

References

1. Escalante-García, JI and Sharp, JH (1998) Effect of temperature on the hydration of the main clinker phases in portland cements: part i, neat cements. Cement and Concrete Research 28(9): 1245-1257.
2. Lothenbach, B, Winnefeld, F, Alder, C, Wieland, E, and Lunk, P (2007) Effect of temperature on the pore solution, microstructure and hydration products of Portland cement pastes. Cement and Concrete Research 37(4): 483-491.
3. Kjellsen, KO, Detwiler, RJ, and Gjørv, OE (1990) Backscattered electron imaging of cement pastes hydrated at different temperatures. Cement and Concrete Research 20(2): 308-311.
4. Kjellsen, KO, Detwiler, RJ, and Gjørv, OE (1991) Development of microstructures in plain cement pastes hydrated at different temperatures. Cement and Concrete Research 21(1): 179-189.
5. Kjellsen, KO (1996) Heat curing and post-heat curing regimes of high-performance concrete: Influence on microstructure and C-S-H composition. Cement and Concrete Research 26(2): 295-307.
6. Kjellsen, KO, Detwiler, RJ, and Gjørv, OE (1990) Pore structure of plain cement pastes hydrated at different temperatures. Cement and Concrete Research 20(6): 927-933.
7. Scrivener, KL and Taylor, HFW (1993) Delayed ettringite formation: a microstructural and microanalytical study. Advances in cement research 5(20): 139-146.
8. Zhang, X (2007) PhD thesis, Quantitative microstructural characterisation of concrete cured under realistic temperature conditions, in Material Science. EPFL: Lausanne. p. 283.

9. Halse, Y, Jensen, H-U, and Pratt, PL. (Year) The effect of the curing temperature on the pozzolanic reaction in fly ash blended cement. in 8th ICCC. Rio de Janeiro, Brasil.
10. Escalante-García, JI and Sharp, JH (1998) Effect of temperature on the hydration of the main clinker phases in portland cements: part ii, blended cements. Cement and Concrete Research 28(9): 1259-1274.
11. Escalante-García, JI and Sharp, JH (2001) The microstructure and mechanical properties of blended cements hydrated at various temperatures. Cement and Concrete Research 31(5): 695-702.
12. Escalante-Garcia, JI and Sharp, JH (2004) The chemical composition and microstructure of hydration products in blended cements. Cement and Concrete Composites 26(8): 967-976.
13. De Weerdt, K, Sellevold, EJ, Justnes, H, and Kjellsen, KO (2010) Fly ash-limestone ternary cements: effect of component fineness. Advances in cement research (accepted).
14. De Weerdt, K, Justnes, H, Kjellsen, KO, and Sellevold, E (2010) Fly ash -limestone ternary composite cements: synergetic effect at 28 days. Nordic Concrete Research 42(2).
15. De Weerdt, K, Kjellsen, KO, Sellevold, EJ, and Justnes, H (2011) Synergy between fly ash and limestone powder in ternary cements. Cement and Concrete Composites 33(1): 30-38.
16. De Weerdt, K, Ben Haha, M, Le Saout, G, Kjellsen, KO, Justnes, H, and Lothenbach, B (2010) Hydration mechanisms of ternary Portland cements containing limestone powder and fly ash. Cement and Concrete Research In review.
17. Lothenbach, B, Le Saout, G, Gallucci, E, and Scrivener, K (2008) Influence of limestone on the hydration of Portland cements. Cement and Concrete Research 38(6): 848-860.
18. Le Saout, G, Füllmann, T, Kocaba, V, and Scrivener, K (2007) Quantitative study of cementitous materials by X-ray diffraction/Rietveld analysis using an external standard, in 12th International Congress on the Chemistry of Cement Montréal, Canada.
19. Scrivener, KL (2004) Backscattered electron imaging of cementitious microstructures: understanding and quantification. Cement and Concrete Composites 26(8): 935-945.
20. Ben Haha, M, Gallucci, E, Guidoum, A, and Scrivener, KL (2007) Relation of expansion due to alkali silica reaction to the degree of reaction measured by SEM image analysis. Cement and Concrete Research 37(8): 1206-1214.
21. Ben Haha, M, De Weerdt, K, and Lothenbach, B (2010) Quantification of the degree of reaction of fly ash. Cement and Concrete Research 40(11): 1620-1629.
22. Maltais, Y and Marchand, J (1997) Influence of curing temperature on cement hydration and mechanical strength development of fly ash mortars. Cement and Concrete Research 27(7): 1009-1020.
23. Payá, J, Monzó, J, Borrachero, MV, Peris-Mora, E, and Amahjour, F (2000) Mechanical treatment of fly ashes: Part IV. Strength development of ground fly ash-cement mortars cured at different temperatures. Cement and Concrete Research 30(4): 543-551.
24. Soroka, I and Stern, N (1976) Calcareous fillers and the compressive strength of portland cement. Cement and Concrete Research 6(3): 367-376.
25. Soroka, I and Setter, N (1977) The effect of fillers on strength of cement mortars. Cement and Concrete Research 7(4): 449-456.
26. De Weerdt, K and Justnes, H. (Year) Synergic reactions in triple blended cements. in 11th NCB International Seminar on Cement and Building Materials. New Delhi.
27. Taylor, HFW, Mohan, K, and Moir, GK (1985) Analytical study of pure and extended Portland cement pastes: II, fly ash- and slag-cement pastes. Journal of the American Ceramic Society 68(12): 685-690.
28. Dalziel, JA and Gutteridge, WA (1986) The influence of pulverized-fuel ash upon the hydration characteristics and certain physical properties of a Portland cement paste. Cement and Concrete Association: Technical Report: Wexham Springs. p. 28.
29. Lukas, W (1976) The influence of an Austrian fly ash on the reaction processes in the clinker phases of Portland cements. Materials and Structures 9(5): 331-337.
30. Sakai, E, Miyahara, S, Ohsawa, S, Lee, S-H, and Daimon, M (2005) Hydration of fly ash cement. Cement and Concrete Research 35(6): 1135-1140.

31. Ogawa, K, Uchikawa, H, Takemoto, K, and Yasui, I (1980) The mechanism of the hydration in the system C_3S-pozzolana. Cement and Concrete Research 10(5): 683-696.
32. Justnes, H. (Year) Kinetics of reaction in cementitious pastes containing silica fume as studied by ^{29}Si NMR. in Nuclear Magetic Resonance Spectroscopy of Cement-Based Materials. Berlin: Springer.
33. Escalante, JI, Gómez, LY, Johal, KK, Mendoza, G, Mancha, H, and Méndez, J (2001) Reactivity of blast-furnace slag in Portland cement blends hydrated under different conditions. Cement and Concrete Research 31(10): 1403-1409.
34. Le Saoût, G, Lécolier, E, Rivereau, A, and Zanni, H (2006) Chemical structure of cement aged at normal and elevated temperatures and pressures, Part II: Low permeability class G oilwell cement. Cement and Concrete Research 36(3): 428-433.
35. Gómez-Zamorano, LY and Escalante-García, JI (2010) Effect of curing temperature on the nonevaporable water in portland cement blended with geothermal silica waste. Cement and Concrete Composites 32(8): 603-610.
36. Kjellsen, KO and Detwiler, RJ (1992) Reaction kinetics of portland cement mortars hydrated at different temperatures. Cement and Concrete Research 22(1): 112-120.
37. Escalante-Garcia, JI (2003) Nonevaporable water from neat OPC and replacement materials in composite cements hydrated at different temperatures. Cement and Concrete Research 33(11): 1883-1888.
38. Matschei, T and Glasser, FP (2010) Temperature dependence, 0 to 40°C, of the mineralogy of Portland cement paste in the presence of calcium carbonate. Cement and Concrete Research 40(5): 763-777.
39. Luke, K and Glasser, FP (1988) Internal chemical evolution of the constitution of blended cements. Cement and Concrete Research 18(4): 495-502.
40. Kakali, G, Tsivilis, S, Aggeli, E, and Bati, M (2000) Hydration products of C_3A, C_3S and Portland cement in the presence of $CaCO_3$. Cement and Concrete Research 30(7): 1073-1077.
41. Bonavetti, VL, Rahhal, VF, and Irassar, EF (2001) Studies on the carboaluminate formation in limestone filler-blended cements. Cement and Concrete Research 31(6): 853-859.
42. Hoshino, S, Yamada, K, and Hirao, H (2006) XRD/Rietveld analysis of the hydration and strength development of slag and limestone blended cement. Journal of Advanced Concrete Technology 4(3): 357-367.
43. Famy, C, Scrivener, KL, and Crumbie, AK (2002) What causes differences of C-S-H gel grey levels in backscattered electron images? Cement and Concrete Research 32(9): 1465-1471.

List of tables:

Table 1: Chemical composition of the clinker, fly ash and limestone powder..... 12
Table 2: Mineral composition of the clinker determined by XRD-Rietveld analysis. 12
Table 3: Experimental matrix 12
Table 4: Compressive and flexural strength 13
Table 5: Quantification of anhydrous clinker phases and % of OPC reacted by XRD-Rietveld analysis..... 14
Table 6: the %OPC and FA reacted and coarse porosity determined by BSE-IA. 15
Table 7: Amount of calcium hydroxide (CH) and bound water (H) determined by TGA..... 15

List of figures

Figure 1: Compressive strength of OPC and OPC-FA-L in function of the curing temperature and time. 16
Figure 2: % OPC reacted as a function of the curing time and temperature for OPC and OPC-FA-L determined by BSE-IA. 16
Figure 3: Fly ash reactivity at the different curing temperatures tested. 16
Figure 4: The amount of bound water (H) and calcium hydroxide (CH) of OPC and OPC-FA-L as a function of time and curing temperature. 17
Figure 5: The amount of bound water (H) relative to the amount of OPC reacted for the OPC and OPC-L cements at 5˚C, 20˚C and 40˚C. 17
Figure 6: XRD patterns for OPC and OPC-FA-L cured for 180 days at 5, 20 and 40°C (with E = ettringite, Ms = monosulphate, Hc = hemicarbonate, Mc = monocarbonate). 18
Figure 7: Coarse porosity determined by BSE-IA as a function of curing time at 5, 20 and 40˚C for all tested combinations. 18
Figure 8: BSE images of hydrated pastes. Left: OPC 5˚C 90 days; right: OPC 40˚C 90 days. 19
Figure 9: BSE images of hydrated pastes. Left: OPC-FA* 5˚C 90 days; right: OPC-FA* 40˚C 90 days..... 19
Figure 10: Compressive strength versus the amount of bound water (%H), % OPC and FA reacted, and the coarse porosity for OPC (triangles) and OPC-FA-L (spheres) cured for 1, 7, 28 and 90 days at 5, 20 and 40°C (resp. white, grey and black). 19

Table 1: Chemical composition of the clinker, fly ash and limestone powder

	Clinker	Fly ash	Limestone
SiO_2	20.0	50.0	12.87
Al_2O_3	5.4	23.89	2.68
Fe_2O_3	3.14	6.03	2.04
CaO	60.6	6.32	42.29
MgO	2.9	2.12	1.84
SO_3	1.5	0.43	-
P_2O_5	0.10	1.07	-
K_2O	1.2	1.42	0.62
Na_2O	0.5	0.63	0.49
LOI	0.33	3.60	37.66
Carbon	-	3.13	-
Chloride	0.051	0.00	-
Free CaO	1.85	-	-
Gypsum	3.7	-	-
Blaine surface [m^2/kg]	450*	450	810
Density [kg/m^3]	3150*	2490	2740

* for OPC = clinker + gypsum

Table 2: Mineral composition of the clinker determined by XRD-Rietveld analysis.

Minerals	[%]
C_2S	19
C_3S	54
C_3A	11
C_4AF	8

Table 3: Experimental matrix

name	OPC	FA	L
OPC	100	-	-
OPC-L	95	-	5
OPC-FA*	70	30	-
OPC-FA	65	35	-
OPC-FA-L	65	30	5

Table 4: Compressive and flexural strength

	Compressive strength [MPa]					Flexural strength [MPa]				
time [days]	1	3	7	28	90	1	3	7	28	90
OPC										
5°C	5.9	24.4	36.0	50.6	57.1	1.7	5.3	7.0	7.8	8.2
20°C	22.1	31.6	36.1	45.6	48.0	5.3	7.2	7.7	7.1	6.9
40°C	26.3	29.7	34.1	40.3	42.2	5.0	6.4	6.3	6.0	5.1
OPC-L										
5°C	5.8	24.7	38.4	52.9	60.1	1.6	5.1	6.9	8.0	8.3
20°C	21.9	32.8	38.1	43.9	51.5	5.0	7.0	7.4	7.4	7.5
40°C	26.9	30.8	35.1	40.8	44.2	5.3	6.5	6.4	5.6	5.7
*OPC-FA**										
5°C	2.3	14.2	25.9	36.3	46.0	0.5	3.3	5.2	6.7	7.6
20°C	13.7	23.8	28.5	39.8	55.2	3.5	5.0	5.9	6.3	7.7
40°C	19.5	26.4	37.9	50.0	53.8	3.9	5.1	7.1	8.1	7.7
OPC-FA										
5°C	1.8	12.2	22.5	31.2	41.4	0.4	3.0	4.9	6.2	6.9
20°C	12.1	21.5	25.7	37.8	52.3	3.1	4.7	5.2	7.0	6.8
40°C	18.0	25.0	36.3	51.6	54.5	3.5	5.0	7.3	8.1	7.8
OPC-FA-L										
5°C	1.9	12.8	23.6	34.8	44.7	0.5	2.9	5.1	6.3	7.7
20°C	12.4	23.8	28.8	39.8	55.3	3.2	4.8	5.7	6.0	8.5
40°C	19.6	26.2	36.8	50.0	53.6	3.7	4.9	7.6	8.9	7.9

Table 5: Quantification of anhydrous clinker phases and % of OPC reacted by XRD-Rietveld analysis

	Alite [%]						Belite [%]						Ferrite [%]						Aluminate [%]						% OPC reacted				
time [days]	0	1	7	28	90	180	0	1	7	28	90	180	0	1	7	28	90	180	0	1	7	28	90	180	1	7	28	90	180
OPC																													
5°C	54.6	25.9	7.5	4.0	1.5	-	18.7	17.6	18.8	17.1	15.4	14.5	8.0	6.0	5.0	3.2	2.1	2.1	10.6	7.3	3.8	1.9	0.8	1.2	41.7	62.9	72.1	78.4	80.6
20°C	54.6	15.3	6.5	4.5	2.0	1.4	18.7	17.8	17.1	15.5	8.2	6.5	8.0	5.9	3.7	2.5	2.5	2.7	10.6	5.9	2.5	1.5	1.5	1.5	53.5	68.4	74.5	84.0	86.4
40°C	54.6	9.9	5.9	3.8	2.1	-	18.7	18.7	14.5	9.5	5.8	6.2	8.0	3.9	3.3	3.4	3.4	3.7	10.6	2.7	1.8	1.8	2.0	2.0	63.2	72.7	79.9	85.6	87.0
OPC-L																													
5°C	54.6	25.1	6.8	3.2	1.7	1.1	18.7	17.3	18.3	17.3	14.8	13.4	8.0	6.1	5.0	2.9	2.0	2.2	10.6	7.1	3.5	1.5	0.8	0.9	42.8	64.8	73.5	79.2	80.6
20°C	54.6	13.7	6.4	3.0	2.3	1.7	18.7	17.6	16.3	14.1	8.2	6.1	8.0	5.8	3.6	2.6	2.3	2.3	10.6	5.7	1.9	1.4	1.5	1.5	55.6	69.8	77.1	83.9	86.7
40°C	54.6	9.4	5.0	4.1	-	-	18.7	18.8	14.6	8.6	6.2	4.4	8.0	4.0	3.1	2.7	3.1	3.2	10.6	2.9	2.0	1.7	1.8	2.1	63.1	73.6	81.4	87.6	89.3
*OPC-FA**																													
5°C	54.6	28.4	7.9	3.2	-	-	18.7	17.6	18.7	17.5	14.4	11.9	8.0	7.0	5.0	1.9	2.2	2.6	10.6	8.0	3.7	-	-	-	37.1	62.5	75.2	81.3	83.2
20°C	54.6	17.3	3.6	-	-	-	18.7	18.3	18.7	16.8	11.0	11.9	8.0	6.0	3.3	2.9	2.6	2.2	10.6	5.1	1.3	1.2	1.2	-	51.1	71.0	76.9	83.1	83.6
40°C	54.6	10.7	2.5	2.2	1.1	2.5	18.7	17.9	17.1	15.4	12.5	13.2	8.0	3.6	3.2	3.4	2.7	2.2	10.6	1.5	1.1	1.2	0.8	1.6	64.6	73.8	75.8	81.0	78.9
OPC-FA																													
5°C	54.6	31.9	7.4	1.7	-	-	18.7	18.2	18.6	18.3	14.0	11.9	8.0	7.1	4.9	2.0	1.5	2.8	10.6	8.4	3.3	-	-	-	32.3	63.5	75.7	82.4	82.9
20°C	54.6	14.2	3.7	-	-	-	18.7	18.8	17.9	16.2	12.0	11.0	8.0	6.2	3.9	2.4	2.3	-	10.6	5.9	1.3	-	-	-	52.9	70.8	79.2	83.7	86.9
40°C	54.6	13.0	1.5	1.1	1.2	-	18.7	18.6	18.4	15.1	14.4	13.1	8.0	3.7	3.1	3.0	3.6	3.4	10.6	2.6	0.9	0.9	1.0	1.2	60.1	73.7	78.1	78.0	80.5
OPC-FA-L																													
5°C	54.6	30.3	5.4	-	-	-	18.7	17.6	18.7	18.5	15.3	11.5	8.0	7.1	5.9	1.3	-	-	10.6	8.4	3.3	-	-	-	34.6	64.4	78.1	82.4	86.0
OPC-FA-L	54.6	13.5	2.8	0.9	-	-	18.7	18.4	17.8	14.3	11.2	9.3	8.0	5.9	3.3	-	-	-	10.6	5.8	1.1	-	-	-	54.3	72.5	82.8	86.4	88.5
OPC-FA-L	54.6	8.6	1.9	1.6	1.5	-	18.7	18.8	15.8	12.0	12.4	12.6	8.0	3.9	2.5	2.1	2.7	1.2	10.6	2.0	1.1	0.9	1.3	1.5	64.7	76.5	81.5	80.4	82.8

Table 6: the %OPC and FA reacted and coarse porosity determined by BSE-IA.

	OPC reacted [%]					FA reacted [%]					Coarse porosity [%]				
time [days]	1	7	28	90	180	1	7	28	90	180	1	7	28	90	180
OPC															
5°C	38.2	68.2	76.5	85.4	88.9						33.2	12.5	3.3	2.1	2.2
20°C	55.9	74.9	82.7	83.9	85.8						22.7	12.6	5.7	4.9	4.8
40°C	65.2	74.5	83.1	85.4	88.2						19.0	12.5	8.8	8.2	8.1
OPC-L															
5°C	37.8	69.4	78.3	86.2	89.3						31.8	13.7	3.9	2.4	1.9
20°C	54.3	73.7	84.6	86.3	89.5						23.3	12.2	6.2	4.2	4.7
40°C	67.3	73.9	84.5	87.2	89.5						19.7	13.2	8.7	7.9	7.9
*OPC-FA**															
5°C	36.5	71.4	84.2	88.9	92.3	0.0	0.9	4.1	8.1	13.7	35.4	17.4	13.9	8.7	7.4
20°C	61.4	79.3	88.0	88.8	89.3	1.1	6.4	19.6	28.4	32.9	29.7	19.9	11.4	3.1	2.8
40°C	73.2	83.2	88.2	89.2	90.2	4.2	11.6	29.6	31.2	34.8	22.9	11.4	3.2	3.1	2.8
OPC-FA															
5°C	34.5	72.3	85.3	90.7	91.5	0.0	1.0	4.6	8.7	12.5	37.6	18.2	13.2	9.4	7.7
20°C	61.5	80.1	86.7	87.4	87.5	0.6	6.1	20.8	27.6	32.7	29.9	20.0	13.4	4.7	3.4
40°C	73.1	82.5	89.7	90.3	90.4	4.8	12.0	29.4	31.7	35.4	24.9	10.2	3.1	2.9	2.7
OPC-FA-L															
5°C	36.2	73.7	84.7	89.6	91.7	0.0	0.9	4.5	8.2	13.2	34.7	19.7	13.6	9.1	7.5
20°C	61.8	84.3	84.4	85.7	86.9	0.8	6.1	18.5	26.4	32.2	30.0	18.9	12.8	3.0	3.1
40°C	72.4	83.3	89.1	89.9	90.7	4.6	12.3	28.5	30.6	34.3	23.9	12.7	3.3	3.1	2.9

Table 7: Amount of calcium hydroxide (CH) and bound water (H) determined by TGA.

	CH [%]					H [%]				
time [days]	1	7	28	90	180	1	7	28	90	180
OPC										
5°C	8.0	17.9	18.8	21.4	22.6	10.8	21.8	24.1	28.5	30.6
20°C	12.3	18.6	20.1	22.6	23.4	15.1	21.9	24.1	26.3	28.2
40°C	15.7	19.5	20.6	22.9	23.1	17.9	21.2	23.2	25.0	26.2
OPC-L										
5°C	7.3	15.7	18.1	19.5	20.7	10.0	19.8	23.7	25.8	29.7
20°C	11.9	16.3	17.9	19.3	20.5	14.6	21.0	23.4	25.0	27.3
40°C	14.6	18.2	19.3	21.0	21.0	16.9	20.7	23.0	24.4	26.1
*OPC-FA**										
5°C	6.1	12.9	14.1	14.3	14.7	7.6	15.7	18.4	20.4	23.0
20°C	9.4	11.4	11.8	11.2	11.2	12.1	16.7	18.8	20.5	23.2
40°C	11.5	12.7	11.8	11.7	11.0	14.3	17.7	18.8	19.8	21.3
OPC-FA										
5°C	4.6	12.3	13.0	13.5	14.1	6.8	14.8	17.3	19.3	22.1
20°C	9.1	13.1	13.5	12.5	12.1	11.2	16.0	18.2	19.8	22.1
40°C	11.1	11.2	10.3	11.0	10.3	13.7	16.9	18.1	18.8	20.2
OPC-FA-L										
5°C	4.7	12.0	12.5	13.1	13.4	7.1	15.3	18.5	20.6	23.5
20°C	9.6	12.9	12.7	11.9	11.4	11.4	17.0	19.4	21.1	22.9
40°C	10.9	11.7	10.1	10.3	9.9	14.2	17.8	19.3	20.0	21.6

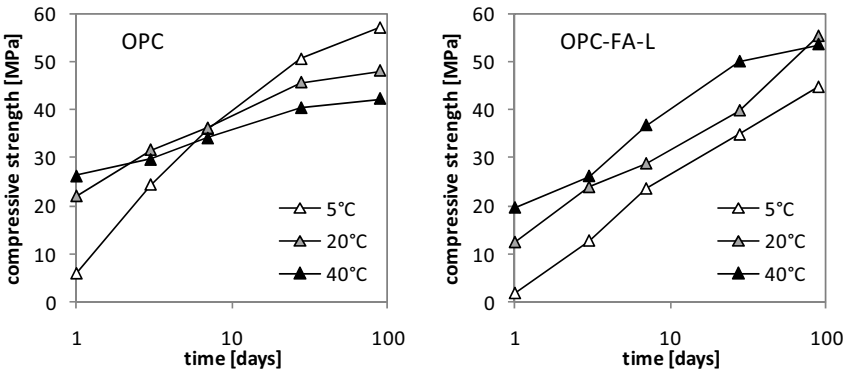

Figure 1: Compressive strength of OPC and OPC-FA-L in function of the curing temperature and time.

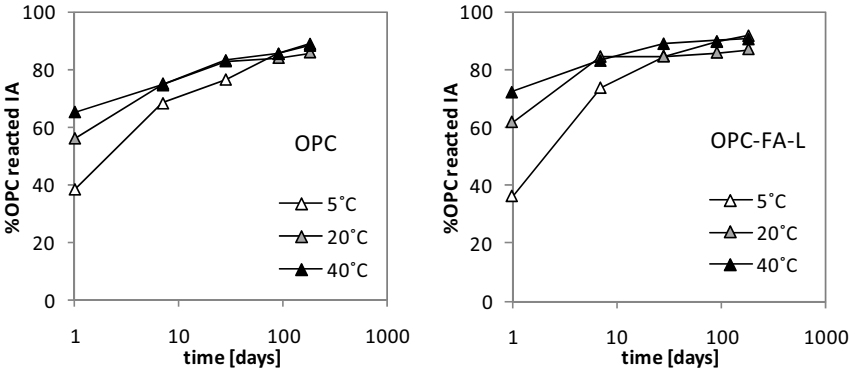

Figure 2: % OPC reacted as a function of the curing time and temperature for OPC and OPC-FA-L determined by BSE-IA.

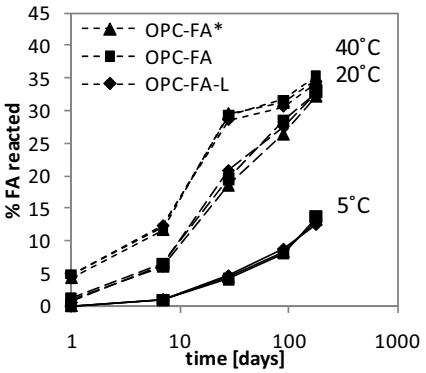

Figure 3: Fly ash reactivity at the different curing temperatures tested.

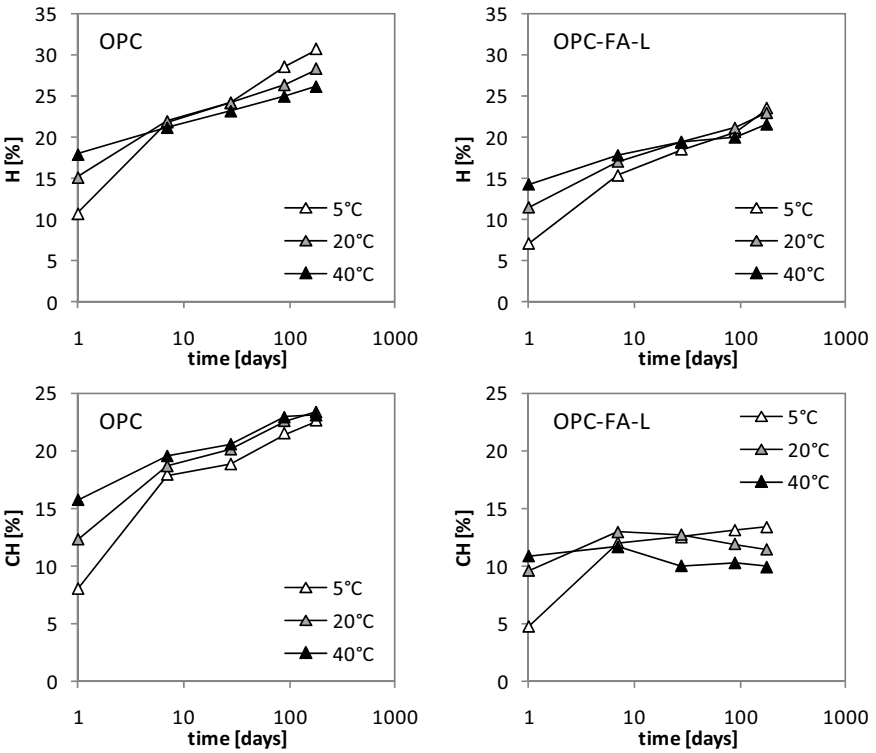

Figure 4: The amount of bound water (H) and calcium hydroxide (CH) of OPC and OPC-FA-L as a function of time and curing temperature.

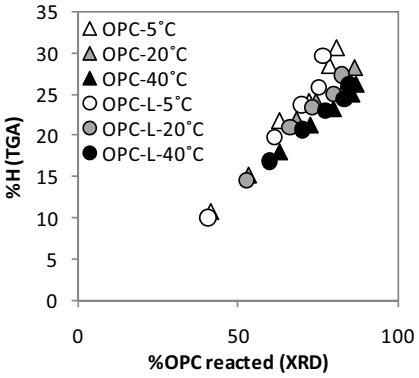

Figure 5: The amount of bound water (H) relative to the amount of OPC reacted for the OPC and OPC-L cements at 5˚C, 20˚C and 40˚C.

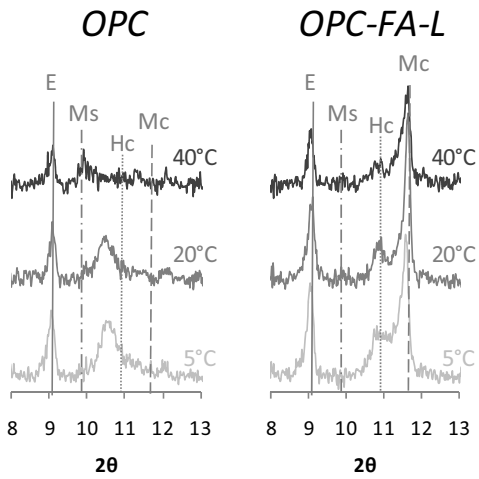

Figure 6: XRD patterns for OPC and OPC-FA-L cured for 180 days at 5, 20 and 40°C (with E = ettringite, Ms = monosulphate, Hc = hemicarbonate, Mc = monocarbonate).

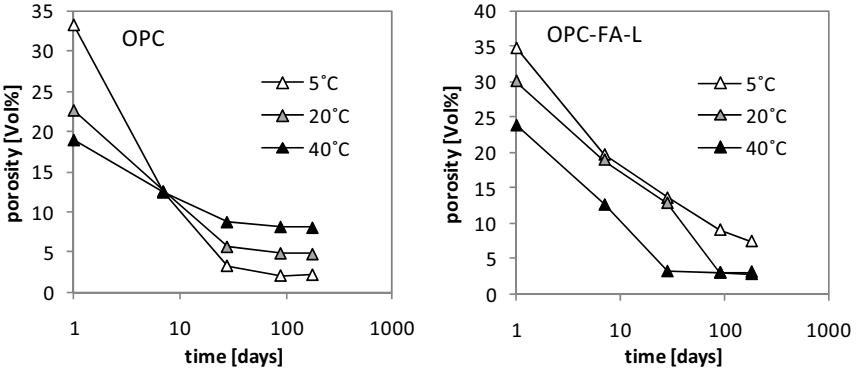

Figure 7: Coarse porosity determined by BSE-IA as a function of curing time at 5, 20 and 40˚C for all tested combinations.

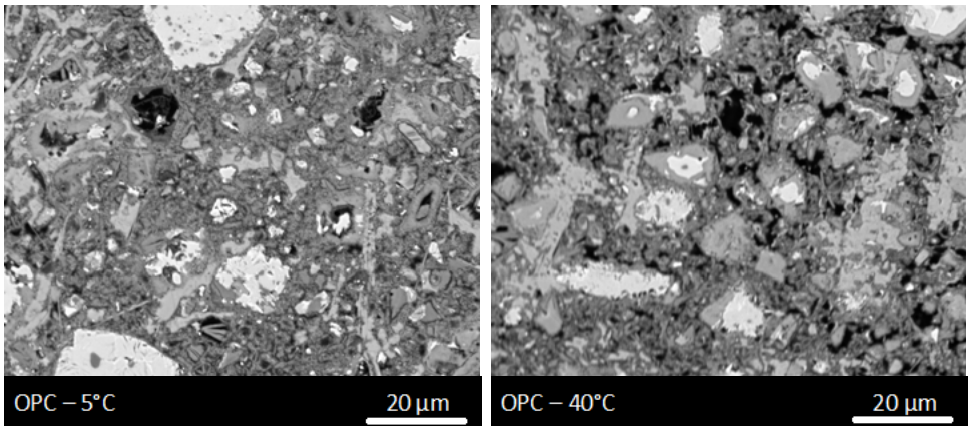

Figure 8: BSE images of hydrated pastes. Left: OPC 5˚C 90 days; right: OPC 40˚C 90 days.

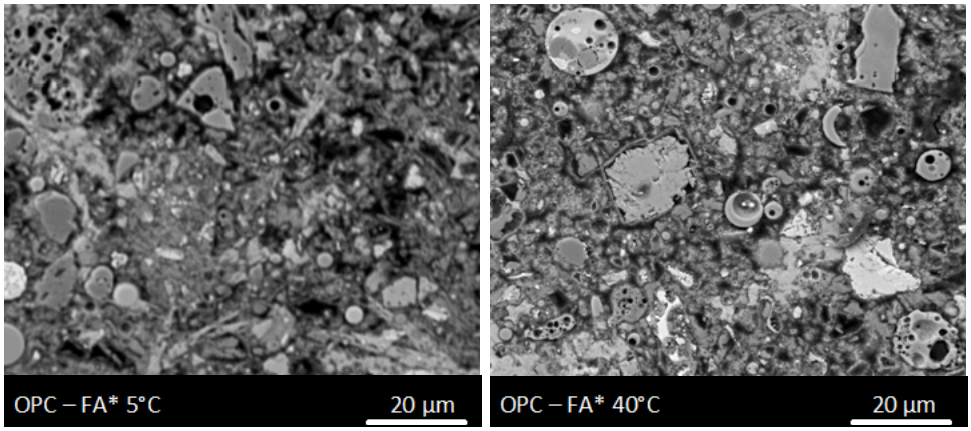

Figure 9: BSE images of hydrated pastes. Left: OPC-FA* 5˚C 90 days; right: OPC-FA* 40˚C 90 days.

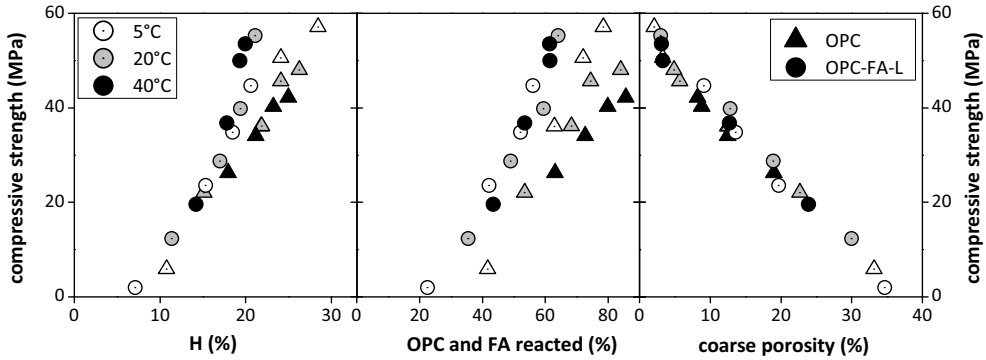

Figure 10: Compressive strength versus the amount of bound water (%H), % OPC and FA reacted, and the coarse porosity for OPC (triangles) and OPC-FA-L (spheres) cured for 1, 7, 28 and 90 days at 5, 20 and 40°C (resp. white, grey and black).

Doctoral Theses at the Department of Structural Engineering
at the Norwegian University of Science and Technology

DEPARTMENT OF STRUCTURAL ENGINEERING
NORWEGIAN UNIVERSITY OF SCIENCE AND TECHNOLOGY

N–7491 TRONDHEIM, NORWAY
Telephone: +47 73 59 47 00 Telefax: +47 73 59 47 01

"Reliability Analysis of Structural Systems using Nonlinear Finite Element Methods",
C. A. Holm, 1990:23, ISBN 82-7119-178-0.

"Uniform Stratified Flow Interaction with a Submerged Horizontal Cylinder",
Ø. Arntsen, 1990:32, ISBN 82-7119-188-8.

"Large Displacement Analysis of Flexible and Rigid Systems Considering Displacement-Dependent Loads and Nonlinear Constraints",
K. M. Mathisen, 1990:33, ISBN 82-7119-189-6.

"Solid Mechanics and Material Models including Large Deformations",
E. Levold, 1990:56, ISBN 82-7119-214-0, ISSN 0802-3271.

"Inelastic Deformation Capacity of Flexurally-Loaded Aluminium Alloy Structures",
T. Welo, 1990:62, ISBN 82-7119-220-5, ISSN 0802-3271.

"Visualization of Results from Mechanical Engineering Analysis",
K. Aamnes, 1990:63, ISBN 82-7119-221-3, ISSN 0802-3271.

"Object-Oriented Product Modeling for Structural Design",
S. I. Dale, 1991:6, ISBN 82-7119-258-2, ISSN 0802-3271.

"Parallel Techniques for Solving Finite Element Problems on Transputer Networks",
T. H. Hansen, 1991:19, ISBN 82-7119-273-6, ISSN 0802-3271.

"Statistical Description and Estimation of Ocean Drift Ice Environments",
R. Korsnes, 1991:24, ISBN 82-7119-278-7, ISSN 0802-3271.

“Properties of concrete related to fatigue damage: with emphasis on high strength concrete”,
G. Petkovic, 1991:35, ISBN 82-7119-290-6, ISSN 0802-3271.

"Turbidity Current Modelling",
B. Brørs, 1991:38, ISBN 82-7119-293-0, ISSN 0802-3271.

"Zero-Slump Concrete: Rheology, Degree of Compaction and Strength. Effects of Fillers as Part Cement-Replacement",
C. Sørensen, 1992:8, ISBN 82-7119-357-0, ISSN 0802-3271.

"Nonlinear Analysis of Reinforced Concrete Structures Exposed to Transient Loading",
K. V. Høiseth, 1992:15, ISBN 82-7119-364-3, ISSN 0802-3271.

"Finite Element Formulations and Solution Algorithms for Buckling and Collapse Analysis of Thin Shells",
R. O. Bjærum, 1992:30, ISBN 82-7119-380-5, ISSN 0802-3271.

"Response Statistics of Nonlinear Dynamic Systems",
J. M. Johnsen, 1992:42, ISBN 82-7119-393-7, ISSN 0802-3271.

"Digital Models in Engineering. A Study on why and how engineers build and operate digital models for decisison support",
J. Høyte, 1992:75, ISBN 82-7119-429-1, ISSN 0802-3271.

"Sparse Solution of Finite Element Equations",
A. C. Damhaug, 1992:76, ISBN 82-7119-430-5, ISSN 0802-3271.

"Some Aspects of Floating Ice Related to Sea Surface Operations in the Barents Sea",
S. Løset, 1992:95, ISBN 82-7119-452-6, ISSN 0802-3271.

"Modelling of Cyclic Plasticity with Application to Steel and Aluminium Structures",
O. S. Hopperstad, 1993:7, ISBN 82-7119-461-5, ISSN 0802-3271.

"The Free Formulation: Linear Theory and Extensions with Applications to Tetrahedral Elements with Rotational Freedoms",
G. Skeie, 1993:17, ISBN 82-7119-472-0, ISSN 0802-3271.

"Høyfast betongs motstand mot piggdekkslitasje. Analyse av resultater fra prøving i Veisliter'n",
T. Tveter, 1993:62, ISBN 82-7119-522-0, ISSN 0802-3271.

"A Nonlinear Finite Element Based on Free Formulation Theory for Analysis of Sandwich Structures",
O. Aamlid, 1993:72, ISBN 82-7119-534-4, ISSN 0802-3271.

"The Effect of Curing Temperature and Silica Fume on Chloride Migration and Pore Structure of High Strength Concrete",
C. J. Hauck, 1993:90, ISBN 82-7119-553-0, ISSN 0802-3271.

"Failure of Concrete under Compressive Strain Gradients",
G. Markeset, 1993:110, ISBN 82-7119-575-1, ISSN 0802-3271.

"An experimental study of internal tidal amphidromes in Vestfjorden",
J. H. Nilsen, 1994:39, ISBN 82-7119-640-5, ISSN 0802-3271.

"Structural analysis of oil wells with emphasis on conductor design",
H. Larsen, 1994:46, ISBN 82-7119-648-0, ISSN 0802-3271.

"Adaptive methods for non-linear finite element analysis of shell structures",
K. M. Okstad, 1994:66, ISBN 82-7119-670-7, ISSN 0802-3271.

"On constitutive modelling in nonlinear analysis of concrete structures",
O. Fyrileiv, 1994:115, ISBN 82-7119-725-8, ISSN 0802-3271.

"Fluctuating wind load and response of a line-like engineering structure with emphasis on motion-induced wind forces",
J. Bogunovic Jakobsen, 1995:62, ISBN 82-7119-809-2, ISSN 0802-3271.

"An experimental study of beam-columns subjected to combined torsion, bending and axial actions",
A. Aalberg, 1995:66, ISBN 82-7119-813-0, ISSN 0802-3271.

"Scaling and cracking in unsealed freeze/thaw testing of Portland cement and silica fume concretes",
S. Jacobsen, 1995:101, ISBN 82-7119-851-3, ISSN 0802-3271.

"Damping of water waves by submerged vegetation. A case study of laminaria hyperborea",
A. M. Dubi, 1995:108, ISBN 82-7119-859-9, ISSN 0802-3271.

"The dynamics of a slope current in the Barents Sea",
Sheng Li, 1995:109, ISBN 82-7119-860-2, ISSN 0802-3271.

"Modellering av delmaterialenes betydning for betongens konsistens",
Ernst Mørtsell, 1996:12, ISBN 82-7119-894-7, ISSN 0802-3271.

"Bending of thin-walled aluminium extrusions",
Birgit Søvik Opheim, 1996:60, ISBN 82-7119-947-1, ISSN 0802-3271.

"Material modelling of aluminium for crashworthiness analysis",
Torodd Berstad, 1996:89, ISBN 82-7119-980-3, ISSN 0802-3271.

"Estimation of structural parameters from response measurements on submerged floating tunnels",
Rolf Magne Larssen, 1996:119, ISBN 82-471-0014-2, ISSN 0802-3271.

“Numerical modelling of plain and reinforced concrete by damage mechanics”,
Mario A. Polanco-Loria, 1997:20, ISBN 82-471-0049-5, ISSN 0802-3271.

“Nonlinear random vibrations - numerical analysis by path integration methods”,
Vibeke Moe, 1997:26, ISBN 82-471-0056-8, ISSN 0802-3271.

“Numerical prediction of vortex-induced vibration by the finite element method”,
Joar Martin Dalheim, 1997:63, ISBN 82-471-0096-7, ISSN 0802-3271.

“Time domain calculations of buffeting response for wind sensitive structures”,
Ketil Aas-Jakobsen, 1997:148, ISBN 82-471-0189-0, ISSN 0802-3271.

"A numerical study of flow about fixed and flexibly mounted circular cylinders",
Trond Stokka Meling, 1998:48, ISBN 82-471-0244-7, ISSN 0802-3271.

“Estimation of chloride penetration into concrete bridges in coastal areas”,
Per Egil Steen, 1998:89, ISBN 82-471-0290-0, ISSN 0802-3271.

“Stress-resultant material models for reinforced concrete plates and shells”,
Jan Arve Øverli, 1998:95, ISBN 82-471-0297-8, ISSN 0802-3271.

“Chloride binding in concrete. Effect of surrounding environment and concrete composition”,
Claus Kenneth Larsen, 1998:101, ISBN 82-471-0337-0, ISSN 0802-3271.

“Rotational capacity of aluminium alloy beams”,
Lars A. Moen, 1999:1, ISBN 82-471-0365-6, ISSN 0802-3271.

“Stretch Bending of Aluminium Extrusions”,
Arild H. Clausen, 1999:29, ISBN 82-471-0396-6, ISSN 0802-3271.

“Aluminium and Steel Beams under Concentrated Loading”,
Tore Tryland, 1999:30, ISBN 82-471-0397-4, ISSN 0802-3271.

"Engineering Models of Elastoplasticity and Fracture for Aluminium Alloys",
Odd-Geir Lademo, 1999:39, ISBN 82-471-0406-7, ISSN 0802-3271.

"Kapasitet og duktilitet av dybelforbindelser i trekonstruksjoner",
Jan Siem, 1999:46, ISBN 82-471-0414-8, ISSN 0802-3271.

“Etablering av distribuert ingeniørarbeid; Teknologiske og organisatoriske erfaringer fra en norsk ingeniørbedrift”,
Lars Line, 1999:52, ISBN 82-471-0420-2, ISSN 0802-3271.

“Estimation of Earthquake-Induced Response”,
Símon Ólafsson, 1999:73, ISBN 82-471-0443-1, ISSN 0802-3271.

“Coastal Concrete Bridges: Moisture State, Chloride Permeability and Aging Effects”
Ragnhild Holen Relling, 1999:74, ISBN 82-471-0445-8, ISSN 0802-3271.

”Capacity Assessment of Titanium Pipes Subjected to Bending and External Pressure”,
Arve Bjørset, 1999:100, ISBN 82-471-0473-3, ISSN 0802-3271.

“Validation of Numerical Collapse Behaviour of Thin-Walled Corrugated Panels”,
Håvar Ilstad, 1999:101, ISBN 82-471-0474-1, ISSN 0802-3271.

“Strength and Ductility of Welded Structures in Aluminium Alloys”,
Miroslaw Matusiak, 1999:113, ISBN 82-471-0487-3, ISSN 0802-3271.

“Thermal Dilation and Autogenous Deformation as Driving Forces to Self-Induced Stresses in High Performance Concrete”,
Øyvind Bjøntegaard, 1999:121, ISBN 82-7984-002-8, ISSN 0802-3271.

“Some Aspects of Ski Base Sliding Friction and Ski Base Structure”,
Dag Anders Moldestad, 1999:137, ISBN 82-7984-019-2, ISSN 0802-3271.

"Electrode reactions and corrosion resistance for steel in mortar and concrete",
Roy Antonsen, 2000:10, ISBN 82-7984-030-3, ISSN 0802-3271.

"Hydro-Physical Conditions in Kelp Forests and the Effect on Wave Damping and Dune Erosion. A case study on Laminaria Hyperborea",
Stig Magnar Løvås, 2000:28, ISBN 82-7984-050-8, ISSN 0802-3271.

"Random Vibration and the Path Integral Method",
Christian Skaug, 2000:39, ISBN 82-7984-061-3, ISSN 0802-3271.

"Buckling and geometrical nonlinear beam-type analyses of timber structures",
Trond Even Eggen, 2000:56, ISBN 82-7984-081-8, ISSN 0802-3271.

”Structural Crashworthiness of Aluminium Foam-Based Components”,
Arve Grønsund Hanssen, 2000:76, ISBN 82-7984-102-4, ISSN 0809-103X.

“Measurements and simulations of the consolidation in first-year sea ice ridges, and some aspects of mechanical behaviour”,
Knut V. Høyland, 2000:94, ISBN 82-7984-121-0, ISSN 0809-103X.

”Kinematics in Regular and Irregular Waves based on a Lagrangian Formulation”,
Svein Helge Gjøsund, 2000-86, ISBN 82-7984-112-1, ISSN 0809-103X.

”Self-Induced Cracking Problems in Hardening Concrete Structures”,
Daniela Bosnjak, 2000-121, ISBN 82-7984-151-2, ISSN 0809-103X.

"Ballistic Penetration and Perforation of Steel Plates",
Tore Børvik, 2000:124, ISBN 82-7984-154-7, ISSN 0809-103X.

"Freeze-Thaw resistance of Concrete. Effect of: Curing Conditions, Moisture Exchange and Materials",
Terje Finnerup Rønning, 2001:14, ISBN 82-7984-165-2, ISSN 0809-103X

Structural behaviour of post tensioned concrete structures. Flat slab. Slabs on ground",
Steinar Trygstad, 2001:52, ISBN 82-471-5314-9, ISSN 0809-103X.

"Slipforming of Vertical Concrete Structures. Friction between concrete and slipform panel",
Kjell Tore Fosså, 2001:61, ISBN 82-471-5325-4, ISSN 0809-103X.

"Some numerical methods for the simulation of laminar and turbulent incompressible flows",
Jens Holmen, 2002:6, ISBN 82-471-5396-3, ISSN 0809-103X.

“Improved Fatigue Performance of Threaded Drillstring Connections by Cold Rolling”,
Steinar Kristoffersen, 2002:11, ISBN: 82-421-5402-1, ISSN 0809-103X.

"Deformations in Concrete Cantilever Bridges: Observations and Theoretical Modelling",
Peter F. Takâcs, 2002:23, ISBN 82-471-5415-3, ISSN 0809-103X.

"Stiffened aluminium plates subjected to impact loading",
Hilde Giæver Hildrum, 2002:69, ISBN 82-471-5467-6, ISSN 0809-103X.

"Full- and model scale study of wind effects on a medium-rise building in a built up area",
Jónas Thór Snæbjørnsson, 2002:95, ISBN82-471-5495-1, ISSN 0809-103X.

“Evaluation of Concepts for Loading of Hydrocarbons in Ice-infested water”,
Arnor Jensen, 2002:114, ISBN 82-417-5506-0, ISSN 0809-103X.

”Numerical and Physical Modelling of Oil Spreading in Broken Ice”,
Janne K. Økland Gjøsteen, 2002:130, ISBN 82-471-5523-0, ISSN 0809-103X.

”Diagnosis and protection of corroding steel in concrete”,
Franz Pruckner, 20002:140, ISBN 82-471-5555-4, ISSN 0809-103X.

“Tensile and Compressive Creep of Young Concrete: Testing and Modelling”,
Dawood Atrushi, 2003:17, ISBN 82-471-5565-6, ISSN 0809-103X.

“Rheology of Particle Suspensions. Fresh Concrete, Mortar and Cement Paste with Various Types of Lignosulfonates”,
Jon Elvar Wallevik, 2003:18, ISBN 82-471-5566-4, ISSN 0809-103X.

“Oblique Loading of Aluminium Crash Components”,
Aase Reyes, 2003:15, ISBN 82-471-5562-1, ISSN 0809-103X.

“Utilization of Ethiopian Natural Pozzolans”,
Surafel Ketema Desta, 2003:26, ISSN 82-471-5574-5, ISSN:0809-103X.

“Behaviour and strength prediction of reinforced concrete structures with discontinuity regions”,
Helge Brå, 2004:11, ISBN 82-471-6222-9, ISSN 1503-8181.

“High-strength steel plates subjected to projectile impact. An experimental and numerical study”,
Sumita Dey, 2004:38, ISBN 82-471-6282-2 (printed version), ISBN 82-471-6281-4 (electronic version), ISSN 1503-8181.

“Alkali-reactive and inert fillers in concrete. Rheology of fresh mixtures and expansive reactions.”
Bård M. Pedersen, 2004:92, ISBN 82-471-6401-9 (printed version), ISBN 82-471-6400-0 (electronic version), ISSN 1503-8181.

“On the Shear Capacity of Steel Girders with Large Web Openings”.
Nils Christian Hagen, 2005:9 ISBN 82-471-6878-2 (printed version), ISBN 82-471-6877-4 (electronic version), ISSN 1503-8181.

”Behaviour of aluminium extrusions subjected to axial loading”.
Østen Jensen, 2005:7, ISBN 82-471-6873-1 (printed version), ISBN 82-471-6872-3 (electronic version), ISSN 1503-8181.

”Thermal Aspects of corrosion of Steel in Concrete”.
Jan-Magnus Østvik, 2005:5, ISBN 82-471-6869-3 (printed version), ISBN 82-471-6868 (electronic version), ISSN 1503-8181.

”Mechanical and adaptive behaviour of bone in relation to hip replacement.” A study of bone remodelling and bone grafting.
Sébastien Muller, 2005:34, ISBN 82-471-6933-9 (printed version), ISBN 82-471-6932-0 (electronic version), ISSN 1503-8181.

“Analysis of geometrical nonlinearities with applications to timber structures”.
Lars Wollebæk, 2005:74, ISBN 82-471-7050-5 (printed version), ISBN 82-471-7019-1 (electronic version), ISSN 1503-8181.

“Pedestrian induced lateral vibrations of slender footbridges”,
Anders Rönnquist, 2005:102, ISBN 82-471-7082-5 (printed version), ISBN 82-471-7081-7 (electronic version), ISSN 1503-8181.

“Initial Strength Development of Fly Ash and Limestone Blended Cements at Various Temperatures Predicted by Ultrasonic Pulse Velocity”,
Tom Ivar Fredvik, 2005:112, ISBN 82-471-7105-8 (printed version), ISBN 82-471-7103-1 (electronic version), ISSN 1503-8181.

“Behaviour and modelling of thin-walled cast components”,
Cato Dørum, 2005:128, ISBN 82-471-7140-6 (printed version), ISBN 82-471-7139-2 (electronic version), ISSN 1503-8181.

“Behaviour and modelling of selfpiercing riveted connections”,
Raffaele Porcaro, 2005:165, ISBN 82-471-7219-4 (printed version), ISBN 82-471-7218-6 (electronic version), ISSN 1503-8181.

”Behaviour and Modelling og Aluminium Plates subjected to Compressive Load”,
Lars Rønning, 2005:154, ISBN 82-471-7169-1 (printed version), ISBN 82-471-7195-3 (electronic version), ISSN 1503-8181.

”Bumper beam-longitudinal system subjected to offset impact loading”,
Satyanarayana Kokkula, 2005:193, ISBN 82-471-7280-1 (printed version), ISBN 82-471-7279-8 (electronic version), ISSN 1503-8181.

“Control of Chloride Penetration into Concrete Structures at Early Age”,
Guofei Liu, 2006:46, ISBN 82-471-7838-9 (printed version), ISBN 82-471-7837-0 (electronic version), ISSN 1503-8181.

"Modelling of Welded Thin-Walled Aluminium Structures",
Ting Wang, 2006:78, ISBN 82-471-7907-5 (printed version), ISBN 82-471-7906-7 (electronic version), ISSN 1503-8181.

"Time-variant reliability of dynamic systems by importance sampling and probabilistic analysis of ice loads",
Anna Ivanova Olsen, 2006:139, ISBN 82-471-8041-3 (printed version), ISBN 82-471-8040-5 (electronic version), ISSN 1503-8181.

"Fatigue life prediction of an aluminium alloy automotive component using finite element analysis of surface topography".
Sigmund Kyrre Ås, 2006:25, ISBN 82-471-7791-9 (printed version), ISBN 82-471-7791-9 (electronic version), ISSN 1503-8181.

"Constitutive models of elastoplasticity and fracture for aluminium alloys under strain path change",
Dasharatha Achani, 2006:76, ISBN 82-471-7903-2 (printed version), ISBN 82-471-7902-4 (electronic version), ISSN 1503-8181.

"Simulations of 2D dynamic brittle fracture by the Element-free Galerkin method and linear fracture mechanics",
Tommy Karlsson, 2006:125, ISBN 82-471-8011-1 (printed version), ISBN 82-471-8010-3 (electronic version), ISSN 1503-8181.

"Penetration and Perforation of Granite Targets by Hard Projectiles",
Chong Chiang Seah, 2006:188, ISBN 82-471-8150-9 (printed version), ISBN 82-471-8149-5 (electronic version), ISSN 1503-8181.

"Deformations, strain capacity and cracking of concrete in plastic and early hardening phases",
Tor Arne Hammer, 2007:234, ISBN 978-82-471-5191-4 (printed version), ISBN 978-82-471-5207-2 (electronic version), ISSN 1503-8181.

"Crashworthiness of dual-phase high-strength steel: Material and Component behaviour",
Venkatapathi Tarigopula, 2007:230, ISBN 82-471-5076-4 (printed version), ISBN 82-471-5093-1 (electronic version), ISSN 1503-8181.

"Fibre reinforcement in load carrying concrete structures",
Åse Lyslo Døssland, 2008:50, ISBN 978-82-471-6910-0 (printed version), ISBN 978-82-471-6924-7 (electronic version), ISSN 1503-8181.

"Low-velocity penetration of aluminium plates",
Frode Grytten, 2008:46, ISBN 978-82-471-6826-4 (printed version), ISBN 978-82-471-6843-1 (electronic version), ISSN 1503-8181.

"Robustness studies of structures subjected to large deformations",
Ørjan Fyllingen, 2008:24, ISBN 978-82-471-6339-9 (printed version), ISBN 978-82-471-6342-9 (electronic version), ISSN 1503-8181.

"Constitutive modelling of morsellised bone",
Knut Birger Lunde, 2008:92, ISBN 978-82-471-7829-4 (printed version), ISBN 978-82-471-7832-4 (electronic version), ISSN 1503-8181.

"Experimental Investigations of Wind Loading on a Suspension Bridge Girder",
Bjørn Isaksen, 2008:131, ISBN 978-82-471-8656-5 (printed version), ISBN 978-82-471-8673-2 (electronic version), ISSN 1503-8181.

"Cracking Risk of Concrete Structures in The Hardening Phase",
Guomin Ji, 2008:198, ISBN 978-82-471-1079-9 (printed version), ISBN 978-82-471-1080-5 (electronic version), ISSN 1503-8181.

"Modelling and numerical analysis of the porcine and human mitral apparatus",
Victorien Emile Prot, 2008:249, ISBN 978-82-471-1192-5 (printed version), ISBN 978-82-471-1193-2 (electronic version), ISSN 1503-8181.

"Strength analysis of net structures",
Heidi Moe, 2009:48, ISBN 978-82-471-1468-1 (printed version), ISBN 978-82-471-1469-8 (electronic version), ISSN1503-8181.

"Numerical analysis of ductile fracture in surface cracked shells",
Espen Berg, 2009:80, ISBN 978-82-471-1537-4 (printed version), ISBN 978-82-471-1538-1 (electronic version), ISSN 1503-8181.

"Subject specific finite element analysis of bone – for evaluation of the healing of a leg lengthening and evaluation of femoral stem design",
Sune Hansborg Pettersen, 2009:99, ISBN 978-82-471-1579-4 (printed version), ISBN 978-82-471-1580-0 (electronic version), ISSN 1503-8181.

"Evaluation of fracture parameters for notched multi-layered structures",
Lingyun Shang, 2009:137, ISBN 978-82-471-1662-3 (printed version), ISBN 978-82-471-1663-0 (electronic version), ISSN 1503-8181.

"Modelling of Dynamic Material Behaviour and Fracture of Aluminium Alloys for Structural Applications"
Yan Chen, 2009:69, ISBN 978-82-471-1515-2 (printed version), ISBN 978-82 471-1516-9 (electronic version), ISSN 1503-8181.

"Nanomechanics of polymer and composite particles"
Jianying He 2009:213, ISBN 978-82-471-1828-3 (printed version), ISBN 978-82-471-1829-0 (electronic version), ISSN 1503-8181.

"Mechanical properties of clear wood from Norway spruce"
Kristian Berbom Dahl 2009:250, ISBN 978-82-471-1911-2 (printed version) ISBN 978-82-471-1912-9 (electronic version), ISSN 1503-8181.

"Modeling of the degradation of TiB_2 mechanical properties by residual stresses and liquid Al penetration along grain boundaries"
Micol Pezzotta 2009:254, ISBN 978-82-471-1923-5 (printed version) ISBN 978-82-471-1924-2 (electronic version) ISSN 1503-8181.

"Effect of welding residual stress on fracture"
Xiabo Ren 2010:77, ISBN 978-82-471-2115-3 (printed version) ISBN 978-82-471-2116-0 (electronic version), ISSN 1503-8181.

"Pan-based carbon fiber as anode material in cathodic protection system for concrete structures" Mahdi Chini 2010:122, ISBN 978-82-471-2210-5 (printed version) ISBN 978-82-471-2213-6 (electronic version), ISSN 1503-8181.

"Structural Behaviour of deteriorated and retrofitted concrete structures" Irina Vasililjeva Sæther 2010:171, ISBN 978-82-471-2315-7 (printed version) ISBN 978-82-471-2316-4 (electronic version) ISSN 1503-8181.

"Prediction of local snow loads on roofs" Vivian Meløysund 2010:247, ISBN 978-82-471-2490-1 (printed version) ISBN 978-82-471-2491-8 (electronic version) ISSN 1503-8181.

"Behaviour and modelling of polymers for crash applications" Virgile Delhaye 2010:251, ISBN 978-82-471-2501-4 (printed version) ISBN 978-82-471-2502-1 (electronic version) ISSN 1503-8181.